

The Mediator of Transcription in *Candida albicans*: Roles in
cell wall biogenesis, morphogenesis and host-pathogen
interactions

Nathalie Uwamahoro

A thesis submitted to Monash University in total fulfillment of the
requirement for the degree of Doctor of Philosophy

March 2015

Department of Biochemistry and Molecular Biology
Science and Technology Research and innovation Precinct
Monash University

Copyright Notices

Notice 1

Under the Copyright Act 1968, this thesis must be used only under the normal conditions of scholarly fair dealing. In particular no results or conclusions should be extracted from it, nor should it be copied or closely paraphrased in whole or in part without the written consent of the author. Proper written acknowledgement should be made for any assistance obtained from this thesis.

Notice 2

I certify that I have made all reasonable efforts to secure copyright permissions for third-party content included in this thesis and have not knowingly added copyright content to my work without the owner's permission.

Table of Contents

LIST OF FIGURES	IV
LIST OF TABLES	VI
DECLARATION	VII
ABSTRACT	VIII
ACKNOWLEDGEMENTS	X
PREFACE:	XIV
PUBLICATIONS ARISING FROM THESIS:	XV
CONFERENCE PRESENTATIONS:	XVI
1. CHAPTER 1	1
1.1. Introduction.....	1
1.1.1. Current antifungal strategies and antifungal drug resistance	2
1.1.2. <i>C. albicans</i> morphogenesis: the chief virulence factor	3
1.1.3. Cellular morphogenesis: cell surface adhesion molecules are downstream targets of yeast to hyphal signalling pathways and are essential for biofilm formation	9
1.1.3.1. Yeast morphogenesis and signalling pathways	11
1.2. Thesis Objectives	21
2. CHAPTER 2	22
2.1. General Materials and Methods	22
2.1.1. Yeast strains	22
2.2. Chapter 3 Materials and Methods	26
2.2.1. Fungal growth conditions	26
2.2.2. Cell staining	26
2.2.3. RNA extraction, quantitative PCR, and microarray analysis	28
2.2.4. Analysis of microarray results and motif identification:	29
2.2.5. Biofilm assays and agar invasion	35
2.3. Chapter 4 Materials and Methods	36
2.3.1. Standard growth conditions for <i>C. albicans</i> and macrophages	36
2.3.2. Quantification of <i>C. albicans</i> survival in macrophages	36
2.3.3. Experiments to assess fungal morphology within macrophages, escape and phagocytosis, and Lamp1 association.....	37
2.3.4. Quantification of macrophage cell death using time-lapse imaging	39
2.3.5. Quantification of IL-1 β production	40
2.3.6. Quantification of <i>Candida</i> gene expression in macrophages.....	40
2.3.7. Fluorescence microscopy and quantification of 1,3 β -glucan exposure using flow cytometry.....	41
2.3.8. Atomic force microscopy	42
3. CHAPTER 3: THE ROLES OF THE <i>C. ALBICANS</i> MEDIATOR IN THE DIMORPHIC SWITCH AND CELL WALL REMODELLING	44
3.1. Introduction.....	44
3.2. Results.....	46
3.2.1. <i>C. albicans</i> Mediator subunits co-regulate genes with morphogenesis associated transcription factors: the link between Ace2 and Med31	46
3.2.2. The <i>C. albicans</i> Med31 controls the expression of genes involved in cell wall integrity and filamentous growth.....	48
3.2.3. Med31 has divergent roles in adhesion between <i>C. albicans</i> and <i>S. cerevisiae</i> in adhesion.....	67
3.2.4. The Mediator Kinase domain plays a role in cell wall gene expression in <i>C. albicans</i>	72
3.2.5. Effects of Mediator mutations on stress-responsive phenotypes in <i>C. albicans</i>	74
3.3. DISCUSSION	77

3.3.1. The Mediator complex is required for <i>C. albicans</i> morphological remodelling and general cellular processes	77
3.3.2. Mediator interacts with transcription factors involved in cellular morphogenesis	77
3.3.3. Core Mediator and Kinase domain mutants have distinct phenotypes	79
3.3.4. The Mediator complex plays complex roles in fungal adhesion and cell wall proteome expression	80
4. CHAPTER 4: THE FUNCTIONS OF MEDIATOR AND HOST PROGRAMMED CELL DEATH PATHWAYS IN	
C. ALBICANS MACROPHAGE EVASION	83
4.1. Introduction:	83
4.1.1. Phagocyte invasion.....	83
4.1.2. Fungal immune evasion and escape	84
4.1.3. <i>C. albicans</i> morphology inside macrophages.....	85
4.1.4. Intracellular signalling in immune cells in response to fungal infection	86
4.1.5. Inflammasome activation and programmed cell death	90
4.2. RESULTS	92
4.2.1. Mediator is required for <i>C. albicans</i> replication in macrophages.....	92
4.2.2. Mediator mutants present various morphologies within macrophages.....	94
4.2.3. A novel macrophage killing assay detects roles of Mediator in <i>C. albicans</i> –induced macrophage cell death.....	99
4.2.4. <i>C. albicans</i> kills macrophages in two distinct phases and Mediator subunits are required for macrophage killing.....	102
4.2.5. <i>C. albicans</i> Mediator subunit Srb9 is required for the establishment of proper cell surface structure of hyphae.....	109
4.2.6. <i>C. albicans</i> activates a programmed cell death pathway for killing macrophages	114
4.2.7. <i>C. albicans</i> cells restructure cell surface architecture to hijack pyroptosis and escape from macrophages	121
4.3. DISCUSSION:	126
4.3.1. Functions of Mediator in immune evasion by <i>C. albicans</i>	126
4.3.2. <i>C. albicans</i> triggers pyroptotic programmed cell death in macrophages	127
5. CHAPTER 5: THESIS SUMMARY AND FUTURE DIRECTIONS	132
5.1. Thesis summary.....	132
5.2. Future directions.....	136
6. REFERENCES	137
APPENDIX 1 APPENDIX FIGURES AND TABLES FOR CHAPTER 3	157
7. APPENDIX 2 APPENDIX FIGURES FOR CHAPTER 4.....	217

List of Figures

Figure 1.1. <i>C. albicans</i> morphological transitions and signalling pathways that lead to virulence.	6
Figure 1.2. Schematic diagram of the <i>C. albicans</i> cell wall and plasma membrane structure.	10
Figure 1.3. Schematic diagram depicting stages of cell division and the stage at which Ace2 dependent genes are expressed.....	12
Figure 3.1. Mediator mutant morphology under nutrient rich conditions	48
Figure 3.2. Chromosomal view of the transcriptional profile of the <i>med31</i> Δ/Δ mutant of <i>C. albicans</i>	49
Figure 3.3. Transcriptional profiling of the <i>med31</i> deletion strain.....	52
Figure 3.4. Motif identification in gene targets of Med31	58
Figure 3.5. Mediator Subunits are required for the regulation of cell wall genes	60
Figure 3.6. The Med31 subunit co-regulates the expression of components in the cAMP signalling pathway.	63
Figure 3.7. Mediator Med31 is required for filamentation in various hyphal inducing conditions.	65
Figure 3.8. The Med31 subunit is required for biofilm formation.	66
Figure 3.9. The Med31 (Soh1) subunit in the model yeast <i>S. cerevisiae</i> regulates cytokinesis, adherence and flocculation.	69
Figure 3.10 The Med31 (Soh1) subunit in the model yeast <i>S. cerevisiae</i> regulates biofilm formation and agar invasion.	71
Figure 3.11. Mediator Med20 and Srb9 are required for adhesin gene expression....	73
Figure 3.12. Sensitivities of the <i>C. albicans</i> Mediator mutants to various stresses. ..	75
Figure 4.0. Signalling pathways that lead to inflammasome activation in macrophages during <i>C. albicans</i> infection.	89
Figure 4.1. Mediator subunits impact on replication of <i>C. albicans</i> in macrophages.	93
Figure 4.2 Mediator mutants present various morphologies within macrophages....	96
Figure 4.3. Late phagosomal association of <i>C. albicans</i> Mediator mutants.....	97
Figure 4.4. Optimization of the live cell macrophage death assay.....	101
Figure 4.5 Filamentous morphology is required for macrophage killing.....	105
Figure 4.6. Phagocytosis of <i>C. albicans</i> Mediator mutants by macrophages.....	107
Figure 4.7. <i>C. albicans</i> filamentation within macrophages requires the adhesin regulator <i>BCR1</i>	108
Figure 4.8. Cells deleted for <i>SRB9</i> are deficient in 1, 3 β glucans in hyphal morphology.....	111
Figure 4.9. Srb9 is required for correct hyphal cell surface architecture	113
Figure 4.10. The two phases of macrophage killing by <i>C. albicans</i> depicted in RAW 264.7 and primary macrophages.....	115

Figure 4.11 Pyroptotic cell death induced in the first phase of macrophage killing.	118
Figure 4.12. Macrophage killing requires components of the inflammasome.	120
Figure 4.13. <i>C. albicans</i> morphogenesis and surface architecture of hyphae are required for triggering macrophage pyroptosis.	124
Appendix 2, Figure 1. Actual experimental results of IL-1 β levels depicted in Figure 4.14.	219
Appendix 2, Figure 2. <i>URA3</i> expression levels of the <i>srb9</i> Δ/Δ mutant within macrophages.	220

List of Tables

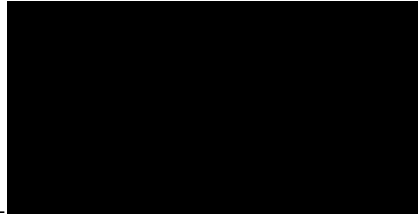
Table 1.1. The Yeast Mediator of Transcription	17
Table 1.2. Phenotypic impairments observed in <i>S. cerevisiae</i> null mutants deficient in non-essential MED subunits.....	18
Table 2.1. <i>S. cerevisiae</i> strains used in this thesis	24
Table 2.2. <i>C. albicans</i> strains used in this thesis	25
Table 2.3. Key growth and phenotyping media used	27
Table 2.4. Primers used in this thesis	31
Table 3.1. Go Slim process of the up-regulated genes in the <i>C. albicans med31Δ/Δ</i> mutant.....	53
Table 3.2. Go Slim process down-regulated genes in <i>C. albicans med31Δ/Δ</i> mutant.....	54
Table 3.3. GO term analysis of genes differentially expressed in the <i>C. albicans med31Δ/Δ</i> mutant.....	55
Appendix Table 1. Go Term process for down- regulated genes in the <i>med31Δ/Δ</i> mutant hits	159
Appendix Table 2. Go Term process for up- regulated genes in the <i>med31Δ/Δ</i> mutant hits	163
Appendix 1, Table 3. Go SLIM classification by process of all significantly altered genes in the <i>C. albicans med31Δ/Δ</i> mutant	164
Appendix 1, Table 4. Go Slim functions <i>down-regulated</i> in the <i>med31Δ/Δ</i> mutant.....	171
Appendix 1, Table 5. Go Slim processes <i>down-regulated</i> in the <i>med31Δ/Δ</i> mutant.....	174
Appendix 1, Table 6. Go SLIM classification by component of all significantly altered genes in the <i>C. albicans med31Δ/Δ</i> mutant	179
Appendix 1, Table 7. Significantly altered genes of the complete transcriptome analysis data for the <i>med31Δ/Δ</i> mutant.	187

Declaration

This is to certify that:

- i. The thesis comprises only of my original work towards the PhD except where indicated in the Preface and figure footnotes.
- ii. Due acknowledgements have been made in the text to all other material used and
- iii. The thesis is less than 100,000 words in length, exclusive of tables, maps, bibliographies and appendices.

Signature of the *Candidate*: _



Date

6 March 2015

Abstract

The fungal pathogen *Candida albicans* is the fourth leading cause of nosocomial infections and continues to cause life-threatening candidiasis. *C. albicans* virulence results from the intricate gene regulatory pathways that dictate morphogenesis, particularly cell wall remodelling, dimorphism and biofilm formation that allows the organism to evade the host. Studies in non pathogenic yeasts have demonstrated that gene regulatory networks rely on multi-subunit transcriptional complexes such as the Mediator of transcription to modulate gene activation and repression in association with RNA polymerase II. While Mediator is well-studied in non-pathogenic model yeasts, before the commencement of this project its roles in *C. albicans* were unknown. In this thesis work, I characterised the roles of three Mediator subunits in *C. albicans*, Med20 from the Head domain of the complex, Med31 from the Middle domain and Srb9 from the Kinase module. I identified global roles for Mediator in the genetic programs that regulate morphogenesis, including conserved roles with non-pathogenic yeasts in the regulation of components of the RAM (regulation of Ace2 and morphogenesis) cell wall remodelling pathway in association with the Ace2 transcription factor. Phenotypic and gene expression comparison using deletion mutants of the most evolutionarily conserved subunit Med31, provided evidence for both conserved and divergent roles, with differences observed in the regulation of cellular adhesion. Med31 controls the yeast to hyphal transition, and it affects the expression of genes coding for key morphogenesis regulators including transcription factors required in the nutrient-sensing cAMP filamentation signalling pathway, (e.g. *EFG1*, *TEC1*, *CPH2* and *RIM101*). The downstream targets of the Mediator complex in *C. albicans* also include the adhesion genes *ALS1*, *ALS3* and *HWPI*, as well as other cell surface molecules such as the immunologically relevant cell wall component 1,3 β -glucan. Collectively, the above mentioned effects of Mediator on cell wall regulation and cellular morphogenesis translate into cellular roles in biofilm formation by *C. albicans*, which is a key virulence attribute, as well as essential functions for Mediator in the ability of *C. albicans* to escape the innate immune response by evading macrophages. Overall, the Mediator complex was essential for *C. albicans* pathogenesis and my published work with collaborators showed the Mediator is also required for *C. albicans* virulence *in vivo*.

I further used *C. albicans* Mediator mutants and a novel assay that I developed, which monitors in real time the killing of macrophages by *C. albicans*, to discover that macrophages are killed in a biphasic fashion by *C. albicans* hyphal cells. I demonstrated for the first time that *C. albicans* hyphal cells trigger the inflammatory suicide response in macrophages – pyroptosis. This work further demonstrated that the long-standing view that *C. albicans* hyphal cells mechanically damage macrophages has to be revised – instead, hyphal cells activate pyroptosis, which is lytic, and then hijack this processes to escape. I showed that hyphal morphogenesis is necessary for pyroptotic macrophage death, and have data that implicate hyphal cell wall 1,3 β -glucan in the mechanism.

The pathogen and host factors and mechanisms of *C. albicans* morphogenesis and immune evasion identified and characterised in my thesis work add to the knowledge base and provide a platform for the identification of future strategies against human fungal infections.

Acknowledgements

Looking back, the years of my PhD have been overall undeniably some of the best years of my life. These past years I realized my long life dream, to be around people who thought about the betterment of humanity, who appreciated and were fascinated by the complexity of the life under the Sun (and beyond) and people who obsessively worked not because they wanted fame, but because they were passionate about finding new discoveries that would make our lives better. I got to work as much as I wanted, read as much as wanted, travelled locally and overseas to engage with other scientists whom I am really grateful for the great discussion and inclusion.

This amazing journey could not have been possible if it wasn't for my awesome supervisor Dr. Ana Traven. I am grateful for a work environment that has been conducive for productive work without politics and drama, and that being among my colleagues did not reduce but instead increased my overall love for doing science. Thank you for supporting me mentally, financially and scientifically...which are analogous to a grad student's basic human needs (food, shelter and clothing). I am truly blessed to have gotten a great role model as my supervisor. Thank you for letting me freely explore during my microscopy experiments, trying different things and giving me freedom to find ways to make our experimental findings better even though my endeavors rewarded me with many failures along the way, fortunately we made great findings eventually. Thank you for being able to point out great findings when I was too delirious with lack of sleep or just plain unaware to notice the findings...yes I am referring to srb9 crescent morphology that I would have dismissed to "funny fungal cells forming moon shapes". Without you, I could have missed one of the greatest findings in fungal host pathogen interactionsso thank you for being awake for both of us! Thank you for teaching me that what is most important is knowing what to do with the information you get...teaching me to learn *how* to think during scientific investigations rather than focusing on the massive amounts of information that can be found on Google in a matter of seconds. Most of all, thank you for being a great mentor.

This journey would not have been completed without the guidance of Dr. Thomas Naderer. I did not like immunology before you showed up, but after working with you I am actually pursuing a career towards that field. Thank you for making immunology easy to understand and increasing my fascination with host-pathogen interactions. Without you I probably would have never discovered that macrophages are killed in two the phases ---that was really cool... Thank you for teaching me that great teachers are teachers willing to serve and that... ..*“even if you’re on the right track, you’ll get run over if you just sit there”*~unknown

Thanks to Professor Trevor Lithgow for inviting me into this great environment. I am truly grateful for all my supervisors and I hope that your level of integrity never changes with the pressures that come with trying to do great science in a world that has forgotten what it’s all about; so my wish for you all are in the words of Richard Feynman...

“So I have just one wish for you – the good luck to be somewhere where you are free to maintain the kind of integrity where you do not feel forced by a need to maintain your position in the organization, or financial support, or so on, to lose your integrity. May you have that freedom.” — Richard P. Feynman, Surely You're Joking, Mr. Feynman!

To my colleagues, thank you for being my science family...to the post docs, thank you for the brotherly banter and the laughs! Thank you for rescuing my experiments with great insights and discussions. To the PhD students, thank you for your generosity. I have never been in a lab where people share their belongings so freely. Thank you for the freedom to take reagents and materials during the times when I was running low. You will never comprehend how grateful I was to be able to reach out and take as much materials and reagents as I wanted when I run out during those late night experiments. Mary...thanks for the cells. Every time I had a new experiment, I knew I could count on you to help me get to the results faster by giving me cells to work with. Yue Qu thanks for allowing me to use anything I wanted on your bench without asking and Jiyoti thanks for missing a few trains home because I needed your input and you couldn’t go home until I was satisfied with our conclusions. I will never forget you all, for you have been an inspiring bunch.

To our beloved RA, Tricia Lo, Thank you for expecting better out of me than I would have expected from myself.

“Open rebuke is better than love carefully concealed”~Proverbs 27:5

Not many people care like that, but you do. For that I will always be grateful and have great respect for you.

To the entire Host- Pathogen Umbrella group, thank you for always helping me when I needed you, you made it a great place to work in.

To my family and large extended family, especially my mother and father, thank you for teaching me that we pursue more knowledge, not to put ourselves on a higher pedestal compared to others, but to increase our capacity to contribute and leave this world a little better than we found it. Thank you for your wisdom and for guiding me in the process.

To my great friends, Leisa, Diana, Josephine, Fera, Elisa, Hanna, Catriona, Li yin, Paulette, Marlies, Dana, Blessing, Sun young, Osasehi, Shruchie, this thesis is also partly your own. Thank you for picking up the phone during my M.I.A moments. To MCC, Monash Christian Union and F.O.C.U.S., thank you for making grad school more than just study and the endless deep discussions on the “meaning of life”.

“You will be the same person in five years as you are today except for the people you meet and the books you read” ~Charlie Jones

Since I am now a “true” scientist, it would be plagiarism to claim that I did this all by myself. Great scientific work is gained by the work of many, past and present and credit should be awarded to all who made way for me to investigate the work in this thesis...I thank God for everyone in my life who has helped me get where I am today including those who published the work referenced in this thesis.

My Sincere thanks to the technical support from the Monash University Micro Imaging facility as well as microarray analysis conducted in Canada by Andre Nantel and Elisa sample processing in James Vince’ laboratory at WEHI. I also acknowledge the Australian government for funding our work.

“One never notices what has been done; one can only see what remains to be done.”~Marie Curie

Preface:

The contributions of collaborators are outlined below:

- i. Dr. Hsing- Hui Shen performed Atomic Force microscopy (AFM) on samples for the AFM results discussed in this thesis (Chapter 4, Figure 4.8).
- ii. The biofilm analyses were performed by Dr. Yue Qu (Chapter 3, Figure 3.8).
- iii. The glucans analyses by flow cytometry and the quantitative PCR in macrophages were conducted by Dr. Jiyoti Verma-Gaur (Chapter 4, Figure 4.7A, C-F7).
- iv. Microarray analysis of the transcriptome was performed by the facility at the Biotechnology Research Institute in Montreal, in collaboration with Dr. Andre Nantel.
- v. Quantitative Polymerase chain reaction (qPCR) analysis for Figure 3.10 panel A, was conducted by Dr. Branka Jeličić
- vi. IL-1 β quantification by ELISA was performed by Drs. James Vince and Rowena Lewis (WEHI).

All other experiments comprises of my own work.

A majority of the work undertaken towards this degree has been published in the papers listed below.

Publications arising from thesis:

- **Nathalie Uwamahoro**, Jiyoti Verma-Gaur, Hsin-Hui Shen, Yue Qu, Rowena Lewis, Jingxiong Lu, Keith Bambery, Seth L. Masters, James E. Vince, Thomas Naderer and Ana Traven (2013), The pathogen *Candida albicans* hijacks macrophage pyroptosis for immune evasion, *mBio*, 5(2),doi: 10.1128/mBio.00003-14
- **Nathalie Uwamahoro**, Yue Qu, Branka Jelicic, Tricia L Lo, Cecile Beaurepaire, Farkad Bantun, Tara Quenault, Peter R Boag, Georg Ramm, Judy Callaghan, Traude H Beilharz, André Nantel, Anton Y Peleg, and Ana Traven (2012) The functions of Mediator in *Candida albicans* support a role in shaping species-specific gene expression, *PLoS Genetics* 8(4): p. e1002613.
- **Nathalie Uwamahoro** and Ana Traven (2010) Yeast, Filaments and Biofilms in Pathogenesis of *Candida albicans*, *Australian Biochemist* 41: 16 (Invited mini-review)

Other publications to which I have contributed, but which are not part of the thesis:

- Michael Dagley, Ian Gentle, Traude Beilharz, Filomena Pettolino, Julianne Djodjevic, Tricia Lo, **Nathalie Uwamahoro**, Thusitha Rupasinghe, Dedreja Tull, Malcom McConville, Andre Nantel, Trevor Lithgow, Aaron Mitchell and Ana Traven, Cell wall integrity is linked to mitochondria and phospholipid homeostasis in *Candida albicans* through the activity of the post-transcriptional regulator Ccr4-Pop2. *Molecular Microbiology*, 2011. 79(4): 968-989.
- Tricia L. Lo, Yue Qu, **Nathalie Uwamahoro**, Tara Quenault, Traude H. Beilharz and Ana Traven. *A Regulation of FLO11 expression and biofilm formation in Saccharomyces cerevisiae by the mRNA decay pathway*. *Genetics*, 2012. 191(4): p. 1387-1391

Conference presentations:

Nathalie Uwamahoro, Jiyoti Verma-Gaur, Hsin-Hui Shen, Yue Qu, Rowena Lewis, Jingxiong Lu, Keith Bambery, James Vince, Thomas Naderer and Ana Traven, Mediator regulates transcriptional programs important for pathogenicity of *Candida albicans*, Lorne Genome Conference, Lorne Australia (poster presentation) **2013**

Nathalie Uwamahoro, Yue Qu, Branka Jelacic, Tricia L Lo, Cecile Beaurepaire, Farkad Bantun, Tara Quenault, Peter R Boag, Georg Ramm, Judy Callaghan, Traude H Beilharz, André Nantel, Anton Y Peleg, and Ana Traven, The functions of Mediator in *Candida albicans* support a role in shaping species-specific gene expression, Lorne Genome Conference, Lorne Australia (poster presentation) **2012**

Nathalie Uwamahoro, Yue Qu, André Nantel, Anton Y Peleg, and Ana Traven, The Mediator subunit Med31 regulates morphogenesis and biofilm formation in *Candida albicans*, Fourth FEBS Advanced Lecture Course Human Fungal Pathogens: Molecular Mechanisms of Host-Pathogen Interactions and Virulence, La Colle sur Loup, France (poster presentation) **2011 Supported by FEBS Youth Travel Fund (YTF) Grant**

Nathalie Uwamahoro, Yue Qu, André Nantel, Anton Y Peleg, and Ana Traven, The Mediator from *Candida albicans* and the virulence-related transcriptional programs, Department of Biochemistry and Molecular Biology PhD Conference, Monash University (Talk presentation) **2011**

Nathalie Uwamahoro and Ana Traven The Mediator subunit Med31 regulates morphogenesis in the fungal pathogen *Candida albicans* Lorne Genome Conference, Lorne Australia (poster presentation) **2010**

Nathalie Uwamahoro and Ana Traven The Mediator subunit Med31 regulates morphogenesis in the fungal pathogen *Candida albicans* Annual Postgraduate Research conference Monash University (poster presentation) **2009**

Nathalie Uwamahoro and Ana Traven The Mediator subunit Med31 regulates morphogenesis in the fungal pathogen *Candida albicans* Victorian Infection and Immunity student symposium (poster presentation) **2009**

Chapter 1

1.1. Introduction

Humans generally harbour commensal fungi that colonise the gastrointestinal and genitourinary tracks [1]. While fungi are normally tolerated as commensals by healthy individuals, fungal disease occurs primarily in immunocompromised hosts. Immunocompromised hosts include a significant proportion of the world population [2-5]. The degree of diseases caused by fungi are classified as either superficial (acute) or systemic (severe). Superficial infections, such as thrush, are treated with antifungal drugs. Seventy five percent of healthy women also experience acute Vulvovaginal Candidiasis (VVG), and after antifungal treatment many patients experience recurring infections [6]. In contrast, systemic infections are much harder to treat and are often life threatening. Systemic infections are common in babies, the elderly and in immunocompromised hosts including HIV and cancer patients. In up to 50% of cases of systemic infections, the patients do not survive even with treatment [7-9]. There are over 600 different fungi that infect humans and the cases of life threatening fungal infections continue to rise [10]. For instance, fungal disease caused by fungal pathogens in the genus *Cryptococcus* results in approximately one million infections each year, while *Candida* is ranked as the fourth source of hospital acquired infections causing 8-9% of blood disseminated infections [11]. The most commonly isolated species in the clinic is *Candida albicans*, and this species causes 80% of cases of oropharyngeal and vulvovaginal candidiasis [12, 13]. Indeed, oropharyngeal candidiasis is often the key symptom of untreated HIV positive patients and affects 90% of AIDS patients [14, 15].

1.1.1. Current antifungal strategies and antifungal drug resistance

A characteristic of *C. albicans* is the use of cell morphogenesis to evade host defences and in resistance of antifungal treatments [16-19]. Currently available antifungal drugs target components of the fungal cell that are different from the host, but these therapies are inefficient because some are fungistatic, and those that are fungicidal are toxic. Furthermore, fungal pathogens continue to develop resistance mechanisms against the current drugs. The antifungals that are currently in use include the polyenes, the azoles, allylamines, echinocandins, pyrimidine analogues, mitotic inhibitors, and others that are not orally bioavailable (eg. tea tree oil). These drugs target components of the cell wall and plasma membrane. For example, azoles target the enzyme 1-4 α -lanosterol demethylase encoded by the gene *ERG11* [20, 21]. This enzyme is required for ergosterol biosynthesis. Azoles such as the drug fluconazole are generally fungistatic, but in some cases can be fungicidal [22], and clinical resistant fungal strains are observed commonly. In the case of the azole drugs, resistance occurs through mutations in the *ERG11* gene [20, 21] or by increasing the rate of drug expulsion from the cells through both ATP binding cassette and major facilitator superfamily transporters [17, 23]. Other mechanisms include resistance via up-regulation of drug targets and inhibition of the drug as found in *Candida krusei* drug resistant strains [24]. Polyenes like amphotericin B are efficient because they bind to the fungal specific sterol molecule ergosterol and also form channels in the membrane [25]. However, prolonged exposures to the drug have toxic effects because, while more specific for ergosterol, amphotericin can also interact with the sterol found in host membrane, cholesterol, leading to organ failure in patients [26]. The problem of toxicity remains a challenge pharmacologically and demonstrates the need for more efficient drugs. The newest and most pathogen-specific antifungal drugs are the echinocandins, such as caspofungin, which target the 1-3 β glucan synthase enzyme that is required for cell wall biogenesis and synthesis of glucan molecules in the cell wall. The disadvantage in the use of these drugs is the emergence of resistant *Candida* strains, mainly via mutations in the gene encoding the target, glucan synthase [27]. Moreover, these drugs are also very expensive and are not orally available [28].

A further problem for treatment of fungal infections is represented by biofilm structures. Some fungal pathogens, particularly *Candida* sp. are able to form communities of cells known as biofilms – these structures are highly adherent to abiotic and biotic surfaces, including host organs and medical devices, such as catheters and heart valves [29]. The high resistance of fungal biofilms to treatment means that for many patients invasive surgery is required to extract the device infected with the biofilm [30]. These surgeries may also be life threatening and costly for patients. In addition to inadequate treatment options, we also lack accurate diagnosis for clinical identification of fungal infections, and autopsies are not usually performed on non-surviving patients to identify whether proper treatment was administered [31]. The continued isolation of resistant clinical isolates implies that fungal cell biology is highly dynamic and adaptable to currently available treatment. Clearly, fungal pathogens impose a significant burden on the world health system and more specific antifungals are required. An integral part of this will involve better understanding of fungal morphogenesis and genetic programs that dictate pathogenesis.

1.1.2. C. albicans morphogenesis: the chief virulence factor

Current knowledge suggests that one of the key differences between non-pathogenic and pathogenic fungi is the patterns of cellular morphogenesis [32]. Cellular morphogenesis may be described as the alteration prompted by an environmental stimulus to aid survival of cellular programs at both molecular and macromolecular levels leading to alterations of cell surface and/or cell shape. Both pathogenic and non-pathogenic fungi may acquire different cell shapes in response to the environment. The non-pathogenic yeast *Saccharomyces cerevisiae*, which is distantly related to *C. albicans*, is capable of morphological transitions and growth as yeast and pseudohyphal cells, but it is not known to make true hyphal filaments [33]. In contrast, *C. albicans* is able to form true hyphae. *C. albicans* morphogenesis is highly dynamic and the pathogen may thrive in several morphological and developmental states, including yeast, pseudohyphae and hyphae, white and opaque cells, biofilms, and the newly discovered grey or GUT cells [34]. The dimorphic switch from round yeast cells to elongated hyphae is the most studied and perhaps the best-characterised virulence-related developmental transition in this organism [19].

C. albicans dimorphism is a threat to the host in two ways: 1) the ability to switch from round yeast cells to hyphae, and 2) the ability of these cells to form biofilms. The round yeast cells have the capacity to allow fungal cell dissemination during an invasive systemic infection. These cells also provide the first highly adherent layer in various host organs including skin, spleen and brain [35, 36]. The yeast to hyphal switch may be triggered by host physiological pH of 7.4 host temperature, serum, nutrient limitations, and changing levels of oxygen [37, 38].

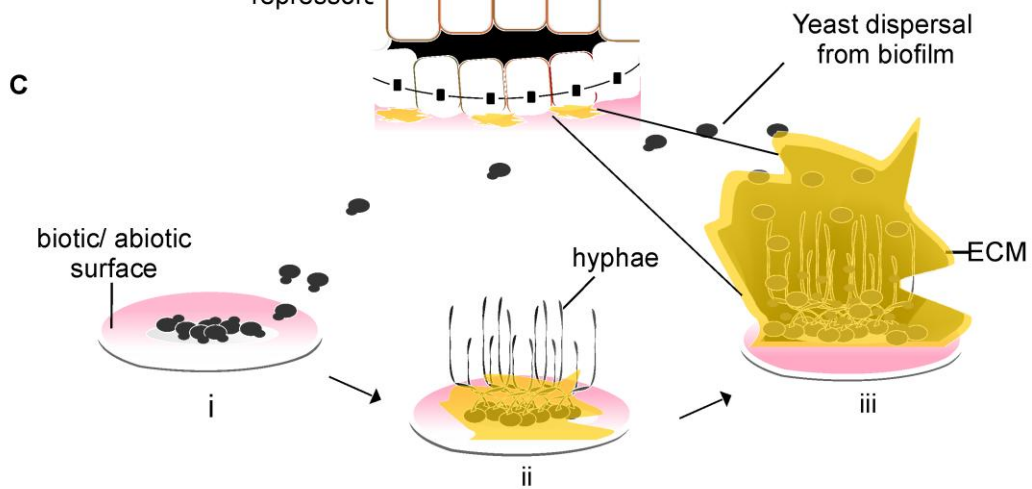
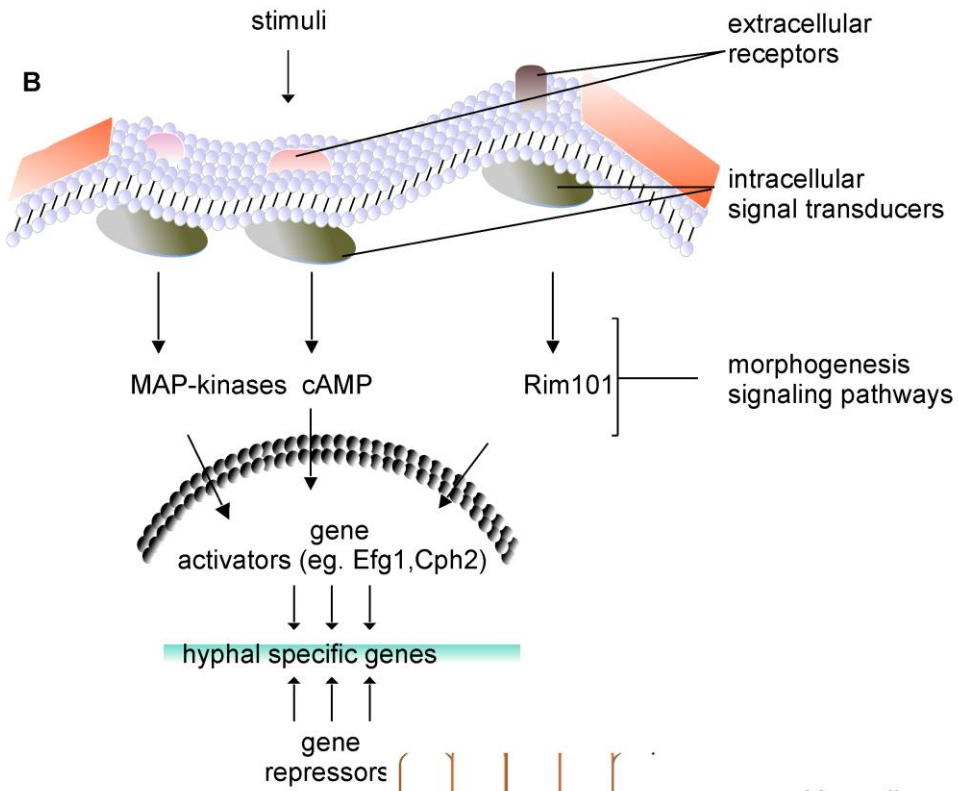
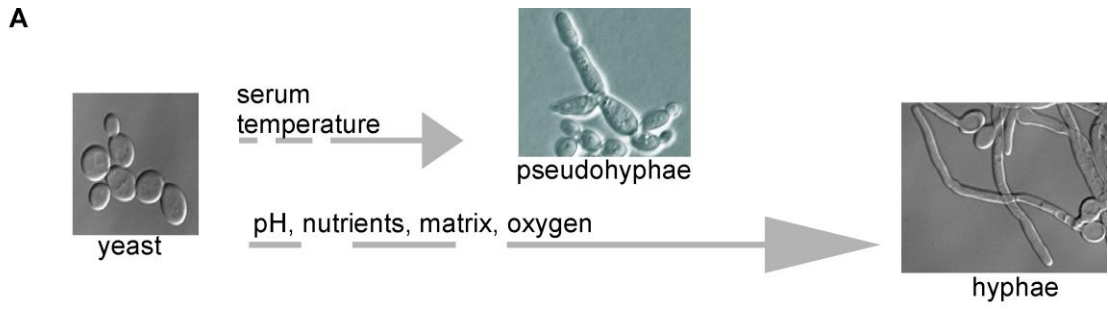


Figure 1.1. *C. albicans* morphological transitions and signalling pathways that lead to virulence. **A)** *C. albicans* pleomorphism is induced by environmental stimuli. Shown are DIC images of cells grown in YPD (yeast), YPD at 37°C (psuedohyphae), and Spider media (hyphae). **B)** Yeast to hyphae morphogenesis signalling pathways in *C. albicans* that lead to the expression of virulence related adhesin genes (schematic diagram information was obtained and is well described by Sudbery, 2011 [39]. **C)** Stages of biofilm formation as described by Hawser and Douglas, 1994 and Richard *et al.*, 2006 [40, 41]. Yeast cells form the first layer of adherent cells (colonization) and may establish a mature biofilm (maturation) on host tissues or medical transplant devices. Studies on biofilm dispersion by Uppuluri *et al.*, showed that at different stages of biofilm, the maturing biofilm serve as a reservoir for more biofilm establishment (dissemination) and the extent of dispersion is greatest at the intermediate stage (**ii**) of biofilm growth [42].

Hyphal cells formed may be either psuedohyphae or true hyphae. Pseudohyphal cells are like dividing yeast cells as they have constrictions at the site of cell separation and are wider than hyphae (Figure 1.1A). Hyphae are long, completely parallel, tube-like filaments. Pseudohyphae were suggested to be an intermediate between yeast and hyphal morphology, a proposition supported by a recent report that showed that the levels of Ume6, a transcription factor related to morphogenesis, are sufficient to trigger the transition from yeast to hyphae via an intermediate pseudohyphal stage [43]. The constrictions at the site of separation in pseudohyphal cells may expose immunologically relevant components of the fungal cell surface that are hidden in hyphae. For example, when yeast cells divide they leave glucan rich bud scars on mother cells that are recognized by host immune cells and engage the receptor Dectin 1, but these glucans are hidden in hyphae [44]. *C. albicans* hyphae are considered an advantage in evasion of the host immune system compared to other fungi. The mycellial nature of hyphae has been shown to be important for tissue invasion and phagocyte escape. All morphotypes can be found in tissues, and fungal mutants that are unable to switch between forms are less virulent, however the specific roles of these distinct morphotypes in virulence are still unclear, and remain under intense investigation [45].

The distinct morphologies of *C. albicans* display specific gene transcription programs and several transcription factors have been identified that control the yeast to hyphae transition [46]. For example Efg1 and Cph1 are transcriptional activators of the

hyphal transition and *C. albicans* deletion strains that have both *EFG1* and *CPH1* deleted cannot transition from yeast to hyphal morphology [47]. Nrg1 is a transcriptional repressor of the hyphal program, and the *nrg1* deletion strains retain hyphal morphology even in yeast growth conditions [48, 49]. The distinct transcriptional regulators of the yeast morphogenetic program in *C. albicans* are shown in Figure 1.1B, together with the signalling pathways that control their activity.

The cell surface properties of yeast or hyphal morphotypes differ and this leads to differential antifungal susceptibility and interactions with the host immune system. Yeast and hyphal-locked mutants are often more susceptible to antifungal treatment [50-53] and yeast and hyphal cells produce different immunological responses. For instance, though the hyphal cell wall may contain 3-5 times more chitin, most chitin in yeast cells is exposed in bud scars and may be recognized by immune cells [54, 55]. Yeast cells are also known to induce Toll-like receptor 4 (TLR4) responses, while during hyphal germination these TLR4 mediated signals are lost [56]. Fè d'Ostiani *et al.* suggested that immune cells are able to discriminate between yeast and hyphal cells based on the type of immunological responses elicited by these cell types [57]. It is generally accepted that hyphal cells are more invasive, but there have been rare reports of non-invasive hyphal cells [47, 58]. There have also been reports suggesting fungal morphology may be different in different tissues [59, 60]. Hyphal cells are usually observed in kidneys, but are not found in the spleen or liver during invasive candidiasis [61, 62]. Other reports suggest that both hyphae and yeast cells are found in infected organs and that there is no clear evidence on which morphology predominates [63, 64]. Although the yeast to hyphal transition is clearly important, aspects of these morphotypes cell biology that lead to an immunological response essential for host evasion remain under investigation.

The second threat to the host by *C. albicans* is biofilm formation, which may also include other microorganisms harboured by the host, such as bacteria, as well as host immune cells [65, 66]. As mentioned above, biofilms are highly resistant to treatment. The various stages of biofilm formation are described in Figure 1.1C. The dimorphic nature of *C. albicans* plays a critical role in biofilm formation, as mutants that cannot make hyphae are usually unable to make biofilms [47, 67]. These mutants include

strains that lack the hyphal morphogenesis transcription factors Efg1 and Cph1 [47, 68]. Deletion mutants that are defective in biofilm formation, also often present poor substrate adherence phenotypes [41]. The specific interactions that occur between cells and the surrounding environment have been shown to dictate the resistant nature of biofilms in response to antifungal treatments. Biofilm antifungal resistance depends on cell density, altered gene expression, matrix properties, persister cells and stress response mechanisms (reviewed by Mathé *et al.*, [69]). The ECM present in a mature biofilm provides an antifungal sequester effect that prevents antifungals from reaching their targets. For example, *FKSI* has been implicated in synthesis and deposition of β -1,3 glucans in the matrix, and these glucans sequester triazoles [70]. Consistent with this, *C. albicans FKSI* mutants produce antifungal susceptible biofilms [71]. Biofilms also contribute to antifungal resistance via persister cells. Persister cells are phenotypic variants of wild type cells, which are highly multidrug resistant and can thrive even after death of the general cell population in a biofilm that occurs after antifungal treatment [72]. *C. albicans* biofilms also serve as a source for peripheral yeast cells that may seed the bloodstream to colonize other sites in the host [42]. The ability of colonizing cells to adhere to host tissues or implant devices is the limiting factor for biofilm formation. Fungal cells unable to adhere are generally avirulent [73]. In addition to this, cells that are not able to form mature biofilms have impaired virulence [74]. This is because aside from antifungal resistance, the mature biofilm structure provides the pathogen with protection from the environment, resistance to mechanical stress and metabolic cooperation and community based regulation of gene expression that can be advantageous for host survival. Although *in vivo* biofilm studies are complicated by the presence of host cells and other interfering microorganisms, experiments in most part suggest that *in vitro* biofilm characteristics are applicable to those found *in vivo*. For example, the yeast cell, hyphae and ECM of *C. albicans* biofilm from denture stomatitis in humans are also found in animal catheter models [75]. However, it should be kept in mind that examples have been reported of differences between *in vitro* and *in vivo* biofilm phenotypes of *C. albicans* mutants [76, 77]. Therefore, while we are able to extrapolate our observations *in vitro* to *in vivo* conditions and deduce possible interplay between transcriptional programs, the reservation is that validation studies *in vivo* remain a necessary step for future studies.

1.1.3. Cellular morphogenesis: cell surface adhesion molecules are downstream targets of yeast to hyphal signalling pathways and are essential for biofilm formation

1.1.3.1 The yeast cell wall:

The fungal cell wall is the first structure that comes into contact with the host cells, carrying antigenic determinants. The factors present on the fungal cell surface are very important in the context of disease as they dictate pathogen adherence to host tissues or synthetic substrates, establish cell-cell communication with the host, including host immune cells, and also are responsible for interactions with other microbial cells, such as for example bacterial species in polymicrobial biofilms [66, 78, 79]. Figure 1.2 shows the structure of fungal cell wall. The communication between fungi and their environment and other cells that is mediated by the cell wall is dependent on what is known as the 'glycan code', and which involves the modifications in the chemical composition and linkages of cell wall polysaccharides [80].

The structure of the fungal cell wall is highly organized containing two distinct and functional layers. Inside, beyond the fibrillar protein coat, the cell wall contains polysaccharides (1,3 and 1,6 beta glucans and chitin) that have a role in cell wall strength and protection from turgor pressure [81, 82]. A recent study comparing the glucans levels from yeast and hyphal cells, identified the 2,3 linkage which was found to be immunologically relevant [83]. The external coat is composed of glycosyl-phosphatidylinositol (GPI)-modified glycoproteins covalently linked to the internal polysaccharide layer (Figure 1.2). These and other non-GPI anchored proteins extend outwards from cell surface for interactions with other cells and the host environment (reviewed in [82, 84, 85]) Aside from preventing the internal cell wall polysaccharides from being recognised by the immune system, these proteins also play several other roles in pathogenesis, such as binding to host and microbial cells, detoxification of oxygen radicals in the extracellular environment, and acquisition of essential nutrients, such as iron for which the Als3 adhesin is a receptor [82, 86-88]. It is clear therefore that the cell wall proteome plays a central role in the communications of fungi with their surroundings and in survival – therefore the genes encoding the proteins in the cell wall

are under tight regulatory control to respond appropriately to the external pressures [88]. For example the aforementioned adhesion molecules in *C. albicans* cell wall contain large and complex promoter regions, containing several regulatory sites that enable combinatorial regulation by environmentally-controlled signalling pathways [89].

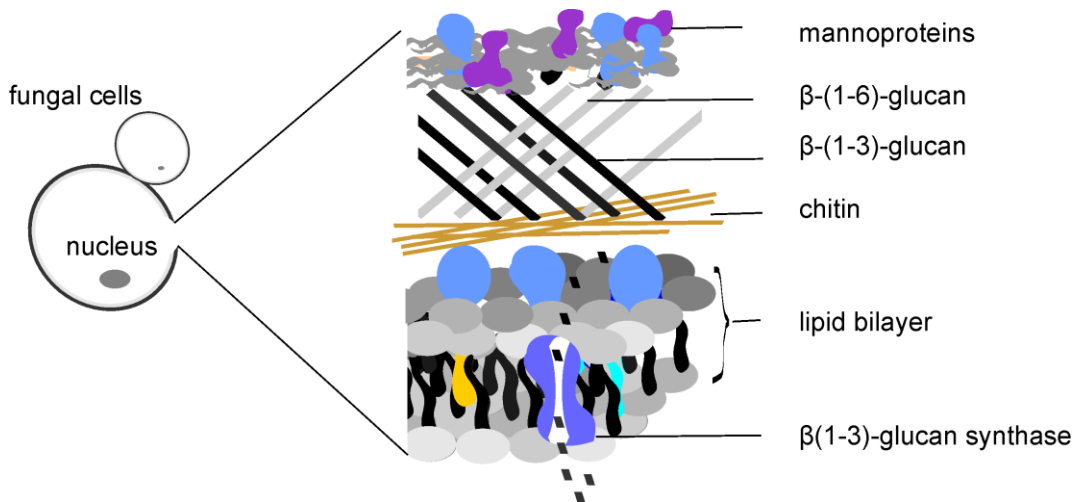


Figure 1.2. Schematic diagram of the *C. albicans* cell wall and plasma membrane structure. The yeast cell wall is usually 100-200 nm thick, and is responsible for 20 to 30% of the cell dry mass. The cell wall is composed of carbohydrate molecules (β -glucans, chitin, and mannan) and glycosylated proteins and glycosphingolipids. Glucans (β -1,6 and 1-3 linked) provide the strength of the cell wall by forming a network (80-90% β -1, 3 chains with some β -1,6 branches). Chitin is a polymer of N-acetylglucosamine, representing only 1-2% of the cell wall [90]. Chitin contributes to the mechanical strength, and also to the elasticity of the cell wall structure. The cell wall proteins are mannosylated, with α -1-6-linked mannan as the inner core and α -1,2 and α -1,3 linkages in the side chains [91]. The outer layer of cell wall proteins has a protective role, both by preventing degrading enzymes, such as glucanases from attacking the inner glucan layers and thus causing cell lysis, as well as prevention host immune recognition in the case of fungal pathogens. The cell wall proteins further have important functions in for cell-cell recognition, and also in adherence to substrates as a prerequisite for biofilm formation. The cell wall proteome consists of two major classes of cell surface glycoproteins-glycosylphosphatidylinositol (GPI) anchored proteins and Pir proteins[82]. The plasma membrane sits underneath the cell wall and is composed of the yeast phospholipids and sphingolipids, and the specific sterol ergosterol, in addition to several membrane proteins, including cell wall biosynthetic enzymes such as glucan synthase [92, 93]. It also contains permeases, efflux pumps and other proteins that mediate intracellular cell signaling in response to external stimuli [94].

The transcriptional networks in *C. albicans* that regulate the remodelling of the cell wall proteome between the yeast and hyphal forms are being studied in detail. In *S. cerevisiae*, the *FLO* gene family mediates adhesion, and of the best studied adhesins in laboratory strains is *FLO11* [95-97]. The expression of *FLO11* is regulated by the pathways that regulate pseudohyphal growth and cell surface adherence and invasion [47]. The adhesin functionally similar to Flo11 is Als1 in *C. albicans*. Als1 facilitates cell to cell adherence and binding to host endothelial cells [98]. However, though the adhesins perform similar cellular functions and share common structure, the *FLO* and *ALS* genes are unrelated in regards to their evolution (i.e. they are not derived from a common ancestral gene) [98]. Another key adhesin is the hyphal specific adhesion Als3. Als3 is interesting, because it performs various functions that are important for pathogenesis. Als3 mediates biofilm formation [99, 100]. It functions as a fungal invasin that mimics host cell cadherins for *C. albicans* endocytosis [101], and it also plays a role in iron assimilation, with iron being a critical nutrient which is very scarce in host niches [99]. Als3 is a promising target for therapeutic antibody and vaccine development against *C. albicans* [99]. Expression of the hyphal wall protein gene, *HWPI*, is also hyphal specific unlike the Als1 adhesin, which is expressed in both yeast and hyphal cells [102, 103]. *ALS1* is also required for both filamentation and virulence in the mouse model of systemic candidiasis [98]. *HWPI* assists fungal attachment to epithelial cells and is also required for systemic candidiasis [39]. It is interesting that it has been found that homologous transcription factors control the expression of cell wall adhesion molecules in distantly related fungal species, although the actual adhesin genes are often not related in an evolutionary sense. For example, the *S. cerevisiae* *FLO* genes and the *C. albicans* *ALS* genes are positively regulated by Efg1/Phd1, Cph1/Ste12 and Tec1 and Flo8, where as Sfl1 and Tup1 for example are negative regulators of adhesion in both yeasts [97, 98, 104].

1.1.3.1. Yeast morphogenesis and signalling pathways

The regulation of cell wall biogenesis is conserved between *C. albicans* and model yeasts. This regulation occurs via multiple signalling pathways (reviewed in 22).

The cell wall integrity pathway (CWI) is the key pathway that is known to direct cell wall biogenesis in response to various challenges. These challenges include cellular replication or cell division depending on availability of nutrients. The signalling pathway that regulates cell division is the Regulation of Ace2 and Morphogenesis (RAM) network, which is well characterised in model yeasts.

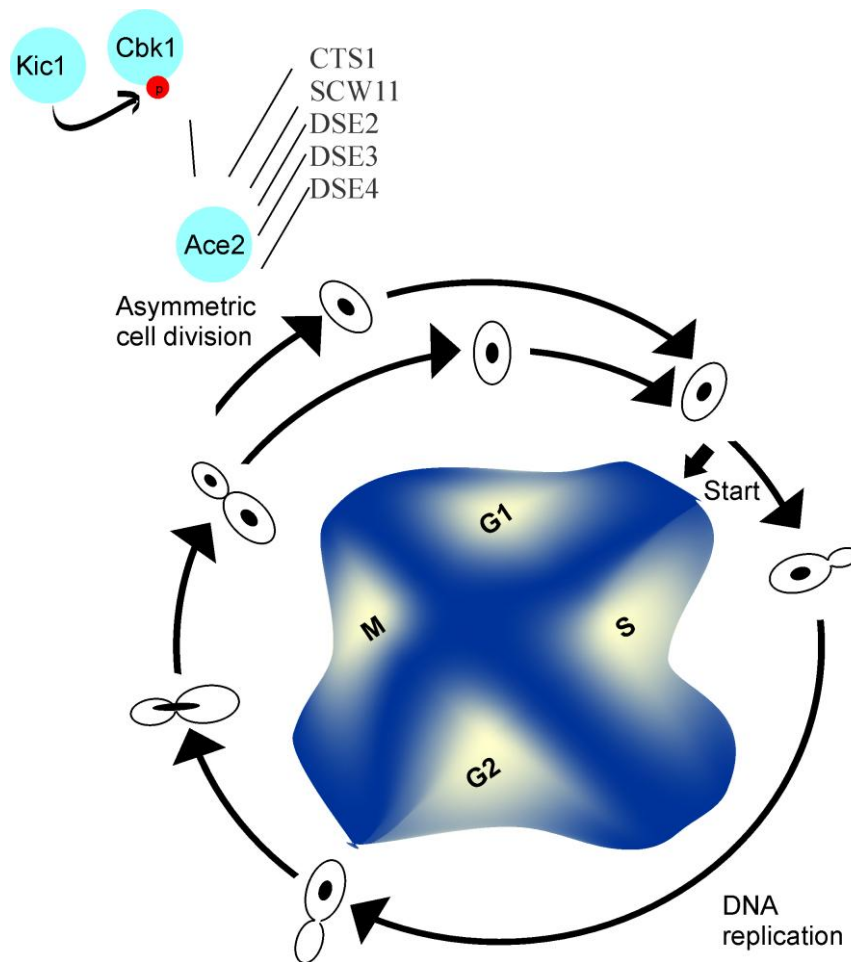


Figure 1.3. Schematic diagram depicting stages of cell division and the stage at which Ace2 dependent genes are expressed. The RAM signalling pathway is activated as mother and daughter cells form primary and secondary septa. Among downstream factor in the signalling pathway is the the Ndr family protein kinase Cbk1 and its associated proteins. These are subsequently phosphorylated by Kic1 which then activates the Ace2 transcription factor at the M/G1 transition. This leads to the expression of septum degradation factors. The cell cycle sketch information was obtained from [105] and cell cycle information is reviewed and discussed by [106-108].

The RAM network is conserved in higher organisms and has also been characterised in *C. albicans* [109]. Aside from maintenance of cell wall integrity, the RAM network controls cytokinesis (mother and daughter cell separation after cell division), daughter specific gene transcription, cell cycle progression, polarized growth, and stress signalling [107, 110-112]. For example to regulate the process of cell separation via RAM signalling, cell wall proteins activate intracellular signalling, which then in turn leads to the activation of transcription factors for the expression of enzymes required for cell wall remodelling [107]. As mother and daughter cells complete synthesis of the primary and secondary septa, the RAM network is activated. A major target of the RAM network is the transcription factor Ace2. Ace2 activity is controlled by temporally restricting its expression to the G2 phase of the cell cycle (Figure 1.3). Ace2 regulates the expression of genes encoding important septum destruction proteins such as the chitinase Cht3 and the glucanases Eng1 and Scw11. The *ACE2* gene is not essential in fungal species studied to date [113]. However, the phenotypes displayed by *ACE2* deletion mutants indicate severe cell separation defects that lead to the formation of cell chains that resemble pseudohyphae [114]. In other words, daughter cells produced during cell division of *ace2* mutants remain attached to mother cells, because of lack of Cht3 activity to resolve the chitin rich septa. This key function of *ACE2* in cytokinesis is conserved between model yeast and *C. albicans* [115]. Also, deletion of *ACE2* in the laboratory filamentation competent *S. cerevisiae* strain, Sigma 1278b, generates mutants that grow rough, raised colonies on solid agar and produce high levels of pseudohyphae relative to wild type strains [116], similar to the observations found in *C. albicans ace2* mutant cells [109].

Signalling pathways also dictate cell wall biogenesis under yeast and hyphal inducing conditions in *C. albicans* leading to the expression of adhesins and establishment of mature biofilms. Figure 1.1B shows the cyclic adenosine monophosphate (cAMP)–protein kinase A (PKA) pathway and other filamentation pathways. These nutrient-sensing pathways are conserved between *C. albicans* and *S. cerevisiae*, and lead to expression of pathogenesis related cell surface proteins [39]. Notice that the transcription factors that are required for the expression of cell wall remodelling program are also critical in facilitating the hyphal to yeast transition that is required for *C. albicans* survival within the human host [117].

Also targeted by these signalling pathways are transcription factors that are essential for biofilm formation. For example, signal transduction induced by *C. albicans* yeasts in contact with serum leads to activation of the cAMP pathway (Figure 1.1B). The downstream effector of this pathway is the transcription factor Bcr1. Bcr1 controls the expression of key cell wall adhesins, *ALS1*, *ALS3* and *HWPI* [77], and its inactivation leads to defects in biofilm formation *in vivo* and *in vitro* [118]. Consistent with a key function in biofilm growth, deletion mutants lacking these adhesins form biofilms that are unable to colonize surfaces and thus are unable to establish mature biofilms [119]. *BCR1* expression is regulated by another transcription factor Tec1, which is also part of the cAMP morphogenesis pathway [119]. Other biofilm related transcription factors include *ACE2*, *GCN4*, and *TYE7* as deletion mutants show defects at different stages of biofilm formation [39, 117]. An interesting feature of the regulatory networks that control biofilm development is that the transcription regulators regulate each other's expression, as mentioned above for Tec1 and Bcr1. Aside from Bcr1, the transcription factors Efg1, Tec1, Ndt80, Rob1 and Brg1 are known as the six master transcription factors that regulate *C. albicans* biofilm development [120]. Tec1 also directly regulates *EFG1* expression, which directly regulates additional target genes and Ndt80 [120]. This characteristic of *C. albicans* gene regulation wherein morphologically relevant transcription factors co-regulates each other suggests complex gene expression programs that allow for dynamic and simultaneous cell surface remodelling, as well as cell shape reconstruction. Furthermore, transcription regulatory networks that dictate the yeast to hyphal switch, cell wall morphogenesis and biofilm

formation are interconnected [39]. Since multiple transcription factors have similarities in their downstream targets, understanding the individual transcriptional networks and their specific targets may provide insights on how fungal pathogens like *C. albicans* utilize these networks to express cell surface molecules essential for morphogenesis and therefore pathogenesis.

Transcriptional co-regulators in C. albicans pathogenesis

As described above, a multitude of transcriptional activators and repressors has been characterised that influence morphogenesis, cell wall integrity and biofilm formation in *C. albicans*. The same is not true if one considers large multi-subunit transcriptional co-regulators such as SAGA and Mediator. Gene regulators coordinate transcription initiation with chromatin modification. Co-regulators are central transcriptional regulators in all eukaryotes, well conserved from yeast to man, and have been extensively studied in model yeast to elucidate their functions in fundamental mechanisms of gene transcription [121, 122]. A recent study by Xiao-Fen Chan *et al.* showed the Mediator assists the assembly of pre-initiation factors that are important for RNA polymerase II-dependent transcription, together with chromatin-remodelling complexes into the so-called pre-initiation complex (PIC), while SAGA acts after PIC assembly to assist transcription on the chromatin template [123]. Here, I will summarise the main features of Mediator, which is the topic of my PhD work, with the focus being mainly on the cellular roles of this complex in model yeasts *S. cerevisiae* and *S. pombe*, particularly in regards to pathways that impact on virulence of pathogenic fungal species, such as cell wall biogenesis and cellular morphogenesis [124-128]. My studies of Mediator did not address fundamental mechanisms of transcription, and so this aspect of Mediator function will only be briefly touched upon in this introduction.

The Mediator is a large protein complex that binds directly to RNA polymerase II and is essential for mRNA transcription. Originally it was designated as a co-activator (co-regulator), however new evidence re-categorised the complex as a general transcription factor [123]. The complex was discovered in *S. cerevisiae* by genetic and biochemical means, and was subsequently found to be conserved in higher eukaryotes [129, 130]. The components of the Mediator complex were first identified in RNA pol II related functional phenotypic screens and the complex was subsequently

biochemically shown to consist of four functional modules: the Head, Middle, Tail and Kinase modules. Table 1.1 shows the Mediator modules and their respective subunits in *S. cerevisiae* and *C. albicans*. Although these modules are conserved, several subunits show high primary sequence divergence when compared between fungi and mammals [131-134], suggesting that perhaps the *C. albicans* Mediator might be considered as an antifungal drug target. The number of subunits may vary between species. For instance, there are more subunits in mammals in addition to the core set found in fungi, and *C. albicans* has 15 paralogues of the *MED2* gene, which are designated as TLO genes and which were biochemically shown to co-purify with the *C. albicans* Mediator complex [135, 136]. Early studies of Mediator suggested a simplified model of two functional structures that influence transcription, (1) the core complex (Head, Middle and Tail) required for positive transcription and the Kinase domain that mediates gene repression [137]. However, further studies revealed that the functions of the various subunits are more dynamic [138]. Not only do the different subunits have overlapping and different functions in transcription initiation, but the Mediator is also required for post initiation steps allowing for flexibility in gene expression [137-140]. For example, the Srb9/Med13 subunit of the Kinase module has been shown to act as a transcription repressor of the cell wall adhesin genes and more generally genes that are repressed in rich nutrient conditions [141]. However, deletion of the Head module subunit, Med1, also show similar phenotypes to Kinase mutants and this was suggested to occur as a result of Med1 involvement in tethering the Core Mediator to the Kinase module [142]. Moreover, Kinase domain subunits have been shown to have activating roles in transcription, in addition to their more recognised roles in repression [143].

Table 1.1. The Yeast Mediator of Transcription

	Mediator submodule	<i>Candida albicans</i>	<i>Saccharomyces cerevisiae</i> homologue
Core Mediator	Head	MED6	MED6
		MED8	MED8
		MED11	MED11
		MED17	SRB4
		MED18	SRB5
		MED19	ROX3
		MED20	SRB2
		MED22	SRB6
	Middle	MED1	MED1
		MED4	MED4
		MED7	MED7
		MED9	CSE2/MED9
		MED21	SRB7
		MED10	NUT2/MED10
		MED31	SOH1
	Tail	MED2/CTA216/TLO1	MED2
		MED2/CTA215/TLO2CTA26	
		MED2/CTA2/TLO1	
		MED2/CTA224/TLO11	
		MED2/CTA213/TLO12	
		MED2/CTA227/TLO16	
		MED2/CTA222/TLO5	
		MED2/CTA212/TLO9	
		MED2/CTA211/TLO10	
		MED2/CTA218/ TLO34	
		MED3	PGD1/HRS1/MED3
MED5	NUT1		
MED14	RGR1		
MED15	GAL11		
MED16	SIN4		
Kinase module	Kinase	MED12	SRB8
		MED13/SRB9	SSN2/SRB9/MED13
		CycC	SRB11/SSN8/UME3/NUT9 /GIG3/RYE2
		CDK8	SRB10/SSN3/UME5

Table 1.2. Phenotypic impairments observed in *S. cerevisiae* null mutants deficient in non-essential MED subunits

Mediator subunit	Null phenotypes (classical genetics, and large scale survey in nutrient rich media)¹
Med1	homozygous diploid, competitive growth, decreased endocytosis
Med2	Abnormal lipid particle morphology, decreased osmotic stress resistance
Med3	vegetative growth: absent, competitive fitness: decreased
Med4	Essential
Med5	Decreased resistance to fluconazole, increased respiratory growth, decreased resistance to caffeine
Med6	Essential
Med7	Essential
Med8	Essential
Med9	Increased cold/heat sensitivity, decreased resistance to fluconazole
Med10	Essential
Med11	Essential
Med12	Decreased vegetative growth rate, decreased resistance to Fluconazole Decreased competitive fitness
Med13/Srb9	Increased cell flocculation, decreased stress resistance, decreased vegetative growth, survival rate in stationary phase decreased
Med14	Essential
Med15	Decreased Low pH resistance, decreased oxidative stress resistance
Med16	Decreased filamentous growth, invasive growth absent Abnormal cell shape, increased flocculation
Med17	Essential
Med18	Decreased resistance to formamide, increased biofilm formation Abnormal bud morphology
Med19	Decreased vegetative growth rate, increased filamentous growth, heat sensitive, decreased oxidative stress
Med20	Decreased biofilm formation, decreased resistance to ethanol, Decreased respiratory growth
Med21	Essential
Med22	Essential
CDK8	Increased flocculation, increased chitin deposition, decreased vegetative growth
CycC	Decreased filamentous growth, invasive growth absent
Med31	Abnormal vegetative growth, decreased vegetative growth

¹ Phenotype information was obtained from the *Saccharomyces* genome database

In addition to transcription activation and repression the Mediator also appear to act as an ‘*integrative hub*’ where many signalling pathways required in cellular homeostasis, cell growth and cellular differentiation act via Mediator interactions that may occur with various transcription activators and repressors [144]. In model yeasts, the Kinase module is a target of the Ras/PKA repression of components required for yeast entry into stationary phase of growth [145]. In addition to this, comparative characterization of Mediator components in *S. cerevisiae* and *Schizosaccharomyces pombe* indicated that Mediator is required for yeast morphogenesis [127, 146]. Although these two yeasts are divergent, these studies showed conserved roles of Mediator in the regulation of cell wall and cell structure remodelling as well as essential roles in stress response. For example, the *MED31* subunit is the best conserved subunit of the Mediator across eukaryotes [126]. In *S. pombe*, genome-wide gene profiles of *med31Δ/Δ* deletion mutants showed that this subunit is required for transcriptional co-regulation of a large set of genes in conjunction with other transcription factors including Sep1 and Ace2 to control cytokinesis. Table 1.2 shows currently known phenotypic defects that result from the deletion of genes encoding Mediator subunits in the *S. cerevisiae* as described in the Saccharomyces Genome Database (updated list March, 2014) [147]. Interestingly, these defects include defects in biofilm formation, antifungal susceptibility, various growth impairments and cell flocculation/aggregation due to increased cell to cell adhesion. Aside from studies in model yeasts, studies on roles of the Mediator complex in fungal pathogens are beginning to emerge. For example, in the human pathogen *C. neoformans*, vegetative growth is carried out in yeast form, while filamentation is mainly associated with mating. The CycC/Ssn8 subunit of the Kinase domain of Mediator has been shown to be involved in the suppression of physiological process including invasive growth, capsule formation, melanin, maintenance of cell wall integrity and virulence [148]. In addition, in *Fusarium graminearum*, a plant fungal pathogen that causes wheat destruction, the CycC/Ssn8 subunit regulates vegetative growth, sexual development, conidation and pathogenesis [149]. Furthermore, the Med15 subunit of *Candida glabrata* appears to have conserved roles as in *S. cerevisiae* in the regulation of the drug resistance virulence

factors including drug efflux pumps and MDR (multidrug resistance) via the transcription factor Pdr1 [150].

The evidence described above led me to predict that Mediator would be important for several pathogenesis related functions in *C. albicans*. In my thesis, I show this to be the case, both in regards to morphogenesis and cell wall integrity, and for interactions with host innate immunity and immune evasion through macrophage killing and escape.

1.2. Thesis Objectives

The global aim of my project was to characterize the cellular role of the Mediator complex in the human fungal pathogen *C. albicans*. Since the yeast Mediator is huge, I focused on characterizing subunits in the Middle, Head and Kinase modules with the specific focus on identifying possible roles of the Mediator in cell morphogenesis in *C. albicans*, as morphogenesis is a key virulence factor of the pathogen. My goal was to use molecular genetics coupled with transcriptomics and cell biology to understand the functions of Mediator in *C. albicans* morphogenesis, and identify the downstream gene targets that control *C. albicans* pathogenesis-related functions. A further goal was to use the *C. albicans* Mediator mutants to understand how *C. albicans* evade the innate immune response, thus shedding light on a process that is key for virulence.

In the following chapters and in my published work, I present the findings that *C. albicans* Mediator subunits have conserved functions with model yeasts in cytokinesis and cell stress responses. Furthermore, I show that *C. albicans* Mediator has fundamental role in the regulation of virulence factors described above, including cell wall remodelling, cell division via Ace2 transcription factor, and the regulation of components and targets of the yeast to hyphae signalling pathways and biofilm formation (Chapter 3). In Chapter 4, I developed a novel assay that shows for the first time *C. albicans* macrophage killing profiles over an extended period of time, and through this assay I demonstrate that the Mediator controls the fungal factors that are required for appropriate host immune cell responses during *C. albicans* invasion. This work also allowed me to make a paradigm-shifting discovery that showed how *C. albicans* hyphal cells do not simply pierce through macrophages for escape, but rather they use specific cell surface properties to activate a lytic host cell death pathway (pyroptosis) which is hijacked by the pathogen for evasion.

Chapter 2

2.1. General Materials and Methods

2.1.1. Yeast strains

The *C. albicans* strains used in this study were derivatives of the BWP17 background strain [88], while the *med31* deletion in *S. cerevisiae* strains was derived from the filamentous Sigma 1278b strain using the KANMX4 cassette. The *C. albicans* mutants were conducted using standard PCR and homologous recombination methods. The two alleles of the *MED31*, *SRB9* or *MED20* genes were replaced with the selective markers *ARG4* and *URA3*. To create complemented the strains, the respective genes, including the upstream and downstream regulatory regions, were reintroduced into the *HIS1* locus of each mutant strain using the integrative plasmid pDDB78. To be able to compare the mutants to wild type and complemented strains, the empty pDDB78 vector was also integrated into the mutant strains. Table 2.1 and Table 2.2 shows the mutant strains and complemented strains, as well as stock numbers in our lab². The *C. albicans* *ace2Δ/Δ*, *bcr1* and the *srb10* mutants were a gift from Aaron Mitchell³. The *srb10* mutant was part of a Kinase mutant collection derived by use of the UAU1 marker deletion strategy [151], and is described in [152]. The *bcr1* mutant was constructed with the same strategy as part of the Transcription Factor Library and is described in [119].

² Ana Traven, Department of Biochemistry, Monash University, Clayton, Victoria, Australia

³ Department of Biological Sciences, Carnegie Mellon University, Pittsburgh, PA 15213, USA

The *S. cerevisiae flo11*Δ mutant and the parental Sigma 1278b strain [67] were a gift from Todd Reynolds⁴.

⁴ University of Tennessee, Department of Microbiology, F321 Walters Life Sciences Building, Knoxville, TN 37996

Table 2.1. *S. cerevisiae* strains used in this thesis

Traven Database code	genotype	source
YAT6	Sigma 1278-b MAT alpha <i>URA3-52 his3::hisG leu2::hisG</i>	Todd Reynolds ³
YAT327	BY4741 <i>srb9Δ::KAN</i>	SGDP ⁵
YAT328	BY4741 <i>med31Δ::KAN</i>	SGDP
YAT480	Sigma 1278-b <i>soh1Δ :KAN</i>	This study
YAT481	Sigma 1278-b <i>soh1Δ :KAN</i>	This study
YAT482	Sigma 1278-b <i>soh1Δ :KAN</i>	This study
YAT483	Sigma 1278-b <i>soh1Δ :KAN</i>	This study
YAT484	Sigma 1278-b <i>soh1Δ :KAN</i>	This study
YAT485	Sigma 1278-b <i>soh1Δ :KAN</i>	This study
YAT495	Sigma 1278-b <i>soh1Δ :KAN+</i> p416 MET25: <i>SOH1</i>	This study

⁵ Saccharomyces Genome Deletion Project

Table 2.2. *C. albicans* strains used in this thesis

Traven database code	Genotype	source
YCAT439	BWP17	[88], [153]
YCAT14	wild type/ BWP17 (<i>ARG4+</i> , <i>URA3+</i> , <i>HIS1-</i>)	[88], [153]
YCAT19	wild type/ BWP17 (<i>ARG4+</i> , <i>URA3+</i> , <i>HIS1+</i>)	[88], [153]
YCAT120	med20Δ:: <i>ARG4</i> /med20Δ:: <i>URA3</i> pDDB78- <i>HIS1</i>	This study
YCAT121	med20Δ:: <i>ARG4</i> /med20Δ:: <i>URA3</i> pDDB78- <i>HIS1</i>	This study
YCAT122	med20Δ:: <i>ARG4</i> /med20Δ:: <i>URA3</i> pDDB78- <i>HIS1</i>	This study
YCAT123	med20Δ:: <i>ARG4</i> /med20Δ:: <i>URA3</i> pDDB78- <i>HIS1</i>	This study
YCAT124	med20Δ:: <i>ARG4</i> /med20Δ:: <i>URA3</i> pDDB78- <i>HIS1-MED20</i>	This study
YCAT125	med20Δ:: <i>ARG4</i> /med20Δ:: <i>URA3</i> pDDB78- <i>HIS1-MED20</i>	This study
YCAT126	med20Δ:: <i>ARG4</i> /med20Δ:: <i>URA3</i> pDDB78- <i>HIS1-MED20</i>	This study
YCAT127	med20Δ:: <i>ARG4</i> /med20Δ:: <i>URA3</i> pDDB78- <i>HIS1-MED20</i>	This study
YCAT114	med31Δ:: <i>ARG4</i> /med31Δ:: <i>URA3</i> pDDB78- <i>HIS1-MED31</i>	This study
YCAT116	med31Δ:: <i>ARG4</i> /med31Δ:: <i>URA3</i> pDDB78- <i>HIS1-MED31</i>	This study
YCAT130	med31Δ:: <i>ARG4</i> /med31Δ:: <i>URA3</i> pDDB78- <i>HIS1</i>	This study
YCAT430	med31Δ:: <i>ARG4</i> /med31Δ:: <i>URA3</i> pDDB78- <i>HIS1</i>	This study
YCAT293	med13Δ:: <i>ARG4</i> /med13Δ:: <i>URA3</i> pDDB78- <i>HIS1</i>	This study
YCAT295	med13Δ:: <i>ARG4</i> /med13Δ:: <i>URA3</i> pDDB78- <i>HIS1</i>	This study
YCAT298	med13Δ:: <i>ARG4</i> /med13Δ:: <i>URA3</i> pDDB78- <i>HIS1</i>	This study
YCAT301	med13Δ:: <i>ARG4</i> /med13Δ:: <i>URA3</i> pDDB78- <i>HIS1-MED13</i>	This study
YCAT303	med13Δ:: <i>ARG4</i> /med13Δ:: <i>URA3</i> pDDB78- <i>HIS1-MED13</i>	This study
YCAT305	med13Δ:: <i>ARG4</i> /med13Δ:: <i>URA3</i> pDDB78- <i>HIS1-MED13</i>	This study
YCAT230	bcr1:Tn7-UAU1/bcr1:Tn7: <i>URA3</i>	[151]
YCAT308	srb10:Tn7-UAU1/srb10:Tn7: <i>URA3</i>	[151]

2.2. Chapter 3 Materials and Methods⁶

2.2.1. Fungal growth conditions

The standard growth media used for the thesis are presented in Table 2.3. The standard growth conditions were in YPD or synthetic media at 30°C. *S. cerevisiae* cells were cultured at 200 rpm, while *C. albicans* cells were cultured at 250 rpm. Filamentation induction in *C. albicans* was conducted at 37°C, using overnight cultured cells diluted to $OD^{600} = 0.05$ in all the filamentation media stated in Table 2.3, except that cells were cultured with shaking (~ 150 rpm) as described by [154]. Deviations from these standard conditions are as indicated in Figure legends. Sensitivity to various drugs and chemicals were conducted using standard media (YPD). Ten fold serial dilutions of cultures from indicated strains were dropped on control plates or on plates containing indicated compounds. Cells were incubated at 30°C unless otherwise indicated, for 3-4 days and photographed.

2.2.2. Cell staining

Images showing calcofluor white-stained chitin in the mother and daughter cell junctions were generated by incubating cells in calcofluor white (1 μ M) for 8 minutes in the dark, followed by three washes with phosphate buffered saline (PBS). For the cell morphology images shown in Figure 3.1, cells were grown under standard growth conditions (YPD at 30°C) and counted. Data was calculated from at least 200 cells per sample that were counted and the experiment was repeated three times with at least 3 independent cultures. The average and standard error are shown in the Figures.

All imaging, morphology analysis and cell staining was conducted using the Olympus IX81 microscope with the Olympus Cell^M software, using the 100x objective with DIC or the DAPI filter for calcofluor white-stained cells. For filamentation in Figure 3.7A, the images represent 10x magnification of the edges of colonies grown of filamentation inducing solid media and incubated for 3 days at 37°C.

⁶ Presented here are the methods for experiments I was involved in executing. All other methods are included in my published work including the work of collaborators (Uwamahoro *et al.*, 2012)

Table 2.3. Key growth and phenotyping media used⁷

Growth media	Content	use
YPD	2% glucose, 2% peptone, 1% yeast extract	<i>S. cerevisiae</i> standard growth
YPD G418	2% glucose, 2% peptone, 1% yeast extract, 200 µg/ml G418 plates	<i>S. cerevisiae sohl</i> mutant selection
Low agar YPD	2% glucose, 2% peptone, 1% yeast extract, 0.3% agar	<i>S. cerevisiae</i> biofilm mats
CSM	As described in [155] with 2% glucose	<i>C. albicans</i> or <i>S. cerevisiae</i> minimal and selection media
YPD	2% glucose, 2% peptone, 1% yeast extract, 80 µg/ml uridine	<i>C. albicans</i> standard growth
Pre-warmed YPD+ 10% serum	2% glucose, 2% peptone, 1% yeast extract, 80 µg/ml Uridine, 10% Fetal bovine serum (FBS)	<i>C. albicans</i> filamentation
Spider media	1% nutrient broth, 1% D-mannitol, 2 g K ₂ HPO ₄ , 80 µg/ml Uridine	<i>C. albicans</i> filamentation
M199	M199 liquid media, filtered, pH7.4, Invitrogen	<i>C. albicans</i> filamentation
Lee's	As described in [155]	<i>C. albicans</i> filamentation
N-acetylglucosamine (NAG)	9 g NaCl, 6.7 g yeast nitrogen base and 0.56 g N-acetylglucosamine per liter	<i>C. albicans</i> filamentation

⁷ When preparing solid media 2% agar was added unless stated otherwise. Uridine was added when working with derivatives of BWP17 background strain.

2.2.3. RNA extraction, quantitative PCR, and microarray analysis

All RNA extractions were conducted using the hot-phenol method [156], on cells grown in conditions indicated in the Figures. Yeast cells were generally grown under standard conditions (Table 2.3) from freshly streaked overnight cultures and diluted to $OD^{600} = 0.1$ and incubated at 30°C to a final $OD^{600} = 1$. In the case of gene expression under filamentous conditions, Spider media was used as described in [77]. In all other cases the type of growth medium is stated in the Figures.

For quantitative PCR (qPCR) analysis, 1 µg of total RNA was treated with DNase (Promega A), prior to making cDNA which was conducted using SuperScript® III Reverse transcriptase kit (Invitrogen) according to the manufacturer's instructions (Invitrogen, Carlsbad, CA, USA). qPCR reactions were conducted using Fast-Start Sybr Green Master mix (Roche) on an Eppendorf Realplex master cycler and analysed by absolute quantification with the following PCR conditions; step1) 95°C 10 min, step 2:95°C 20 seconds, step 3: 60°C 20 seconds, step 4: 74°C 20 seconds, (40 cycles of steps 2-4), step 5: 95°C 15 seconds, step 6: 60°C 15 seconds, step 7: 20 min Melting curve ramp, 8: 95°C 15 seconds, 9: 12°C pause. The sequences of all the primers used in this study are listed in Table 2.4. Gene expression levels of mRNAs were normalized to the levels of *ACT1* or *TDH3* encoding yeast GAPDH. To specifically amplify the *C. albicans* adhesins *ALS1* and *ALS3* against other *ALS* genes, the specific primers from Green *et al.* were used [157]. A threshold of greater than 1.5 fold change in transcript levels of a gene was considered significant.

For Figure 3.11A, the PCR products specific to the genes shown in the Figure were generated using cDNA as the template and analysed using 2% high-resolution agarose gel (Ambion® Agarose-HR™). PCR amplification was conducted for 23 amplification cycles and gels were pre-stained with SYBR safe, and imaged against a 100 bp ladder using an LAS 3000 imager and multiguage software (Fujifilm).

For Microarray analysis, 100 µg total RNA extractions, were treated with DNase and purified using RNAeasy kit (Quiagen). The microarray analysis was performed as described [38, 158], in collaboration with Dr. Andre Nantel⁸.

2.2.4. Analysis of microarray results and motif identification:

As described by Vandeputte *et al.* [159], Gene Ontology (GO) analyses were performed on significantly altered transcripts obtained by microarray to identify putative enriched biological functions, processes, or cell compartments (*Candida* Genome Database GO Term Finder; <http://www.Candidagenome.org/cgi-bin/GO/goTermFinder>) and to assign differentially regulated genes to specific biological processes (*Candida* Genome Database GO _Slim_Mapper; [_http://www.Candidagenome.org/cgi-bin/GO/goTermMapper](http://www.Candidagenome.org/cgi-bin/GO/goTermMapper)). Microarray data was published and can be found in [38]. The microarray data was deposited in GEO under accession number GSE31632.

The promoter motif of upstream sequences of morphologically relevant gene components of the cAMP signalling pathway and downstream targets required for biofilm formation, adhesin and cell wall genes set targets of Med31 was identified as described by [115], using the software MEME (<http://meme.sdsc.edu/meme/intro.html>). The intergenic region of 1,000 bp was extracted from upstream of the ATG codon for the following ORFs: orf19.3629,orf19.6420, orf19.6773, orf19.6958, orf19.6387, orf19.4752, orf19.4941,orf19.610, orf19.2331, orf19.4318, orf19.7247, orf19.5389, orf19.5338, orf19.1944, orf19.1187, orf19.5908, orf19.7150, orf19.2758, orf19.1665, orf19.7517, orf19.7586, orf19.7374, orf19.1401, orf19.3066, orf19.2972, orf19.2475, orf19.3803, orf19.220, orf19.5736, orf19.7414, orf19.3893, orf19.5741, and orf19.6321. A maximum number of four motifs with lengths of 6 to 8 bp that occurred in any number of repetitions were identified. The motif selected had the e-value of 5.9e-023. The yeast transcription factor motif database YeTFaSCo (The Yeast Transcription Factor Specificity Compendium), (<http://yetfasco.cabr.utoronto.ca/>) was then used to

⁸ Dr. Andre Nantel laboratory, Biotechnology Research Institute, National Research Council of Canada, Montreal, Quebec, Canada

identify the transcription factor in *S. cerevisiae* that binds to a motif similar to the identified sequence as described in [160].

Table 2.4. Primers used in this thesis

<i>Saccharomyces cerevisiae</i> qPCR primers			
Primer Name	Gene/ORF	Sequences 5' --> 3'	Reference
<i>ACT1</i> Forward	<i>ACT1/</i> YFL039C	CGTCTGGATTGGTGGTTCTA	This study
<i>ACT1</i> Reverse	<i>ACT1/</i> YFL039C	GATGGACCACTTTCGTCGTA	This study
<i>FLO1</i> Forward	<i>FLO1/</i> YAR050W	TGGCAGTCTTTACACTTCTGGCAC T	This study
<i>FLO1</i> Forward	<i>FLO1/</i> YAR050W	CCTGCTGGTAAGCACGCCTCT	This study
<i>FLO5</i> Forward	<i>FLO5/</i> YHR211W	TGGTAATCTTGGCCTTTCTGGCAC T	This study
<i>FLO5</i> Forward	<i>FLO5/</i> YHR211W	GCCTGCTGGTAAGCACGCCT	This study
<i>FLO9</i> Forward	<i>FLO9/</i> YAL063C	ATTCTGAGGTTGCTGCTTTGG	This study
<i>FLO9</i> Forward	<i>FLO9/</i> YAL063C	GAAGATTGAGCAGCGGTTTGC	This study
<i>FLO10</i> Forward	<i>FLO10/</i> YKR102W	TGCACCTACCGACATAAAGG	This study
<i>FLO10</i> Forward	<i>FLO10/</i> YKR102W	CCCAGGATACAGCATTTGAA	This study
<i>FLO11</i> Forward	<i>FLO11/</i> YIR019C	AGA CTT CAA TTG GCA CAT GG	This study
<i>FLO11</i> Reverse	<i>FLO11/</i> YIR019C	GAA CCC AAG AAA CGG AAG TC	This study
<i>Candida albicans</i> qPCR primers			
Primer Name	Gene/ORF	Sequences 5' --> 3'	Reference
<i>ACT1</i> Forward	<i>ACT1/</i> C1_13700W_A	CCCAGGTATTGCTGAACGTA	[158]
<i>ACT1</i> Reverse	<i>ACT1/</i> C1_13700W_A	GAACCACCAATCCAGACAGA	[158]
<i>ALS1</i> Forward	<i>ALS1/</i> C6_03700W_A	TTCTCATGAATCAGCATCCACAA	[157]
<i>ALS1</i> Reverse	<i>ALS1/</i> C6_03700W_A	CAGAATTTTCACCCATACTTGGTTTC	[157]
<i>ALS3</i> Forward	<i>ALS3/</i> CR_07070C_A	AATGGTCCTTATGAATCACCATCTACT	[157]
<i>ALS3</i> Reverse	<i>ALS3/</i> CR_07070C_A	GAATTTTCATCCATACTTGATTTCACA	[157]

<i>ALS1</i> -forward	<i>ALS1/</i> C6_03700W_A	ACCAATCCAGTTCCAACCTGTGGCA	This study
<i>ALS1</i> - reverse	<i>ALS1/</i> C6_03700W_A	TGGATGCTGATTCATGAGAACCGCT	This study
<i>ALS3</i> - forward	<i>ALS3/</i> CR_07070C_A	ACTTCCACAGCTGCTTCCACTTCT	This study
<i>ALS3</i> - reverse	<i>ALS3/</i> CR_07070C_A	TCCACGGAACCGGTTGTTGCT	This study
<i>HWP1</i> Forward	<i>HWP1/</i> C4_03570W_A	AATCCTCCTCAACCTGATCAGCCTG	This study
<i>HWP1</i> Reverse	<i>HWP1/</i> C4_03570W_A	AGCTGGAGTTGTTGGCTTTTCTGGA	This study
<i>EAP1</i> Forward	<i>EAP1/</i> C2_09530W_A	TGCCCCAGGTACTGAAACCACTC	This study
<i>EAP1</i> Reverse	<i>EAP1/</i> C2_09530W_A	AGTGCCTGGGATAACGGGTTGAG	This study
<i>PIR1</i> Forward	<i>PIR1/</i> C2_08870C_A	ACCAAACCGCCAAGGCCACT	This study
<i>PIR1</i> Reverse	<i>PIR1/</i> C2_08870C_A	ACCGTCACTGATTTGAGCCACTGG	This study
<i>CHT3</i> Forward	<i>CHT3/</i> CR_10110W_A	AGGTGGTGCTGCTGGATCTTATGG	This study
<i>CHT3</i> Reverse	<i>CHT3/</i> CR_10110W_A	TGAGCAAATTGTTTGGCAGTGGCA	This study
<i>TYE7</i> Forward	<i>TYE7/</i> C1_13140C_A	AGAACCAGGTACGAAGGCAGCT	This study
<i>TYE7</i> Reverse	<i>TYE7/</i> C1_13140C_A	TGCCGGCAATCTTGGCATTAAATGT	This study
<i>TDH3</i> Forward	<i>TDH3/</i> C3_06870W_A	TAAGAGTTGCTTTGGGCAGA	This study
<i>TDH3</i> Reverse	<i>TDH3/</i> C3_06870W_A	AATGACCAAGTCGTCACCAG	This study
18s rRNA-forward	RDN18 /CR_08770W_A	GGAT GAACAACAACCGATCCCTAGT	This study
18s rRNA-reverse	RDN18 /CR_08770W_A	TTACTGAAGACTAACTACTG	This study

***Candida albicans* complementation primers**

Gene	ORF	Description	Sequences 5' --> 3'	Reference
<i>MED31</i>	C4_05640C_A	<i>MED31</i> forward complementation primer	TTCACACAGGAAACAGCTATGACCATGATT ACGCCAAGCTAATTTAGCTTCAATTTCTTC	This study

<i>MED31</i>	C4_05640C_A	<i>MED31</i> reverse complementation primer	TCGACCATATGGGAGAGCTCCCAACGCGTT GGATGCATAGTCCTCTATTATCAACATAAT	This study
<i>MED13/SRB9</i>	C2_01470W_A	<i>MED13</i> forward complementation primer	TTCACACAGGAAACAGCTATGACCATGATT ACGCCAAGCTAGTACATCTCTTTGCAAGTG	This study
<i>MED13/SRB9</i>	C2_01470W_A	<i>MED13</i> reverse complementation primer	TCGACCATATGGGAGAGCTCCCAACGCGTT GGATGCATAGTGCAAAGATGGTTCCTTTT	This study
<i>MED20/SRB2</i>	C4_02840C_A	<i>MED20</i> forward complementation primer	TTCACACAGGAAACAGCTATGACCATGATT ACGCCAAGCTTTTAAATTCAAAAGTGTAGA	This study
<i>MED20/SRB2</i>	C4_02840C_A	<i>MED20</i> reverse complementation primer	TCGACCATATGGGAGAGCTCCCAACGCGTT GGATGCATAGAGGAAGACTATTCTAGAAAA	This study

***Candida albicans* deletion primers**

Gene	ORF	Description	Sequences 5' --> 3'	Reference
<i>MED31</i>	C4_05640C_A	<i>MED31</i> forward deletion primer	CAGAGAATATTTCCATGGCGAAAACAATTGAAA AAAAAAGCACACACAACAAAGTTTCACCTAA CCAACATCATTACTTTCAAACACTCACCATAACC CTTTCCCAGTCACGACGTT	This study
<i>MED31</i>	C4_05640C_A	<i>MED31</i> reverse deletion primer	ATGTGTTTCCAGCAGTTAAATTAGTTACCAATG CAGCTACTTTTATTCTTGTCATTATTAACACTCT ACTAGATCTTTTGTCTTCCTTCCTTTCATTTCTGT GGAATTGTGAGCGGATA	This study
<i>MED13/SRB9</i>	C2_01470W_A	<i>MED13</i> forward deletion primer	TTCAACTTCGAGGAATCTCATTAACTTCAGCTT TCTTCTGGCTACTACAATCTTCACTTACAACACTAG AATTCATACTAAAACATTCGATAGAAACATCT TTCCCAGTCACGACGTT	This study

<i>MED13/SRB9</i>	C2_01470W_A	<i>MED13</i> reverse deletion primer	TGTAGCATTGTTGAACAACGACTGGGAGGAAA AAAAAAAAATACAGAACTAAAAAAGTCGTGC GAAATGGCCATACTCATTAAACCTATGTACAGC TTGTGGAATTGTGAGCGGAT	This study
<i>MED20/SRB2</i>	C4_02840C_A	<i>MED20</i> forward deletion primer	GGTTTCTAGTTTAAGTAACAACATTGATGTTGA AAACAAGGGTGAATACTTCTTAACAGACCTCGC AACACTTTGTATATACTTTTCGAATCATTAGATT TTCCCAGTCACGACGTT	This study
<i>MED20/SRB2</i>	C4_02840C_A	<i>MED20</i> reverse deletion primer	TGTCTTCTCCTTTAATGATAATATCTATGTGGTC AACTTACAATCTTTATTTCTTATATAATTTATTTT CATTTTCTCAAATAATTACAGTTGTTGACGGTG GAATTGTGAGCGGATA	This study

2.2.5. Biofilm assays and agar invasion

For *S. cerevisiae* biofilms for Figure 3.9H, overnight cultures were grown in synthetic complete media supplemented with 2% glucose. The cells were then resuspended into 96 well polystyrene plates to an $OD^{600} = 0.1$ using synthetic 0.2% glucose media as described by [67]. Adherence was assayed at the time points indicated in the figure using crystal violet staining as described by [161]. For the biofilm mat growth, 1 μ l of culture at OD 0.5 was incubated at 25°C for 5 days and photographed as described by [95]. For the invasive growth assay in Figure 3.10 was as previously described by [162]. Briefly, strains were streaked on YPD plates (2% glucose, 2% agar) and grown at 30°C for 5 days and photographed. Non-invasive cells were washed of using tap water and photographed again. Under running tap water, the adherent cells were rubbed off using a gloved finger to remove all non-invasive cells and photographed. The *C. albicans* biofilm assay in Figures 3.8 and 3.9C were performed together with Dr. Yue Qu⁹ and the methods are described in [163].

⁹ Department of Biochemistry and Molecular Biology, Monash University, Clayton, Victoria, Australia

2.3. Chapter 4 Materials and Methods¹⁰

2.3.1. Standard growth conditions for *C. albicans* and macrophages

For all macrophage co-incubation studies, *C. albicans* cells were cultured under yeast morphology promoting conditions (YPD supplemented with uridine and grown at 30°C over night), followed by dilution as described below. Hyphal morphogenesis was induced using either Spider media, or general macrophage growth media (RPMI 1640 [164] pH 7.2-7.4, 10% heat-inactivated FBS, 100 U/ml penicillin and 100 µg/ml streptomycin (Gibco BRL, Grand Island, NY) at 37°C, 5% CO₂. Bone marrow derived macrophages (BMDMs) were extracted as described by [165]. BMDMs were allowed to differentiate for 10 days and were subsequently co-cultured with fungal cells in BMDM media (RPMI 1640, 20% L-cell conditioned media (LCCM), 15% FBS, 100 U/ml penicillin and 100 µg/m streptomycin). Cells that were used for the assays were no more than 4 days old post-differentiation.

2.3.2. Quantification of *C. albicans* survival in macrophages

Macrophages were seeded in 96 well plates and infected with *C. albicans* (cultured in YPD+uridine at 30°C over night) at a multiplicity of infection of 1:2 (macrophage:*Candida*). After 1 h (T₀), macrophages were washed 4 times with 1x PBS to remove all un-phagocytosed yeast cells (as previously described by Fernandes-Arenas, *et al.* [166]). Cells were replenished with BMDM media and allowed to continue co-incubation for 13.5 h (T_{13.5}). The macrophage lysis buffer (150 µl of 50 mM Tris pH7.5, 2 mM EDTA, 0.1% Triton X-100) was added to the wells, followed by 10 min of incubation. Lysed macrophages were transferred into microcentrifuge tubes and the wells washed with 1x sterile water using a multichannel pipette until all *Candida* cells were transferred to the microcentrifuge tubes (this was confirmed by microscopic analysis of wells at 20x magnification). Samples in microcentrifuge tubes were vortexed for 30 seconds and centrifuged at 5000 rpm. Pelleted cells were washed, and diluted before plating on YPD + uridine plates. Plates were incubated at 30°C for 36-48 h and

¹⁰ Presented here are the methods for experiments I was involved in executing. All other methods are included in my published work including the work of collaborators (Uwamahoro *et al.*,2014). The methods described here are reproduced with minor modifications from the Supplemental data for Uwamahoro et al 2014, as I wrote the Methods sections for the manuscript.

colony forming units (CFUs) counted. The experiments were performed at least 3 independent times with each strain assayed in triplicate wells. Figure 4.1 indicates the relative ($T_{13.5}/T_0$) increase in CFUs.

2.3.3. Experiments to assess fungal morphology within macrophages, escape and phagocytosis, and Lamp1 association

To determine early filament extension of the wild type, *srb9* Δ/Δ and *med31* Δ/Δ mutant cells within macrophages, fungal cells were co-incubated with macrophages as described above and lengths of phagocytosed yeast cells were followed under live cell imaging. Using ImageJ software, the relative length of the filaments was monitored and recorded for 90 min. At least 10 wild type and *srb9* Δ/Δ mutant cells each were sampled at each time point. Shown are the lengths expressed relative to time zero, calculated after determining the averages lengths at each time point. The average length over time and the SEM are plotted. Heat killed cells are added as a control (no change in cell size).

For assaying fungal escape and morphology (Figure 4.2 B-E), experiments were conducted as described by [166]. Freshly streaked *C. albicans* strains were cultured at 30°C in 2 ml of YPD+ uridine media, while 500,000 cells of primary macrophages were seeded into wells of a 24 well plate containing microscope glass slide coverslips and incubated at 37°C, 5% CO₂ atmosphere overnight. *Candida* and macrophages were co-incubated for 1 hour at the multiplicity of infection 1 macrophage: 2 *Candida*, and unphagocytosed cells washed off with PBS. One milliliter of BMDM medium was added and cells were allowed to co-incubate a further 3 hours. For monitoring escape, cells were stained with 5 μ g/ml calcofluor white for 10 min, washed 4 times and mounted on glass slides with Dako fluorescent medium (Invitrogen). Imaging was done using an Olympus IX81 microscope with the Olympus cellM software, using the 60x objective with DIC, or the DAPI filter for calcofluor white stained cells. Three independent experiments were performed and at least 200 cells/strain counted in each of 2 the experiments. Phagocytosis rates were also determined.

To determine *C. albicans* phagocytosis, in Figure 4.6 and 4.14F-G, images at the 30 min time point post the 1h co-incubation were used from three independent experiments conducted together for wild type and *casp1^{-/-}casp11^{-/-}* BMDMs in Figure 4.6 and 4.14F-G (the experiments are shown in Figures 4.5B and 4.14A). Similarly, for the RAW 264.7 cells, the experiment shown in Figure 4.10B was used for quantification at the 30 min time point post the 1 h co-incubation (two independent experiments). A total of 200 macrophages were counted for each of the independent biological experiments. The MOI was 1:6 (macrophage : *Candida*) cells. Morphology of *Candida* cells within macrophages in Figure 4.10C was determined from the same experiments as above counting 100 *Candida* cells in each of the biological repeats. For all experiments testing phagocytosis, fungal morphology, escape and phagolysosome association, Figures show averages from the biological repeats and the standard error of the mean.

For quantifying the association of *C. albicans* with Lamp1, cells were prepared and stained with calcofluor white as described above, except that cells were allowed to co-incubate for a further 2 h, instead of 3 h. After washes with PBS, cells were fixed with 4% paraformaldehyde for 10 min, and washed thrice with PBS, followed by 10 min incubation in 50 mM ammonium chloride. Cells were washed thrice and permeabilised with 0.1% saponin for 5 min, before adding blocking solution (3% BSA, 0.1% saponin, 1x PBS) for 15 min on ice. A 1/800 dilution of the anti-Lamp1 antibody (CD107a from BD Pharmagen) was added and allowed to bind overnight at 4°C. The next day, cells were washed twice for 15 min with ice cold PBS, and 1/800 dilution of Alexa-fluor 594 Chicken anti-rat IgA was added. Incubation was overnight in blocking solution. The next day, cells were washed thrice with 50 ml PBS and mounted. Cells were imaged using confocal microscopy on the Nikon C1 Invert Microscope (Monash MicroImaging facility). Three independent experiments were performed and Lamp1 association was counted for at least 50 *Candida* cells for each of the strains in each of the independent experiments. Calcofluor white staining was used to discriminate between internal and external *Candida* during quantification, as the stain does not permeate live macrophages.

Statistical analysis was performed using the Graph Pad Prism version 6.00 for Windows, GraphPad Software (La Jolla California USA, www.graphpad.com), using the unpaired, two tailed student t-test. The asterisk above error bars indicates *p*-values (*<0.05, **<0.01, ***<0.001 and ****<0.0001).

2.3.4. Quantification of macrophage cell death using time-lapse imaging

Primary macrophages or RAW 264.7 macrophage cell lines (500,000 cells) were seeded in 24 well plates and infected with *C. albicans* (cultured in YPD+uridine at 30°C overnight) at a multiplicity of infection of 1:6 (macrophage:*Candida*). After 1 h, macrophages were washed 4 times with 1x PBS to remove all un-phagocytosed yeast cells as previously described by Fernandez-Arenas *et al.*, [167]. Cells were replenished with 1 ml of RPMI media containing 10 µg/ml propidium iodide (PI) (Invitrogen). Experiments were performed on the Leica AF6000 LX live cell imaging system with an inverted, fully motorized microscope, driven by the Leica Advanced Suite Application software (Monash MicroImaging facility). During the course of the experiment, cells were maintained in a humidified chamber at 37°C and 5% CO₂. Time-lapse images were acquired with bright field and TxRed filter every 15 min for up to 24 h using a 20x/0.8A objective, typically capturing over 300 cells per well. Macrophage cell death was determined after conversion of propidium iodide images into binary images using the Fiji ImageJ software [168], the same signal threshold was applied for all samples. The binary images were then used to measure PI signal for the area of each image with the particle analyser function in the software. The percentage of macrophage cell death at specific time points was determined from the PI signal was described in the Results. Calculations were done with Microsoft Excel and data analyzed by the GraphPad Prism Software. Each experiment was performed independently at least 3 times using macrophages derived from different mice and independent *Candida* cultures, except for the RAW 264.7 experiments, which were conducted twice. Graphs show the mean of the biological repeats and the standard error of the mean (SEM). Statistical significance was determined using the unpaired Student *t*-test with two-tailed *p*-values (GraphPad Prism Software La Jolla California USA, www.graphpad.com). Asterisk above error bars indicate *p*-values (*<0.05, **<0.01, ***<0.001 and ****<0.0001)

2.3.5. Quantification of IL-1 β production

Experiments were conducted as described by Joly *et al.*, [169]. Briefly, BMDMs were primed with 50 ng/ml LPS for 3.5 h in 6 well plates. Overnight cultures of *C. albicans* strains were counted and co-incubated with primed BMDMs at a ratio of 1:6 (BMDM:*Candida*) for the time points indicated in the figure. The relative IL-1 β levels are presented in Figure 4.13C and 4.13D. In one of the experiments comparing wild type and *srb9 Δ/Δ* Mediator mutant of *Candida*), after the 1 h of co-incubation non-phagocytosed cells were washed off with PBS (Figure 4.13E). This additional washing step did not cause an observable difference in IL-1 β levels. Therefore, relative IL-1 β levels for the *srb9 Δ/Δ* mutant in Figure 4.13E were calculated using data from all four experiments. To obtain heat killed fungal cells, wild type *Candida* were heated for 1 h at 80°C before co-incubation with BMDMs.

Supernatants were collected sent for IL-1 β quantification by ELISA according to the manufacturer's recommendations (R&D systems). IL-1 β quantification was performed by Dr. James Vince and Rowena Lewis (WEHI)¹¹.

2.3.6. Quantification of *Candida* gene expression in macrophages¹²

Gene expression was studied following co-incubation of macrophages and *Candida* (1 macrophage : 6 *Candida*) in 100 mm dishes for 3 h. Isolation of *Candida* cells was done by washing the dishes with PBS, followed by addition of 5 ml/plate of Trizol reagent to lyse the macrophages. Fungal cells were collected by centrifugation and washed two times with Trizol to remove most of macrophage DNA and RNA. Cells were frozen in dry-ice and stored at -80°C until use. RNA was extracted using the hot-phenol method and contaminating genomic DNA removed by treatment with DNase I (Ambion). Reverse transcription was performed as mentioned in section 2.2.3 with the following modifications. The expression levels of the transcripts were normalized to the

¹¹ James E. Vince, The Walter and Eliza Hall Institute of Medical Research, Parkville, Victoria 3052, Australia

¹² Assay conducted together with Dr. Jiyoti Verma Gau, Department of Biochemistry, Monash University, Clayton, Victoria, Australia

level of 18s rRNA. Three independent biological experiments were performed, with two technical replicates each. Averages shown in Figure 4.8A are from the biological repeats and the error bars represent the standard error of the mean (SEM).

2.3.7. Fluorescence microscopy and quantification of 1,3 β -glucan exposure using flow cytometry

For immunofluorescence labeling of 1,3 β -glucan, overnight YPD grown *C. albicans* strains were washed twice with PBS and transferred into a 24 well tissue culture plate with coverslips at OD⁶⁰⁰=0.05 in RPMI with 10% serum, followed by incubation for 4 h at 37°C in a humidified atmosphere with 5% CO₂. These conditions mimic the conditions during the macrophage infection experiments. *Candida* bound coverslips were collected after 4 h of filamentation, washed twice with 1 ml PBS, and incubated for 10 min with PBS containing 0.1% BSA. β -glucan staining was done by incubating coverslips with 200 μ l monoclonal mouse anti- β -1,3-glucan antibody (Biosupplies Australia, 1 μ g/ml in PBS with 0.1 % BSA), at room temperature for 30 min. After washing with PBS to remove unbound primary antibody, cells were incubated with 200 μ l AlexaFluor 488-labelled goat anti-mouse IgG (Invitrogen, 4 μ g/ml in PBS with 0.1% BSA). In negative control samples, only the secondary antibody was added (no signal was detected in these negative control experiments, data not shown). After incubation at room temperature for 30 min, cells were washed 3 times with PBS, mounted on slides and observed using the Nikon1 confocal microscope (Monash MicroImaging Facility) as described above.

For flow cytometry¹³, overnight YPD grown *C. albicans* strains were washed twice with PBS and transferred to 37°C into pre-warmed Spider medium at OD₆₀₀=0.05 and incubated for 3 hours at 37°C. Cells were washed twice with PBS, collected by centrifugation (200 rpm) and re-suspended in 500 μ l of monoclonal mouse anti- β -1,3- glucan antibody. After 30 min at room temperature, cells were collected by centrifugation and washed three times with 1 ml PBS, followed by 30 min incubation with AlexaFluor 488-labelled goat anti-mouse IgG as above. After washing, cells were

¹³ Assay conducted by Dr. Jiyoti Verma Gau, Department of Biochemistry, Monash University, Clayton, Victoria, Australia

re-suspended in PBS and immediately analyzed by flow cytometry (FACSCalibur, BD Biosciences). For data acquisition, forward and side scatter were detected on linear scales, while AlexaFluor 488 fluorescence was analysed on logarithmic scales. The AlexaFluor 488 fluorescence intensity of at least 10000 gated cells was calculated using FACSDiva 5.0 software (BD Biosciences). The fluorescence graphs were made in Weasel 3.1 (WEHI, Australia). The experiment was performed on three independent occasions.

2.3.8. Atomic force microscopy¹⁴

Freshly streaked *C. albicans* strains were cultured at 30°C in 2 ml of YPD+ Uridine media, while sterile microscope glass slides were immersed in petri dishes containing 15 ml of RPMI media at 37°C in a humidified atmosphere with 5% CO₂. The following day, *C. albicans* cells were washed with sterile water and diluted into the prepared dishes to OD⁶⁰⁰ = 0.05 and incubated 37°C in a humidified atmosphere with 5% CO₂. *Candida* bound slides were collected after 4 h of filamentation and washed twice with Milli-Q water before imaging. The experiment comparing wild type and *srb9Δ/Δ* mutant hyphae was performed three times, and at least 10 individual hyphae measured for each of the strains across the independent experiments. In one of the experiments, the complemented *srb9Δ/Δ* + *SRB9* strain was also included, and 5 hyphae measured for this strain. Immediately before measurement, the glass slides were washed 3 times with water and were dried in air.

AFM¹⁵ measurements were performed at room temperature using NanoWizard® II AFM system at Melbourne Centre for Nanofabrication. AFM contact mode images were obtained using Si₃N₄ cantilevers (MSNL-10, Bruker, Santa Barbara, CA). Prior to making measurements, the spring constant was corrected and a scan rate was set at 1 Hz. Deflection images were simultaneously acquired and analyzed with the JPK data software (JPK instruments AG, Germany). Force-distance measurements were collected on a single *C. albicans* cell by approaching the cantilever tip towards the cell, pressing

¹⁴ I prepared the samples for AFM images were produced by Dr. Hsin Hui Shen.

¹⁵ Assay conducted by Dr. Hsing Hui, Department of Microbiology, Monash University, Clayton, Victoria, Australia

against the cell surface and retracting the tip from the cell. The force-map of wild type and mutant cells consisted of ~64 measurements in a selected region on individual cells (1.7 μm x 1.7 μm for the wild type strain, and a 1.2 μm x 1.2 μm section for the *srb9 Δ / Δ* strain). For the complemented strain, a 1.7 μm x 1 μm region was selected with 31 measurements.

Chapter 3: The roles of the C. albicans

Mediator in the dimorphic switch and cell wall remodelling

3.1. Introduction

As mentioned in Chapter 1, the ability to developmentally switch between distinct cell morphologies, such as yeast and hyphal cells, is a key virulence trait for *C. albicans*. Cell morphology is determined by complex developmental programs, with changes to gene regulatory networks being a key part of the process. While several transcriptional activators and repressors have been characterised in *C. albicans* that control yeast and hyphal morphologies, very little is known about transcriptional co-regulators in this context. In model yeasts *S. cerevisiae* and *S. pombe*, the Mediator complex has been implicated in the regulation of morphogenesis [127, 170]. For example, studies in *S. pombe* showed that mutagenesis of the *MED1*, *MED12*, *MED18*, *MED20*, *MED27*, *MED15* and *MED31* subunits of Mediator results in cell morphology defects including inability to undergo cell separation after cell division [125]. In contrast, deletion of the subunits in the Kinase module has been shown to greatly enhance cellular flocculation [141], but no septation defects were observed in these mutants, suggesting that the different subunits of Mediator have different roles in morphogenesis. Similarly, for other phenotypes such as stress responses, the mutations

in the distinct Mediator subunits can have similar or distinct phenotypes (as described by similar phenotypes obtained through mutagenesis of various Mediator subunits presented in Table 1.2).

In *S. pombe*, the Kinase module was suggested to be required as a repressor of the expression of adhesins. The *srb10Δ* and *med12Δ* mutants produced increased transcript levels of adhesins including genes related to the *S. cerevisiae* *FLO* gene family [127]. The fold increase of these genes was higher in the *srb10Δ* mutant, which corresponds well with the stronger flocculation phenotype that is observed in this strain as compared to the milder phenotype observed for the *med12Δ* mutant. The role of the Kinase module as a repressor of Flo-like adhesins is conserved between *S. pombe* and *S. cerevisiae* as these adhesins are also up-regulated in the *S. cerevisiae* Cdk8 module mutants [125]. In addition to this, components of the Mediator have also been shown to act in response to physiological signals and influence morphological changes. For example, in *S. cerevisiae*, the Srb10 regulates gene-specific activators in response to the physiological signals via phosphorylation of Ste12 for filamentous growth in response to nitrogen limitation [171].

The approach taken in this thesis to characterize the Mediator of *C. albicans* was the deletion of components of the Mediator, and through analysis of the morphological defects, identified possible gene regulatory roles. The subunits focused on were the highly conserved Med31 from the Middle module, the Kinase domain subunit Srb9, and the Head module subunit Med20.

3.2. Results

3.2.1. *C. albicans* Mediator subunits co-regulate genes with morphogenesis associated transcription factors: the link between *Ace2* and *Med31*

To start addressing the function of Mediator in morphogenesis of *C. albicans*, I deleted the highly conserved *MED31* subunit in the Middle domain of the complex. I also constructed a complemented strain, where the wild type *MED31* gene was ectopically re-expressed in the mutant. The morphology of *med31Δ/Δ* mutant cells showed a cell-chain phenotype when compared to wild type and complemented strains, consistent with defective cell separation after cell division (Figure 3.1 A). This phenotype was a result of cytokinesis defects, rather than cells simply adhering to each other as shown by calcofluor white staining that demonstrated that the cells failed to separate at the mother daughter junctions (septa) resulting in a chained phenotype (Figure 3.1A). Furthermore, the cells remained attached even after light sonication, indicating that they were not merely more “sticky”. Quantification showed that 43% of cells from *med31Δ/Δ* cultures showed the cell-chain phenotype (Figure 3.1B). This phenotype was observed in two independently constructed homozygous deletion mutants and was significantly complemented in the reconstituted strain (Figure 3.1A and B).

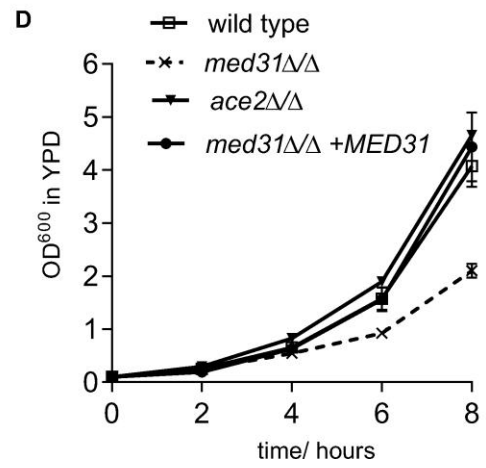
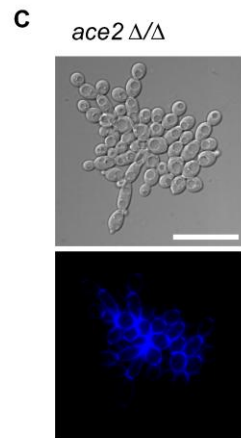
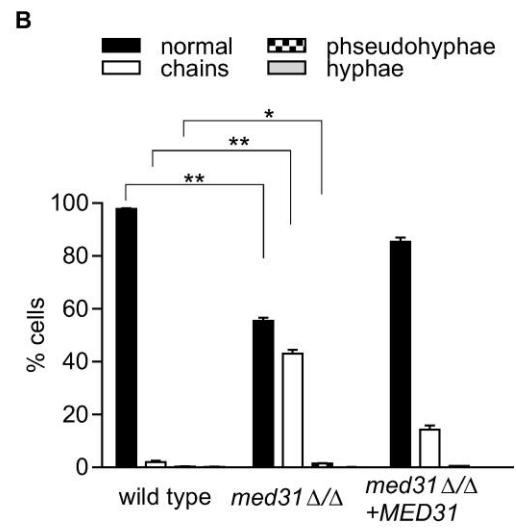
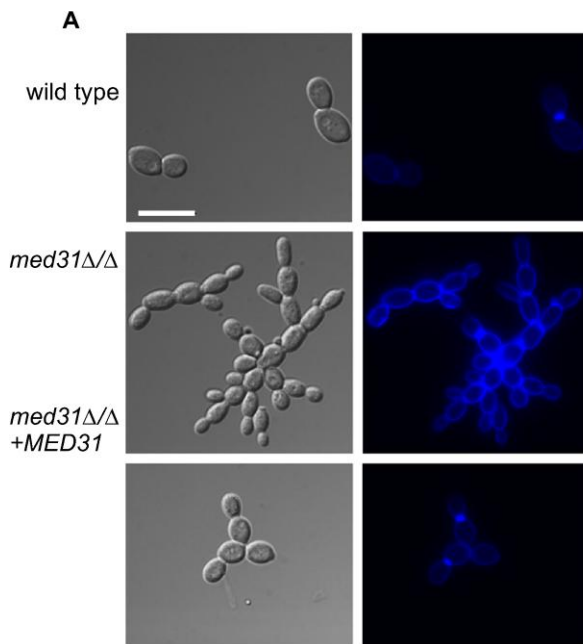


Figure 3.1. Mediator mutant morphology under nutrient rich conditions. Cultures of wild type *C. albicans*, the *med31Δ/Δ* and *ace2Δ/Δ* mutants and the complemented *med31Δ/Δ+MED31* strains and were grown to log phase in YPD at 30°C, and cells observed by microscopy using DIC (differential interference contrast) for bright field (**A** and **C**) or through the DAPI filter for calcofluor white-stained cells (**A** right panel and **C** bottom panel). The scale bar is 20μm. **B**) Quantification of the morphogenesis of *C. albicans* strains. Shown are the averages from three experiments and the error bar represents the SEM. * $p \leq 0.05$, ** $p \leq 0.01$. **D**) The growth of strains was monitored for 8 hours, from at least three experiments and the error bar represents the SEM.

In *C. albicans* and many other fungal species, cell separation is controlled by the transcription factor Ace2. Figure 3.1C shows highly impaired cytokinesis in an *ace2Δ/Δ* deletion mutant. Compared with the *ace2Δ/Δ* mutant (Figure 3.1A and 3.1C), the cytokinesis defect in the *med31Δ/Δ* mutant is milder (Figure 3.1A). Assessment of the growth of these two mutants showed that the *ace2Δ/Δ* mutant showed no growth defect compared to wild type cells, however the *med31Δ/Δ* strain showed significantly slower growth (Figure 3.1D). Collectively, these results suggested that the *C. albicans* Med31 might have a conserved role with *S. pombe* and *S. cerevisiae* in Ace2-dependent regulation of genes necessary for cytokinesis, but it also has Ace2-independent roles in cell fitness.

3.2.2. The *C. albicans* Med31 controls the expression of genes involved in cell wall integrity and filamentous growth

To obtain a global view of the functions of Med31 in gene regulation in *C. albicans*, microarray-based transcriptomics was performed in collaboration with Prof. Andre Nantel at the Biotechnology Research Institute in Montreal. Cells from the *med31Δ/Δ* mutant and the *med31+MED31* complemented strain were grown under yeast growth conditions (YPD, 30°C), total RNA extracted and microarrays performed with four independent biological repeats. Microarray analysis was used to identify any chromosomal changes that may have occurred as a result of genetic manipulation during mutant construction which would affect transcriptome analysis results. No gross

chromosomal defects were identified between the *med31Δ/Δ* mutant and the complemented strain (Figure 3.2).

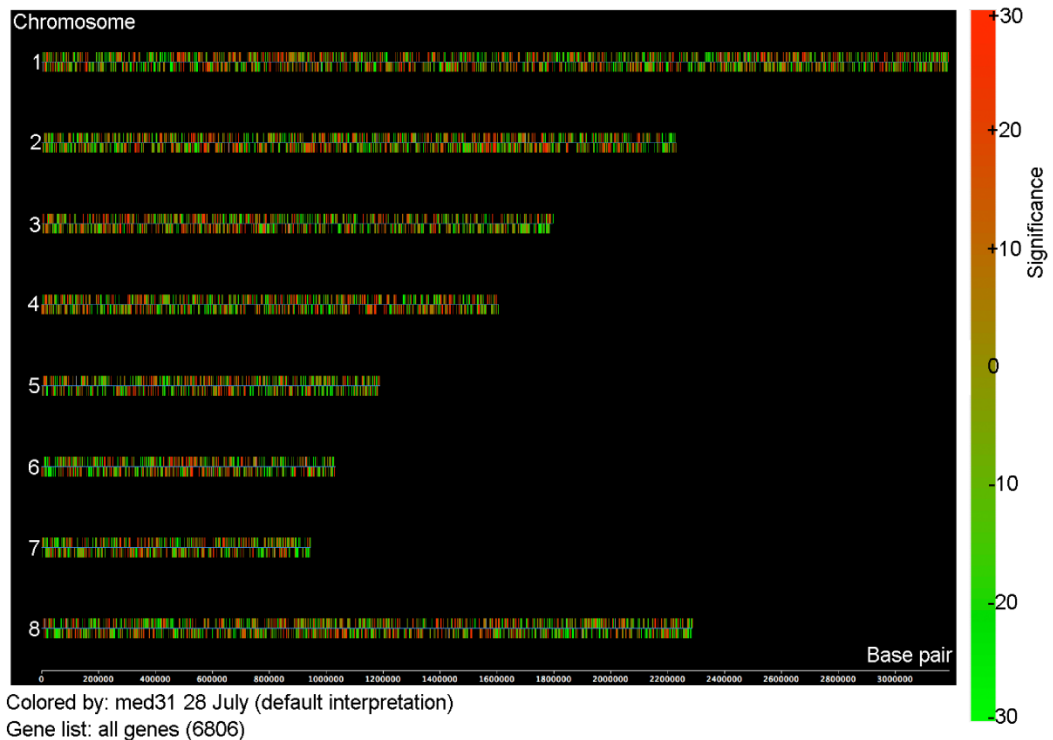


Figure 3.2. Chromosomal view of the transcriptional profile of the *med31Δ/Δ* mutant of *C. albicans*. Presented is a pictorial representation of changes gene expression of all 6806 genes analysed on all eight *C. albicans* chromosomes of the *med31Δ/Δ* mutant relative to the *med31Δ/Δ* +*MED31* complemented strain. Colour scale on the right indicates the changes in gene expression levels (log₂) on the individual chromosomes.

Figure By Andre Nantel¹⁶

¹⁶ Dr. Andre Nantel laboratory, Biotechnology Research Institute, National Research Council of Canada, Montreal, Quebec, Canada

Figure 3.3A and 3.3B and Tables 1-7 show the genes differentially expressed in the *med31Δ/Δ* mutant. Changes were observed in the expression of 510 genes or 7% of the *C. albicans* genome by considering genes that were up-regulated and down-regulated 1.5 fold (*p*-value was less than 0.05) (Figure 3.3A). An updated (2014) GO-term enrichment analysis of published data [163], is presented in Appendix 1 Table 1 and Table 2.

Out of the 510 differentially regulated genes, 61.7% (315) were down-regulated and 38.2% (195) were up-regulated (Figure 3.3A). This is consistent with a predominantly positive role of Med31 in transcription, suggesting that the *C. albicans* Med31 subunit is primarily required for transcriptional activation, similar to its functions in *S. cerevisiae* and *S. pombe* [124, 125, 146, 172].

To obtain a global view of the roles of Med31 transcription target genes, the GO Slim Mapper tool in *Candida* Genome Database (CGD) was used to identify putative enriched biological functions, processes, or cell compartments (Appendix 1 Table 3). The biological processes of a quarter (24.5%) of all significantly altered genes are still unknown in *C. albicans*. In addition to this, 32.9% had no known molecular function (Appendix 1 Table 3). Some significantly up-regulated and down-regulated genes are presented in Table 3.1 and Table 3.2 respectively. Since a majority of genes were down-regulated and to stay in line with my thesis aims, I focused on Med31 target genes (significantly down-regulated set) that had classifications related to *C. albicans* morphogenesis and cell stress.

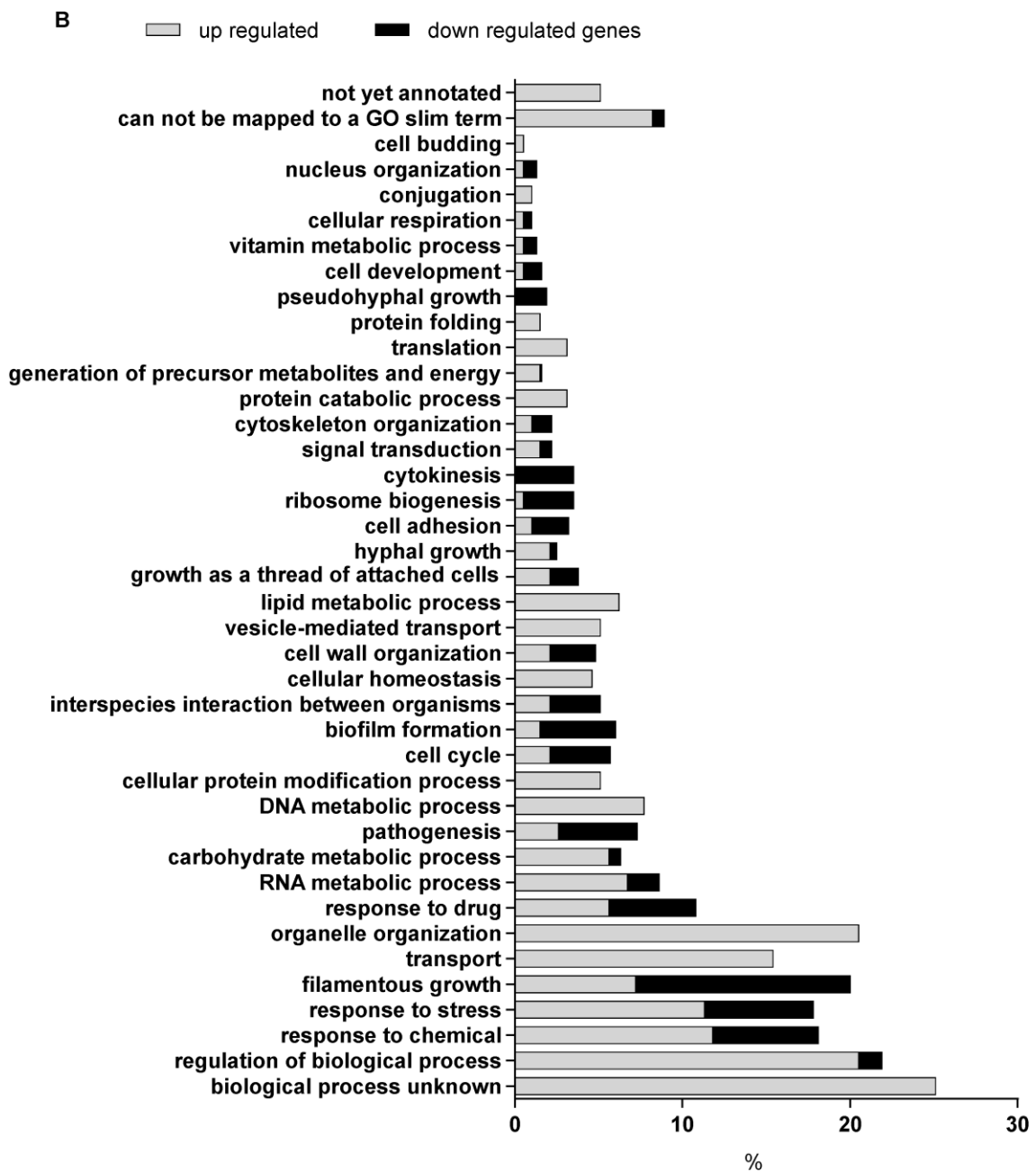
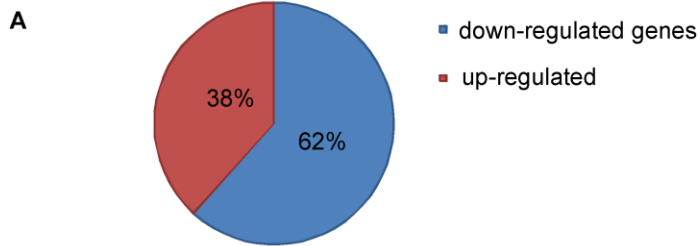


Figure 3.3. Transcriptional profiling of the *med31* deletion strain. (A) Compared to the complemented strain *med31+MED31*, 7.8% of genome was significantly altered in the mutant and the full list of genes is provided in Appendix 1, Table 7. (B) Major Gene Ontology (GO) categories of the *C. albicans* genes with altered expression in the *med31* deletion strain. The genes that were found to be significantly up-regulated or down-regulated in the *med31Δ/Δ* mutant cells were analysed with the GO Slim Mapped tool of the *Candida* Genome Database and classified by biological processes. The redundant occurrence of the most represented GO terms was calculated (total exceeds 100%, taking into account that several GO terms could be assigned to one single gene). Other categories are depicted in Appendix 1 Table 3. *p*-values for enrichment are presented of Go-terms as published in [163] and are updated Table 3.3 below. The complete list of Go-terms is presented in Appendix 1, Table 1 [163].

Table 3.1. Go Slim process of the up-regulated genes in the *C. albicans med31Δ/Δ* mutant

Go-Slim	Cluster frequency (%)	Genes annotated to the term
organelle organization	20.5	<i>ACSI, ARC18, CDC68, CLN3, COX19, DPB4, ESC4, EXO1, GCF1, MAS2, MRP20, PEX11, PHB2, PRI2, RAD54, RAD7, RHO2, RIM1, SEC5, TIM13, TIP1, USO1, orf19.1085, orf19.1195, orf19.1483, orf19.185, orf19.2201, orf19.3223.1, orf19.3581, orf19.439, orf19.5459, orf19.5515, orf19.6100, orf19.6458.1, orf19.6563.1, orf19.6607, orf19.6861, orf19.7196, orf19.7538, orf19.954</i>
organelle organization	20.5	<i>ACSI, ARC18, CDC68, CLN3, COX19, DPB4, ESC4, EXO1, GCF1, MAS2, MRP20, PEX11, PHB2, PRI2, RAD54, RAD7, RHO2, RIM1, SEC5, TIM13, TIP1, USO1, orf19.1085, orf19.1195, orf19.1483, orf19.185, orf19.2201, orf19.3223.1, orf19.3581, orf19.439, orf19.5459, orf19.5515, orf19.6100, orf19.6458.1, orf19.6563.1, orf19.6607, orf19.6861, orf19.7196, orf19.7538, orf19.954</i>
transport	15.4	<i>ARC18, BET4, CFL4, CHS7, CLC1, COX19, HGT3, HXT5, MAC1, MAS2, RHO2, RPB4, SEC5, TIM13, TIP1, USO1, VCX1, VMA11, VMA5, orf19.1195, orf19.1210, orf19.1564, orf19.1795.1, orf19.2302, orf19.4731, orf19.4981, orf19.5095, orf19.516, orf19.6264.3, orf19.954</i>
RNA metabolic process	6.7	<i>CDC68, PRI2, RNY11, RPB4, SEN2, TAF19, orf19.1356, orf19.1794, orf19.5239, orf19.5459, orf19.6458.1, orf19.7196, orf19.7265</i>
lipid metabolic process	6.2	<i>ARE2, AYRI, CAT2, FAA21, INO1, OPI3, PEX11, orf19.1092, orf19.276, orf19.2761, orf19.4066, orf19.6100</i>
carbohydrate metabolic process	5.6	<i>ARA1, CHS7, EXG2, GLK4, INO1, MDH1-3, PYC2, orf19.1092, orf19.338, orf19.7214, orf19.7426</i>
cellular homeostasis	4.6	<i>DOT5, MAC1, TRR1, VCX1, VMA5, orf19.1195, orf19.2302, orf19.2516, orf19.6100</i>
protein catabolic process	3.1	<i>RAD7, orf19.1085, orf19.229, orf19.6861, orf19.7196, orf19.7265</i>
signal transduction	1.5	<i>CEK1, RHO2, orf19.5620</i>

Table 3.2. Go Slim process down-regulated genes in *C. albicans med31Δ/Δ* mutant

Go-Slim	Cluster frequency (%)	Genes annotated to the term
response to stress	17.8	<i>ADAEC, ADE1, ADE2, AHR1, CAS5, CDR1, CPH2, CTF18, DAC1, DCK1, DCK2, DED1, ECM29, EFG1, FCRI, FGR14, FGR6, FGR6-3, FGR6-4, GAD1, GAL10, GPR1, GPX2, HGT1, HSM3, HSP104, HSP21, HYM1, MAL2, MHP1, NRG1, PDE2, PGA26, PHHB, PHO4, PTC8, RIM101, SFU1, SHA3, SNQ2, SOD5, SRR1, SSU1, TEC1, TYE7, VAM3, YTM1, ZCF13, orf19.2175, orf19.2208, orf19.3481, orf19.3854, orf19.512, orf19.6720, orf19.7213</i>
response to drug	10.8	<i>AHR1, CAS5, CDR1, CPH2, DIP5, EFG1, FCRI, FCY21, GSL1, HGT1, HOL4, HYM1, LEU4, MIG1, NRG1, OPT1, PDE2, RIM101, RRP6, SNQ2, STP3, UTP22, VPS28, YTH1, orf19.1308, orf19.173, orf19.304, orf19.3228, orf19.341, orf19.3854, orf19.4116, orf19.5401, orf19.6586, orf19.7029</i>
pathogenesis	7.3	<i>ADE2, ADE5,7, AHR1, ALS1, CAS5, DAC1, EFG1, HSP104, HSP21, LEU2, MNT1, NRG1, PDE2, PGA26, RHD3, RIM101, SOD5, SRR1, TEC1, TYE7, VAM3, VPS28</i>
cell cycle	5.7	<i>CHT3, CTF18, DAD3, DIT2, ENGI, FKH2, HYM1, INNI, PHHB, PWP2, RIM101, RME1, SCW11, SDS24, orf19.1619, orf19.3854, orf19.7450</i>
ribosome biogenesis	3.5	<i>DBP2, DBP7, PWP2, RRP6, TSRI, UTP22, YTM1, orf19.1578, orf19.1687, orf19.512, orf19.7107</i>
signal transduction	2.2	<i>ARF1, DCK1, DCK2, GPR1, PDE2, RIM101, SRR1</i>
<i>Cellular morphogenesis</i>		
cytokinesis	3.5	<i>CHT3, ENGI, HYM1, INNI, PWP2, RIM101, SCW11, SDS24, orf19.1619, orf19.7450</i>
pseudohyphal growth	1.9	<i>CPH2, EFG1, GPR1, NRG1, TEC1, orf19.3228</i>
cell adhesion	3.2	<i>AHR1, ALS1, ALS5, ALS6, DEF1, EAP1, EFG1, MNT1, PDE2, TEC1</i>
cell wall organization	4.8	<i>CAS5, DCK1, DIT2, HYM1, MHP1, MNT1, PDE2, PGA13, PGA26, PHHB, PIR1, RHD3, VPS28, orf19.215, orf19.6741</i>
biofilm formation	6.0	<i>AHR1, ALS1, ALS5, ALS6, CAS5, DEF1, EAP1, EFG1, HSP104, NRG1, PDE2, PGA26, ROB1, SUC1, TEC1, TRY6, TYE7, VAM3</i>
filamentous growth	20	<i>ADE5,7, AHR1, ALS1, CAS5, CHT1, CPH2, CTA4, CUP9, DAC1, DCK1, DCK2, DEF1, DOT6, ECM29, EFG1, ENA2, FCRI, FGR14, FGR6, FGR6-1, FGR6-3, FGR6-4, FKH2, GAL10, GPR1, HAL9, HGT1, HSP21, HYM1, MAL2, MHP1, MIG1, MNT1, NRG1, PDE2, PGA13, PGA26, PHHB, PHO4, PTC8, RIM101, ROB1, SHA3, SNQ2, SRR1, SSU1, STP3, STP4, SUC1, TEC1, TYE7, VAM3, VPS28, YTM1, ZCF13, ZCF16, orf19.2397.3, orf19.3228, orf19.6720, orf19.6868, orf19.6874, orf19.7111</i>

Table 3.3. GO term analysis of genes differentially expressed in the *C. albicans med31Δ/Δ* mutant

GOID	GO term	Cluster frequency (%)	Background frequency (%)	Corrected P-value	False Discovery ate (%)
<i>Down regulated genes</i>					
50896	response to stimulus	29.4	16.5	7.52E ⁻⁰⁶	0
30447	filamentous growth	20.9	8.8	2.95E ⁻⁰⁸	0
42221	response to chemical	19.3	8.7	4.25E ⁻⁰⁶	0
6950	response to stress	18	9.2	7.90E ⁻⁰⁴	0
31667	response to nutrient levels	12.4	4.6	2.36E ⁻⁰⁵	0
42710	biofilm formation	6.5	2.1	8.31E ⁻⁰³	0
7124	pseudohyphal growth	2.6	0.4	2.18E ⁻⁰²	0
<i>Up regulated genes</i>					
7005	mitochondrion organization	10	2.3	4.77E ⁻⁰⁵	0
10821	regulation of mitochondrion organization	2.6	0.1	3.00E ⁻⁰⁴	0
10821	regulation of mitochondrion organization	2.6	0.1	3.00E ⁻⁰⁴	0

Twenty per cent of genes down-regulated in the *med31Δ/Δ* mutant cells were involved in the filamentous growth process, 18.1%, 17.8% and 12.7% in response to stimuli (chemicals, drugs, and stresses respectively), and 10.8% in processes required in response to drugs (Figure 3.3B, Table 3.2, and Appendix 1, Table 5). Furthermore, 50.2% of Med31 target genes were cytoplasmic, 26.9% were nuclear proteins (mainly transcription factors), and the cellular component of 25.3% of target genes were unknown (Appendix 1, Table 6). Interestingly, genes impacted by Med31 included the transcription factors that control the yeast to hyphal transition such as *EFG1*, *MIG1*, and *NRG1* (Table 3.2, Filamentous growth). Only a select few targets were localized in the cell wall (5.1%) and these included key adhesins and other GPI anchored proteins, namely Als1, Als5, Als6, Cht1, Cht3, Csh1, Ddr48, Eap1, Ecm331, Eng1, Exg2, Glx3, Hyr3, Iff6, Ino1, Met15, Pga13, Pga31, Phhb, Pir1, Pst2, Rhd3, Scw11, Sod4, Sod5, and Xyl2 (Table 3.2 and Appendix 1 Table 6).

Consistent with the cell morphology defects and Ace2-dependent gene regulation, several Ace2-dependent genes were down-regulated in the microarray analysis of the *med31Δ/Δ* mutant including *CHT3*, *SCW11*, *DSE1*, as well as the genes *ENG1*, *HYM1*, *INN1*, *PWP2*, *RIM101*, *SDS24* that are assigned to the GO term cytokinesis (Table 3.1 and Table 3.2). Several other genes that were found to be positively regulated by Med31 are known to function in cell wall biogenesis and integrity, for example there was a significant enrichment for genes that encode GPI-anchored cell wall proteins including *PGA13*, *PGA26*, *EAP1*. In addition to this, cell surface adhesion molecules were significantly down-regulated including those in the *ALS* gene family (*ALS1*, *ALS5* and *ALS6*) and the transcription factors known to regulate the expression of adhesins and cell wall remodelling (*EFG1*, *TEC1*). Six out of eight FGR (filamentous growth regulator) family genes, of which there are no orthologues in *S. cerevisiae*, were down-regulated in the mutant. In addition, several DNA binding transcription factors appear to be under the control of Med31 (Table 3.2). A significant proportion of these factors required for pathogenesis were transcription factors involved in the Ras-cAMP morphogenesis pathway and they were down-regulated in the absence of *MED31*. This includes *NRG1*, *EFG1*, *MIG1*, *TEC1*, *CPH2* and *RIM101*.

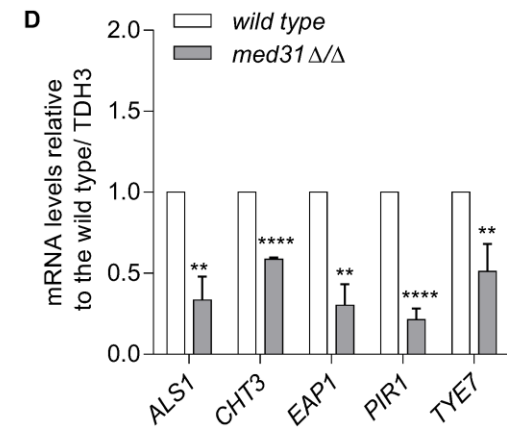
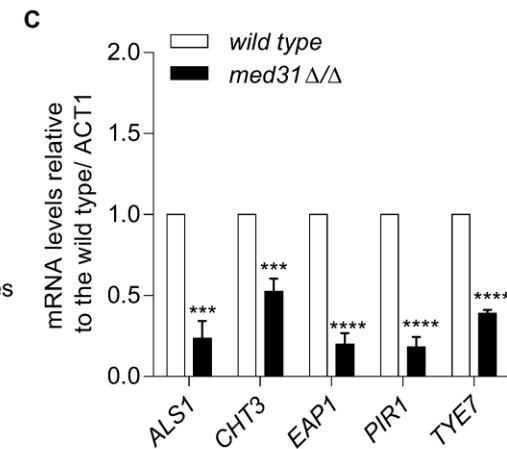


Figure 3.4. Motif identification in gene targets of Med31 **(A)** A selection of genes known to be required for adhesion, hyphal switch signalling and cell wall morphogenesis were down-regulated in the *med31Δ/Δ* mutant. Error bars represent the standard error of the mean (SEM) of the *med31Δ/Δ* mutant normalised levels of four separate microarray experiments against the complemented strain *med31+MED31*. **(B)** A motif present in the upstream sequences of most members of the selected morphogenesis related Med31 target genes shown in panel A was identified using MEME. This represents a *Candidate* binding site for Mss11 based on the known binding site of the homolog in *S. cerevisiae*. **(C)** Confirmation of down-regulated Ace2 dependent genes and adhesins. Cells were grown in YPD at 30°C to a final OD⁶⁰⁰ = 1 (yeast morphology), and levels of the indicated genes determined by quantitative PCR. The expression levels were normalised to *ACT1* and expressed relative to wild type levels, which were set to 1. Equivalent results were obtained when the glyceraldehyde-3-phosphate dehydrogenase (GAPDH) encoding gene *TDH3* was used for normalization **(D)**. ** $p \leq 0.01$, *** $p \leq 0.001$, **** $p \leq 0.0001$.

Focusing on the regulatory roles of Mediator in cell morphogenesis, a selection of genes (Figure 3.4A) known to be required for adhesion, components of the RAM network and Ras-cAMP morphogenesis pathways and cell wall proteins were used, based on their GO process and function classification (Appendix 1, Table 3 and Appendix 1, Table 4), to identify the possible motif target using MEME. Nucleotide sequences of 1080 bp upstream of opening reading frames were used. MEME analysis produced the motif [GAAAAAAAAA], p -value 5.9e-023 (Figure 3.4B). YeTFaSCo, which is based on transcription factors in *S. cerevisiae* [1], identified that the Mss11 transcription factor from *S. cerevisiae* recognises such a motif (p -value 1.355e-06). Given that the DNA binding specificity of the *C. albicans* homolog of this transcription factor is conserved with *S. cerevisiae* [173], this analysis suggests a possible co-regulatory role between Med31 and Mss11. The Mss11 transcription factor in *C. albicans* is required for hyphal growth [173], and the Mss11 protein in *S. cerevisiae* is also a critical regulator of filamentous growth [97].

Next, I used qPCR analysis to confirm transcript down-regulation of the levels of several Ace2-dependent genes in the *med31Δ/Δ* mutant (Figure 3.4C-D). Next I wanted to address whether other subunits of Mediator were also involved in Ace2-dependent gene expression. To that end, I analysed the expression levels of the Ace2-dependent genes in mutants inactivated in the subunits of the Head and Kinase modules of Mediator, *MED20* and *SRB9* respectively. Figure 3.5A shows the extent of down-regulation of the adhesins and the Ace2 dependent *CHT3* gene levels in the *ace2Δ/Δ* mutant as a control for chitin levels in a cytokinesis defective mutant. The *CHT3* gene was at wild type levels in the *med20Δ/Δ* mutant (Figure 3.5B). Similar results were obtained when the genes were normalized to *TDH3* (Figure 3.5C-E). The mild cytokinesis defects and down regulation of the *CHT3* gene in the Mediator mutants compared to the *ace2Δ/Δ* mutant suggests that perhaps several Mediator subunits share a co-regulatory role in the regulation of cytokinesis and thus inactivation of either one of the subunits has a modest overall effect. I found the regulation of the *ALS1* adhesin was 1.5 fold down-regulated in the *ace2Δ/Δ*, 2.6 fold down-regulated in the *med20Δ/Δ* mutants, (Figure 3.5C-D). The cell wall gene *EAP1* was down-regulated in the *ace2Δ/Δ* mutant (9.7 fold) and modestly down-regulated in the *med20Δ/Δ* mutant (1.6 fold) Figure 3.5C-D). There was similar morphology between wild type and *med20* mutants (Figure 3.5E).

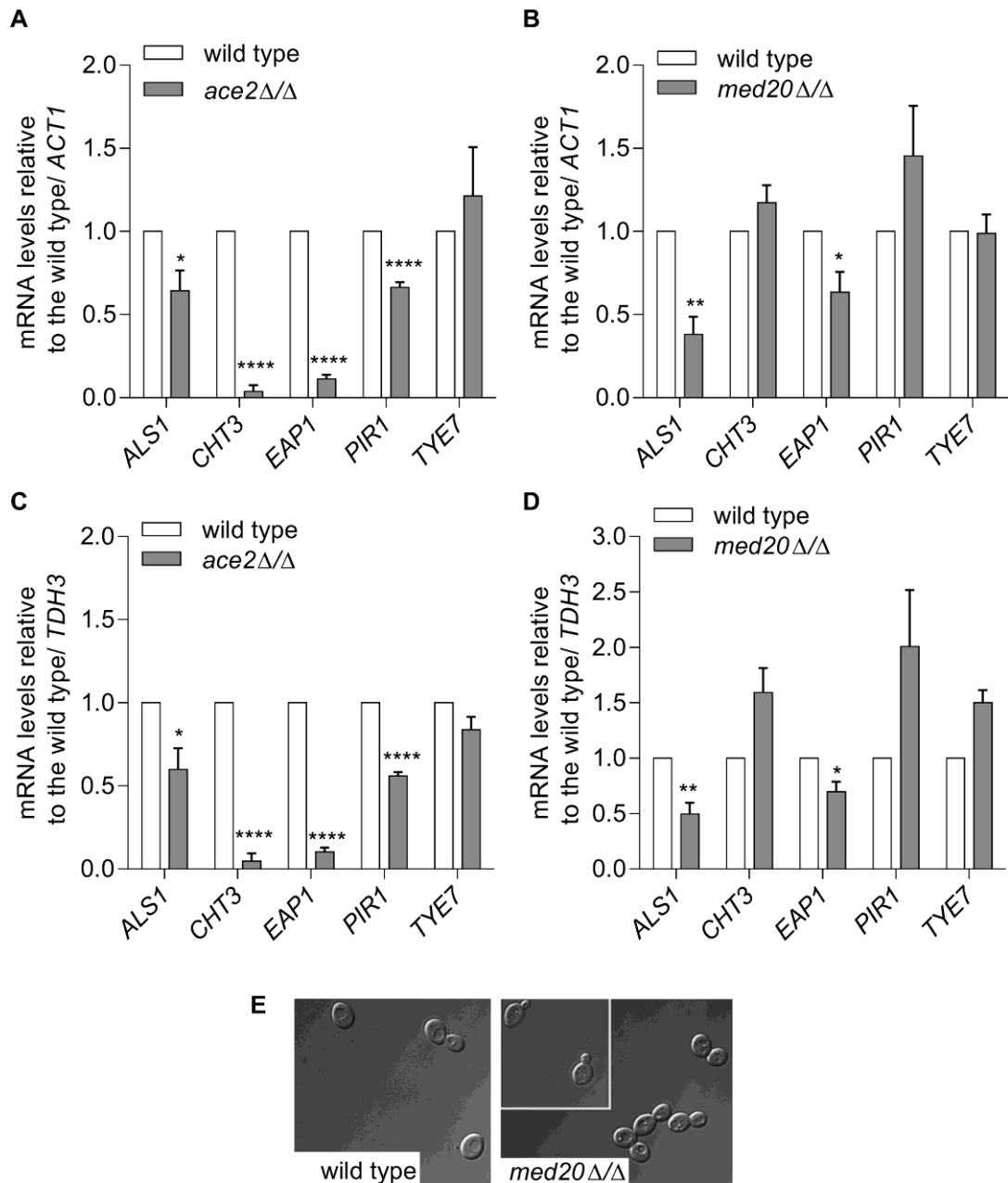
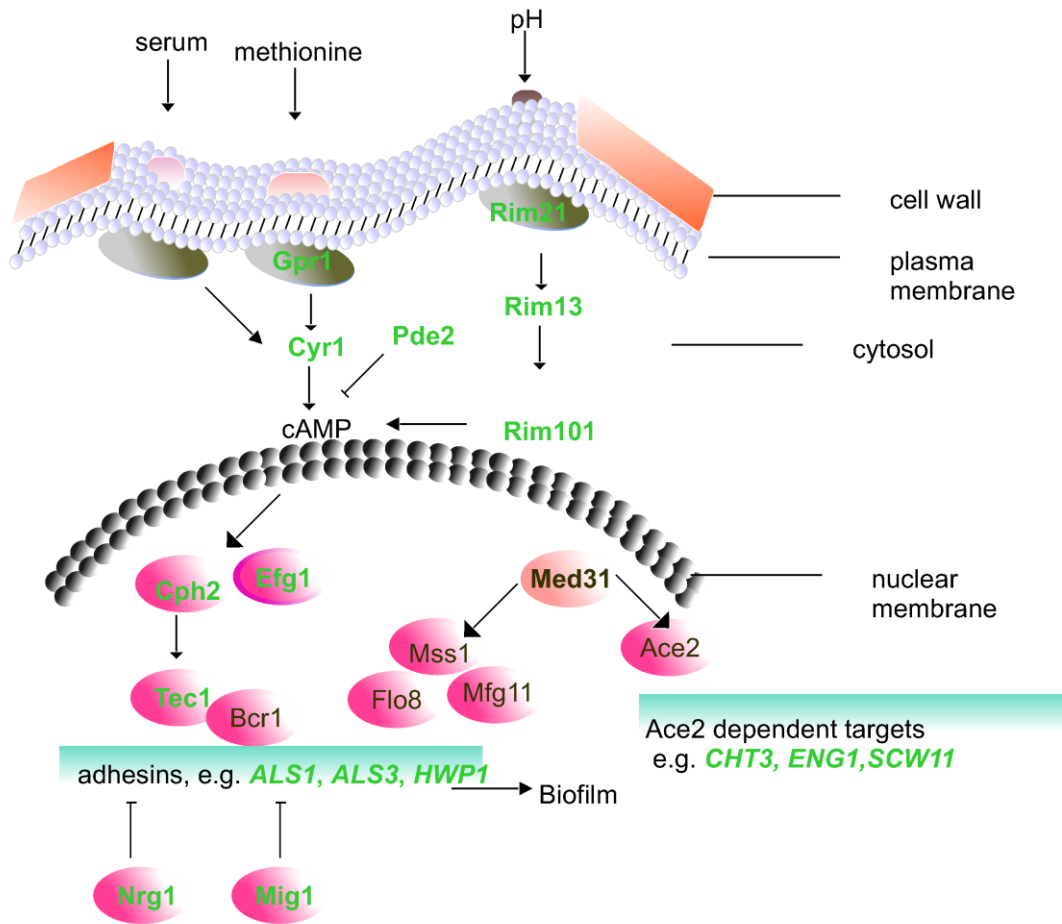


Figure 3.5. Mediator Subunits are required for the regulation of cell wall genes **A-D)** Cells from wild type, *ace2Δ/Δ*, or *med20Δ/Δ* mutants were grown in YPD at 30°C (yeast morphology) and levels of the indicated genes determined by quantitative PCR. The expression of the indicated genes was normalised to *ACT1* (A-B) and expressed relative to wild type levels, which were set to 1. Equivalent results were obtained when the glyceraldehyde-3-phosphate dehydrogenase (*GAPDH*) encoding gene *TDH3* was used for normalization (C-D). Shown are the averages of at least three independent experiments and the SEM. * $p \leq 0.05$, ** $p \leq 0.01$, *** $p \leq 0.001$, **** $p \leq 0.0001$. **E)** Cultures of wild type *C. albicans* and *med20Δ/Δ* mutants were grown to log phase and cells were observed by microscopy using DIC for bright field at 100x magnification.

It was interesting to find that the *med31Δ/Δ* mutant showed down regulation of transcription factors including *TYE7*, *TEC1*, *EFG1*, *NRG1*, *MIG1* and *CPH2*, all of which are required for the regulation of *C. albicans* hyphal switch morphology (Figure 3.6A). In addition to this, other components of the hyphal morphogenesis pathways were down-regulated including *GPR1*, *CYR1*, *PDE2*, *RIM101*, *RIM21*, and *RIM13* (Figure 3.6A). These results suggested that *med31Δ/Δ* mutant cells were compromised in the ability to correctly sense environmental cues and induce the morphological switch from yeast to hyphal cells. Furthermore, the adhesin *ALS1* and the hyphal specific *ALS3* and *HWPI* were down-regulated relative to *ACT1* levels in the *med31Δ/Δ* mutant compared to the levels in complemented strain when cells were grown in hyphal inducing conditions (Figure 3.6B).

A



B

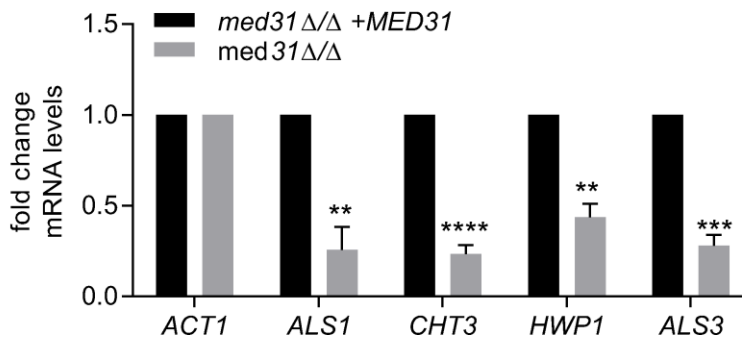


Figure 3.6. The Med31 subunit co-regulates the expression of components in the cAMP signalling pathway. A) The cartoon represents the steps in signalling occurring in the cytosol (upper section) and the transcription regulation within the nucleus including suggested possible factors that may interact with Med31 based on this study and other studies [45].¹⁷ Genes shown in green are down-regulated and had the consensus motif in Figure 3.4B similar to the Mss11 transcription factor in *S. cerevisiae* required for the expression of adhesin genes. Transcription factors are encircled in pink. Aside from the regulation of Ace2 dependent genes, the Mediator Med31 subunit may co-regulate genes with the Mss11 transcription factor. In *S. cerevisiae*, Mss11 interacts with Flo8 and Mfg1 to regulate the expression of adhesin genes [97]. **B)** Med31 expression of adhesin genes under hyphal inducing conditions. Cells from *med31Δ/Δ* mutant and *med31Δ/Δ+MED31* complemented strain were grown in Spider media at 37°C and levels of the indicated genes determined by quantitative PCR. The expression of the indicated genes was normalised to *ACT1* and presented values are relative to the levels in the complemented strain as this was used for microarray analysis. Shown are the averages of three independent experiments and the standard error of the mean. ** $p \leq 0.01$, *** $p \leq 0.001$, **** $p \leq 0.0001$.

¹⁷ Figure 3.6A contains combined information from this study and information obtained from Sudbery, 2011

To determine the ability of *med31Δ/Δ* mutant cells to switch morphology, wild type, *med31Δ/Δ* mutant and *med31Δ/Δ+MED31* strains were grown in various hyphal inducing liquid media for 6 hours, or on plates and the morphology of cells imaged. No filamentation was detected for the *med31Δ/Δ* mutant on solid media (Figure 3.7A) or in liquid cultures (Figure 3.7B) consistent with down regulation of hyphal morphogenesis components as determined in the microarray (Figure 3.4, 3.5 and 3.6). The *C. albicans med31Δ/Δ* mutant eventually formed some hyphal cells at later time points (Figure 3.8A), indicating it is delayed in making hyphal filaments, rather than completely defective. The *ace2* mutant as used as a comparison, and this revealed that the filamentation phenotypes of the *med31Δ/Δ* mutant were significantly stronger than any defects in the absence of ACE2 (Figure 3.7), suggesting Med31 acts via a different transcription factor in the filamentation program. The *med31Δ/Δ* mutant was also deficient in biofilm formation on serum-coated silicone squares (Figure 3.8B).

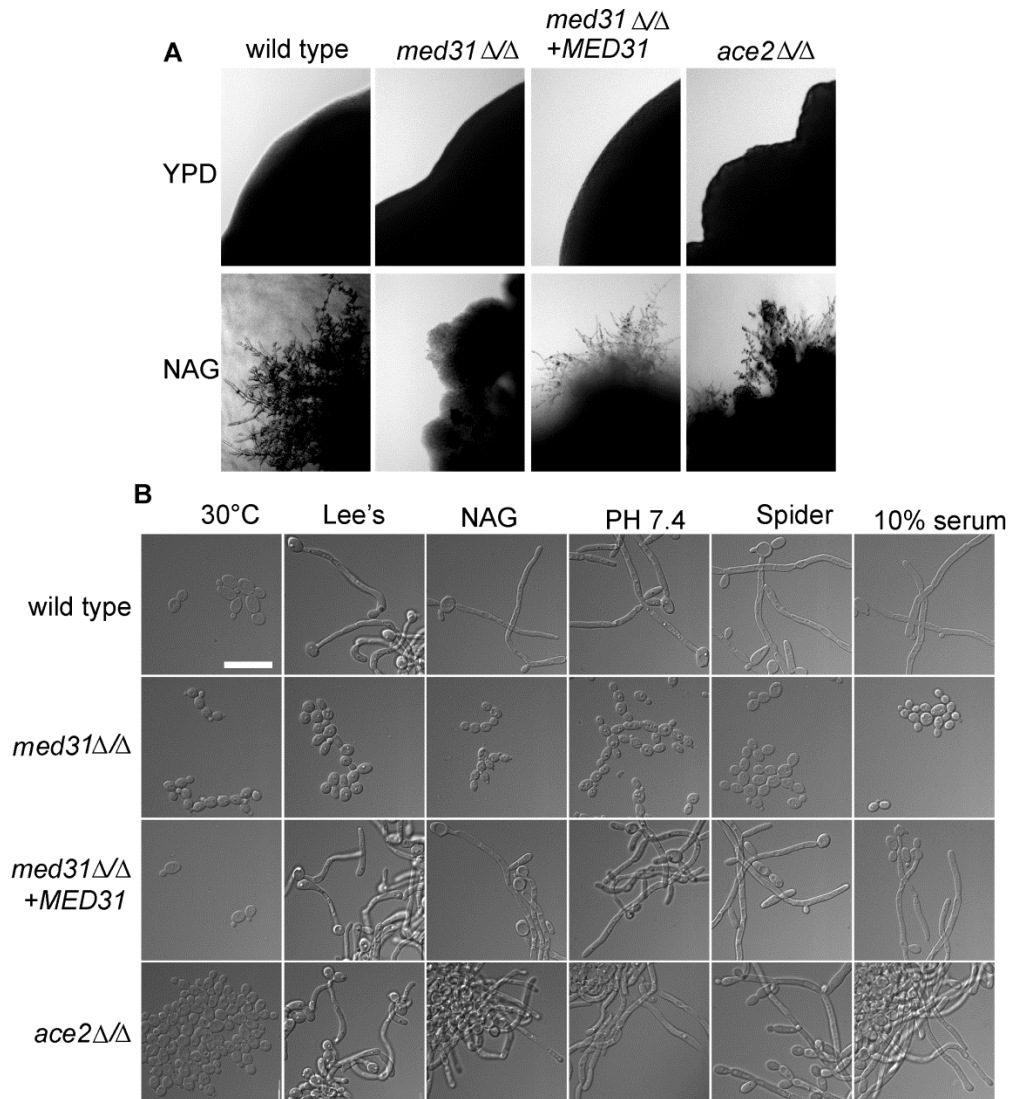


Figure 3.7. Mediator Med31 is required for filamentation in various hyphal inducing conditions. **A)** Representative images of the edges of colonies from wild-type, *med31*, *med31*+*MED31* and *ace2* deletion strains were photographed using the Olympus IX81 microscope at 10x magnification. **B)** Overnight cultures were grown in YPD to saturation and cells diluted into pre-warmed filamentation media. Control shows cells grown in YPD medium at 30°C, while filamentous growth was assessed at 37°C for cells grown under Lee's, N-Acetyl-glucosamine (NAG), pH7.4, Spider, and YPD +10% serum hyphal inducing conditions. Photographs were taken after 6 hours of growth in filamentation media. Scale bar is 20μm.

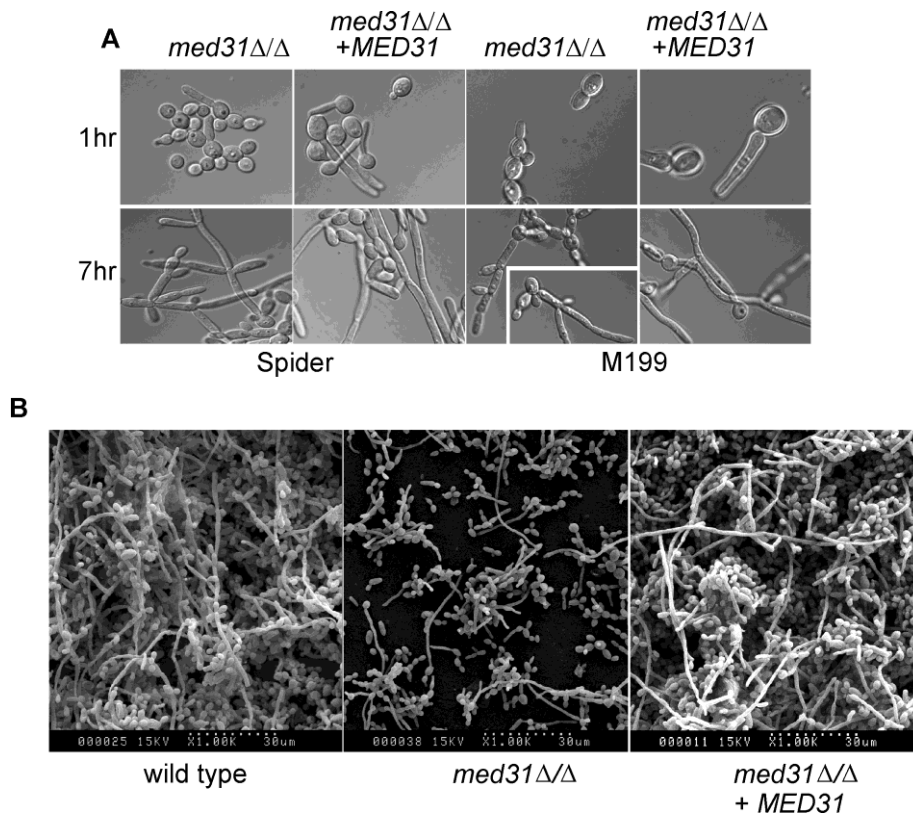


Figure 3.8. The Med31 subunit is required for biofilm formation. A) The *med31Δ/Δ* mutant eventually forms hyphal structures. Overnight cultures were grown in YPD to saturation and cells diluted into pre-warmed filamentation media. Filamentous growth was assessed at 37°C for cells grown under Spider and M199 hyphal inducing media. **B)** *In vitro* biofilm analysis of the *med31Δ/Δ* mutant. Scanning electron microscopy (SEM) of wild type and *med31Δ/Δ* mutant biofilms. Biofilms were formed *in vitro* on serum coated silicone disks. Mature biofilms (48 h) were imaged by SEM as described in [38].

Figure data BY: Yue Que¹⁸

¹⁸ Department of Biochemistry and Molecular Biology, Monash University, Clayton, Victoria, Australia

3.2.3. Med31 has divergent roles in adhesion between C. albicans and S. cerevisiae in adhesion

Previous reports suggested that the orthologue of the Med31 subunit in model yeasts *S. cerevisiae* and *S. pombe* co-regulates Ace2 dependent genes [126], however the Med31 protein was not implicated in regulation of hyphal morphogenesis, as these studies were conducted in the non-filamentous strains of *S. cerevisiae*. In order to determine whether the role of the Med31 subunit in adhesion is conserved in model yeasts, I deleted the Med31 orthologue *SOH1* in the filamentous *S. cerevisiae* Sigma1278b strain. The *soh1Δ* mutant was sensitive to formamide as expected based on previous published studies [127] in *S. pombe* and *S. cerevisiae* BY4741 strain, and this was complemented by re-introduction of the *SOH1* gene into the mutant (Figure 3.9A).

Growth of the *soh1Δ* mutant on non-hyphal inducing conditions (YPD agar) produced wrinkled colony morphology (Figure 3.9B). The wrinkled colony morphology depends on the adhesin gene *FLO11*, as deletion of *FLO11* results in smooth colonies (Figure 3.9B and [95]). Similar to *C. albicans* cells, the nutrient sensing cyclic adenosine monophosphate (cAMP)–protein kinase A (PKA) pathway control filamentous growth leading to activation of *FLO11*. *FLO11* belongs to a family with five other members *FLO1*, *FLO5*, *FLO9* and *FLO10*. Interestingly, these other members are adjacent to their respective telomeres, but *FLO11* is neither adjacent to a telomere nor a centromere and is generally the only member expressed in the Sigma 1278b strain genetic background, while other *FLO* genes remain silent [174]. The Flo11 adhesin facilitates *S. cerevisiae* invasive growth, biofilm formation and diploid pseudohyphal growth phenotypes [174, 175].

Wrinkled morphology could also result from a cytokinesis defect, as observed in the *C. albicans med31Δ/Δ* and *ace2Δ/Δ* mutants (Figure 3.1B and [115, 116]). In rich media (YPD), the levels of *FLO11* were not different between the wild type and the *soh1Δ* mutant (Figure 3.9C). They increased slightly in the mutant when minimal media with 2% glucose was used (Figure 3.9C). However, in low 0.2% glucose media, which promotes *S. cerevisiae* Σ1278b strain adherence to plastic, ~40 fold

increase in transcript of *FLO11* in *soh1Δ* cells was observed (Figure 3.9C). The other *FLO* gene family members (*FLO1*, *FLO5*, *FLO9* and *FLO10*) were not differentially expressed in the mutant under any of the tested conditions (Figure 3.9). The *soh1Δ* mutant cells also showed a flocculation phenotype (Figure 3.9D). Morphological analysis of cells sonicated and grown in YPD to log phase suggested that a combination of a cytokinesis defect and overexpression of adhesion genes lead to the hyper- wrinkled morphology (Figure 3.9E).

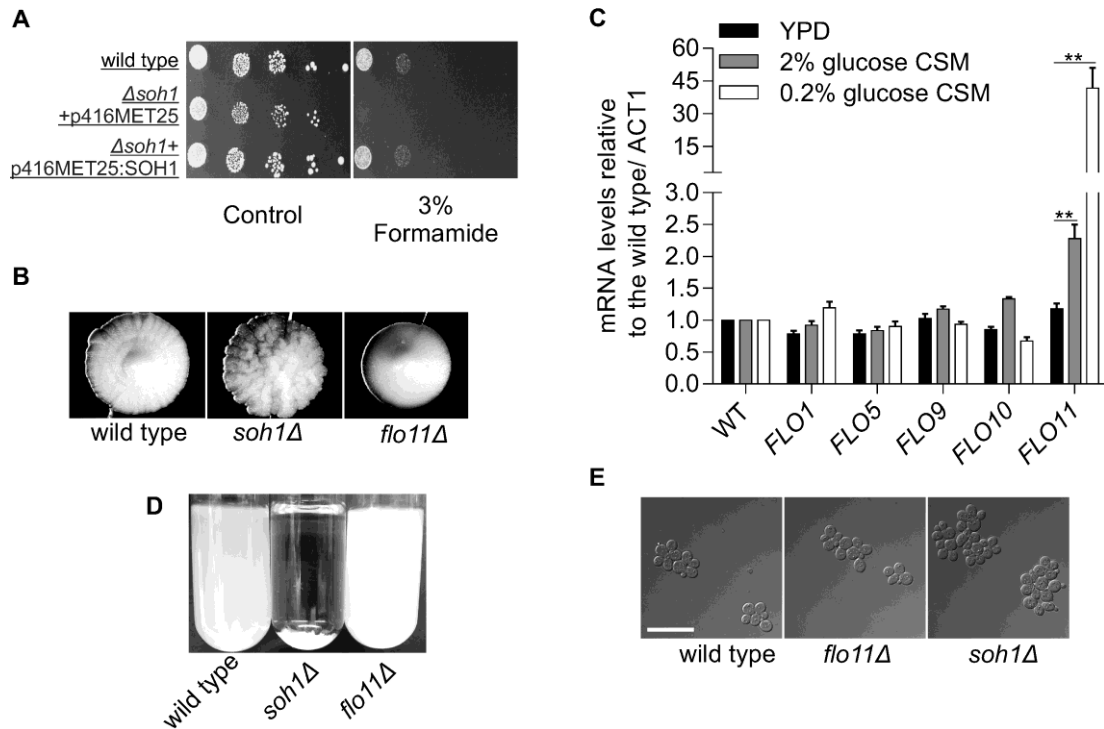


Figure 3.9. The Med31 (Soh1) subunit in the model yeast *S. cerevisiae* regulates cytokinesis, adherence and flocculation. **A)** Sensitivity assay of *soh1* to formamide. Wild type *S. cerevisiae* $\Sigma 1278b$, *soh1* Δ mutant and complemented strain containing a single copy of the SOH1 gene was subcloned into the centromeric plasmid p416MET25 plasmid downstream of the MET25 promoter and under the CYC1 terminator. For the control, cells were grown at 30°C on CSM plates containing low methionine (20mg/L) [176] while 3% formamide was added on test plate. **(B)** Colonies of wild type *S. cerevisiae* $\Sigma 1278b$ and the *soh1* Δ mutant were grown on YPD plates at 30°C and photographed. The *flo11* Δ strain was used as a control, to show smooth colony morphology in the absence of FLO11. **(C)** Wild type and mutant cells were cultured in different growth media and cells were harvested during log phase. Levels of FLO11 were normalized to ACT1, and expressed relative to the wild type, which was set to 1. Shown are averages from three independent biological cultures and the standard error. ** $p \leq 0.01$. **(D)** Flocculation of *soh1* Δ cells. Flocculation assessment of wild type *S. cerevisiae* $\Sigma 1278b$ and the *soh1* Δ mutant were grown overnight in YPD media at 30°C with shaking (200rpm) and photographed. **(E)** Cells were grown in YPD at 30°C with shaking (200rpm) and sonicated. Shown here are DIC images. The Scale bar is 20 μm .

Next, the influence of Soh1 in adherence to plastic and biofilm formation was evaluated. Cells depleted of Flo11 are unable to form a highly structured pattern of multicellular confluent mat or biofilm on 0.3% YPD agar. The Flo11 protein also facilitates a process called “sliding motility” that favours reduced friction between the cells and the substrate in addition to the expansive forces of the growing cell population forming the wild type biofilm (Figure 3.10A, wild type) [95]. The mat or biofilm has two parts; the central core (hub) is composed of cells that exhibit very little growth in the biofilm and the outer area (rim) where cells are actively growing outward. The outward extension of the biofilm is facilitated by Flo11-dependent cell to cell adhesion. Assessment of the biofilm formation shows that the wild type cells form a biofilm that extends outward (Figure 3.10A). In comparison the *soh1Δ* mutants showed less biofilm extension, instead, the *soh1Δ* biofilm showed an elevated structure, as if the biofilm was growing upward instead of extending outwards extension to colonize all the media (Figure 3.10B). *soh1Δ* biofilms did not show a smooth structure similar to the biofilm that lacks the Flo11 protein, instead, the biofilm surface morphology albeit more compact, was similar to wild type hub morphology (Figure 3.10A). The biofilms formed by the *soh1Δ* mutant were smaller compared to wild type cells however with greater ability to adhere to plastic culture plates (Figure 3.10C). A recent whole-genome study in the *S. cerevisiae* Sigma1278b strain ability to form biofilms showed consistent results with our findings suggesting that the *soh1Δ* mutant make smaller biofilm mats [97], although adherence is increased (Figure 3.10C).

Invasive growth was also assessed where wild-type cells streaked on a solid (2% agar) YPD agar adhered to the surface of the agar plate, even when washed with water. There was no measurable difference between wild type and *soh1Δ* mutant cells, however, when the plate was rubbed with a gloved finger to more thoroughly remove non-invasive *soh1Δ* cells, the mutant showed a greater level of invasive growth compared to the wild type (Figure 3.10D).

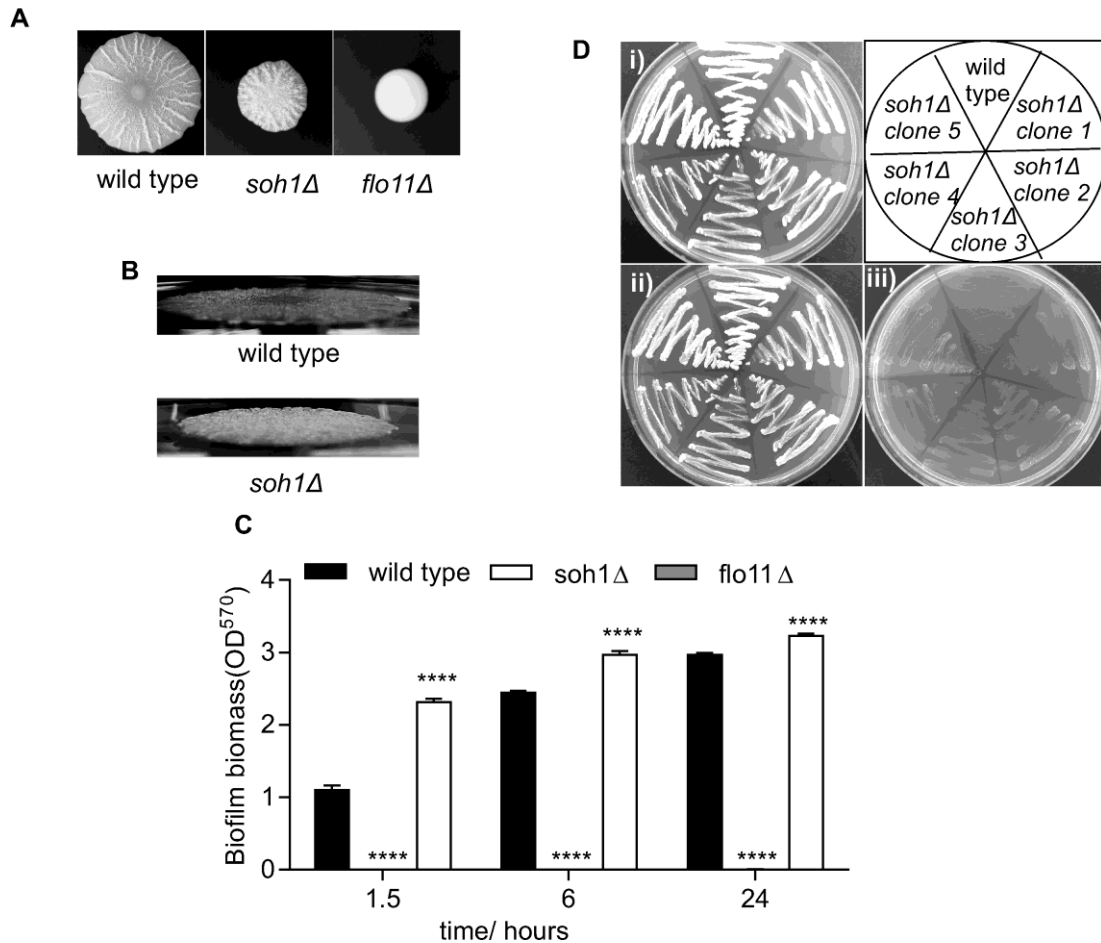


Figure 3.10 The Med31 (Soh1) subunit in the model yeast *S. cerevisiae* regulates biofilm formation and agar invasion. **A-B** Elevation of biofilm formation in *soh1Δ* mutants. Wild type *S. cerevisiae* $\Sigma 1278b$ and the *soh1Δ* mutant were grown for 7 days on 0.3% agar, 2% glucose YPD media. The formation of *S. cerevisiae* biofilm mats was documented. Shown are the top (**A**) and the side (**B**) view of the biofilm mat. **C**) *S. cerevisiae* adherence to polystyrene. *S. cerevisiae* wild type and *soh1Δ* mutant cells were cultured in 0.2% glucose synthetic complete media (CSM) as described in Materials and Methods. Quantification was performed by crystal violet staining. At least three independent cultures were used, assayed in quadruplicates. For the mutant, two independently constructed deletion strains were used and gave equivalent results. The *flo11Δ* mutant was assayed in parallel as a negative control and showed no adherence at any of the time points (not shown). Error bars represent SEM. Biomass significant difference of mutants compared to wild type biomass **** $p < 0.0001$. **D**) Med31 in *S. cerevisiae* affects invasive growth. **i**) The strains were streaked onto YPD plates and grown at 30°C for 5 days. **ii**) The plates were then washed with water to remove non-invasive cells. **iii**) The plates were washed with water and rubbed with a gloved finger to more thoroughly remove non-invasive cells. The diagram at upper right indicates the placement of the different strains on the plates.

3.2.4. *The Mediator Kinase domain plays a role in cell wall gene expression in C. albicans*

Previous studies in *S. cerevisiae* showed the requirement of components of Kinase module in the regulation of genes required during yeast diauxic shift. The subunits of the Kinase domain were required for proper entry of cells into the stationary phase of growth, and lack of these subunits led to altered expression of the cell wall-related secretory glycoprotein, *YPG1* [177]. Hence I investigated whether the role of cell surface components was conserved in *C. albicans* by looking at the expression levels of adhesins in kinase module *srb9* Δ/Δ mutant at log and stationary phases of growth using complete synthetic medium. The levels of the *ALS1* at log phase were similar between wild type and *srb9* Δ/Δ mutant cells (Figure 3.11A). However, greater *ALS1* levels compared to wild type cells were observed at stationary phase (Figure 3.11A).

ALS3 appeared up-regulated in the mutant in both logarithmic and stationary phase of growth, while *HWPI* was up-regulated in stationary phase (Figure 3.11A). The overexpression of these adhesins in cells lacking *Srb9* suggested that *Srb9* acts in the repression of these adhesion genes, particularly in the stationary phase of growth (Figure 3.11A). It appears however that the roles of the Kinase domain in adhesion in *C. albicans* are complex, as studies in our lab have shown that the levels of the adhesins *ALS3* and *HWPI* tend to expressed at lower levels in the *srb9* Δ/Δ mutant when grown in hyphal growth conditions (Spider media at 37°C) *in vitro* (shown in Figure 3.10B and published in [38]), and the *srb9* Δ/Δ mutant shows biofilm formation defects in polystyrene [38]. Interestingly, the *srb9* Δ/Δ mutant cells appeared to have a mild cytokinesis defect (Figure 3.11C).

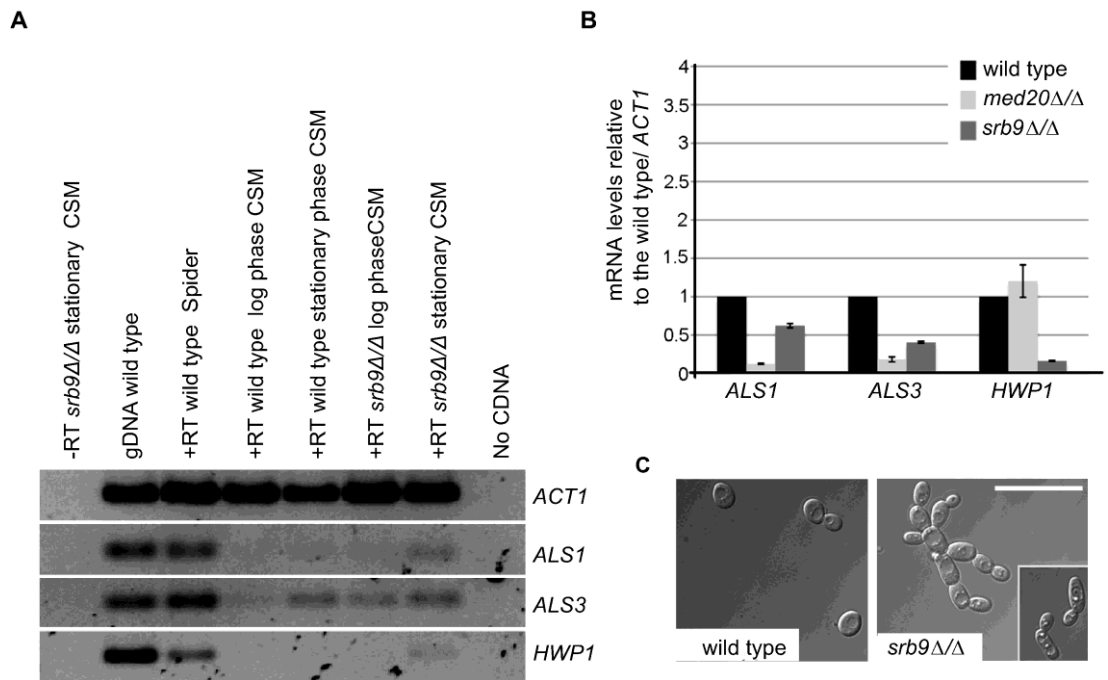


Figure 3.11. Mediator Med20 and Srb9 are required for adhesin gene expression. **A)** Wild type DAY286 and *srb9Δ/Δ* mutant were grown in CSM media and sampled at either log or stationary phase of growth and RNA was extracted for RT PCR. The PCR reactions were compared by 2% high resolution TBE-agarose gel electrophoresis. *ACT1* transcript levels served as control. Wild type grown in hyphal growth media (Spider, 37 °C) was used as a positive control, as this condition leads to up-regulation of the transcription of the adhesin genes. **B**¹⁹ and **C)** wild type and mutant strains were grown in Spider growth media and cells were harvested for qPCR analysis. Levels of genes were normalized to *ACT1*, and expressed related to the wild type, which was set to 1. Shown are averages from at least three independent biological repeats in with standard error. * $p \leq 0.05$, ** $p \leq 0.001$. **C)** Cultures of wild type *C. albicans* and *srb9Δ/Δ* mutants were grown in YPD to log phase and cells were observed by microscopy. The wild type is the same as in Figure 3.5E. Shown are DIC images with cells at 100x magnification.

¹⁹ Figure 3.10B was conducted by Branka Jelacic, Department of Molecular Biology, Rud-er Boskovic' Institute, Bijenic'ka 54, 10000 Zagreb, Croatia

3.2.5. Effects of Mediator mutations on stress-responsive phenotypes in *C. albicans*

To further examine the global effect of the lack of Mediator components on *C. albicans* cell wall and cell membrane integrity and stress responses, I tested the sensitivity of Mediator mutants to cell wall and cell membrane targeting agents, as well as several other stressors (Table 3.4 and Figure 3.12). The *med31Δ/Δ* mutant showed high sensitivity to membrane targeting agents including formamide, DMSO and nystatin and was also sensitive to growth at lower temperatures (16°C) (Figure 3.11). A compromised cell surface structure was further reiterated by the sensitivity of this mutant to Congo red and SDS agents, and a higher resistance of the *med31Δ/Δ* mutant to calcofluor white. Calcofluor white is toxic to yeast cells as it binds chitin in the cell wall. The *med31Δ/Δ* mutant was also mildly sensitive to the oxidative agent, H₂O₂, severely sensitive to salt stress and ethanol, but able to grow at high temperatures.

The *med20Δ/Δ* mutant showed mild sensitivity or no sensitivity to cell wall, cell membrane, oxidative and salt stress relative to *med31Δ/Δ* cells (the *med20Δ/Δ* phenotypes were intermediate between *med31Δ/Δ* and wild type cells). Calcofluor white sensitivity of the *med20Δ/Δ* mutant was similar to the wild type. The *srb9Δ/Δ* mutant did not show sensitivity to any of the membrane compromising agents, but was sensitive to all the cell wall compromising agents, oxidative stress and ethanol. Menadione is also another compound that produces deadly ROS [178]. Interestingly treatment of the *C. albicans med31Δ/Δ* and *srb9Δ/Δ* mutant showed higher sensitivity to menadione compared to wild type, consistent with our findings on treatment with hydrogen peroxide (Figure 3.12B). Collectively, these results suggest that Med31 regulate cell wall and cell membrane integrity. Srb9 is important for cell wall integrity, but not for membrane integrity.

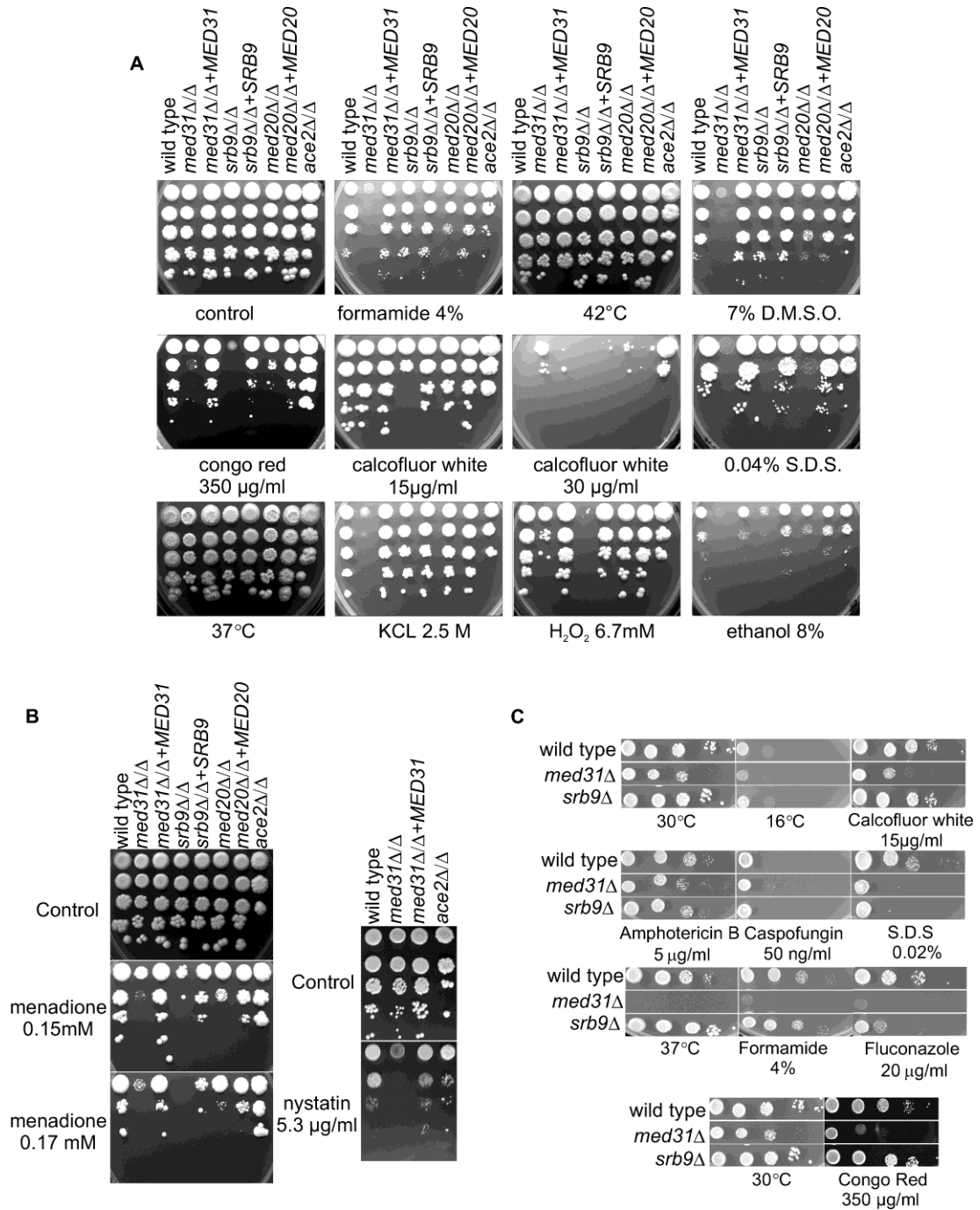


Figure 3.12. Sensitivities of the *C. albicans* Mediator mutants to various stresses. 10 fold serial dilutions of the wild type, Mediator mutants and complemented strains were dropped on YPD plates containing the indicated compounds. The plates were incubated at 30°C (unless stated otherwise) for 3–4 days and photographed. **B)** Oxidative stress was also tested using menadione. **C)** Sensitivities of the *S. cerevisiae* Mediator mutants to various stresses.

Table 3.4. Stress responsive phenotypes of Mediator mutants

	<i>S. cerevisiae</i>		<i>C. albicans</i>			
	<i>med31Δ</i>	<i>srb9Δ</i>	<i>med31Δ/Δ</i>	<i>ace2Δ/Δ</i>	<i>med20Δ/Δ</i>	<i>srb9Δ/Δ</i>
Conditions affecting membrane integrity						
Formamide	++	–	++	–	+/-	–
DMSO	+	R	++	–	+/-	–
Nystatin	–	–	++	+/-	ND	ND
16°C	ND	ND	+	+	–	–
Conditions affecting cell wall integrity						
Congo red	+	–	+	–	+/-	++
Calcofluor white	+	–	R	R	–	+
SDS	+	R	++	–	+	+
Other stresses						
Oxidative stress (H2O2)	+	R	+	-/+	–	++
Salt stress (NaCl)	–	–	++	–	–	–
37°C	+	–	–	–	–	–
Ethanol	+	+	++	–	+/-	+
++ very sensitive; + sensitive; +/- mildly sensitive; – wild type phenotype; R resistant; ND not determined.						

Similar sensitivity assay was conducted on Mediator genes deleted using the *S. cerevisiae* BY4741 strain (Table 3.3 and Figure 3.12C). There was a conserved role of the Med31 in cell wall and cell membrane biogenesis, but in contrast to the resistance observed in *C. albicans*, the *S. cerevisiae med31Δ (soh1Δ)* cells were sensitive to calcofluor white and 37°C (Figure 3.12). More interesting was that the *S. cerevisiae srb9Δ* mutant cells which showed no sensitivity to either cell wall or cell membrane compromising agents. Instead, I observed resistance to DMSO, SDS, and oxidative stress (Figure 3.12C and Table 3.3). These sensitivity assays in *S. cerevisiae*, suggested a shared role between the Med31 subunits in regulation of cell wall and membrane morphogenesis, while some resistance to antifungals required the Srb9 subunit.

3.3. DISCUSSION

3.3.1. *The Mediator complex is required for C. albicans morphological remodelling and general cellular processes*

Morphological analysis of the Mediator mutants showed conserved and divergent roles between *C. albicans* and model yeast *S. cerevisiae* and *S. pombe*. I was able to delete both alleles encoding the Med31, Med20 or Srb9 subunits showing that these subunits are not essential in *C. albicans*, consistent with previous reports in model yeasts [125, 146]. I identified three major roles of the Middle module Med31 subunit in dictating *C. albicans* cellular features required for correct morphogenesis: 1) Med31 co-regulates genes required for cytokinesis via the Ace2 transcription factor and possibly also interacts with other transcription factors including Mss11; 2) Med31 is required for filamentation and positive transcription of components of the PKA/cAMP pathway, 3) *med31* Δ/Δ mutant cells are inefficient in biofilm formation and expression of adhesin genes under hyphal/ biofilm growth conditions. I also found there were similarities in the function of Med20 in *C. albicans* and model yeasts. Interestingly, analysis of the components of the Kinase module, suggested that the roles of the Mediator complex in cell wall biogenesis are dynamic and depending on stimuli, the subunits may act in gene activation or repression.

3.3.2. *Mediator interacts with transcription factors involved in cellular morphogenesis*

Mediator has an important role in sending regulatory information from activators and repressors of genes that are bound to upstream promoter elements to the RNA polymerase II transcription initiation machinery [129]. The cytokinesis defect observed in the *med31* Δ/Δ mutant (Figure 3.1A) suggested functional associations with the Ace2 transcription factor. Analysis of the *med31* Δ/Δ mutant transcriptome suggested that Med31 is required for transcription of Ace2-dependent genes, including *CHT3*, which encodes the chitinase responsible for cell wall remodelling and cytokinesis in *C. albicans*. This is in agreement with a previous study [124] in model yeast where deletion of *MED31* reduced the expression of

Ace2-dependent genes. The *C. albicans med31Δ/Δ* mutant did not show differential regulation of the *ACE2* transcript, suggesting that Med31 does not regulate Ace2 dependent genes through down regulation of *ACE2*, but rather it might be physically interacting with Ace2. That this mechanism might be at play is supported by studies in *S. pombe*, where it has been shown that the essential Mediator Head domain subunit Med8 interacts with Ace2, and links the transcriptional activator to RNA pol II by also interacting with the Rpb4 subunit of the polymerase [179]. The difference in the degree of cytokinesis defects and the growth rate between *med31Δ/Δ* and *aceΔ/Δ* strains suggested that Med31 is not absolutely essential for Ace2-dependent transcription, and also that Med31 has Ace2-independent roles in cell growth and division. *C. albicans*.

Genome wide analysis of the *C. albicans med31Δ/Δ* mutant showed that although Med31 is not essential for transcription, it is involved in differential regulation of a large set of genes pertaining to many important cellular processes (Figure 3.3, Table 3.1 and Table 3.2). Consistent with this large effect on gene transcription, *med31Δ/Δ* grow significantly slower than wild type cells. A larger proportion of genes were down-regulated in comparison to the up-regulated genes, suggesting that Med31 is primarily a co-activator of transcription in *C. albicans*. The up-regulated genes corresponded to similar process categories of the down-regulated genes, and thus they were up-regulated possibly as a compensatory response to the down-regulated genes (Table 3.1). With regards to the regulation of genes required for the control of *C. albicans* morphogenesis, the motif identified in a subset of Med31 gene targets suggests that the Med31 subunit may also interact with the *C. albicans* transcription factor Mss11. Levels of *MSS11* were not affected in the *med31Δ/Δ* mutant, suggesting that the effect on Mss1-dependent genes is not indirect. In *S. cerevisiae*, Mss11 has roles in filamentous growth regulated by both the MAPK cascade and the cAMP-PKA pathway ([180] and role depicted in a sketch Figure 3.6A). The Mss11 protein was previously identified as a regulator of filamentous growth required for the transcriptional activation of the glucoamylase *STA2* and expression of *FLO11* in some conditions [180]. The *C. albicans* Mss11 has been shown to interact with Flo8 and to be an activator in hyphal development and hyphal-specific gene expression (Figure 3.6A). Mss11 deletion in *C. albicans*

impairs hyphal formation and expression of hyphal specific genes including *HWP1*. Indeed, we find similar morphological impairments in the *med31Δ/Δ* mutant suggesting the Med31 and Mss11 may coordinate transcriptional activity to regulate hyphal morphology *C. albicans* (Figure 3.6A). The transcript levels of *FLO8* were not affected in the *med31Δ/Δ* mutant, supporting possible co-factor activity between Med31, Flo8 and Mss11, although the exact association still needs to be examined. Only recently, the Flo8 and Mss11 and Mfg1 were shown to interact for the expression of adhesins in *S. cerevisiae* (Figure 3.6 and [97]). Previous studies suggested that the dependency of the transcription factors Flo8, Msn1 and Ste12 on Mss11 for strong transcriptional activation in response to nutrients could be the result of Mss11 associations with co-regulators [180]. My results suggest that this may include Mediator.

3.3.3. Core Mediator and Kinase domain mutants have distinct phenotypes

Mutagenesis of the *MED31* and *MED20* genes in model yeasts lead to similar phenotypes and these Mediator subunit have overlapping functions in gene regulation [125]. Consistently, the *C. albicans med20Δ/Δ* mutant had similar phenotypes, although generally milder, to those observed for the *med31Δ/Δ* mutant, in regards to sensitivity to cell wall and membrane targeting agents (Table 3.4 and Figure 3.12), but also hyphal morphogenesis (Figure 3.7). These results suggest conservation in *C. albicans* of the reported functional overlap in gene regulation between the Med31 and Med20 subunits of Mediator. Transcriptomics across Mediator mutants in *S. cerevisiae* showed that the Kinase domain subunits have distinct roles in gene expression to the core Mediator complex [172]. My data in *C. albicans* reflects this as well – the Kinase domain mutant *srb9Δ/Δ* displayed different phenotypes to the core complex mutants *med31Δ/Δ* and *med20Δ/Δ*. This was true in regards to stress responses and cell wall and cell membrane targeting drugs (Table 3.4) and morphogenesis (see Chapter 4).

3.3.4. The Mediator complex plays complex roles in fungal adhesion and cell wall proteome expression

My results suggest that in *C. albicans* Mediator has complex roles both as an activator and as a repressor of adhesion-dependent phenotypes in fungi. Consistent with reports in *S. cerevisiae* [181], the *C. albicans* Kinase domain mutant *srb9Δ/Δ* overexpressed some cell wall adhesin genes under conditions in which these are normally repressed (Figure 3.11A). Interestingly, under conditions inducing for filamentation, we found that adhesin gene expression tends to be down-regulated in cells lacking Srb9 [163]. The Kinase domain of Mediator is mainly considered to be involved in gene repression, however the subunits can have both positive and negative effects on transcription [182]. Our results suggest that the activity of the Kinase module is utilized by *C. albicans* in the regulation of adhesins in such a way that the role of Kinase subunits is varied to accommodate the cell wall remodelling required in the yeast and hyphal morphologies. The precise nature of the effect of Kinase domain subunits on adhesion gene expression appeared to be dependent on nutrient conditions. With this in mind, it is of note that Spider medium is inducing for hyphal morphogenesis but it is also nutrient limiting. A subsequent study in our lab described in Chapter 4 of this thesis showed no differences in adhesion gene expression between wild type hyphal cells and the *srb9Δ/Δ* mutant upon ingestion of *C. albicans* by macrophages, suggesting that the effect of Srb9 on cell wall proteome expression is very much condition-dependent. A similar conclusion was reached for other transcriptional regulators of *C. albicans* cell wall proteome expression, most notably Bcr1 [103]. More work is required to understand precisely how the Kinase domain of Mediator regulates adhesion in *C. albicans* and other fungi.

The core Mediator subunits Med31 and Med20 were required for positive transcription of adhesin genes in both yeast and hyphal morphology (Figure 3.5A and Figure 3.6B). The transcriptional deregulation of adhesins and transcription factors in the cAMP pathway was reflected in the inability of the *med31Δ/Δ* mutants to induce hyphal morphogenesis (Figure 3.7) and biofilm formation (Figure 3.8). Of note, *med31Δ/Δ* mutant cells eventually form filamentous structures, and so this mutant is

not completely defective, but rather delayed in transitioning to the hyphal state. It is well established that under conditions used in our study, the adhesin genes affected in *med31Δ/Δ* cells are targets of the *C. albicans* transcription factor Bcr1 [77, 119]. There was no significant changes observed in transcript levels of *BCR1* in the *med31Δ/Δ* mutant (data not shown but published in [163]). Hence Med31 may be required for the expression of adhesins as a co-activator for Bcr1.

In contrast to reduced adherence of the *med31Δ/Δ* mutant in *C. albicans*, my results show that the *S. cerevisiae*, *med31Δ (soh1Δ)* mutant has phenotypes consistent with hyper-adherence: the mutant is highly flocculent, it produces wrinkled colonies, it is hyper-adherent to polystyrene and forms biofilm mats that, although smaller, are of aberrant, elevated structure. The mutant is also hyper-invasive into the agar. My results are consistent with these phenotypes resulting from a combination of effects on cytokinesis through Ace2-dependent gene expression, and effects on *FLO11* transcription. The levels of *FLO11* transcript showed an increased expression in the *med31Δ (soh1Δ)* mutant, but only under some conditions (Figure 3.9C). The condition where *FLO11* was overexpressed was low glucose, 0.2% glucose synthetic complete media, the same condition in which the *med31Δ (soh1Δ)* mutant hyper-adhered to polystyrene. This suggests that *FLO11* overexpression might be causative of the increase adherence.

The *med31Δ (soh1Δ)* mutant showed a smaller biofilm of elevated structure, which entirely resembled the hub of wild type biofilm. This phenotype could be a result of variation in intercellular and cell to agar adhesive strength leading to a more compact biofilm relative to wild type cells [183]. The biofilm mat formation assay was performed in 2% glucose conditions in rich YPD media, in conditions in which the *FLO11* gene was not overexpressed in the *med31Δ (soh1Δ)* mutant. Therefore, effects of Med31 on cytokinesis and the increased attachment of cells to each other that result from that could be the cause of the “tall mat” phenotype in the mutant. Consistent with this idea, in a recent whole genome analysis of biofilm in the Sigma

1278b strain of *S. cerevisiae ace2* mutant was shown to have a similar biofilm mat phenotype to my *med31Δ (soh1Δ)* mutant [97]²⁰.

Conclusions and end of chapter summary

In this Chapter I presented the functions of the *C. albicans* Mediator in the regulation of immunologically relevant morphogenesis factors. Mediator subunits were shown to regulate cytokinesis, filamentation and biofilm related factors, likely in collaboration with known transcription factors. The results in this Chapter also highlighted the divergence in some cellular roles of the Med31 subunit between *C. albicans* and *S. cerevisiae* that are relevant for *Candida* pathogenesis, namely adhesion and invasion properties. In the next chapter, the role of *C. albicans* Mediator in host immune recognition and evasion was studied.

²⁰ Ryan *et al.*, 2012, Table S3

Chapter 4: The functions of Mediator and host programmed cell death pathways in C. albicans macrophage evasion

4.1. Introduction:

In Chapter 1, basic concepts on the roles of yeast and hyphal morphologies and host-pathogen interaction were introduced including cell surface adhesion and biofilm formation. The cell surface of *C. albicans* also mediates interactions with the host immune system. Macrophages in particular are at the forefront of innate immunity with functions in detecting the pathogen, and triggering the immune response including phagocytosis and destruction of the pathogen [61, 184]. We are only beginning to understand the specific mechanisms that enable *C. albicans* cells to survive phagocytosis by host innate immune cells, as well as to escape to sustain the infection, but studies in murine macrophages have provided the basic principles.

4.1.1. Phagocyte invasion

To facilitate fungal cell recognition, host cells employ receptors known as pattern recognition receptors (PRRs) [185]. PRRs include Toll-like receptors (TLRs), C-type lectin receptors (CLRs) and Nod-like receptors (NLRs), which are expressed in immune cells such as dendritic cells and macrophages [44]. These receptors recognize specific types of fungal components known as pathogen associated

molecular patterns or PAMPs (reviewed by [186]); the interaction of PRRs with PAMPs leads to the induction of host cell intracellular signalling, eventually resulting in distinct gene expression profiles and activation of signaling pathways to mount an immune response [187-190]. β -glucan, chitin and, mannoprotein are carbohydrate polymer components of the fungal cell wall which play important roles for fungal recognition by phagocytes [44, 191]. For example, the PRR dendritic cell associated C-type lectin- 1 (Dectin 1) which is present on several immune cells, binds the fungal PAMP β -1,3 glucan [192], while the Dectin-2 receptors recognize α -mannan, and the Toll-like receptors (TLRs), TLR2 and TLR4 recognize phospholipomannan and O-linked mannan respectively [193]. Chitin was suggested to possibly associate with TLR2, Dectin-1 or the macrophage mannose receptor (MR), but the exact mechanism remains under investigation [194]. Fungal uptake is dependent on host cell type and anatomical location, opsonins and fungal cell wall composition [185]. Once pathogens are phagocytosed, phagosomes mature, which involves vesicle fission and fusion with lysosome leading to the development of the phagolysosome. The phagolysosome is a compartment in macrophages in which the fungus is killed using potent antimicrobial activities such as acidification and respiratory burst [195].

4.1.2. Fungal immune evasion and escape

To counteract immune destruction, pathogens have mechanisms to avoid death within phagolysosomes. For example, in the case of the bacterial pathogen *Mycobacterium tuberculosis*, the pathogen is capable of inhibiting phagosome-lysosome fusion, which allows for the establishment of a latent infection that can last for years [196]. *Histoplasma capsulatum* blocks the fusion of the phagosome to the lysosome and modifies intra-phagosomal pH [197]. However, the magnitude of these activities depends on the type of host phagocyte [197-199]. *C. albicans* cells may evade phagosomal destruction by expressing detoxifying enzymes on the cell surface (e.g. catalase, superoxide dismutases) that abolish oxidative-stress associated species including reactive oxygen and nitrogen species (ROS/RNS) [200, 201]. In addition to this, *C. albicans* cells are able to switch to gluconeogenic metabolism [202], and it was proposed that cells could be surviving on an amino acids within macrophages

due to the induction of the arginine biosynthetic pathway which also acts to neutralize intra-phagosomal pH and could be promoting hyphal differentiation inside macrophages [201].

C. albicans can also use non-lytic egress, where there is no lysis of the phagocyte and so the host cell survives after pathogen escape, but this mechanism is rare and so its importance remains to be understood [203]. *Cryptococcus neoformans* phagocytosis leads to formation of “leaky” phagolysosomes [204]. Similar to *C. albicans*, *C. neoformans* escape may also not lead to host cell death, but rather involve an expulsion from the macrophage that was termed “vomocytosis” [205, 206]. *C. neoformans* contains a protective capsule on its surface, which can be significantly enlarged as a protection mechanism against the damaging phagolysosomal environment [207]. This then in turn enables replication of the pathogen and causes macrophage lysis [208]. Inhibition of phagosomal maturation has been observed in *C. krusei* [209], and *C. albicans*, also uses this survival mechanism inside epithelial cells [167, 210, 211]. A major advantage of *C. albicans* and *Aspergillus fumigatus* is that these pathogens can escape from the phagosome by generating hyphae, which leads to destruction of the host cell [212]. Curiously, this only occurs in certain phagocytes such as selected macrophage and monocyte populations, while in neutrophils *C. albicans* filamentation is inhibited [212]. The presumed mechanism by which hyphal filaments enable fungal escape is mechanical destruction of macrophage cell integrity. However, as further discussed below, not all experimental data can be reconciled with this model [85, 213, 214]. It is established that bacterial pathogens can induce lytic suicide pathways in host cells, such as pyroptosis and use them for escape [215, 216], but whether fungal pathogens do the same was unknown at the commencement of my project.

4.1.3. *C. albicans* morphology inside macrophages

Wozniok *et al.* demonstrated that phagocytes are able to discriminate between wild type yeast or hyphal cells of *C. albicans*, as neutrophil migration and phagocytosis was specifically towards hyphal cells [217]. Surprisingly, the *TUPI* deletion mutant which remains constitutively filamentous, was unable to elicit

similar response from neutrophils as wild type hyphae, suggesting that other factors aside from filamentation are necessary in fungal-host cell induced responses [217]. When phagocytosed by macrophages, *C. albicans* yeast cells switch to hyphal cells [47]. The specific factors that lead to this transition are unknown as the phagosomal environment is acidic and thus not conducive to *C. albicans* filamentous transition; metabolic changes in the macrophage environment, perhaps even driven by *C. albicans* itself, might lead to changes in pH and CO₂ levels resulting in a host situation that would promote hyphal differentiation [202, 213].

It has been firmly established, starting with early work from Gerry Fink's lab, that hyphal morphogenesis is a key determinant for the escape of *C. albicans* from macrophages [47, 86, 169, 218, 219]. As mentioned the current view suggests that the polarized growth of hyphae leads to piercing of macrophage membranes and fungal escape [220]. This view is supported by the fact that yeast cells are unable to escape from macrophages [219-221]. However, it has become clear in recent years that the ability of *C. albicans* to grow as hyphae does not necessarily result in the ability of cells to escape from macrophages. For example, some cell wall mannosylation mutants make hyphae in macrophages as well as wild type strains, but do not egress as efficiently [213]. Additionally, some transcription factor mutants are able to filament in macrophages, but are defective in killing them [214]. While it appears to be the case that hyphal formation is *condition sine qua non* for the escape of *C. albicans* from macrophages (i.e. yeast-locked mutants do not escape), the data discussed above question the precise role of hyphal filaments in macrophage evasion by *C. albicans* [47, 214, 219, 222].

4.1.4. Intracellular signalling in immune cells in response to fungal infection

Cells of the innate immune system possess extracellular and intracellular receptors that monitor signs of infection to mount an appropriate immune response. Central players in this process are complexes known as inflammasomes [223]. The human and mice inflammasomes come in two known families, the pyrin domain (PYD) and HIN domain-containing (PYHIN) or the nucleotide-binding-and-oligomerization domain (Nod) and leucine-rich-repeat-containing or NLR family

(reviewed by [224]). Inflammasomes are complexes that survey and bind, directly or indirectly, to foreign or local molecules from dying or damaged cells [225]. The NLR inflammasomes activate the pro-inflammatory protease caspase-1 [226]. The mammalian NLRs are divided into four sub-families based on their ligand binding domain, and this includes the NLRPs or NLRCs which have a pyrin domain or a caspase-recruiting domain (CARD) respectively (reviewed by [227]). The NLRs, NLRP1, NLRP3, NLRC4, are distinct from PYHIN (e.g. AIM2) as they require the adaptor molecule ASC (apoptosis speck protein with CARD (caspase-recruitment-and-activation domain)), to bind pro-caspases (reviewed by [225]). Activation of the inflammasome leads to autoproteolytic cleavage of pro-caspases, where active caspases are then able to process cytokine precursor molecules [224]. Although many caspases have been implicated in the programmed cell death process that leads to apoptosis (e.g. caspase-3), only a few are known as inflammatory caspases including, caspase-1 and caspase-5 in humans, and their murine homologues caspase-1 and caspase-11 [228]. Caspase-5 or caspase-11 has been shown to interact with caspase-1 and increase its proteolytic activity (reviewed by [229]). Caspase-1 is known to cleave the pro-inflammatory cytokines interleukin-1 β (IL-1 β) and IL-18 [230]. IL-1 β exist in the form of pro-IL-1 β , non-bioactive precursor, and because its activity potentiates tissue damage and autoimmune diseases [226, 231], the processing of this cytokine to mature IL-1 β , is tightly regulated by the inflammasome complexes. In fact, mutations in *NLRP3* gene has been linked to NLRP3 inflammasome hyper-activation and over production of IL-1 β , and there is current research underway to develop antagonists as cures for IL-1 β related genetic disorders including hereditary periodic fever syndrome [232]. In addition, single nucleotide polymorphism in *NLRP3* has been associated with other diseases including psoriasis, celiac disease and increased susceptibility to human immunodeficiency virus-type-1 (HIV-1) infections (reviewed by [227]).

Inflammasome complexes have been shown to assemble during fungal infections, with the NLRP3-inflammasome playing an important role in response to *C. albicans* [169, 189, 233-235]. Mice devoid of ASC, NLRP3 or caspase-1 activity are more susceptible to both systemic fungal disease and to mucosal candidiasis [236]. Although NLRP3 is known to be active in response to various stimuli, there is

scarce information on whether NLRP3 actually binds these activators; instead, the current thought is that its activation is generated by signaling intermediates [237]. Joly *et al.* investigated whether NLRP3 inflammasome activation and IL-1 β secretion, using various *Candida* species, was dependent on hyphae, psuedohyphae and yeast cell morphology. Although they found that inflammasome activation required hyphae formation, *C. albicans* hyphal cells failed to induce IL-1 β secretion so it was suggested that the ability of *Candida* cells to filament may not necessarily be the cause of inflammasome activation [169, 222].

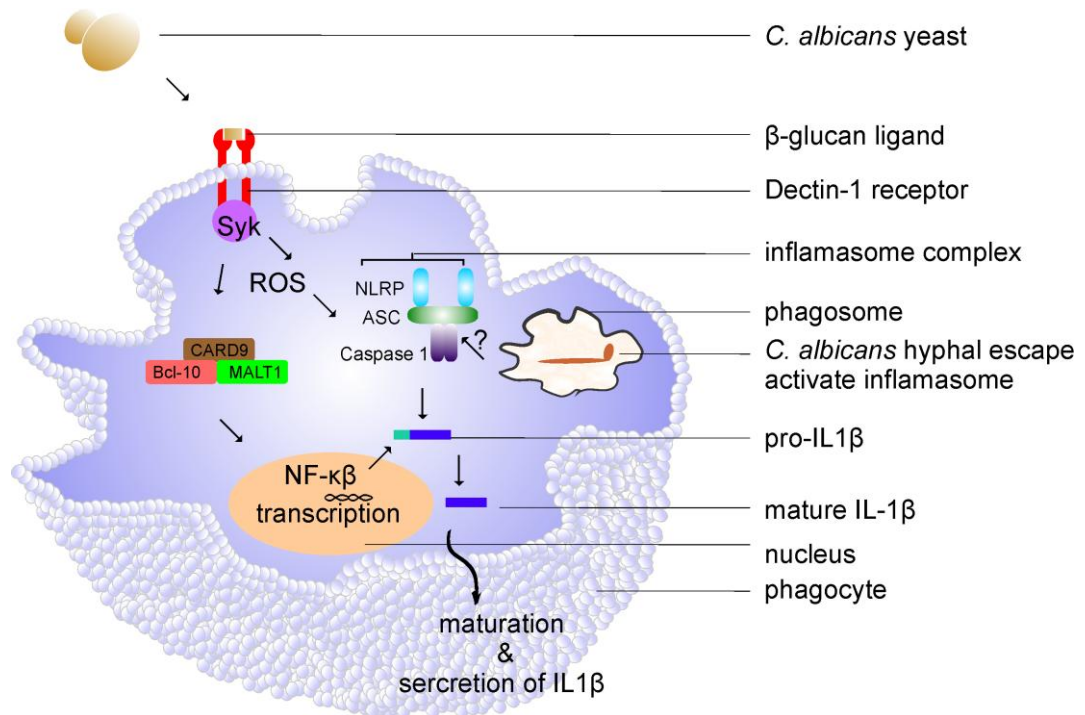


Figure 4.0. Signalling pathways that lead to inflammasome activation in macrophages during *C. albicans* infection. Dectin-1 recognizes fungal 1, 3 β -glucan, resulting in activation of the Syk kinase signaling pathway and the expression of the pro-inflammatory cytokine IL-1 β . Activation of the CARD9/Bcl10/MALT1 complex and the cytoplasmic inflammasome complex that contains NLRP3, ASC and caspase-1 occurs. This leads to processing of the IL1 β precursor and secretion of mature IL1beta [189, 233, 238]. For activation of the inflammasome to occur, *C. albicans* needs to form intracellular hyphae in phagosomes [218], as yeast cells are incompetent for inflammasome activation and caspase-1-dependent IL-1 β secretion [169]. The precise mechanisms that enable NLRP3/ASC inflammasome activation by *C. albicans* are not fully defined [169, 239-241].

Inflammasome activation by *C. albicans* needs extracellular and intracellular signals (Figure 4.0). The processes that lead to Dectin-1 and NLRP3 activation are illustrated in Figure 4.0 [189, 233, 238]. Once fungal cells are phagocytosed, the NLRP3 inflammasome is activated by fungal 1,3 beta glucan in manner dependent on the kinase Syk1 [242]. We know that Dectin-1 may also act as an extracellular sensor for some *C. albicans* isolate and may induce both IL-1 β production and maturation through a non-canonical caspase-8-dependent inflammasome, instead of the canonical caspase-1 inflammasome for protective immunity [190].

4.1.5. Inflammasome activation and programmed cell death

It has been shown in response to bacterial pathogens that inflammasome activation is associated with the activation of programmed cell death pathways. An infected immune cell may commit suicide using genetic programs to benefit the remaining cells, with the goal that foreign material of pathogen are disposed with it. Immune cells may activate the major cell death pathways, apoptosis, necrosis, and pyroptosis as a defense against pathogens (reviewed by [243]).

Death by apoptosis is non-inflammatory as it leads to cell body shrinkage forming 'apoptotic bodies' that are rapidly phagocytosed without extracellular cytoplasmic content spillage [244]. In contrast, necrotic cells increase in volume and the processes that follows lead to intracellular content spillage into the extracellular milieu. For this reason, necrosis is pro-inflammatory and is known as the cell death pathway that leads to extensive tissue damage [245]. Pyroptosis is a prototypical lytic host cell death pathway which has characteristics of both apoptosis and necrosis, including nuclear condensation and osmotic lysis [243]. Different caspases are known to be required in apoptosis and pyroptosis. The key difference between necrosis and pyroptosis is that pyroptotic cell death is caspase-1 dependent cell death [246]. Caspase-11 is another pyroptotic caspase. In comparison apoptosis requires caspase-2,-8 and -9 which activate the effector caspases (caspase-3,-6,-7) [247]. The same inflammasomes that induce IL-1 β secretion can also trigger programmed pyroptotic cell death via caspase-1 [248]. NLRP1, NLRP3, NLRC4 and AIM2

inflammasomes all appear to trigger pyroptosis in cells of monocyte/macrophage lineage [166, 249, 250].

Programmed cell death pathways in host cells can be manipulated by microbial pathogens to their advantage, to keep their replicative niches or to trigger lytic pathways that enable them to escape. Pyroptosis protects against microbial infections because it is lytic and enhances inflammation, but it can also contribute to pathological inflammation, as mentioned above as a result of NLRP3 defects, or as seen in the condition Muckle–Wells Syndrome [251, 252]. Although as mentioned before, the inflammasome pathway is required for mounting an inflammatory response against microbial pathogens, in some instances deletion of factors in the pyroptotic pathway has been shown to be protective to the host. For instance, IL-18 deficient mice are protected against septic shock by *Salmonella enterica* serovar Typhimurium [253]. Furthermore the deletion of caspase-1 has been shown to be protective in various disease models. For example, caspase-1 deletion is protective in animals with progressive ventricular dilatation and heart failure [254] and renal ischemic acute renal failure [255]. Collectively, these studies suggest that a carefully balancing act is required in the host to ensure the inflammatory response is triggered and pathogens are destroyed, but hyper-inflammation must be prevented.

In this second part of the thesis, the *med31* Δ/Δ and *srb9* Δ/Δ Mediator mutants were used to discern the effect of these mutations on the ability of *C. albicans* cells to interact with host immune cells, specifically looking at macrophage cytosolic interactions and provide insights on fungal escape. As a result, I showed for the first time the ability of a fungal pathogen to trigger pyroptotic cell death in macrophages [256]. We proposed that this lytic pathway is “hijacked” by *C. albicans* for immune evasion [256].

4.2. RESULTS

4.2.1. Mediator is required for *C. albicans* replication in macrophages

Oxidative burst is an important mechanism that professional phagocytes utilise to destroy pathogens [257]. As introduced in section 4.1.2, *C. albicans* cells avoid phagosomal destruction through cellular morphogenesis, and also have potent stress-responsive mechanism to counteract oxidative bursts [200]. It was evident from experiments conducted in Chapter 3 that Mediator mutants were sensitive to oxidative stress *in vitro* (Table 3.4). Hence, I hypothesized that gene regulation by the Mediator complex is required for survival of *C. albicans* upon phagocytosis by macrophages. To test this, wild type and mutant cells were co-incubated at a multiplicity of infection (MOI) of 1:1 or 2:1 (macrophage:*Candida*) for 3 hours, and survival of *Candida* strains determined by plating for and counting colony forming units. After 3 hours post phagocytosis, there was no significant difference in survival of *Candida* cells between those fungal cells incubated with macrophages and those without (Figure 4.1A) as was previously found [258]. Hence, to study the ability of fungal strains to replicate in macrophages, the co-incubation time was extended to 13.5 hours and CFUs were determined at an MOI of 1:2 (macrophage:*Candida*). I hypothesised that at this point *C. albicans* cells would have undergone enough cycles of replication in macrophages to show clear differences between the wild type and mutants. The number of CFUs obtained after 13.5 hours was normalised to the time just post the 1 hour co-incubation (time 0), to take into account the slower growth of the *med31Δ/Δ* mutant. This allowed me to compare the percentage increase in CFUs in the RAW264.7 cell line and wild type murine bone marrow derived macrophages (WT BMDMs) (Figure 4.1B).

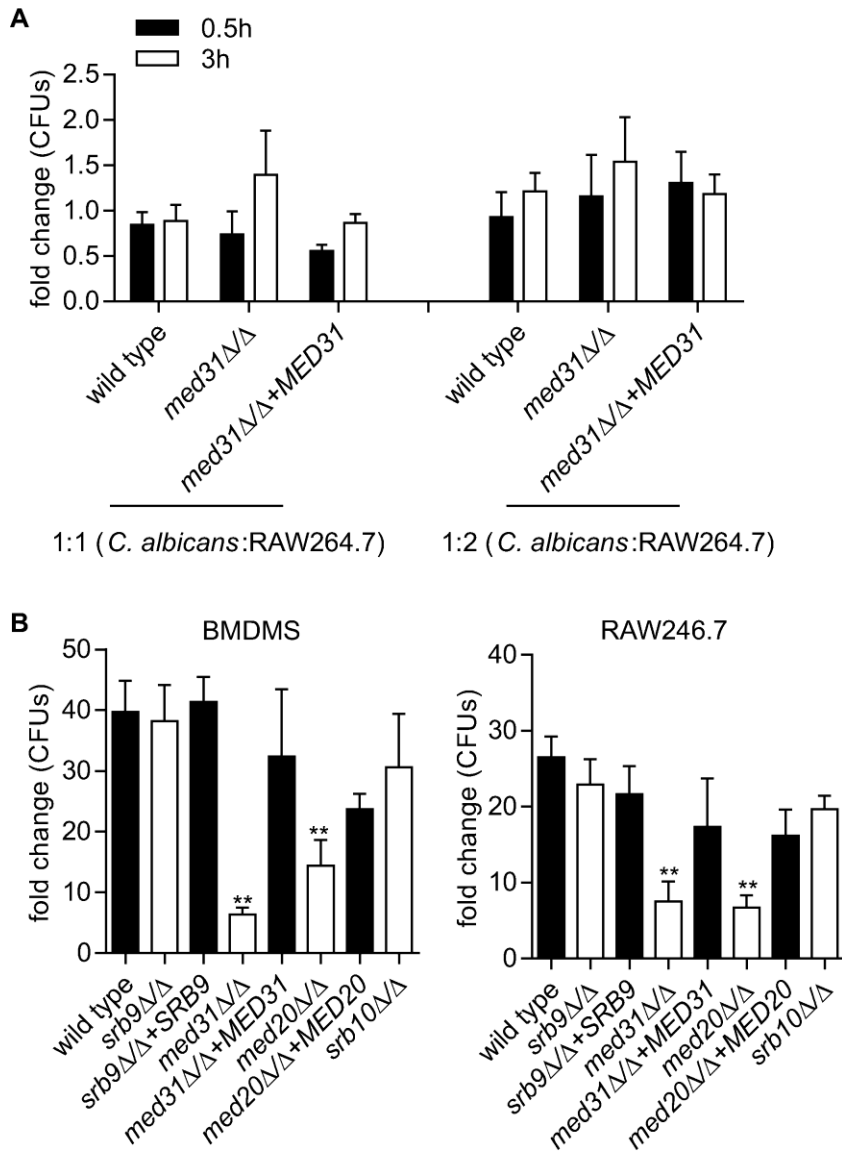


Figure 4.1. Mediator subunits impact on replication of *C. albicans* in macrophages. **A)** Survival of *C. albicans* in RAW264.7 macrophages. Shown is the ratio of CFUs of *Candida* incubated with and without RAW264.7 macrophages. Error bars represent the standard deviation. The multiplicity of infection (MOI) was 1:1 or 2:1 (macrophage:*Candida*). The assay was repeated only twice as the lack of *Candida* death in macrophages was previously reported [258]. **B)** Replication of Mediator mutants of *C. albicans* in BMDMs and RAW264.7 macrophages. Macrophages were incubated with *C. albicans* for 1 h, after which non-ingested cells were washed away. Colony forming units (CFUs) for the indicated strains were determined at time 13.5 h relative to time 0 h, which corresponds to the time just post the 1 h co-incubation. The fold change in CFUs is shown. The experiment was performed on at least 3 separate occasions. The (MOI) was 1:2 (macrophage:*Candida*). Shown are the averages from the biological repeats and the SEM. ** $p \leq 0.01$.

All mutants were able to replicate after co-incubation with macrophages as the fold increase was greater than zero (Figure 4.1B). It was interesting that although the highest levels of sensitivity to oxidative stress *in vitro* was observed for the *srb9* Δ/Δ mutant (as was shown in Chapter 3, Table 3.4); there was no significant difference between the *srb9* Δ/Δ mutant cells and wild type cells in their survival within macrophages whether in RAW264.7 or BMDMs (Figure 4.1B). The *srb10* mutant also showed wild type levels of replication within macrophages (Figure 4.1B). There was a significant difference between wild type cells and *med31* Δ/Δ and *med20* Δ/Δ mutant cells, which is likely due to the slower growth of these mutants, and their morphogenesis defects that results in less escape (see below).

4.2.2. Mediator mutants present various morphologies within macrophages

The ability to form hyphae is critical for the escape of *C. albicans* from macrophages. I have described in Chapter 3 the morphogenesis defects of the Mediator mutants *in vitro*. Here the ability of Mediator mutants to facilitate the yeast to hyphal transition upon engulfment by macrophages was tested. The ability of the *srb9* Δ/Δ mutant to filament within macrophages was quantified by co-incubating *srb9* Δ/Δ yeast cells and macrophages, phagocytosis and then followed by live video measurements of hyphae using ImageJ software. As shown in Figure 4.2A, the *srb9* Δ/Δ mutant was able to filament at a similar rate to wild type cells, consistent with the *in vitro* results described in Uwamahoro *et al.*, 2012 [256]. During this quantification, I observed that the *srb9* Δ/Δ mutant did not show the same degree of hyphal protrusion from macrophages compared to wild type cells. Wild type hyphae displayed consistent directionality in their movement, but this was not the case for the mutant hyphae. A proportion of *srb9* Δ/Δ mutant hyphae curved and coiled inside macrophages over time. To further address the impact of Mediator on morphogenesis in macrophages, wild type and mutant *C. albicans* cells were co-incubated with RAW264.7 macrophages or BMDMs at an MOI of 1:2 (macrophage:*Candida*) for 3 hours, followed by staining with the chitin specific dye calcofluor white to discriminate between internalised and escaped cells (Figure 4.2B and C).

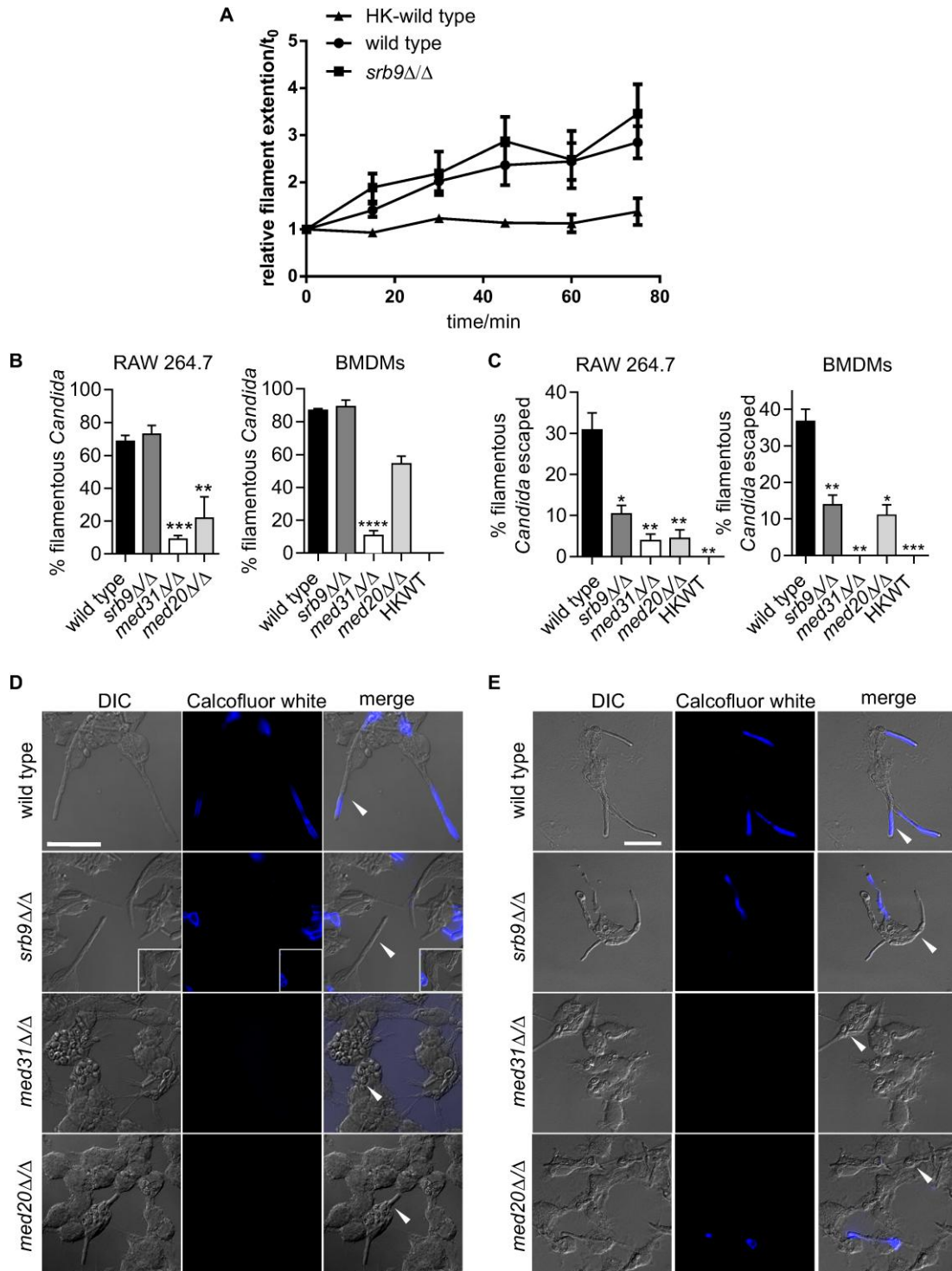


Figure 4.2 Mediator mutants present various morphologies within macrophages. **A)** Filament extension within macrophages was followed using live cell imaging in RAW264.7 cells. The relative length of filaments was determined over time using the ImageJ software. Shown are the lengths of hyphal cells relative to time zero. Ten filaments of wild type and *srb9Δ/Δ* mutant cells were measured and the average length over time and the SEM are plotted. Heat killed cells are added as a control. **B)** Filamentation and escape of Mediator mutants in macrophages. Numbers of escaped *C. albicans* hyphae were determined by counting total cells in macrophages from bright field images, and also calcofluor white (CW)-stained hyphae (see images in D and E). CW only stains fungal cells that have escaped, while the phagocytosed cells are protected. At least 200 cells/strain were counted. Shown are averages and the SEM (n=3). * $p \leq 0.05$ ** $p \leq 0.01$ **** $p \leq 0.0001$. **C)** An MOI of 2:1 (*Candida* : macrophage) was used. Fungal cell morphology was assessed by microscopy and quantified at 3 h post-phagocytosis. **D) and E)** Images of *C. albicans* incubated with RAW264.7 at 100x magnification (D) or BMDMs at 60x magnification (E). *Candida* cells outside macrophages are stained by CW, while fungal cells inside macrophages are not. Arrows indicate hyphal or yeast cells and wild type hyphal cells are able to escape macrophages indicated by blue stained hyphae.

The mean number of hyphal cells within macrophages after 3 hours was similar between wild type (86%) and *srb9Δ/Δ* (89%) cells, while only 10.7% of *med31Δ/Δ* and 54% of *med20Δ/Δ* cells were found to be filamentous in BMDMs respectively (Figure 4.2B). A similar trend could be observed in co-incubations with the RAW264.7 cell line (Figure 4.2B). Despite similar filamentation rates between wild type and *srb9Δ/Δ* cells, the mutant had a significant defect in escaping from macrophages at this time point (3 hours post-phagocytosis) (13.8% *srb9Δ/Δ* escaped versus 36.7% of the wild type) (Figure 4.2C). In the case of *med31Δ/Δ* and *med20Δ/Δ* mutants, consistent with their morphogenesis defect [163], they were severely impaired in escape (Figure 4.2C). While all (100%) of the *med31Δ/Δ* cells were unable to escape macrophages after 3 hours in BMDMs, 29% of *med20Δ/Δ* cells were able to escape (Figure 4.2C), suggesting Med20 has a more minor role in morphogenesis and macrophage escape than Med31. These results are consistent with the morphogenesis defects of these mutants as observed *in vitro* [259]. The images showing the morphologies of wild type and Mediator mutants in

macrophages are shown in Figure 4.2 D and E. As described further below, phagocytosis of *Candida* cells by macrophages did not differ between the wild type strain and Mediator mutants (Figure 4.6).

Next I determined whether the defects in macrophage escape were related to the ability of Mediator mutants to escape the phagolysosome. Phagolysosomal escape was visualised and quantified using immunofluorescence with a primary antibody for Lamp1, a late phagosomal degranulation marker for both late endosomes and lysosomes [260]. The association of *C. albicans* cells and Lamp1 indicates the formation of phagolysosomes [167]. Confocal images showed that in the first 2 hours, the *srb9* Δ/Δ and *med31* Δ/Δ were associated with Lamp1 positive compartments significantly more compared to wild type cells (Figure 4.3A and B).

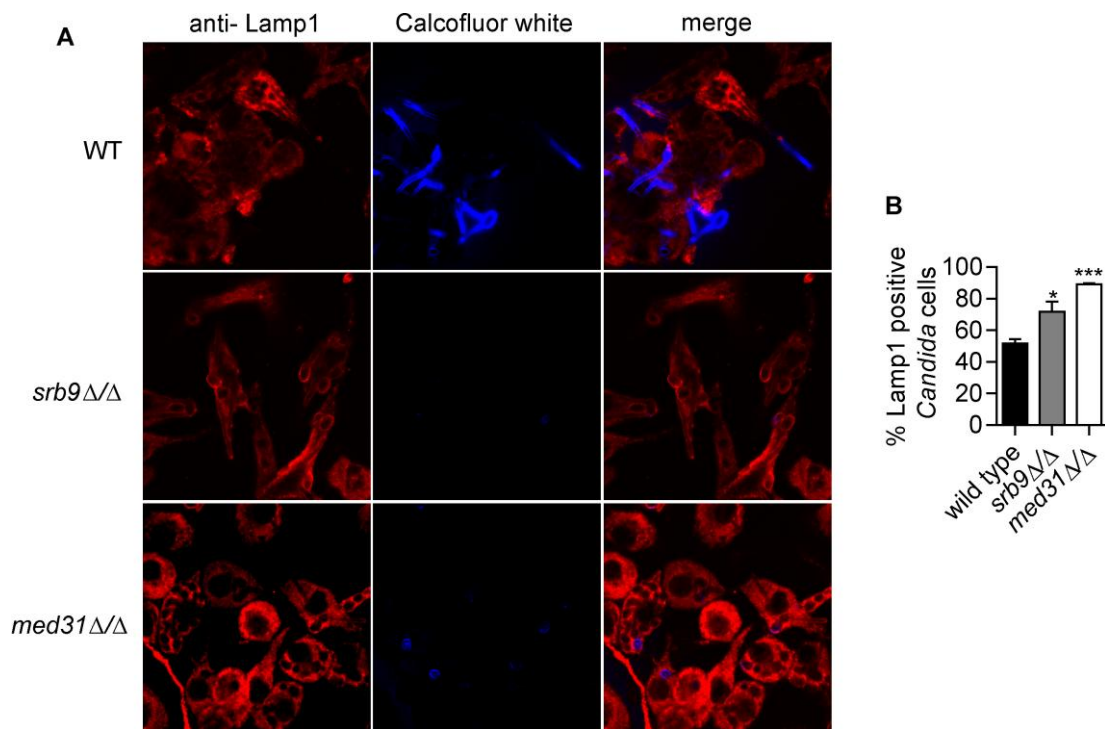


Figure 4.3. Late phagosomal association of *C. albicans* Mediator mutants.

A) Association of *C. albicans* with phagosomes in wild type BMDMs was monitored with immunofluorescence by staining for the late phagosomal marker Lamp1. Shown are slices of images obtained by confocal microscopy. Blue stain represents fungal cells outside macrophage stained by calcofluor white, Lamp1 stain is red. **B)** Lamp1 associated *C. albicans* cells were scored by microscopy at the 2 hour time point. Three independent experiments were

performed and at least 50 *Candida* cells were counted every time. Shown are averages and the SEM. * $p \leq 0.05$, *** $p \leq 0.001$.

4.2.3. A novel macrophage killing assay detects roles of Mediator in *C. albicans* – induced macrophage cell death

To determine the ability of *Candida* cells to kill macrophages, we developed an assay that could efficiently monitor macrophage death over time in a quantitative manner, without relying on microscopy-based counting of dead macrophages by the researcher, which can introduce bias. I developed the assay using time lapse microscopy and propidium iodide (PI)-based staining of dead macrophages. Figure 4.4 describes the methodology.

Candida cells were co-incubated with macrophages for 1 hour, followed by washing off of the non-phagocytosed cells, which left only intracellular *Candida* and fungal cells undergoing phagocytosis (i.e. cells stuck to macrophages). This was followed by co-incubation of macrophages and *Candida* cells in the presence of PI. Macrophage cell death rates (% PI positive cells) were determined every 15 minutes for up to 24 hours using live fluorescent cell imaging. The death of macrophages was converted to total area using the ImageJ software. The Total Area (TA) of PI staining was obtained from time lapse images converted to binary images using the Analyse Particle function in ImageJ. This represented the number of dead macrophages. The total area was used to calculate the percentage of macrophages killed at each time point (t_x) following the formula:

$$t_x = (t_n/t_{max}) * 100 * t_{total}$$

where t_n is the TA generated at each time point, t_{max} is the highest TA generated in the entire experiment (this was 100% for the wild type, but significantly less for some mutants, for example the *med31Δ/Δ* mutant or the control–heat killed cells, which only killed 0.5% macrophages after 24 hours of co-incubation), t_{total} is the ratio of the t_n at t_{max} , compared to actual live macrophages at t_{max} . Furthermore, t_{total} was accurately calculated by merging the PI and BF images to determine whether all macrophages were PI positive. If this was not the case, the maximum macrophage death was manually calculated.

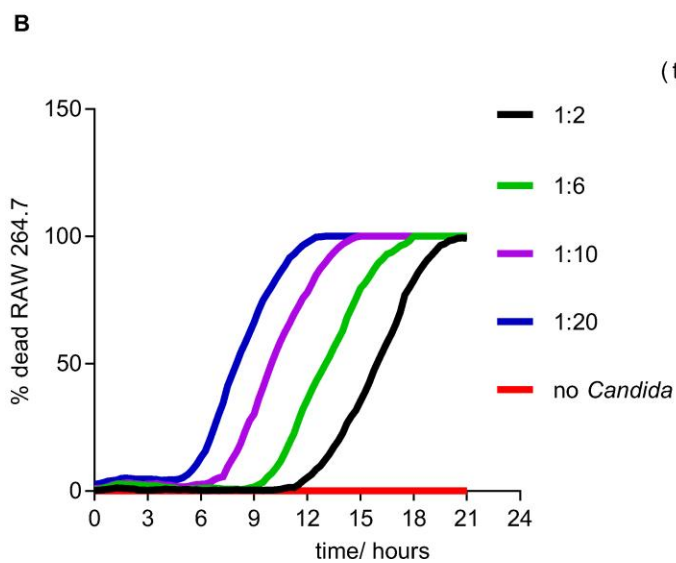
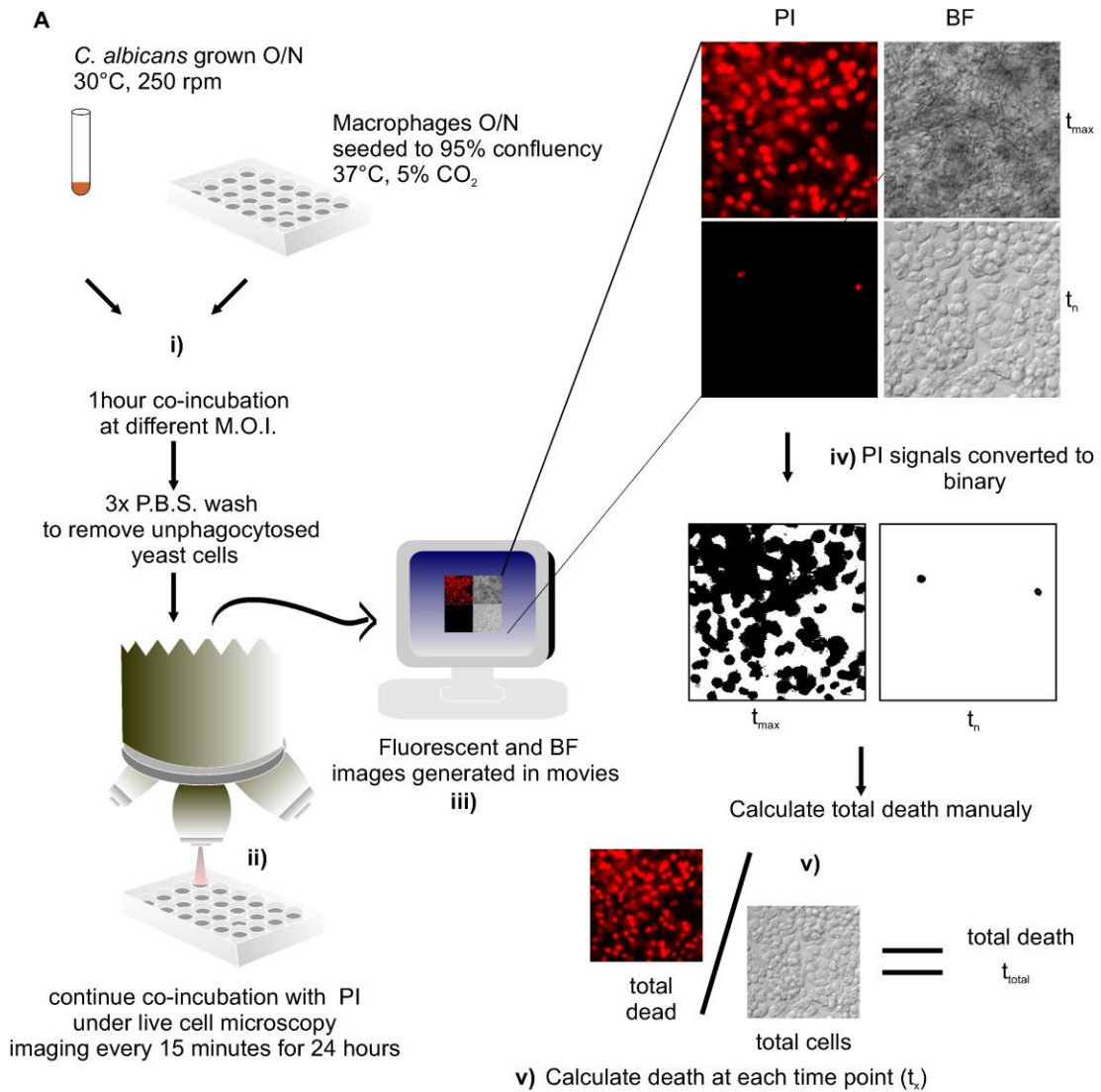


Figure 4.4. Optimization of the live cell macrophage death assay. A) RAW264.7 cells were challenged with *Candida* (i). After 1 hour of co-incubation, non-phagocytosed fungal cells were removed with PBS washes and fresh growth media containing PI was added to detect cell death. Live cell, time-lapse microscopy (ii) was conducted to generate images taken every 15 min for up to 24 hours. Bright field (BF) and fluorescent (PI) images generated (iii) were converted to binary images (iv) using the same PI signal threshold in the image software. The total signal of dead macrophages was measured at each time point (t_n) and the total death (t_{total}) was set as the time point at which maximum macrophage death was achieved (t_{max}). This was calculated by manually (v) counting PI-positive total macrophages (in fluorescent (PI) and bright-field images, respectively). The percentage of dead macrophages at each time point (t_x) was calculated based on the total maximum death (vi). All t_x values were calculated using Microsoft Excel and were plotted and analyzed with GraphPad Prism software to generate the final figure seen in **B. B)** Titration of wild type *Candida* in macrophages using the assay in panel **A**. Increasing the number of *Candida* cells led to faster killing of macrophages. An MOI of 1:6 (macrophage:*Candida*) was chosen in subsequent assays as the optimal MOI in relation to the investigations carried out (see figure 4.4A).

For example, for a 24 hour experiment, if the highest TA (t_{max}) obtained for a strain was 67540.382, but not all macrophages were PI positive (e.g. only 182 out of 476 macrophages were killed at the end of 24 hours), then t_{total} was 182/476 or 0.3823529 Hence, the t_x at the 24 hour (t_{24}) time point would be

$$t_{24} = (67540.382/67540.382)*100 *0.3823529$$

$$t_{24} = 38.24$$

All other data (t_x) prior to 24 hours, would use the formula:

$$t_x = (x /67540.382)*100 *0.3823529$$

A significant component of using this assay was to determine the ideal MOI. This was best determined looking at the death curves generated by wild type *C. albicans* cells (Figure 4.3B). *Candida* titrations showed that the rate at which the maximum macrophage killing was achieved was dependent on the proportion of *Candida* cells introduced in the system, such that the higher the number of *Candida*, the faster the exponential phase of killing was attained. An MOI of 1:6 (macrophage: *Candida*) proved to be best for this assay because at this MOI various macrophages killing phases were most easily observed (these phases are described in more detail below).

4.2.4. C. albicans kills macrophages in two distinct phases and Mediator subunits are required for macrophage killing

The new assay was performed in an *ex vivo* model, using primary bone marrow-derived macrophages, to provide a more realistic macrophage environment in regards to mimicking the conditions in the host. Analysis of macrophage killing by wild type *C. albicans* in wild type BMDMs (WT BMDMs) indicated that two killing phases occurred (Figure 4.5A). The first phase of macrophage killing by wild type cells showed death rates ~20-30% within 6 hours post infection (Figure 4.5A and 4.5C), followed by a second, more rapid phase of macrophage killing. Figure 4.5D shows representative snap-shot images from the live cell microscopy experiments in Figure

4.5A

at

5

hours.

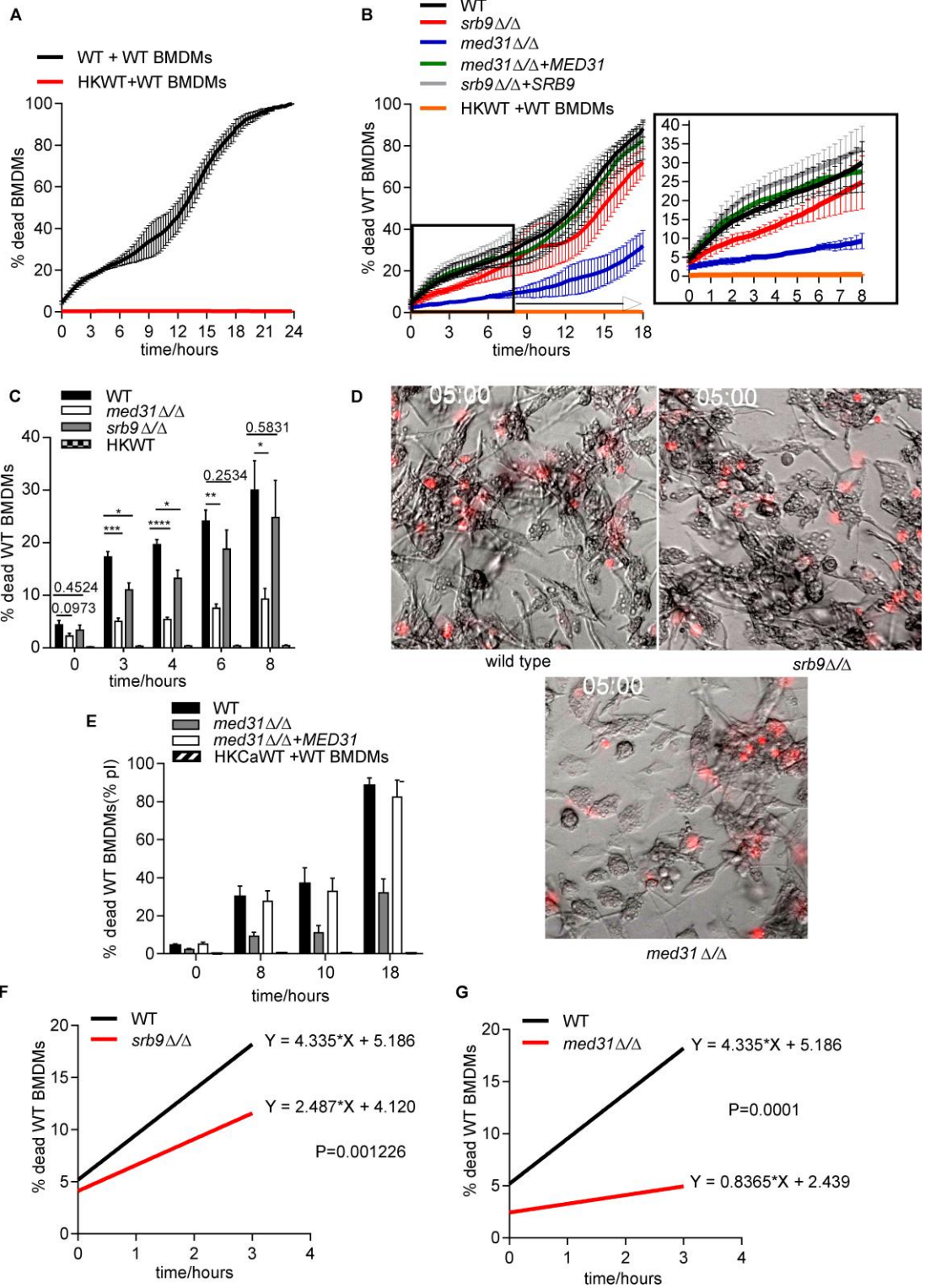


Figure 4.5 Filamentous morphology is required for macrophage killing. A-C and E) Killing of WT BMDMs, by *C. albicans* wild type and Mediator mutants. *Candida* and macrophages were co-incubated at an MOI of 1:6 (macrophage:*Candida*) and the experiment was carried out as described in Figure 4.3A. The same wild type data for A and B are presented separate for clarity. **B)** Boxed image shows the data magnified for the 0-8 hour time points. Heat killed wild type *C. albicans* (HKWT) yeast cells were included as control. Shown are the mean and SEM of results from 4 independent experiments. **C and E)** Bar graph representation of data in A, depicting differences in wild type and Mediator mutants killing of macrophages. *p*-value as indicated (****, $p < 0.0001$, ***, $p < 0.001$, **, $p < 0.01$; *, $p < 0.05$). **D)** Merged images BF and PI at 5 hour post infection. **F-G)** Linear regression analysis of the first phase of macrophage killing in panel A (boxed time points). Shown are the lines of best fit depicting the initial rates of macrophage killing, as indicated by the slope of the line. *p*-values comparing wild type and macrophage killing rates are shown to demonstrate that the rate of killing was significantly diminished for both *med31Δ/Δ* and *srb9Δ/Δ* mutants of Mediator. Video supplementary information is available online in Uwamahoro *et al.*, 2014 [261].

Although the *srb9* Δ/Δ cells were able to filament at the same rate as wild cells (Figure 4.2E), there was a significant difference compared to wild type *C. albicans* in hyphae protrusions from macrophages for up to 4-5 hours after phagocytosis (Figure 4.5D). No difference was observed with the *srb9* Δ/Δ mutant compared to the wild type strain in the second phase of killing (8-18 hours) (Figure 4.5B and 4.5E). Complementation with the *SRB9* gene restored macrophage killing ability to the mutant (Figure 4.5A). In comparison, filamentation of the *med31* Δ/Δ cells was delayed within macrophages (Figure 4.5C), although we did observe filaments starting to form by 6 hours). The *med31* Δ/Δ mutant showed impaired killing in the first and second phases of macrophage killing, where only 5% of macrophages were dead after 3 hours, and an average of 32% after 18 hours of co-incubation compared to 88% by wild type (Figure 4.5B and E). More macrophage death at later time points is consistent with the eventual formation of hyphal filaments by the *med31* Δ/Δ mutant. The differences in the rates of macrophage killing in the first phase could also be determined by regression to a linear function, which demonstrated that the initial slope of the lines presented in Figure 4.5A (box image), is less steep with the mutants than with wild type (Figure 4.5F and 4.5G). This showed that the rates of macrophage killing by *med31* Δ/Δ and *srb9* Δ/Δ mutants were significantly slower.

To ascertain that the difference in fungal escape and killing of macrophages observed between wild type and mutant cells was not an artefact of rates of fungal cell phagocytosis, the rate of phagocytosis and the phagocytic index were determined for wild type and mutant cells using an MOI of 1:6 (macrophage: *Candida*). Cells were counted after 30 min of co-incubation (after allowing cells to co-incubate for 1 hour to allow for phagocytosis to take place, after which un-phagocytosed *Candida* cells were washed off, so that only phagocytosed *Candida* cells remained in the assay). The results show that in RAW264.7 cells and BMDMs wild type and mutant *Candida* were phagocytosed equally with approximately 100% of macrophages containing at least 1 *Candida* cell (Figure 4.6A). This was also consistently reflected in the phagocytosis index (Figure 4.6B). These data demonstrated that Mediator mutants were phagocytosed at the same rate as the wild type cells. The observed

differences between wild type and Mediator mutants in macrophage escape and killing (Figure 4.5) were therefore not due to differences in the rates of phagocytosis.

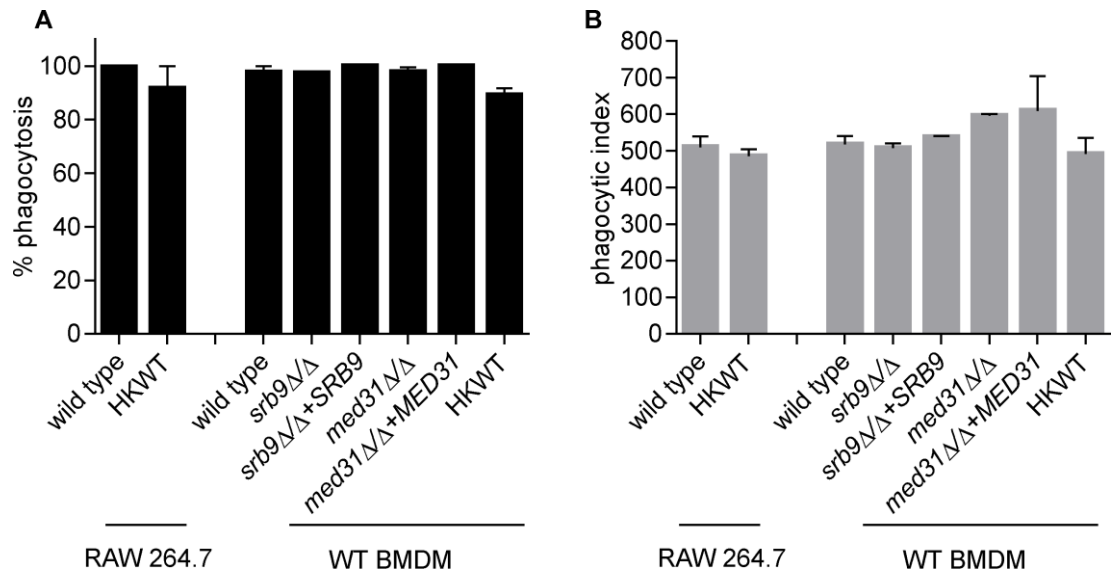


Figure 4.6. Phagocytosis of *C. albicans* Mediator mutants by macrophages. A and B) Percentage of infected macrophages and number of *Candida* cells/100 macrophages were counted from images from the live-cell microscopy experiments in Figure 4.4A and 4.10B (30 min time point after the 1 hour co-incubation period). Three independent biological experiments were performed for BMDMs and two for the RAW 264.7 cell line with two technical repeats per biological sample. At least 100 macrophages were counted from each technical repeat, in each of the independent biological experiments. Values are means \pm SEM. HKWT-heat killed yeast wild type cells. Shown are the percentage of fungal cells phagocytosed by macrophages (A), and the number of phagocytosed yeast cells per 100 macrophages (B).

C. albicans cells that lack the biofilm related transcription factor Bcr1 required for the expression of the *ALS1*, *ALS3* and *HWP1* adhesins share some phenotypes with the *srb9* Δ/Δ mutant (Chapter 3). For example, biofilm formation is impaired but filamentation is not affected by the *BCR1* mutation [119]. Also, the *bcr1* Δ/Δ mutant causes lower macrophage cell death in the J774 macrophage-like cell line [222]. As a transcriptional co-regulator, Srb9 likely impacts on gene transcription via gene-specific DNA binding transcription factors, such as Bcr1.

I therefore hypothesised that Srb9 might be cooperating with Bcr1 in regulating *C. albicans* morphogenesis and macrophage killing pathways. To test this idea, *bcr1* Δ/Δ mutant cells were used to challenge wild type BMDMs and morphogenesis and macrophage survival monitored over time (Figure 4.7).

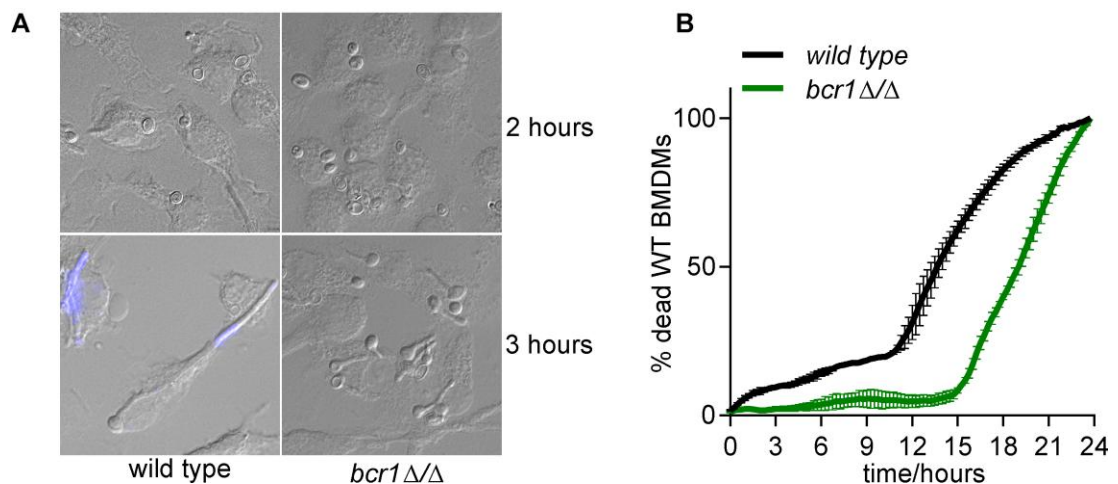


Figure 4.7. *C. albicans* filamentation within macrophages requires the adhesin regulator *BCR1*. **A**) The *bcr1* mutant cells display delayed filamentation within macrophages. Wild type *C. albicans* and *bcr1* mutant cells were incubated with wild type BMDMs (2 *Candida*: 1 macrophage). Fungal cell morphology was assessed by microscopy and images were taken at specified time points post-phagocytosis. **B**) Delayed filamentation of *C. albicans* cells leads to reduced induction of macrophage cell death. Shown are mean data from one biological experiment conducted in two separate wells in replicates and the error bars represent the standard deviation (SD).

The *bcr1* mutant was significantly more impaired in hyphal morphogenesis than the *srb9* Δ/Δ mutant. Hyphae only started forming after 2 hours within macrophages, and after 3 hours only germ tubes and small hyphal filaments were visible (Figure 4.7A). Consistent with the morphogenesis defect, the ability of this mutant to kill macrophages was greatly reduced (Figure 4.7B). These data suggest that Bcr1 is not functionally related to Srb9, at least not in respect to hyphal morphogenesis and macrophage killing pathways.

4.2.5. *C. albicans* Mediator subunit Srb9 is required for the establishment of proper cell surface structure of hyphae

As presented above, the *srb9* Δ/Δ mutant could form hyphae in macrophages with similar kinetics compared to that of wild type cells. Thus it was not clear why this mutant was delayed in escaping and killing of macrophages. The hypothesis was that while filamentous morphology was normal, the *srb9* Δ/Δ mutant hyphae likely display changes to their surface architecture. Since I previously found that Srb9 is required in the expression of cell surface adhesion molecules *in vitro* (Chapter 3), the levels of several adhesins were measured upon phagocytosis by macrophages. Results suggested that there was no difference between wild type and *srb9* Δ/Δ mutant in the mRNA levels of the hyphal specific *HWPI*, *ALS1* and *ALS3* adhesins in macrophages (Figure 4.8A). As a control, the levels of the *URA3* were also determined to confirm that virulence of morphological characteristics and growth are not due to expression of *URA3* at a different loci during mutant construction (see Chapter 3). The levels of *URA3* were similar to wild type levels as well as the complemented strain (Appendix 2, Figure 2).

Next, I decided to test the cell wall component, 1,3 β -glucan because this major immunogenic component was previously suggested to play a role in the intracellular recognition of *Candida* cells in macrophages [262]. Using an antibody specific to 1,3 β -glucan and confocal microscopy, I assessed the levels of 1,3 β -glucan in *srb9* Δ/Δ mutant cells grown *in vitro*, but in conditions that mimicked macrophage cell growth (in RPMI media at 37°C).

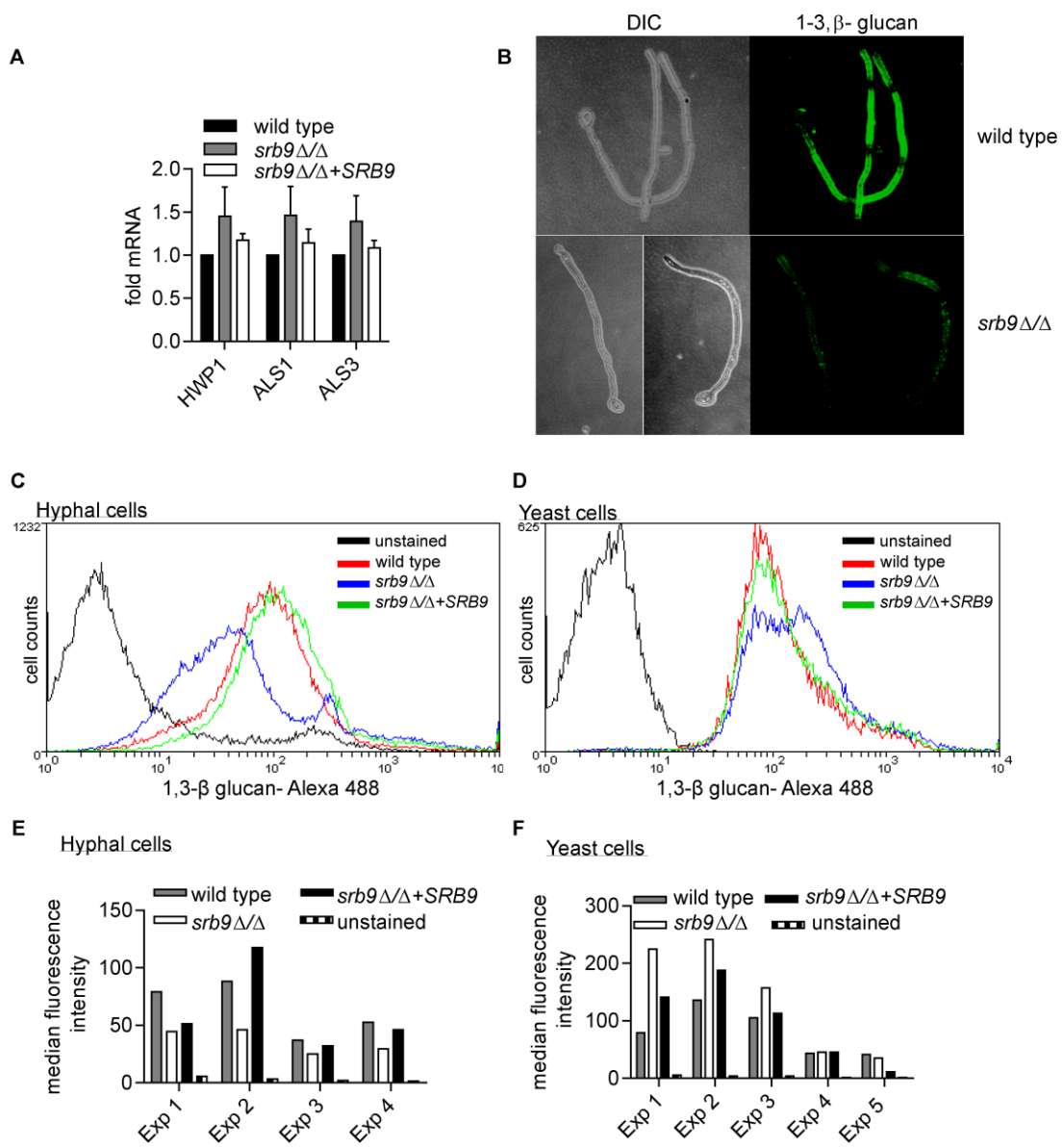


Figure 4.8. Cells deleted for *SRB9* are deficient in 1, 3 β glucans in hyphal morphology. A) Adhesin expression within macrophages was determined using quantitative PCR comparing the *srb9 Δ / Δ* mutant and complemented *C. albicans* strains. The experiment was performed on 3 separate occasions. 18s rRNA was used for normalization. The averages and SEM are shown. Appendix 2, Figure 2 shows the levels of *URA3* as a control. B) Wild type and mutant hyphae were grown in RPMI media at 37°C and stained with the 1,3 β -glucan antibody, followed by visualization by confocal microscopy. Image stacks were used to create 3D renditions. C) Population analysis of 1, 3 β -glucan levels using flow cytometry. Hyphal growth was induced in Spider media at 37°C for 3 hours. Yeast cells were grown in YPD at 30°C. Exposed 1,3 β -glucan was stained using the 1,3 β -glucan antibody. The experiment was performed on several different occasions. The FACS curves (B, C) are representative images from one of the experiments in E. The bar graphs (E, F) show the median fluorescence obtained in the individual experiments. The data in A and C-F was produced by Dr. Jiyoti Verma-Gaur.

The results showed that compared to wild type cells, the *srb9 Δ / Δ* mutant after 4 hours of hyphal growth displayed lower levels of exposed 1,3 β -glucan (Figure 4.8B). A similar result was obtained by flow cytometry using the 1, 3 β -glucan antibody followed by secondary antibody conjugated to Alexa 488. Figure 4.7 E and F show the individual experiments, showing the median fluorescent intensity. Interestingly, the *srb9 Δ / Δ* cells showed low levels of 1,3 β -glucan only during hyphal growth, while during yeast growth the cells showed either no difference or slight more 1,3 β -glucan compared to wild type cells.

To further address the properties of hyphal cell surface, hyphae from wild type *srb9 Δ / Δ* cells grown in macrophage growth conditions were analysed by Atomic force microscopy (AFM), in collaboration with Dr. Hsin-Hui Shen (Monash University). After 1 hour of filamentation there were no significant differences compared to similarly sampled wild type cells (data not shown). However, after 4 hours, *srb9 Δ / Δ* cells presented a breakdown of cell surface structure, which was evident because of smooth surface of hyphae (compared to rough wild type hyphae) and significantly less adhesion force measured in a square matrix area (Figure 4.9).

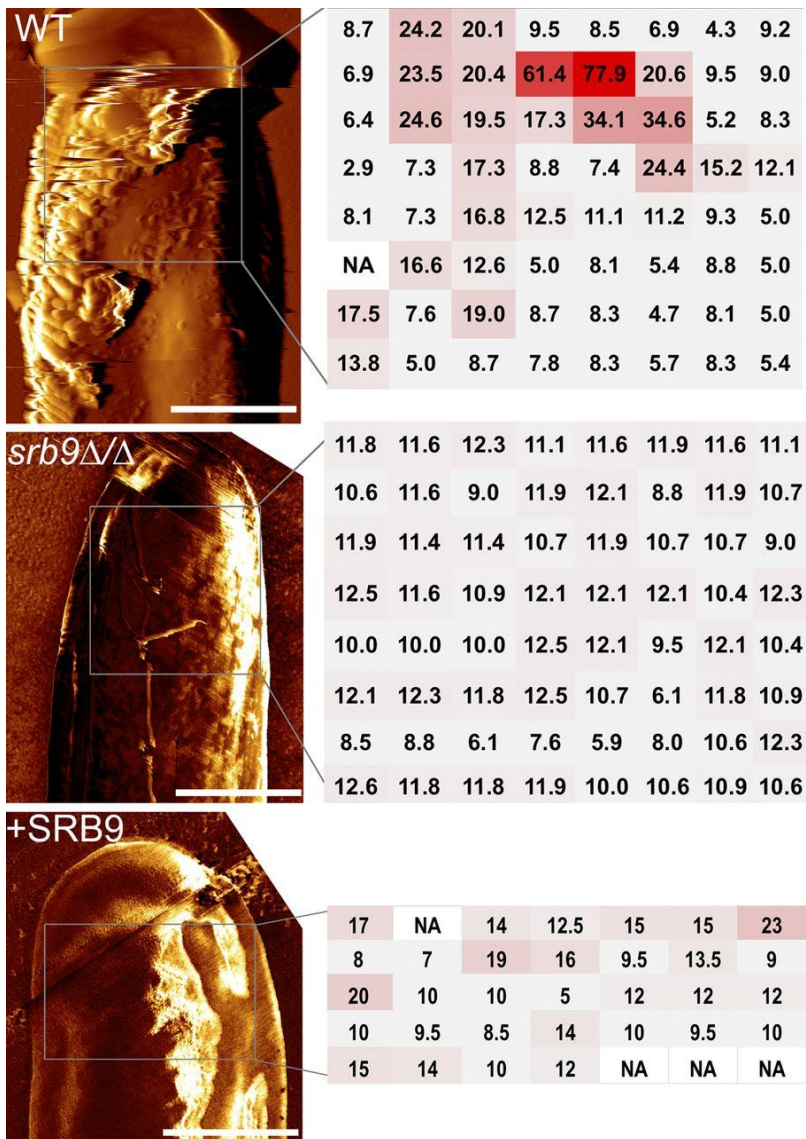


Figure 4.9. Srb9 is required for correct hyphal cell surface architecture. AFM (atomic force microscopy) was performed on hyphae grown *in vitro*. Deflection images of hyphal tips from wild-type and *srb9* Δ/Δ mutant hyphae are presented on the left and the force measurements on the right. The regions in which force measurements were done were squares of the following sizes: 1.7 μm -by-1.7 μm for the wild type, 1.2 μm -by-1.2 μm for *srb9* Δ/Δ , and 1.5 μm -by-1 μm for the complemented strain). The adhesion forces were extracted from force-distance curves (the unit of adhesion force is nN). The force was measured in a matrix region which for the wild type and mutant was 8-by-8-matrix, and 7-by-5 for the complemented strain. The force measurements are color-coded from grey (low) to red (high). Several hyphae were measured for each of the strains and gave similar results. Scale bar 1 μm . This figure was generated in collaboration with Dr. Hsin-hui Shen²¹

²¹ Building 77, Science Technology Research & Innovation Precinct, Monash University, Clayton Campus, Melbourne 3800, Australia

4.2.6. C. albicans activates a programmed cell death pathway for killing macrophages

The current model of macrophage killing is that it occurs via physical shearing of macrophages by *C. albicans* hyphae. My data challenge this assumption. Firstly, with my *in vivo* live cell imaging assay, it was obvious that the initial phase of macrophage killing was generally slower compared to the second phase. Secondly, the first phase of killing was significantly lower when RAW cells were used compared to primary macrophages (BMDMs) (Figure 4.10A and 4.10B), although the extent of filamentation by wild type *C. albicans* was the same in these two macrophage types (Figure 4.10C). Almost no macrophage killing is observed in the first phase (8-10 hours post-phagocytosis) when the RAW264.7 cell are used, whereas up to 40% of BMDMs are killed by wild type *C. albicans* within 9 hours under the same experimental conditions (Figure 4.10A and B).

The impaired macrophage killing profiles of *srb9* Δ/Δ and *med31* Δ/Δ mutants (Figure 4.5A), showed similarity to those of wild type RAW264.7 cell killing, although the mutants were able to kill more BMDMs than what the wild type was able to do with the RAW cells line in the first 8-9 hours (Figure 4.9 and 4.10B). I therefore hypothesised that *C. albicans* morphogenesis and possibly components of the cell wall could be triggering a host cell death pathway that is disabled in RAW264.7 cells making them resistant to *C. albicans* killing.

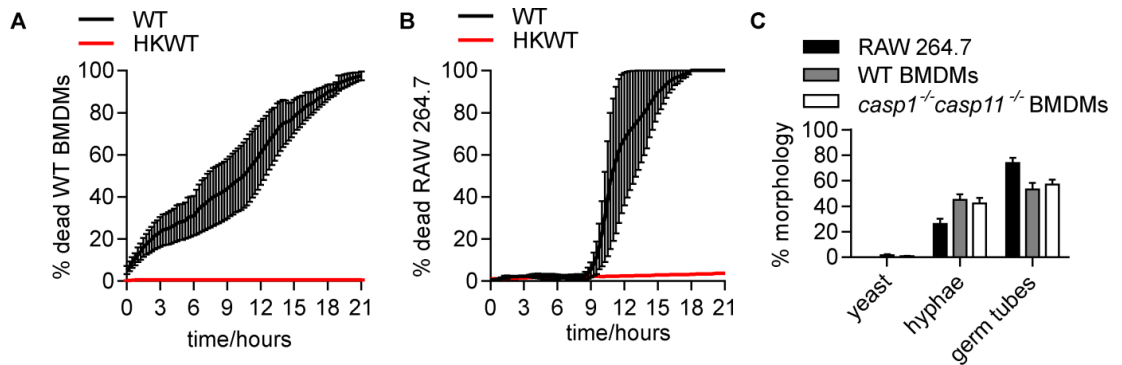


Figure 4.10. The two phases of macrophage killing by *C. albicans* depicted in RAW 264.7 and primary macrophages. **A)** Wild type *C. albicans* was incubated with wild type BMDMs at MOI 1:6 (macrophage:*Candida*), and macrophage cell death monitored over time. The results are averages and the standard error of the mean (SEM) from two independent biological experiments. HKWT-heat killed wild type *C. albicans* cells (yeast morphology). **B)** Experiments were performed as in panel A except that the macrophage cell line RAW 264.7 was used. Shown are the mean and the SEM (n=2). **C)** Yeast and hyphal cells were counted from images from the live-cell microscopy using RAW264.7, primary macrophages from wild type mice (WT BMDMs) and primary macrophages from caspase1/11 mutant mice (*casp1^{-/-}casp11^{-/-}*)²² at 30 min post the 1 hour co-incubation. A total of 100 phagocytosed *Candida* cells were counted for each of the independent biological experiments, and classified as either yeasts or hyphae (hyphae included cells producing germ tubes). Data is from two independent biological experiments for the RAW264.7 cells and 3 experiments for BMDMs. Values shown are means \pm SEM.

²² The studies on *casp1^{-/-}casp11^{-/-}* mutant are presented in subsequent results. All WT BMDM and *casp1^{-/-}casp11^{-/-}* mutant live cell death assay experiments (except for data in figure 4.10A) were conducted containing both cell types, but are plotted separately for simplicity.

As introduced in section 4.1.4, ASC is the adaptor component of the NLRP inflammasome complexes that bind and activate pro-caspases, which then leads to the activation and excretion of the pro-inflammatory cytokine IL-1 β . The macrophage factor that differentiates RAW264.7 and BMDMs is the lack of expression of the inflammasome component ASC [263]. In addition to this, in response to intracellular pathogens, caspase-1 allows for activation of the pro-inflammatory cell death program known as pyroptosis (see section 4.1.5). While pyroptosis is well known to occur in response to intracellular bacteria [264], it was not known to occur in response to intracellular *C. albicans*, although *C. albicans* is known to activate caspase-1 for IL-1 β production [169]. The idea therefore was that *C. albicans* triggers pyroptosis and the RAW264.7 cells are resistant to killing by *C. albicans* because they cannot trigger pyroptotic death due to lack of ASC.

To test the idea that *C. albicans* hyphae trigger pyroptotic macrophage cell death, I used primary macrophages derived from *casp1^{-/-}casp11^{-/-}* mutant mice, and compared them to wild type BMDMs upon infection with wild type *C. albicans*. Consistent with my hypothesis, *casp1^{-/-}casp11^{-/-}* BMDMs were more resistant to macrophage killing in the first phase compared to WT BMDMs (Figure 4.11A). Again, fungal cells produced similar morphological properties within WT BMDMs and *casp1^{-/-}casp11^{-/-}* BMDMs (Figure 4.11 C). Mutant *casp1^{-/-}casp11^{-/-}* BMDMs challenged with wild type *C. albicans* showed similar macrophage cell death in the second phase to wild type macrophages – this phase -starts around 10 hours post-infection (Figure 4.11A and B). This suggests that caspase-1 dependent macrophage killing was mainly required in the first phase, and was dispensable in the second. I observed that in the second phase (around 15 hours), macrophage death occurred simultaneously with the production of large amounts of lateral yeasts by escaped hyphae (Figure 4.11D).

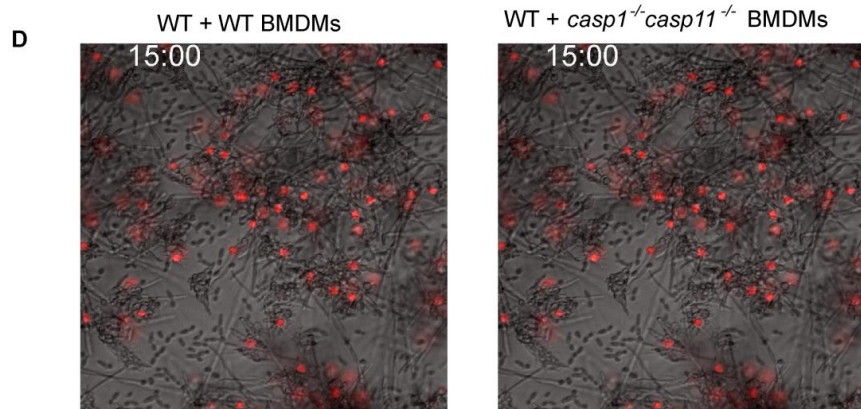
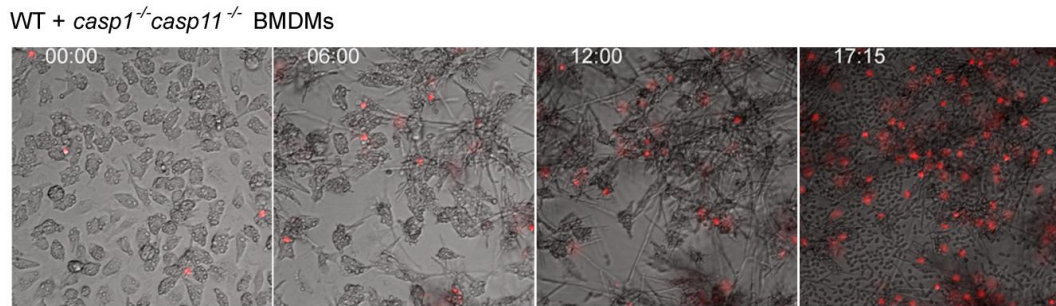
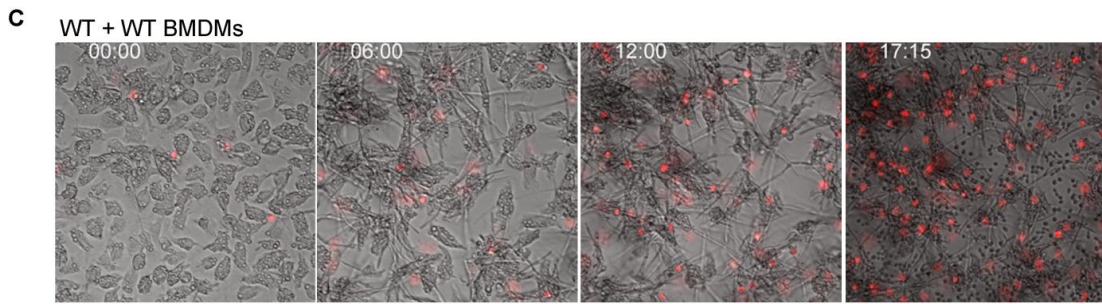
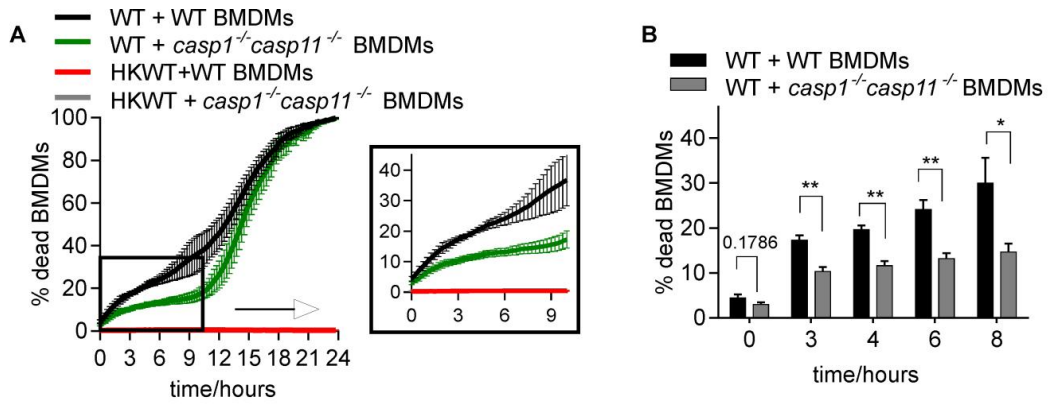


Figure 4.11 Pyroptotic cell death induced in the first phase of macrophage killing. A-B) Wild type *C. albicans* was incubated with wild type or *casp1^{-/-}casp11^{-/-}* BMDMs. Shown are averages of 4 independent experiments and the SEM. These data are the same as the wild type *Candida* control experiments shown in Figure 4.5, 4.10C and 4.12A. They are shown here separately for clarity. Graphs show means and the SEM for percentage of macrophage cell death at selected time points from curves in A) with *p*-values (** $p \leq 0.01$, * $p \leq 0.05$).**C-D)** Images of selected time points from the live cell microscopy of wild type *C. albicans* infecting wild type or *casp1^{-/-}casp11^{-/-}* BMDMs. Corresponding videos (S1-S3) published in [261].

To further establish the role of the NLRP3 inflammasome in *C. albicans*-mediated macrophage cell death, I next tested macrophages lacking the inflammasome components NLRP3 (*nlrp3^{-/-}*) and ASC (*asc^{-/-}*) alongside wild type BMDMs. Indeed live cell analysis showed decreased macrophage killing in mutants lacking ASC and NLRP3 (Figure 4.12A and B). In addition to this, pan-caspase inhibitors, Z-vad and QVD showed suppression of pyroptotic death (Figure 4.13C-E). Of note, in all of these cases (mutant macrophages or caspase inhibitors), the second phase of macrophage killing by *C. albicans* was normal.

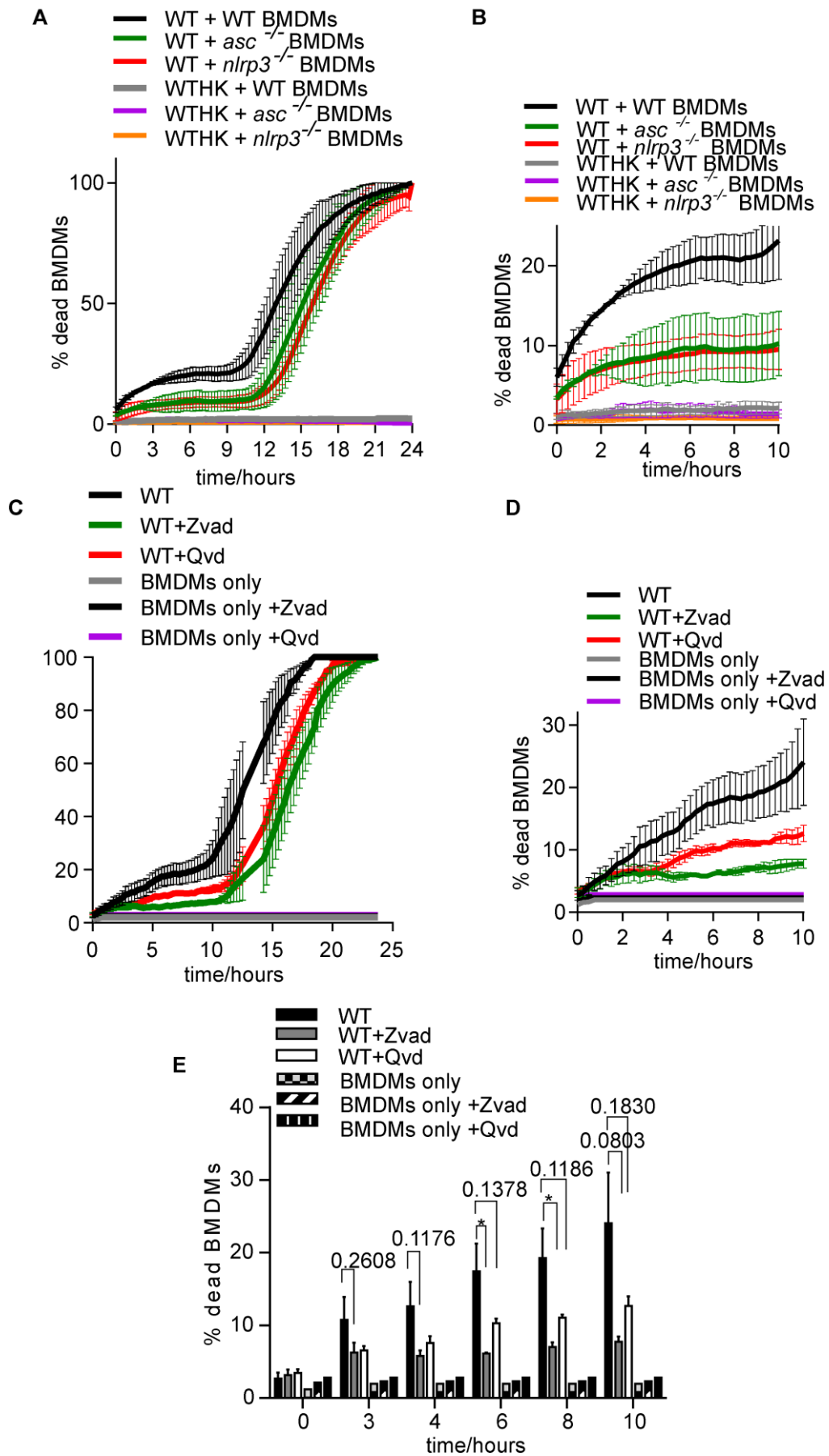


Figure 4.12. Macrophage killing requires components of the inflammasome. **A-B)** Wild type *C. albicans* was incubated with wild type, *nlrp3*^{-/-} or *asc*^{-/-} BMDMs. Lack of these components of the NLRP3 inflammasome complex was protective against *C. albicans* induced macrophage death. Data in **B** is from **A** but re-plotted to show 0-10 hour time points only for easier comparison. Shown are averages of 2 independent experiments and the SEM. **C-E)** Treatment of WT BMDMs with pan-caspase inhibitors Zvad or Qvd. Panel **D** and **E** shows the first 10 hours in panel **C**. Shown are the averages and SEM of data from one experiment conducted using three different *C. albicans* wild type clones as biological repeats. *p*-values are as indicated with the asterix * denoting $p \leq 0.05$).

4.2.7. *C. albicans* cells restructure cell surface architecture to hijack pyroptosis and escape from macrophages

I next decided to test the idea that fungal morphogenesis and wild type hyphal surface architecture are needed to trigger pyroptosis in macrophages. To do this, the *casp1^{-/-}casp11^{-/-}* BMDMs were challenged with *srb9Δ/Δ* mutants that form hyphae similar to wild type cells, but with cell surface defects. In the same experiments, I also used the *med31Δ/Δ* strain, which is defective in hyphal morphogenesis. The idea was that the differences between wild type and Mediator mutant *Candida* in macrophage killing ability would be smaller or not detectable at all in the absence of pyroptosis in *casp1^{-/-}casp11^{-/-}* BMDMs, if Mediator mutants were defective in triggering pyroptosis.

Compared to wild type *C. albicans*, there were differences in the extent of *casp1^{-/-}casp11^{-/-}* BMDM cell death upon infection with the Mediator mutants in the first 8 hours (in the pyroptotic phase), but the differences were not statistically significant to $p < 0.05$ (Figure 4.13A and 4.13B). The *med31Δ/Δ* mutant which display delayed hyphal formation showed less potency in macrophage killing even when pyroptosis was inactive (Figure 4.13B). The *med31Δ/Δ* mutant cells still showed higher death compared to heat killed cells even in *casp1^{-/-}casp11^{-/-}* BMDMs (Figure 4.13A-see boxed image). The second phase of *casp1^{-/-}casp11^{-/-}* macrophage killing, as expected, mimicked what was seen with wild type BMDMs. Only 43% of macrophages were killed by the *med31Δ/Δ* mutant killing after 18 hours, significantly less compared to wild type cells (93% death) (Figure 4.13C).

In regards to *srb9Δ/Δ* cells, there was no significant difference in their ability to cause macrophage death compared to wild type *C. albicans* in pyroptosis-defective *casp1^{-/-}casp11^{-/-}* macrophages (Figure 4.11). The *srb9Δ/Δ* cells also showed different kinetics in *casp1^{-/-}casp11^{-/-}* BMDMs in the second phase of macrophage killing (Figure 4.13A). The similarity in macrophage death between *srb9Δ/Δ* and wild type cells in phase 1 in *casp1^{-/-}casp11^{-/-}* macrophages suggested that *Srb9* is required for the expression of hyphal specific factors that are required in wild type *C. albicans* to

induce pyroptotic macrophage death.

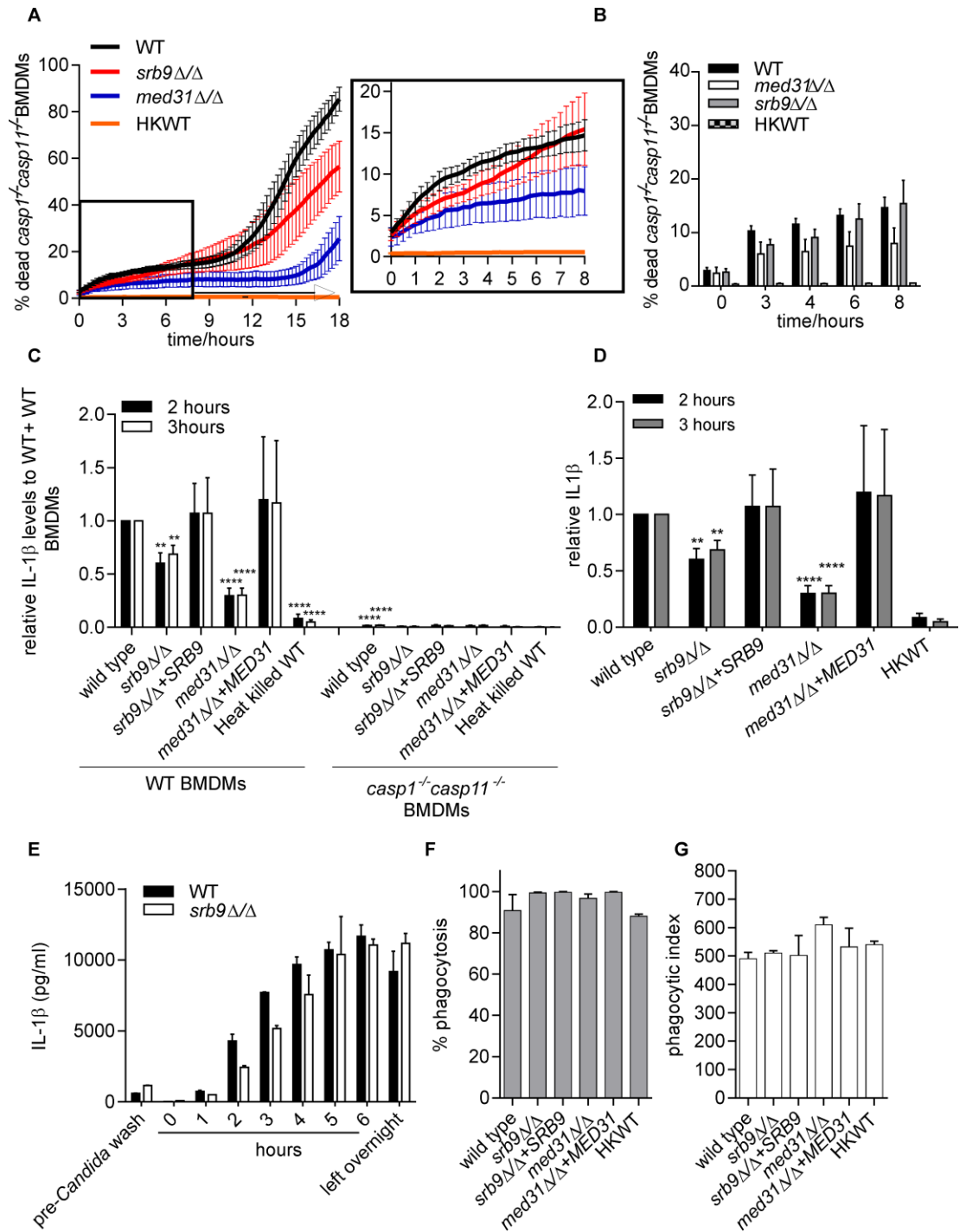


Figure 4.13. *C. albicans* morphogenesis and surface architecture of hyphae are required for triggering macrophage pyroptosis. **A-B)** Wild type *C. albicans* and Mediator mutants incubated with *casp1^{-/-} casp11^{-/-}* mutant BMDMs. Shown are averages of 4 independent experiments and the SEM. Data presented here were conducted at the same time as the data in Figure 4.5A hence the same wild type *Candida* control experiments shown in Figure 4.5A applies. They are shown here separately for clarity of the results. The data in this figure are from experiments performed 3 independent times (for the *med31Δ/Δ* mutant) or 4 independent times (for the *srb9Δ/Δ* mutant). The error bars are the SEM. **C-D)** Effects of Mediator subunits on IL-1 β secretion from macrophages. BMDMs were pre-treated with LPS and infected with *C. albicans*, and IL-1 β levels were determined from supernatants after 2 or 3 h. The experiment was performed 3 independent times (4 for the *srb9Δ/Δ* mutant), and fold differences were calculated, with IL-1 β levels induced by wild-type *C. albicans* in wild-type BMDMs set to 1. Averages and SEM are shown. The individual experiments with IL-1 β concentrations in supernatants (pg/ml) are shown in Appendix 2, Figure 1. A multiplicity of 1:6 (macrophage:*Candida*) was used. *p*-values were calculated for the comparisons between wild-type + WT BMDMs to either WT BMDMs (left side of the graph) or *casp1^{-/-} casp11^{-/-}* BMDMs (right side). Panel D shows mutant killing relative to wild type *C. albicans* within *casp1^{-/-} casp11^{-/-}*. **E)** Time lapse IL-1 β secretion induced by the *srb9Δ/Δ* mutant. Shown are the averages and the standard deviation of two technical repeats from one experiment. The multiplicity of infection was 1:6 (macrophage:*Candida*). Graphs are for individual time points with statistical significance. *p* values are as indicated (**** *p* \leq 0.0001, ** *p* \leq 0.01). **F)** Phagocytosis of *Candida* by *casp1^{-/-} casp11^{-/-}* BMDMs. Figure shows the percentage of fungal cells phagocytosed by macrophages (panel E), and the number of phagocytosed yeast cells per 100 macrophages (panel G). The experiment was conducted at the same time as data in Figure 4.6, but is presented here separately, so wild type BMDM controls in Figure 4.6 apply to this data.

The levels of secreted IL-1 β are a sensitive and quantitative measure of caspase-1 activity. Therefore to quantify the extent of caspase-1 activation by *C. albicans* Mediator mutants, IL-1 β levels were measured during the first phase of macrophage killing (Figure 4.14C-D and Appendix 2, Figure 1). In these assays, the expression of the precursor IL-1 β (pro-IL-1 β) is induced by priming murine macrophages with bacterial lipopolysaccharides (LPS) for 3.5 hours [169]. This is then processed to mature IL-1 β upon activation of caspase-1 during macrophage co-incubation with fungal cells.

The IL-1 β levels induced by wild type and Mediator mutants were determined and expressed relative to levels induced by wild type, which were set to 1 (Figure 4.13C). Mutant *casp1^{-/-} casp11^{-/-}* BMDMs were used as a control to show that the vast majority (>95%) of secreted IL-1 β in this assay is due to caspase-1 and caspase-11 activity (Figure 4.13C and 4.13D). After 3 hours of *med31 Δ/Δ* cells co-incubation with wild type BMDMs, the mutant was able to induce ~30% of IL-1 β levels relative to the levels induced by wild type *C. albicans* cells (Figure 4.13C). This is probably a result of the observed delay in hyphal morphogenesis in this mutant. Cells lacking *SRB9* induced a modest 68.7%, but statistically significant defect. In addition to this, time point analysis of IL-1 β levels induced by the hyphal *srb9 Δ/Δ* mutant showed that initially the mutants was not as competent as the wild type in triggering IL-1 β secretion by BMDMs, but this recovered at the 6 hour time point (Figure 4.13E). This is consistent with slower initial macrophage killing caused by the *srb9 Δ/Δ* mutant, which recovered after four or so hours (Figure 4.5A). The differences in responses observed in *casp1^{-/-} casp11^{-/-}* were not due to differences in phagocytosis of fungal cells (Figure 4.13F-G).

4.3. DISCUSSION:

4.3.1. Functions of Mediator in immune evasion by *C. albicans*

The results in this chapter highlight the role of components of the *C. albicans* Mediator in the regulation of phenotypic characteristics for survival and evasion of macrophages. These characteristics include morphogenesis and modulation of cell wall virulence factors. Lack of Med31 leads to impaired filamentation within macrophages consistent with findings *in vitro* that were presented in Chapter 3. It is reasonable to assume that the transcription regulation impairment of genes related to morphogenesis which was observed in *med31Δ/Δ* cells *in vitro* (Chapter 3) also influences filamentation induced within macrophages. The significant differences between wild type *med31Δ/Δ* cells in growth and replication in macrophages are also paralleled by the fitness and growth defects as observed *in vitro* (Chapter 3). In contrast, the Srb9 subunit of the Mediator is not required for the regulation of the hyphal switch within macrophages and does not impact *C. albicans* survival or proliferation within macrophages. The critical role of this subunit in macrophages appears to be the modulation of cell wall components during the yeast to hyphal transition, as demonstrated by decreased exposed 1,3 β-glucan in *srb9Δ/Δ* hyphal cells. Another independent study from the Krysan lab reported on mutants in transcription factors that were able to switch to hyphae in macrophages, but were defective in killing macrophages [214]. An example is the transcription factor Upc2, a regulator of ergosterol biosynthetic genes. Unlike the *srb9Δ/Δ* mutant, *upc2* mutant cells did not display differences in 1,3 β-glucan levels compared to wild type *Candida*, suggesting that in addition to 1,3 β-glucan, other cell wall components impact on *C. albicans* escape from macrophages [258, 265].

Our results implicate hyphal 1,3 β-glucan in the initial phase of *C. albicans*-macrophage interactions and host cell death, but at the moment it is unclear exactly how 1,3 β-glucan on the surface of internalised *C. albicans* hyphae is required for inflammasome activation and pyroptotic death. The activation of the caspase-1 inflammasome has been suggested to be triggered by the ability of hyphal cells to

disrupt the phagolysosome as this may release molecules that activate the NLRP3 inflammasome [169]. In this context, one possibility is that low levels of 1,3 β -glucan causes a structural defect of the cell, and the weakened hyphae are unable to pierce through the phagolysosome for cytoplasmic macrophage signalling to occur. Infection assays conducted in mice demonstrated that β -glucans are initially masked in the earlier stages of infection but later become exposed in several organs; however glucans are also masked against Dectin 1 during extracellular *C. albicans*-macrophage interactions [258]. Increased 1, 3 β -glucans in the cell wall induce higher levels of IL-1 β [266]. Indeed, decreased levels of IL-1 β were observed in the cells lacking *Srb9*, suggesting that the *Srb9* may co-regulate genes that encode *C. albicans* cell surface components required to elicit such immune responses. Furthermore, for fungal cells to mount an IL-1 β response in human macrophages, cytoplasmic glucan recognition is required [241], and so lower level of glucan on the surface of *srb9 Δ/Δ* mutant cells could lead to lower *C. albicans* recognition by cytoplasmic mechanisms. Future studies will aim to decipher the precise biochemical composition of the glycome and proteome of *srb9 Δ/Δ* mutant hyphae for a better understanding of the mechanisms that impact on *C. albicans* recognition by the NLRP3 inflammasome. In addition, using the systemic infection model in mice, we have shown in our laboratory that the *srb9 Δ/Δ* and *med31 Δ/Δ* mutants are crippled in virulence or avirulent respectively [256], suggesting that the observed defects in macrophage escape may affect the survival of *C. albicans* within the host and the establishment of infection.

4.3.2. C. albicans triggers pyroptotic programmed cell death in macrophages

Introduced here is also a novel assay that significantly changed our understanding of the mechanisms by which macrophages are killed by *C. albicans* and possibly other fungal pathogens. A key advantage provided by the novel assay included sensitive and quantitative analysis of macrophage death over smaller time intervals in real time. This is an important improvement over assays commonly used by investigators in the field [200, 202, 267-269], which use only sample specific time points, followed by visualization under the microscope. This may easily introduce “handling” errors in the number of *C. albicans* induced macrophage deaths, and

furthermore, only the selected time points are analysed, meaning that important events might be missed.

Utilizing the specific morphological differences between wild type, *med31* Δ/Δ and *srb9* Δ/Δ mutant cells I was able to discover that the process of macrophage killing by *C. albicans* is biphasic. The first phase occurred in the first 8-10 h under the experimental conditions that I utilized with an MOI of 6 *Candida* to 1 macrophage, while the second phase was initiated from 8 to 10 hours and ended between 18 and 24 hours. Of great importance was the discovery that, in the first phase of the interaction, the process of macrophage killing occurs via programmed cell death. This was first apparent when little to no macrophage killing occurred in the first phase when the RAW264.7 cell line was used in the assay. *C. albicans* cells continued filamentation for 8 to 10 hours without inflicting macrophage cell death - as if macrophages were “waiting” for *C. albicans* cells to escape before they started to die rapidly in the second phase (see videos as published in [256]). Although *C. albicans* cells are known to be viable and even divide within macrophages [270], this result was unexpected because macrophage killing by hyphae was hypothesized to occur primarily via mechanical piercing of macrophages [219, 220, 271].

For the two macrophage killing phases to occur, it was imperative that phagocytosed yeast cells were able to form hyphae containing wild type cell surface properties, as demonstrated by the results with the hyphae-impaired *med31* Δ/Δ mutant and the *srb9* Δ/Δ mutant which forms hyphae that have defective cell surface properties (Figure 4.2F and 4.5D and Figure 4.7). My results suggested that the type of programmed cell death induced in the first phase of macrophage killing by *C. albicans* is pyroptosis, since intra-macrophage wild type hyphae induced 40% to 50% less death in *casp1*^{-/-}*casp11*^{-/-} BMDMs compared to wild type BMDMs (Figure 4.10 A and B). For our assays, only the double mutant *casp1*^{-/-}*casp11*^{-/-} BMDMs was available for my use. Caspase-1 and caspase-11 both participate in the induction of pyroptosis [272, 273]. Caspase-11 seems to respond mainly to gram-negative bacteria and LPS [274, 275], and it is known that caspase-11 is unable to cleave IL-1 and IL-18, as macrophages lacking NLRP3, ASC or caspase-1 still activate caspase-11, but do not secrete IL-1 β [273]. In addition to this, macrophages killing in *nlrp3*^{-/-}

and *asc*^{-/-} mutant BMDMs revealed that deletion of components of the NLRP3 inflammasome affected macrophage death similar to *casp1*^{-/-}*casp11*^{-/-} BMDMs. Since NLRP3 inflammasome activation is upstream of caspase-1 activity, but not caspase-11, these data suggests that caspase-1 is the major pyroptotic caspase activated by *C. albicans* hyphal cells. Whilst my publication was under peer review, an independent study published by Wellington *et al.*, fully supported my findings by showing that macrophage killing occurs via pyroptosis and showing that death was hyphal induced and dependent on caspase-1 and the inflammasome subunits NLRP3 and ASC [265].

Although it was evident that pyroptosis is induced in the first phase of macrophage killing, results obtained from the macrophage killing assays including *med31*Δ/Δ mutant and heat killed cells revealed that there was death of macrophages that relied on other factors in the first phase. This conclusion is based on several findings. There was no macrophage killing induced by heat-killed cells, although the morphogenesis-defective *med31*Δ/Δ mutant yeast cells induced some macrophage cell death in both WT BMDMs and in *casp1*^{-/-}*casp11*^{-/-} BMDMs (Figure 4.5 and 4.13). These results indicate that, in addition to hyphal cells, live yeast cells participate in the first phase of macrophage killing. Studies have shown that heat killed cells expose more glucans molecules to activate the inflammasome extracellularly via Dectin-1 [241]. Our assay focused on intracellular activation of the inflammasome, and therefore the data suggest that other factors aside from glucan signaling are involved in the ability of live, intracellular yeast cells to kill macrophages to a higher extent than heat killed yeast cells. *C. albicans* cells are known to release soluble compounds that lead to suppression of nitric oxide (NO) production employed by macrophages to kill pathogens. This inhibition only occurs in the presence of live fungal cells and not heat killed or formaldehyde treated cells [276]. It is possible that live yeast cells are also able to induce early macrophage death through mechanisms yet to be identified.

An open question remains whether host cell death pathways other than pyroptosis participate in *C. albicans*-triggered macrophage cell death. We did investigate the possibility that *C. albicans* induces macrophage death via apoptosis. However, our work showed no evidence of activation of the apoptotic caspase-3 in

the first phase of macrophage killing, suggesting no induction of apoptosis [261]. *In vivo* studies using mice infection model addressing *Candida*-macrophage interactions and caspase-3 support the idea that caspase-3 is not activated, or only transiently activated by *Candida* [277]. Other studies also eliminated apoptosis induced through caspase-8 and caspase-9 activation as these are not activated in response to *C. albicans* infection of macrophages [278].

The exact trigger for the logarithmic cell death that occurs in phase two of macrophage killing is currently unknown. My results demonstrated that the second phase of macrophage death is very rapid and it occurs in NLRP3 inflammasome mutants, as well as upon treatment with pan-caspase inhibitors, eliminating all caspase-dependent pathways. The caspase-independent pathway known as necroptosis, which depends on the kinases Rip1 and Rip3 [279] may be involved, and this is an area of current to investigation in our laboratory. Wellington *et al.* suggested that fungal load triggers the second phase of killing that is independent of pyroptosis [265]. However, our detailed time lapse microscopy showed that this second phase does not occur for almost 8 hours, while fungal loads are high before then. Also, when initiated, the second phase of killing occurs very rapidly. Together, these observations argue against simple necrotic death, and instead suggest a regulated mechanism that is triggered by a signal. I noticed that in the second phase a lot of yeast-form cells are visible in the media surrounding macrophages. An intriguing possibility is that the reverse transition, from hyphae to yeast, plays a role in macrophage killing by *C. albicans*, but whether this is indeed the case remains to be determined.

In conclusion, the results in this chapter highlight the influence of Mediator co-regulatory roles in *C. albicans* morphogenesis for the induction of correct immune response and for *C. albicans* pathogenesis. The novel assay designed brought to light the two phases of macrophage killing induced by *C. albicans* challenging our current view on how *C. albicans* evades destruction by macrophages, and showing the ability of fungal cells to employ host pathways to their advantage. We have proposed that *C. albicans* might “hijack” the activation of the lytic macrophage cell death that is pyroptosis to escape from immune attack [256].

Systemic inflammation continues to be a problem caused by fungal infections. Our data suggest that lack of caspase-1 induced pyroptosis may provide a protective role, possibly in the human host. As introduced in section 4.1.5, caspase-1 is known to protect against *C. albicans* infections through induction of other immune effectors including Th1 and Th17 ([280-282]. It is possible that pyroptosis aids the host by inducing an inflammatory response that allows for the development of host adaptive immune system, as well as attracting immune effector cells to the sites of fungal infection. In addition to my work, other studies suggest that *casp1^{-/-}casp11^{-/-}* mice show normal fungal burdens [283, 284]. Therefore host immune cells must constantly balance pro-inflammatory responses with avoiding too much inflammation to mount appropriate immune response against fungal infections for the host to survive.

Chapter 5: Thesis summary and future directions

5.1. Thesis summary

The data in Chapter 3 and Chapter 4 suggest that the Mediator is required for the regulations of virulence genes in *C. albicans*. Moreover, comparative analysis of Mediator subunit functions in *S. cerevisiae* and *C. albicans* showed that both conserved and divergent roles can be detected. The conservation of Mediator functions between the fungal pathogen and non-pathogenic yeasts re-established the current thought of Mediator as an essential co-regulatory factor for transcriptional control in all eukaryotes, while the divergent roles establishes that Mediator can also be a source of gene regulation diversity, through shifts in negative and positive gene regulatory roles [138, 140].

The Mediator subunit Med31 acts via the Ace2 transcription factor in the regulation of *S. cerevisiae* and *C. albicans* cell proliferation through functions in cell separation (cytokinesis). Regulation of aspects of the cell cycle is conserved in the mammalian counterpart. Embryonic deletion of *MED31* leads to severe cell proliferation defects, as well as other roles in embryogenesis [285], showing that the functions in cell division and growth of this Mediator subunit are conserved from yeast to complex metazoans.

My investigations suggest that Mediator regulated important gene expression networks in *C. albicans* that enable the pathogen to survive the environmental pressures at sites colonised within the hosts as an adaptation to the environmental shifts. This concept is supported by a study on the Mediator Srb10 subunit in model yeast which showed roles of both positive and negative regulation as well as multiple roles in nutrient sensing gene control [182].

In Chapter 4, the importance of gene co-regulation of *C. albicans* virulence factors including cell wall components by the Mediator was established. In particular the Mediator control of the yeast to hyphal transition through Med31 and proper hyphal cell wall development via Srb9 proved critical in immune cell evasion. My study showed that Mediator function is required for activation of pyroptotic cell death by *C. albicans*. Furthermore, my study raises questions about the precise functions of hyphal morphogenesis and caspase-1 dependent pathways in disease caused by *C. albicans*. Modulation of caspase-1-dependent inflammatory responses could prove beneficial in restricting hyper-inflammation that results from recognition of *C. albicans* hyphae.

My results underscore the importance of integrating imaging and mechanistic studies. For years, we thought that fungal pathogens kill macrophages simply through hyphal growth extension and destruction of the host cell, however, my study showed that, although we observed fungal escape from immune cells that coincided with hyphal morphogenesis, careful analysis of fungal and host interactions indicated that *C. albicans* achieves this through manipulating a host cell death pathway. To specifically identify the downstream components involved in pathogenesis, one must also scrutinize and dissect even the most obvious observational findings *in vivo*, *ex vivo* and *in vitro* models.

This is well illustrated by our findings that *ex vivo* macrophages phagocytose *Candida* cells and these fungal cells are able to filament and escape macrophages. In contrast, Brothers *et al.* used the zebra fish model to show that *in vivo*, macrophages phagocytose *Candida* cells, but fungal cells do not escape macrophages[270]. It is possible that the ability of macrophages to control *C. albicans* morphogenesis *in vivo* differs from the experiments conducted *in vitro* and *ex vivo*.

In our *ex vivo* analyses of *Candida* phagocytosis by macrophages, the phagocytosis index variable was well controlled to an MOI of 1:6 (macrophage:*C. albicans*). In comparison, the *in vivo* zebra fish study, this variable could not be controlled and variations of MOI could be observed. Interestingly, the *in vivo* study suggested that macrophages were able to restrict *C. albicans* filamentation, however this finding was dependent on MOI. The more fungal cells were phagocytosed, the more filamentous fungal cells were observed and this lead to fungal escape. In comparison, fungal cells with low MOI were able to control filamentation of fungal cells within macrophages, and this lead to less filamentation and fungal escape. Our study findings correlate with the findings in relation to higher MOIs observed in in this study [270], suggesting that *in vitro* and *ex vivo* studies have some limitations to findings which may be obtained using *in vivo* studies.

In addition to this, in experiments with zebra fish the experimental temperature is kept between 28°C and 33°C. This is potentially a problem for evaluating the impact of morphogenesis, as human body temperature of 37°C is the standard trigger for the activation of the hyphal program in *C. albicans*, although *C. albicans* cells were founds to filament extracellularly in the zebrafish model [270]. A recent manuscript described *in vivo* imaging of the *Candida*-macrophage interaction in the mouse kidney using GFP-labelled macrophages and DsTomato-labelled *C. albicans* [286]. Here, yeast and filamentous cells of *C. albicans* were observed inside macrophages early upon infection of mice, while at later stages (24 h post-infection) the *C. albicans* filaments were not in contact with the macrophages any more. Whether the internalised *C. albicans* filaments in this *in vivo* model are due to engulfment of the filaments by macrophages or germination of the engulfed yeast cells (which would parallel our *ex vivo* experiments), is not clear.

Ultimately, full immunity to *C. albicans* in the mouse model *in vivo* requires caspase-1, and activation of caspase-1 can be observed by determining serum levels of IL-1beta post infection [287]. How precisely activation of pyroptosis by *C. albicans* contributes to immune evasion *in vivo* remains to be determined.

At the conclusion of this project, the majority of the aims for the project were fulfilled. The main findings in this thesis are as follows:

1. The *C. albicans* Mediator subunits co-regulate genes associated with cell division, particularly components of the RAM cell signalling network.
2. Subunits in the Kinase, Middle and Head modules are required for the co-regulation of *C. albicans* virulence factors in cell wall integrity and filamentous growth in association with morphogenesis related transcription factors.
3. Mediator has divergent roles between non-pathogenic and pathogenic yeast in the regulation adhesion and invasiveness.
4. Components of the Mediator are required for *C. albicans* morphogenesis and escape from innate immune cells -macrophages.
5. A novel macrophage-killing assay was designed and used to discover the different phases of host immune cell death following phagocytosis of *C. albicans*.
6. *C. albicans* triggers a suicide host cell program known as pyroptosis and then hijacks it to escape from macrophages.
7. The Mediator complex controls components of the *C. albicans* cell surface that might be important for immune evasion.

5.2. Future directions

My study elucidated the functions of the *C. albicans* Mediator o in regards to roles in cell wall biogenesis, morphogenesis and host-pathogen interactions, and my results opened up several questions to be investigated in future work. These questions are outlined below:

1. What transcription factors does Mediator collaborate with to regulate pathways important for *C. albicans* pathogenesis?
2. How are the functions of Mediator in cell wall integrity coordinated with its roles in adherence and biofilm formation? What down-stream targets of Mediator control these pathways?
3. Are the observed defects of Mediator mutants in macrophage escape *ex vivo* recapitulated *in vivo*?
4. Are the biofilm formation defects recapitulated *in vivo* in animal models?
5. How does *Candida* modulate its cell wall composition in hyphae to trigger pyroptotic cell death in macrophages?
6. Precisely what cell wall components are required for macrophage escape?
7. What other host pathways, besides pyroptosis, are involved in macrophage cell death in response to *Candida* infection?
8. What are the mechanistic properties of the rapid phase 2 of macrophage killing by *Candida*?
9. Does yeast morphology play a role in macrophage escape?

Future work using pathogen and host mutants impaired in specific cell wall components, morphogenesis of host responses, coupled with the macrophage-killing assay developed in this project, "omics" approaches (transcriptomics, proteomics and glycomics), animal models and *in vivo* imaging should be able to answer some of these outstanding questions.

References

1. Ruhnke, M., *Epidemiology of Candida albicans Infections and Role of Non-Candidaalbicans Yeasts*. *Curr Drug Targets*, 2006. **7**(4): p. 495-504.
2. Pfaller, M.A. and D.J. Diekema, *Epidemiology of Invasive Candidiasis: a Persistent Public Health Problem*. *Clinical Microbiology Reviews*, 2007. **20**(1): p. 133-163.
3. Iwatani, S., *et al.*, *Successful Management of an Extremely Premature Infant with Congenital Candidiasis*. *AJP Rep*, 2014. **4**(01): p. 005-008.
4. da Silva-Rocha, W., *et al.*, *Candida species distribution, genotyping and virulence factors of Candida albicans isolated from the oral cavity of kidney transplant recipients of two geographic regions of Brazil*. *BMC Oral Health*, 2014. **14**(1): p. 20.
5. Lee, S.-Y., *et al.*, *Prevalence of invasive fungal disease in hematological patients at a tertiary university hospital in Singapore*. *BMC Research Notes*, 2011. **4**(1): p. 42.
6. Sobel, J.D., *et al.*, *Vulvovaginal candidiasis: Epidemiologic, diagnostic, and therapeutic considerations*. *American Journal of Obstetrics and Gynecology*, 1998. **178**(2): p. 203-211.
7. Pfaller, M.A., *et al.*, *Results from the ARTEMIS DISK Global Antifungal Surveillance Study, 1997 to 2005: an 8.5-Year Analysis of Susceptibilities of Candida Species and Other Yeast Species to Fluconazole and Voriconazole Determined by CLSI Standardized Disk Diffusion Testing*. *Journal of Clinical Microbiology*, 2007. **45**(6): p. 1735-1745.
8. Wisplinghoff, H., *et al.*, *Nosocomial Bloodstream Infections in US Hospitals: Analysis of 24,179 Cases from a Prospective Nationwide Surveillance Study*. *Clinical Infectious Diseases*, 2004. **39**(3): p. 309-317.
9. Hajjeh, R.A., *et al.*, *Incidence of Bloodstream Infections Due to Candida Species and In Vitro Susceptibilities of Isolates Collected from 1998 to 2000 in a*

- Population-Based Active Surveillance Program*. Journal of Clinical Microbiology, 2004. **42**(4): p. 1519-1527.
10. Brown, G.D., D.W. Denning, and S.M. Levitz, *Tackling Human Fungal Infections*. Science, 2012. **336**(6082): p. 647.
 11. Trofa, D., A. Gácsér, and J.D. Nosanchuk, *Candida parapsilosis, an Emerging Fungal Pathogen*. Clinical Microbiology Reviews, 2008. **21**(4): p. 606-625.
 12. Vazquez, J.A., *et al.*, *A Multicenter Randomized Trial Evaluating Posaconazole versus Fluconazole for the Treatment of Oropharyngeal Candidiasis in Subjects with HIV/AIDS*. Clinical Infectious Diseases, 2006. **42**(8): p. 1179-1186.
 13. Sobel, J.D., *Recurrent Vulvovaginal Candidiasis*. New England Journal of Medicine, 1986. **315**(23): p. 1455-1458.
 14. Fidel, P.L., *Candida-Host Interactions in HIV Disease: Implications for Oropharyngeal Candidiasis*. Advances in Dental Research, 2011. **23**(1): p. 45-49.
 15. Ramos-e-Silva, M., *et al.*, *Superficial mycoses in immunodepressed patients (AIDS)*. Clinics in Dermatology, 2010. **28**(2): p. 217-225.
 16. Pemán, J., E. Cantón, and A. Espinel-Ingroff, *Antifungal drug resistance mechanisms*. Expert Review of Anti-infective Therapy, 2009. **7**(4): p. 453-460.
 17. Mishra, N., *et al.*, *Pathogenicity and drug resistance in Candida albicans and other yeast species*. Acta Microbiologica et Immunologica Hungarica, 2007. **54**(3): p. 201-235.
 18. White, T.C., *et al.*, *Resistance Mechanisms in Clinical Isolates of Candida albicans*. Antimicrobial Agents and Chemotherapy, 2002. **46**(6): p. 1704-1713.
 19. Mitchell, A.P., *Dimorphism and virulence in Candida albicans*. Current Opinion in Microbiology, 1998. **1**(6): p. 687-692.
 20. Sanglard, D., *Resistance of human fungal pathogens to antifungal drugs*. Current Opinion in Microbiology, 2002. **5**(4): p. 379-385.
 21. Sanglard, D., *Resistance and tolerance mechanisms to antifungal drugs in fungal pathogens*. Mycologist, 2003. **17**(2): p. 74-78.
 22. Longley, N., *et al.*, *Dose Response Effect of High-Dose Fluconazole for HIV-Associated Cryptococcal Meningitis in Southwestern Uganda*. Clinical Infectious Diseases, 2008. **47**(12): p. 1556-1561.
 23. Morschhäuser, J., *The genetic basis of fluconazole resistance development in Candida albicans*. Biochimica et Biophysica Acta (BBA) - Molecular Basis of Disease, 2002. **1587**(2-3): p. 240-248.
 24. Cannon, R.D., *et al.*, *Efflux-Mediated Antifungal Drug Resistance*. Clinical Microbiology Reviews, 2009. **22**(2): p. 291-321.

25. Gray, K.C., *et al.*, *Amphotericin primarily kills yeast by simply binding ergosterol*. Proceedings of the National Academy of Sciences, 2012. **109**(7): p. 2234-2239.
26. Bates, D.W., *et al.*, *Mortality and Costs of Acute Renal Failure Associated with Amphotericin B Therapy*. Clinical Infectious Diseases, 2001. **32**(5): p. 686-693.
27. Niimi, K. and M. Niimi, *The Mechanisms of Resistance to Echinocandin Class of Antifungal Drugs*. Nippon Ishinkin Gakkai Zasshi, 2009. **50**(2): p. 057-066.
28. Olaechea, P.M., *et al.*, *Economic Impact of Candida Colonization and Candida Infection in the Critically Ill Patient*. European Journal of Clinical Microbiology and Infectious Diseases, 2004. **23**(4): p. 323-330.
29. Ramage, G., J.P. Martínez, and J.L. López-Ribot, *Candida biofilms on implanted biomaterials: a clinically significant problem*. FEMS Yeast Research, 2006. **6**(7): p. 979-986.
30. Selma Tobudic, C.K., Andrea Lassnigg, Birgit Willinger, Wolfgang Graninger, Elisabeth Presterl, *Biofilm formation of Candida spp. isolates from patients at a cardiothoracic intensive care unit*. Int J Artif Organs, 2011. **34**(9): p. 818 - 823.
31. De Pauw, B., *et al.*, *Revised Definitions of Invasive Fungal Disease from the European Organization for Research and Treatment of Cancer/Invasive Fungal Infections Cooperative Group and the National Institute of Allergy and Infectious Diseases Mycoses Study Group (EORTC/MSG) Consensus Group*. Clinical Infectious Diseases, 2008. **46**(12): p. 1813-1821.
32. Thompson, D.S., P.L. Carlisle, and D. Kadosh, *Coevolution of Morphology and Virulence in Candida Species*. Eukaryotic Cell, 2011. **10**(9): p. 1173-1182.
33. Gimeno, C.J., *et al.*, *Unipolar cell divisions in the yeast S. cerevisiae lead to filamentous growth: Regulation by starvation and RAS*. Cell. **68**(6): p. 1077-1090.
34. Pande, K., C. Chen, and S.M. Noble, *Passage through the mammalian gut triggers a phenotypic switch that promotes Candida albicans commensalism*. Nat Genet, 2013. **45**(9): p. 1088-1091.
35. Liu, Y., *et al.*, *Mechanisms of Candida albicans Trafficking to the Brain*. PLoS Pathog, 2011. **7**(10): p. e1002305.
36. Mavor, A.L., S. Thewes, and B. Hube, *Systemic Fungal Infections Caused by Candida Species: Epidemiology, Infection Process and Virulence Attributes*. Current Drug Targets, 2005. **6**(8): p. 863-874.
37. S. Nadeem, A.S., S. Hakim, Y. Anjum and S. U. Kazm., *Effect of Growth Media, pH and Temperature on Yeast to Hyphal Transition in Candida albicans*. Open Journal of Medical Microbiology, 2013. **3**(3): p. 185-192.
38. Uwamahoro, N. and A. Traven, *Yeast, Filaments and Biofilms in Pathogenesis of Candida albicans*. 2012.
39. Sudbery, P.E., *Growth of Candida albicans hyphae*. Nature Reviews Microbiology, 2011. **9**: p. 737+.

40. Hawser, S.P., Douglas, L J, *Biofilm formation by Candida species on the surface of catheter materials in vitro*. *Infect. Immun.*, 1994. **62**(3): p. 915-921.
41. Richard, M.L., *et al.*, *Candida albicans Biofilm-Defective Mutants*. *Eukaryotic Cell*, 2005. **4**(8): p. 1493-1502.
42. Uppuluri, P., *et al.*, *Dispersion as an Important Step in the Candida albicans Biofilm Developmental Cycle*. *PLoS Pathog*, 2010. **6**(3): p. e1000828.
43. Carlisle, P.L., *et al.*, *Expression levels of a filament-specific transcriptional regulator are sufficient to determine Candida albicans morphology and virulence*. *Proceedings of the National Academy of Sciences*, 2009. **106**(2): p. 599-604.
44. Netea, M.G., *et al.*, *An integrated model of the recognition of Candida albicans by the innate immune system*. *Nat Rev Micro*, 2008. **6**(1): p. 67-78.
45. Sudbery, P.E., *Growth of Candida albicans hyphae*. *Nat Rev Micro*, 2011. **9**(10): p. 737-748.
46. Biswas, S., P. Van Dijck, and A. Datta, *Environmental Sensing and Signal Transduction Pathways Regulating Morphopathogenic Determinants of Candida albicans*. *Microbiology and Molecular Biology Reviews*, 2007. **71**(2): p. 348-376.
47. Lo, H.-J., *et al.*, *Nonfilamentous C. albicans Mutants Are Avirulent*. *Cell*, 1997. **90**(5): p. 939-949.
48. Dhillon, N.K., S. Sharma, and G.K. Khuller, *Signaling Through Protein Kinases and Transcriptional Regulators in Candida albicans*. *Critical Reviews in Microbiology*, 2003. **29**(3): p. 259-275.
49. Cleary, I. and S. Saville, *An analysis of the Impact of NRG1 Overexpression on the Candida albicans Response to Specific Environmental Stimuli*. *Mycopathologia*, 2010. **170**(1): p. 1-10.
50. Lass-Flörl, C., *et al.*, *Activities of Antifungal Agents against Yeasts and Filamentous Fungi: Assessment according to the Methodology of the European Committee on Antimicrobial Susceptibility Testing*. *Antimicrobial Agents and Chemotherapy*, 2008. **52**(10): p. 3637-3641.
51. Jayatilake, J.A.M.S., *et al.*, *Quantitative evaluation of tissue invasion by wild type, hyphal and SAP mutants of Candida albicans, and non-albicans Candida species in reconstituted human oral epithelium*. *Journal of Oral Pathology & Medicine*, 2006. **35**(8): p. 484-491.
52. Kumamoto, C.A. and M.D. Vices, *Contributions of hyphae and hypha-co-regulated genes to Candida albicans virulence*. *Cellular Microbiology*, 2005. **7**(11): p. 1546-1554.
53. Saville, S.P., *et al.*, *Engineered Control of Cell Morphology In Vivo Reveals Distinct Roles for Yeast and Filamentous Forms of Candida albicans during Infection*. *Eukaryotic Cell*, 2003. **2**(5): p. 1053-1060.

54. Nather, K. and C.A. Munro, *Generating cell surface diversity in Candida albicans and other fungal pathogens*. FEMS Microbiology Letters, 2008. **285**(2): p. 137-145.
55. Cabib, E. and B. Bowers, *Chitin and Yeast Budding: localization of Chitin in Yeast Bud Scars*. Journal of Biological Chemistry, 1971. **246**(1): p. 152-159.
56. van der Graaf, C.A.A., *et al.*, *Differential Cytokine Production and Toll-Like Receptor Signaling Pathways by Candida albicans Blastoconidia and Hyphae*. Infection and Immunity, 2005. **73**(11): p. 7458-7464.
57. d'Ostiani, C.F., *et al.*, *Dendritic Cells Discriminate between Yeasts and Hyphae of the Fungus Candida albicans: Implications for Initiation of T Helper Cell Immunity in Vitro and in Vivo*. The Journal of Experimental Medicine, 2000. **191**(10): p. 1661-1674.
58. Felk, A., *et al.*, *Candida albicans Hyphal Formation and the Expression of the Efg1-Regulated Proteinases Sap4 to Sap6 Are Required for the Invasion of Parenchymal Organs*. Infection and Immunity, 2002. **70**(7): p. 3689-3700.
59. Fradin, C. and B. Hube, *Tissue Infection and Site-specific Gene Expression in Candida albicans*, in *Advances in Applied Microbiology*. 2003, Academic Press. p. 271-290.
60. Hube, B., *From commensal to pathogen: stage- and tissue-specific gene expression of Candida albicans*. Current Opinion in Microbiology, 2004. **7**(4): p. 336-341.
61. Lionakis, M.S., *et al.*, *Organ-Specific Innate Immune Responses in a Mouse Model of Invasive Candidiasis*. Journal of Innate Immunity, 2011. **3**(2): p. 180-199.
62. Scherwitz, C., *Ultrastructure of Human Cutaneous Candidosis*. J Investig Dermatol, 1982. **78**(3): p. 200-205.
63. Gow, N.A.R., *et al.*, *Candida albicans morphogenesis and host defence: discriminating invasion from colonization*. Nat Rev Micro, 2012. **10**(2): p. 112-122.
64. Moyes, D.L., *et al.*, *A Biphasic Innate Immune MAPK Response Discriminates between the Yeast and Hyphal Forms of Candida albicans in Epithelial Cells*. Cell Host & Microbe, 2010. **8**(3): p. 225-235.
65. Donlan, R.M. and J.W. Costerton, *Biofilms: Survival Mechanisms of Clinically Relevant Microorganisms*. Clinical Microbiology Reviews, 2002. **15**(2): p. 167-193.
66. Harriott, M.M. and M.C. Noverr, *Importance of Candida–bacterial polymicrobial biofilms in disease*. Trends in Microbiology, 2011. **19**(11): p. 557-563.
67. Baillie, G.S. and L.J. Douglas, *Role of dimorphism in the development of Candida albicans biofilms*. Journal of Medical Microbiology, 1999. **48**(7): p. 671-679.
68. Ramage, G., *et al.*, *The filamentation pathway controlled by the Efg1 regulator protein is required for normal biofilm formation and development in Candida albicans*. FEMS Microbiology Letters, 2002. **214**(1): p. 95-100.

69. Mathé, L. and P. Van Dijck, *Recent insights into Candida albicans biofilm resistance mechanisms*. Current Genetics, 2013. **59**(4): p. 251-264.
70. Nett, J.E., *et al.*, *Genetic Basis of Candida Biofilm Resistance Due to Drug-Sequestering Matrix Glucan*. Journal of Infectious Diseases, 2010. **202**(1): p. 171-175.
71. Nett, J.E., *et al.*, *Role of Fks1p and Matrix Glucan in Candida albicans Biofilm Resistance to an Echinocandin, Pyrimidine, and Polyene*. Antimicrobial Agents and Chemotherapy, 2010. **54**(8): p. 3505-3508.
72. LaFleur, M.D., C.A. Kumamoto, and K. Lewis, *Candida albicans Biofilms Produce Antifungal-Tolerant Persister Cells*. Antimicrobial Agents and Chemotherapy, 2006. **50**(11): p. 3839-3846.
73. Dieterich, C., *et al.*, *In vitro reconstructed human epithelia reveal contributions of Candida albicans EFG1 and CPH1 to adhesion and invasion*. Microbiology, 2002. **148**(2): p. 497-506.
74. Nobile, C.J. and A.P. Mitchell, *Regulation of Cell-Surface Genes and Biofilm Formation by the C. albicans Transcription Factor Bcr1p*. Current Biology, 2005. **15**(12): p. 1150-1155.
75. Nett, J.E., *et al.*, *Development and Validation of an In Vivo Candida albicans Biofilm Denture Model*. Infection and Immunity, 2010. **78**(9): p. 3650-3659.
76. Řičicová, M., *et al.*, *Candida albicans biofilm formation in a new in vivo rat model*. Microbiology, 2010. **156**(3): p. 909-919.
77. Nobile, C.J., *et al.*, *Critical Role of Bcr1-Dependent Adhesins in C. albicans Biofilm Formation In Vitro and In Vivo*. PLoS Pathog, 2006. **2**(7): p. e63.
78. Jenkinson, H.F. and J. Douglas, *Interactions between Candida Species and Bacteria in Mixed Infections*, in *Polymicrobial Diseases*, G.J. Brogden KA, Editor. 2002, ASM Press: Washington (DC).
79. de Groot, P.W.J., *et al.*, *Adhesins in Human Fungal Pathogens: Glue with Plenty of Stick*. Eukaryotic Cell, 2013. **12**(4): p. 470-481.
80. Poulain, D. and T. Jouault, *Candida albicans cell wall glycans, host receptors and responses: elements for a decisive crosstalk*. Current Opinion in Microbiology, 2004. **7**(4): p. 342-349.
81. Proctor, Stephen A., *et al.*, *Contributions of Turgor Pressure, the Contractile Ring, and Septum Assembly to Forces in Cytokinesis in Fission Yeast*. Current Biology. **22**(17): p. 1601-1608.
82. Chaffin, W.L., *Candida albicans Cell Wall Proteins*. Microbiology and Molecular Biology Reviews, 2008. **72**(3): p. 495-544.
83. Lowman, D.W., *et al.*, *Novel Structural Features in Candida albicans Hyphal Glucan Provide a Basis for Differential Innate Immune Recognition of Hyphae Versus Yeast*. Journal of Biological Chemistry, 2014. **289**(6): p. 3432-3443.

84. Castillo, L., *et al.*, *A study of the Candida albicans cell wall proteome*. PROTEOMICS, 2008. **8**(18): p. 3871-3881.
85. Gow, N.A.R. and B. Hube, *Importance of the Candida albicans cell wall during commensalism and infection*. Current Opinion in Microbiology, 2012. **15**(4): p. 406-412.
86. Gantner, B.N., R.M. Simmons, and D.M. Underhill, *Dectin-1 mediates macrophage recognition of Candida albicans yeast but not filaments*. Vol. 24. 2005. 1277-1286.
87. Klis, F.M., *et al.*, *Covalently linked cell wall proteins of Candida albicans and their role in fitness and virulence*. FEMS Yeast Research, 2009. **9**(7): p. 1013-1028.
88. Brown, A.J.P., *et al.*, *Stress adaptation in a pathogenic fungus*. The Journal of Experimental Biology, 2014. **217**(1): p. 144-155.
89. Verstrepen, K.J. and F.M. Klis, *Flocculation, adhesion and biofilm formation in yeasts*. Molecular Microbiology, 2006. **60**(1): p. 5-15.
90. Ruiz-Herrera, J., *et al.*, *Molecular organization of the cell wall of Candida albicans and its relation to pathogenicity*. FEMS Yeast Research, 2006. **6**(1): p. 14-29.
91. Latgé, J.-P., *The cell wall: a carbohydrate armour for the fungal cell*. Molecular Microbiology, 2007. **66**(2): p. 279-290.
92. Rest, M.E.v.d., *et al.*, *The Plasma Membrane of Saccharomyces cerevisiae: Structure, Function, and Biogenesis*. Microbiol Rev, 1995. **59**(2): p. 304-322.
93. Prasad, R., *The Plasma Membrane of Candida albicans: Its Relevance to Transport Phenomenon*, in *Candida Albicans*, R. Prasad, Editor. 1991, Springer Berlin Heidelberg. p. 108-127.
94. Cabezón, V., *et al.*, *Analysis of Candida albicans plasma membrane proteome*. Proteomics , 2009. **9**(20): p. 4770-4786.
95. Reynolds, T.B. and G.R. Fink, *Bakers' Yeast, a Model for Fungal Biofilm Formation*. Science, 2001. **291**: p. 878.
96. Reynolds, T.B., *et al.*, *Mat Formation in Saccharomyces cerevisiae Requires Nutrient and pH Gradients*. Eukaryotic Cell, 2008. **7**(1): p. 122-130.
97. Ryan, O., *et al.*, *Global Gene Deletion Analysis Exploring Yeast Filamentous Growth*. Science, 2012. **337**(6100): p. 1353-1356.
98. Fu, Y., *et al.*, *Candida albicans Als1p: an adhesin that is a downstream effector of the EFG1 filamentation pathway*. Molecular Microbiology, 2002. **44**(1): p. 61-72.
99. Liu, Y. and S.G. Filler, *Candida albicans Als3, a Multifunctional Adhesin and Invasin*. Eukaryotic Cell, 2011. **10**(2): p. 168-173.
100. Zhao, X., *et al.*, *Candida albicans Als3p is required for wild-type biofilm formation on silicone elastomer surfaces*. Microbiology, 2006. **152**(8): p. 2287-2299.

101. Hoyer, L.L., *et al.*, *Discovering the secrets of the Candida albicans agglutinin-like sequence (ALS) gene family – a sticky pursuit*. Medical Mycology, 2008. **46**(1): p. 1-15.
102. Nobile, C.J., *et al.*, *Function of Candida albicans Adhesin Hwp1 in Biofilm Formation*. Eukaryotic Cell, 2006. **5**(10): p. 1604-1610.
103. Fanning, S., *et al.*, *Divergent Targets of Candida albicans Biofilm Regulator Bcr1 In Vitro and In Vivo*. Eukaryotic Cell, 2012. **11**(7): p. 896-904.
104. Fichtner, L., F. Schulze, and G.H. Braus, *Differential Flo8p-dependent regulation of FLO1 and FLO11 for cell–cell and cell–substrate adherence of S. cerevisiae S288c*. Molecular Microbiology, 2007. **66**(5): p. 1276-1289.
105. Research, E.Z.D.-B.c., *cell cycle figure* <http://www.csb.ethz.ch/research/dynamic>.
106. Bachewich, C., A. Nantel, and M. Whiteway, *Cell cycle arrest during S or M phase generates polarized growth via distinct signals in Candida albicans*. Molecular Microbiology, 2005. **57**(4): p. 942-959.
107. Saputo, S., *et al.*, *The RAM Network in Pathogenic Fungi*. Eukaryotic Cell, 2012. **11**(6): p. 708-717.
108. Weiss, E.L., *Mitotic Exit and Separation of Mother and Daughter Cells*. Genetics, 2012. **192**(4): p. 1165-1202.
109. Nelson, B., *et al.*, *RAM: A Conserved Signaling Network That Regulates Ace2p Transcriptional Activity and Polarized Morphogenesis*. Molecular Biology of the Cell, 2003. **14**(9): p. 3782-3803.
110. Weiss, E.L., *et al.*, *The Saccharomyces cerevisiae Mob2p–Cbk1p kinase complex promotes polarized growth and acts with the mitotic exit network to facilitate daughter cell–specific localization of Ace2p transcription factor*. The Journal of Cell Biology, 2002. **158**(5): p. 885-900.
111. Colman-Lerner, A., T.E. Chin, and R. Brent, *Yeast Cbk1 and Mob2 Activate Daughter-Specific Genetic Programs to Induce Asymmetric Cell Fates*. Cell, 2001. **107**(6): p. 739-750.
112. Laabs, T.L., *et al.*, *ACE2 is required for daughter cell-specific G1 delay in Saccharomyces cerevisiae*. Proceedings of the National Academy of Sciences, 2003. **100**(18): p. 10275-10280.
113. Dohrmann, P.R., *et al.*, *Parallel pathways of gene regulation: homologous regulators SWI5 and ACE2 differentially control transcription of HO and chitinase*. Genes & Development, 1992. **6**(1): p. 93-104.
114. Song, Y., Cheon, Seon Ah., Lee, Kyung Eun., Lee, So-Yeon., Lee, Byung-Kyu., Oh, Doo-Byung., Kang, Hyun Ah., Kim, Jeong-Yoon, *Role of the RAM Network in Cell Polarity and Hyphal Morphogenesis in Candida albicans*. Mol. Biol. Cell, 2008. **19**(12): p. 5456-5477.

115. Mulhern, S.M., M.E. Logue, and G. Butler, *Candida albicans* Transcription Factor *Ace2* Regulates Metabolism and Is Required for Filamentation in Hypoxic Conditions. *Eukaryotic Cell*, 2006. **5**(12): p. 2001-2013.
116. King, L. and G. Butler, *Ace2p*, a regulator of *CTS1* (chitinase) expression, affects pseudohyphal production in *Saccharomyces cerevisiae*. *Current Genetics*, 1998. **34**(3): p. 183-191.
117. Huang, G., *Regulation of phenotypic transitions in the fungal pathogen Candida albicans*. *Virulence*, 2012. **3**(3): p. 251-261.
118. Nobile, C.J. and A.P. Mitchell, *Genetics and genomics of Candida albicans* biofilm formation. *Cell Microbiol*, 2006. **8**(9): p. 1382-91.
119. Nobile, C.J. and A.P. Mitchell, *Regulation of Cell-Surface Genes and Biofilm Formation by the C. albicans* Transcription Factor *Bcr1p*. *Current biology : CB*, 2005. **15**(12): p. 1150-1155.
120. Nobile, Clarissa J., et al., *A Recently Evolved Transcriptional Network Controls Biofilm Development in Candida albicans*. *Cell*. **148**(1): p. 126-138.
121. Conaway, R.C. and J.W. Conaway, *The Mediator complex and transcription elongation*. *Biochimica et Biophysica Acta (BBA) - Gene Regulatory Mechanisms*, 2013. **1829**(1): p. 69-75.
122. Rodríguez-Navarro, S., *Insights into SAGA function during gene expression*. Vol. 10. 2009. 843-850.
123. Chen, X.-F., et al., *Mediator and SAGA Have Distinct Roles in Pol II Preinitiation Complex Assembly and Function*. *Cell Reports*, 2012. **2**(5): p. 1061-1067.
124. Miklos, I., et al., *Genomic expression patterns in cell separation mutants of Schizosaccharomyces pombe defective in the genes sep10 + and sep15 + coding for the Mediator subunits Med31 and Med8*. *Molecular Genetics and Genomics*, 2008. **279**(3): p. 225-238.
125. Linder, T., Rasmussen, N. N., Samuelsen, C. O., Chatzidaki, E., Baraznenok, V., Beve, J., Henriksen, P., Gustafsson, C. M., Holmberg, S., *Two conserved modules of Schizosaccharomyces pombe Mediator regulate distinct cellular pathways*. *Nucleic Acids Res*, 2008. **36**: p. 2489-2504.
126. Linder, T. and C.M. Gustafsson, *The Soh1/MED31 Protein Is an Ancient Component of Schizosaccharomyces pombe and Saccharomyces cerevisiae Mediator*. *J. Biol. Chem.*, 2004. **279**(47): p. 49455-49459.
127. Linder, T., et al., *Two conserved modules of Schizosaccharomyces pombe Mediator regulate distinct cellular pathways*. *Nucleic Acids Research*, 2008. **36**(8): p. 2489-2504.
128. Zhu, X., et al., *Genome-Wide Occupancy Profile of Mediator and the Srb8-11 Module Reveals Interactions with Coding Regions*. *Molecular cell*, 2006. **22**(2): p. 169-178.

129. Kim, Y.-J., *et al.*, *A multiprotein mediator of transcriptional activation and its interaction with the C-terminal repeat domain of RNA polymerase II*. *Cell*, 1994. **77**(4): p. 599-608.
130. Kornberg, R.D., *The mediator Special Issue*, in *Mediator comes of age*, R.D. Kornberg, Editor. 2005, Trends in Biochemical sciences.
131. Björklund, S. and C.M. Gustafsson, *The yeast Mediator complex and its regulation*. Trends in Biochemical Sciences, 2005. **30**(5): p. 240-244.
132. Kim, Y.-J. and J.T. Lis, *Interactions between subunits of Drosophila Mediator and activator proteins*. Trends in Biochemical Sciences, 2005. **30**(5): p. 245-249.
133. Conaway, R.C., *et al.*, *The mammalian Mediator complex and its role in transcriptional regulation*. Trends in Biochemical Sciences, 2005. **30**(5): p. 250-255.
134. Malik, S. and R.G. Roeder, *Dynamic regulation of pol II transcription by the mammalian Mediator complex*. Trends in Biochemical Sciences, 2005. **30**(5): p. 256-263.
135. Bourbon HM, A.A., Ansari AZ, Asturias FJ, Berk AJ, Bjorklund S, Blackwell TK, Borggreffe T, Carey M, Carlson M, Conaway JW, Conaway RC, Emmons SW, Fondell JD, Freedman LP, Fukasawa T, Gustafsson CM, Han M, He X, Herman PK, Hinnebusch AG, Holmberg S, Holstege FC, Jaehning JA, Kim YJ, Kuras L, Leutz A, Lis JT, Meisterernest M, Naar AM, Nasmyth K, Parvin JD, Ptashne M, Reinberg D, Ronne H, Sadowski I, Sakurai H, Sipiczki M, Sternberg PW, Stillman DJ, Strich R, Struhl K, Svejstrup JQ, Tuck S, Winston F, Roeder RG, Kornberg RD *A unified nomenclature for protein subunits of mediator complexes linking transcriptional regulators to RNA polymerase II*. *Molecular Cell*, 2004. **14**(5): p. 553-557.
136. Zhang, A., *et al.*, *The Tlo Proteins Are Stoichiometric Components of Candida albicans Mediator Anchored via the Med3 Subunit*. *Eukaryotic Cell*, 2012. **11**(7): p. 874-884.
137. Poss, Z.C., C.C. Ebmeier, and D.J. Taatjes, *The Mediator complex and transcription regulation*. *Critical Reviews in Biochemistry and Molecular Biology*, 2013. **48**(6): p. 575-608.
138. Ansari, S. and R. Morse, *Mechanisms of Mediator complex action in transcriptional activation*. *Cellular and Molecular Life Sciences*, 2013. **70**(15): p. 2743-2756.
139. Shahi, P., *et al.*, *Differential Roles of Transcriptional Mediator Subunits in Regulation of Multidrug Resistance Gene Expression in Saccharomyces cerevisiae*. *Molecular Biology of the Cell*, 2010. **21**(14): p. 2469-2482.
140. Casamassimi, A. and C. Napoli, *Mediator complexes and eukaryotic transcription regulation: An overview*. *Biochimie*, 2007. **89**(12): p. 1439-1446.
141. Samuelson, C.O., *et al.*, *TRAP230/ARC240 and TRAP240/ARC250 Mediator subunits are functionally conserved through evolution*. *Proceedings of the National Academy of Sciences*, 2003. **100**(11): p. 6422-6427.

142. Balciunas, D., *et al.*, *The Med1 subunit of the yeast mediator complex is involved in both transcriptional activation and repression*. Proceedings of the National Academy of Sciences of the United States of America, 1999. **96**(2): p. 376-381.
143. Galbraith, M.D., A.J. Donner, and J.M. Espinosa, *CDK8: A positive regulator of transcription*. Transcription, 2010. **1**(1): p. 4-12.
144. Malik, S. and R.G. Roeder, *The metazoan Mediator co-activator complex as an integrative hub for transcriptional regulation*. Nature Reviews Genetics, 2010. **11**: p. 761+.
145. Howard, S.C., *et al.*, *The Ras/PKA Signaling Pathway of Saccharomyces cerevisiae Exhibits a Functional Interaction With the Sin4p Complex of the RNA Polymerase II Holoenzyme*. Genetics, 2001. **159**(1): p. 77-89.
146. Koschubs, T., *et al.*, *Identification, structure, and functional requirement of the Mediator submodule Med7N/31*. Embo Journal, 2009. **28**(1): p. 69-80.
147. *Saccharomyces Genome Database* (<http://www.yeastgenome.org/>).
148. Wang, L.-I., *et al.*, *Cryptococcus neoformans Mediator Protein Ssn8 Negatively Regulates Diverse Physiological Processes and Is Required for Virulence*. PLoS ONE, 2011. **6**(4): p. e19162.
149. Zhou, X., *et al.*, *The CID1 cyclin C-like gene is important for plant infection in Fusarium graminearum*. Fungal Genetics and Biology, 2010. **47**(2): p. 143-151.
150. Thakur, J.K., *et al.*, *A nuclear receptor-like pathway regulating multidrug resistance in fungi*. Nature, 2008. **452**(7187): p. 604-609.
151. Nobile, C. and A. Mitchell, *Large-Scale Gene Disruption Using the UAU1 Cassette, in Candida albicans*, R. Cihlar and R. Calderone, Editors. 2009, Humana Press. p. 175-194.
152. Blankenship, J.R., *et al.*, *An Extensive Circuitry for Cell Wall Regulation in Candida albicans*. PLoS Pathog, 2010. **6**(2): p. e1000752.
153. Wilson, R.B., D. Davis, and A.P. Mitchell, *Rapid Hypothesis Testing with Candida albicans through Gene Disruption with Short Homology Regions*. Journal of Bacteriology, 1999. **181**(6): p. 1868-1874.
154. Firon, A., *et al.*, *The SUN41 and SUN42 genes are essential for cell separation in Candida albicans*. Molecular Microbiology, 2007. **66**(5): p. 1256-1275.
155. Homann, O.R., *et al.*, *A Phenotypic Profile of the Candida albicans Regulatory Network*. PLoS Genet, 2009. **5**(12): p. e1000783.
156. Collart, M.A. and S. Oliviero, *Preparation of Yeast RNA*, in *Current Protocols in Molecular Biology*. 2001, John Wiley & Sons, Inc.
157. Green, C.B., *et al.*, *Construction and real-time RT-PCR validation of Candida albicans PALS-GFP reporter strains and their use in flow cytometry analysis of ALS*

- gene expression in budding and filamenting cells.* Microbiology, 2005. **151**(4): p. 1051-1060.
158. Dagley, M.J., *et al.*, *Cell wall integrity is linked to mitochondria and phospholipid homeostasis in Candida albicans through the activity of the post-transcriptional regulator Ccr4-Pop2.* Molecular Microbiology, 2011. **79**(4): p. 968-989.
 159. Vandeputte, P., *et al.*, *Identification and Functional Characterization of Rca1, a Transcription Factor Involved in both Antifungal Susceptibility and Host Response in Candida albicans.* Eukaryotic Cell, 2012. **11**(7): p. 916-931.
 160. de Boer, C.G. and T.R. Hughes, *YeTFaSCo: a database of evaluated yeast transcription factor sequence specificities.* Nucleic Acids Research, 2012. **40**(D1): p. D169-D179.
 161. Deighton, M.A., *et al.*, [17] *Methods for studying biofilms produced by staphylococcus epidermidis*, in *Methods in Enzymology*, J.D. Ron, Editor. 2001, Academic Press. p. 177-195.
 162. Robertson, L.S. and G.R. Fink, *The three yeast A kinases have specific signaling functions in pseudohyphal growth.* Proceedings of the National Academy of Sciences, 1998. **95**(23): p. 13783-13787.
 163. Uwamahoro, N., *et al.*, *The Functions of Mediator in Candida albicans Support a Role in Shaping Species-Specific Gene Expression.* PLoS Genet, 2012. **8**(4): p. e1002613.
 164. SOBS Media and Prep Services. <http://www.med.monash.edu.au/sobs/media-prep-services/>
 165. Vince, James E., *et al.*, *Inhibitor of Apoptosis Proteins Limit RIP3 Kinase-Dependent Interleukin-1 Activation.* Immunity, 2012. **36**(2): p. 215-227.
 166. Fernandes-Alnemri, T., *et al.*, *AIM2 activates the inflammasome and cell death in response to cytoplasmic DNA.* Nature, 2009. **458**(7237): p. 509-513.
 167. Fernandez-Arenas, E., *et al.*, *Candida albicans actively modulates intracellular membrane trafficking in mouse macrophage phagosomes.* Cell Microbiol, 2009. **11**(4): p. 560-89.
 168. Schindelin, J., *et al.*, *Fiji: an open-source platform for biological-image analysis.* Nat Meth, 2012. **9**(7).
 169. Joly, S., *et al.*, *Cutting Edge: Candida albicans Hyphae Formation Triggers Activation of the Nlrp3 Inflammasome.* The Journal of Immunology, 2009. **183**(6): p. 3578-3581.
 170. Lariviere, L., *et al.*, *Structure and TBP binding of the Mediator head subcomplex Med8-Med18-Med20.* Nature Structural & Molecular Biology, 2006. **13**(10): p. 895-901.
 171. Nelson, C., *et al.*, *Srb10/Cdk8 regulates yeast filamentous growth by phosphorylating the transcription factor Ste12.* Nature, 2003. **421**(6919).

172. van de Peppel, J., *et al.*, *Mediator Expression Profiling Epistasis Reveals a Signal Transduction Pathway with Antagonistic Submodules and Highly Specific Downstream Targets*. *Molecular cell*, 2005. **19**(4): p. 511-522.
173. Su, C., *et al.*, *Mss11, a Transcriptional Activator, Is Required for Hyphal Development in Candida albicans*. *Eukaryotic Cell*, 2009. **8**(11): p. 1780-1791.
174. Guo, B., *et al.*, *A Saccharomyces gene family involved in invasive growth, cell–cell adhesion, and mating*. *Proceedings of the National Academy of Sciences*, 2000. **97**(22): p. 12158-12163.
175. Lo, W.-S. and A.M. Dranginis, *The Cell Surface Flocculin Flo11 Is Required for Pseudohyphae Formation and Invasion by Saccharomyces cerevisiae*. *Molecular Biology of the Cell*, 1998. **9**(1): p. 161-171.
176. Knop, C.T.M., *System of centromeric, episomal, and integrative vectors based on drug resistance markers for Saccharomyces cerevisiae*. *BioTechniques*, 2006. **40**(1): p. 73-78.
177. Chang, Y.-W., *et al.*, *The rye Mutants Identify a Role for Ssn/Srb Proteins of the RNA Polymerase II Holoenzyme During Stationary Phase Entry in Saccharomyces cerevisiae*. *Genetics*, 2001. **157**(1): p. 17-26.
178. Loor, G., *et al.*, *Menadione triggers cell death through ROS-dependent mechanisms involving PARP activation without requiring apoptosis*. *Free Radical Biology and Medicine*, 2010. **49**(12): p. 1925-1936.
179. Mehta, S., *et al.*, *The Med8 mediator subunit interacts with the Rpb4 subunit of RNA polymerase II and Ace2 transcriptional activator in Schizosaccharomyces pombe*. *FEBS Letters*, 2009. **583**(19): p. 3115-3120.
180. Gagiano, M., *et al.*, *Mss11p is a transcription factor regulating pseudohyphal differentiation, invasive growth and starch metabolism in Saccharomyces cerevisiae in response to nutrient availability*. *Molecular Microbiology*, 2003. **47**(1): p. 119-134.
181. Chang, Y.-W., S.C. Howard, and P.K. Herman, *The Ras/PKA Signaling Pathway Directly Targets the Srb9 Protein, a Component of the General RNA Polymerase II Transcription Apparatus*. *Molecular Cell*, 2004. **15**(1): p. 107-116.
182. Nemet, J., *et al.*, *The two faces of Cdk8, a positive/negative regulator of transcription*. *Biochimie*, 2014. **97**(0): p. 22-27.
183. Nguyen, B., *et al.*, *Elastic Instability in Growing Yeast Colonies*. *Biophysical Journal*, 2004. **86**(5): p. 2740-2747.
184. Filler, S.G., *Candida–host cell receptor–ligand interactions*. *Current Opinion in Microbiology*, 2006. **9**(4): p. 333-339.
185. Brown, G.D., *Innate Antifungal Immunity: The Key Role of Phagocytes*. *Annual Review of Immunology*, 2011. **29**(1): p. 1-21.

186. Bourgeois, C., *et al.*, *Fungal attacks on mammalian hosts: pathogen elimination requires sensing and tasting*. *Current Opinion in Microbiology*, 2010. **13**(4): p. 401-408.
187. Yates, R.M. and D.G. Russell, *Phagosome Maturation Proceeds Independently of Stimulation of Toll-like Receptors 2 and 4*. *Immunity*, 2005. **23**(4): p. 409-417.
188. Sato, K., *et al.*, *Dectin-2 Is a Pattern Recognition Receptor for Fungi That Couples with the Fc Receptor γ Chain to Induce Innate Immune Responses*. *Journal of Biological Chemistry*, 2006. **281**(50): p. 38854-38866.
189. Gross, O., *et al.*, *Syk kinase signalling couples to the Nlrp3 inflammasome for anti-fungal host defence*. *Nature*, 2009. **459**(7245): p. 433-6.
190. Gringhuis, S.I., *et al.*, *Dectin-1 is an extracellular pathogen sensor for the induction and processing of IL-1beta via a noncanonical caspase-8 inflammasome*. *Nat Immunol*, 2012. **13**(3): p. 246-54.
191. Yang, H., H. He, and Y. Dong, *CARD9 Syk-dependent and Raf-1 Syk-independent signaling pathways in target recognition of Candida albicans by Dectin-1*. *European Journal of Clinical Microbiology & Infectious Diseases*, 2011. **30**(3): p. 303-305.
192. Wheeler, R.T., Kombe, Diana., Agarwala, Sudeep D., Fink, Gerald R., *Dynamic, Morphotype-Specific Candida albicans Glucan Exposure during Infection and Drug Treatment*. *PLoS Pathog*, 2008. **4**(12): p. e1000227.
193. Jouault, T., *et al.*, *Host responses to a versatile commensal: PAMPs and PRRs interplay leading to tolerance or infection by Candida albicans*. *Cellular Microbiology*, 2009. **11**(7): p. 1007-1015.
194. Lee, C.G., *et al.*, *Chitin regulation of immune responses: an old molecule with new roles*. *Current Opinion in Immunology*, 2008. **20**(6): p. 684-689.
195. Philippe, B., *et al.*, *Killing of Aspergillus fumigatus by Alveolar Macrophages Is Mediated by Reactive Oxidant Intermediates*. *Infection and Immunity*, 2003. **71**(6): p. 3034-3042.
196. Nguyen, L. and J. Pieters, *The Trojan horse: survival tactics of pathogenic mycobacteria in macrophages*. *Trends in cell biology*, 2005. **15**(5): p. 269-276.
197. Eissenberg, L.G., W.E. Goldman, and P.H. Schlesinger, *Histoplasma capsulatum modulates the acidification of phagolysosomes*. *The Journal of Experimental Medicine*, 1993. **177**(6): p. 1605-1611.
198. Strasser, J.E., *et al.*, *Regulation of the Macrophage Vacuolar ATPase and Phagosome-Lysosome Fusion by Histoplasma capsulatum*. *The Journal of Immunology*, 1999. **162**(10): p. 6148-6154.
199. Woods, J.P., *Knocking on the right door and making a comfortable home: Histoplasma capsulatum intracellular pathogenesis*. *Current Opinion in Microbiology*, 2003. **6**(4): p. 327-331.

200. Arana, D.M., *et al.*, *Differential susceptibility of mitogen-activated protein kinase pathway mutants to oxidative-mediated killing by phagocytes in the fungal pathogen Candida albicans*. Cellular Microbiology, 2007. **9**(7): p. 1647-1659.
201. Vylkova, S., *et al.*, *The Fungal Pathogen Candida albicans Autoinduces Hyphal Morphogenesis by Raising Extracellular pH*. mBio, 2011. **2**(3).
202. Lorenz, M.C., J.A. Bender, and G.R. Fink, *Transcriptional Response of Candida albicans upon Internalization by Macrophages*. Eukaryotic Cell, 2004. **3**(5): p. 1076-1087.
203. Bain, J.M., *et al.*, *Non-lytic expulsion/exocytosis of Candida albicans from macrophages*. Fungal Genetics and Biology, 2012. **49**(9): p. 677-678.
204. Tucker, S.C. and A. Casadevall, *Replication of Cryptococcus neoformans in macrophages is accompanied by phagosomal permeabilization and accumulation of vesicles containing polysaccharide in the cytoplasm*. Proceedings of the National Academy of Sciences, 2002. **99**(5): p. 3165-3170.
205. Voelz, K. and R.C. May, *Cryptococcal Interactions with the Host Immune System*. Eukaryotic Cell, 2010. **9**(6): p. 835-846.
206. Chayakulkeeree, M., *et al.*, *SEC14 is a specific requirement for secretion of phospholipase B1 and pathogenicity of Cryptococcus neoformans*. Molecular Microbiology, 2011. **80**(4): p. 1088-1101.
207. Zaragoza, O., *et al.*, *Capsule enlargement in Cryptococcus neoformans confers resistance to oxidative stress suggesting a mechanism for intracellular survival*. Cellular Microbiology, 2008. **10**(10): p. 2043-2057.
208. Levitz, S.M., *et al.*, *Chloroquine induces human mononuclear phagocytes to inhibit and kill Cryptococcus neoformans by a mechanism independent of iron deprivation*. The Journal of Clinical Investigation, 1997. **100**(6): p. 1640-1646.
209. García-Rodas, R., *et al.*, *The Interaction between Candida krusei and Murine Macrophages Results in Multiple Outcomes, Including Intracellular Survival and Escape from Killing*. Infection and Immunity, 2011. **79**(6): p. 2136-2144.
210. Marcil, A., *et al.*, *Analysis of PRA1 and Its Relationship to Candida albicans-Macrophage Interactions*. Infection and Immunity, 2008. **76**(9): p. 4345-4358.
211. Zhao, X.R. and C.C. Villar, *Trafficking of Candida albicans through oral epithelial endocytic compartments*. Medical Mycology, 2011. **49**(2): p. 212-217.
212. Bonnett, C.R., *et al.*, *Early Neutrophil Recruitment and Aggregation in the Murine Lung Inhibit Germination of Aspergillus fumigatus Conidia*. Infection and Immunity, 2006. **74**(12): p. 6528-6539.
213. McKenzie, C.G.J., *et al.*, *Contribution of Candida albicans Cell Wall Components to Recognition by and Escape from Murine Macrophages*. Infection and Immunity, 2010. **78**(4): p. 1650-1658.

214. Wellington, M., K. Koselny, and D.J. Krysan, *Candida albicans Morphogenesis Is Not Required for Macrophage Interleukin 1beta Production*. MBio, 2012. **4**(1).
215. Senerovic, L., et al., *Spontaneous formation of IpaB ion channels in host cell membranes reveals how Shigella induces pyroptosis in macrophages*. Cell Death Dis, 2012. **3**: p. e384.
216. Srivastav, S., et al., *Leishmania donovani Prevents Oxidative Burst-mediated Apoptosis of Host Macrophages through Selective Induction of Suppressors of Cytokine Signaling (SOCS) Proteins*. Journal of Biological Chemistry, 2014. **289**(2): p. 1092-1105.
217. Wozniok, I., et al., *Induction of ERK-kinase signalling triggers morphotype-specific killing of Candida albicans filaments by human neutrophils*. Cellular Microbiology, 2008. **10**(3): p. 807-820.
218. Jiménez-López, C. and M.C. Lorenz, *Fungal Immune Evasion in a Model Host-Pathogen Interaction: Candida albicans Versus Macrophages*. PLoS Pathog, 2013. **9**(11): p. e1003741.
219. McKenzie, C.G., et al., *Contribution of Candida albicans cell wall components to recognition by and escape from murine macrophages*. Infect Immun, 2010. **78**(4): p. 1650-8.
220. Miramón, P., L. Kasper, and B. Hube, *Thriving within the host: Candida spp. interactions with phagocytic cells*. Medical Microbiology and Immunology, 2013. **202**(3): p. 183-195.
221. Lo, H.J., et al., *Nonfilamentous C. albicans mutants are avirulent*. Cell, 1997. **90**(5): p. 939-49.
222. Wellington, M., K. Koselny, and D.J. Krysan, *Candida albicans Morphogenesis Is Not Required for Macrophage Interleukin 1β Production*. mBio, 2013. **4**(1).
223. Davis, B.K., H. Wen, and J.P.-Y. Ting, *The Inflammasome NLRs in Immunity, Inflammation, and Associated Diseases*. Annual Review of Immunology, 2011. **29**(1): p. 707-735.
224. Guarda, G. and A. So, *Regulation of inflammasome activity*. Immunology, 2010. **130**(3): p. 329-336.
225. Rathinam, V.A.K., S.K. Vanaja, and K.A. Fitzgerald, *Regulation of inflammasome signaling*. Nat Immunol, 2012. **13**(4): p. 333-332.
226. Martinon, F., K. Burns, and J. Tschopp, *The Inflammasome: A Molecular Platform Triggering Activation of Inflammatory Caspases and Processing of proIL-β*. Molecular Cell, 2002. **10**(2): p. 417-426.
227. Zhong, Y., A. Kinio, and M. Saleh, *Functions of NOD-like receptors (NLRs) in human diseases*. Frontiers in Immunology, 2013. **4**.
228. Wang, S., et al., *Murine Caspase-11, an ICE-Interacting Protease, Is Essential for the Activation of ICE*. Cell, 1998. **92**(4): p. 501-509.

229. Broz, P. and D.M. Monack, *Noncanonical Inflammasomes: Caspase-11 Activation and Effector Mechanisms*. PLoS Pathog, 2013. **9**(2): p. e1003144.
230. Thornberry, N.A., *et al.*, *A novel heterodimeric cysteine protease is required for interleukin-1[beta]processing in monocytes*. Nature, 1992. **356**(6372): p. 768-774.
231. Dinarello, C.A., *Interleukin-1 in the pathogenesis and treatment of inflammatory diseases*. Vol. 117. 2011. 3720-3732.
232. Hoffman, H. and A. Wanderer, *Inflammasome and IL-1 β -Mediated Disorders*. Current Allergy and Asthma Reports, 2010. **10**(4): p. 229-235.
233. Hise, A.G., *et al.*, *An essential role for the NLRP3 inflammasome in host defense against the human fungal pathogen Candida albicans*. Cell Host Microbe, 2009. **5**(5): p. 487-97.
234. Franchi, L., *et al.*, *Function of Nod-like receptors in microbial recognition and host defense*. Immunological Reviews, 2009. **227**(1): p. 106-128.
235. Kumar, H., *et al.*, *Involvement of the NLRP3 inflammasome in innate and humoral adaptive immune responses to fungal beta-glucan*. J Immunol, 2009. **183**(12): p. 8061-7.
236. Hise, A.G., *et al.*, *An Essential Role for the NLRP3 Inflammasome in Host Defense against the Human Fungal Pathogen Candida albicans*. Cell host & microbe, 2009. **5**(5): p. 487-497.
237. Franchi, L., R. Munoz-Planillo, and G. Nunez, *Sensing and reacting to microbes through the inflammasomes*. Nat Immunol, 2012. **13**(4): p. 325-332.
238. Cheng, S.C., *et al.*, *The dectin-1/inflammasome pathway is responsible for the induction of protective T-helper 17 responses that discriminate between yeasts and hyphae of Candida albicans*. J Leukoc Biol, 2011. **90**(2): p. 357-66.
239. Drummond, R.A., *et al.*, *The role of Syk/CARD9 coupled C-type lectins in antifungal immunity*. European Journal of Immunology, 2011. **41**(2): p. 276-281.
240. Franchi, L., R. Munoz-Planillo, and G. Nunez, *Sensing and reacting to microbes through the inflammasomes*. Nature, 2014. **13**(4).
241. Kankkunen, P., *et al.*, *(1,3)- β -Glucans Activate Both Dectin-1 and NLRP3 Inflammasome in Human Macrophages*. The Journal of Immunology, 2010. **184**(11): p. 6335-6342.
242. Cheng, S.-C., *et al.*, *Interplay between Candida albicans and the Mammalian Innate Host Defense*. Infection and Immunity, 2012. **80**(4): p. 1304-1313.
243. Lamkanfi, M. and V.M. Dixit, *Manipulation of Host Cell Death Pathways during Microbial Infections*. Cell Host & Microbe, 2010. **8**(1): p. 44-54.
244. Häcker, G., *The morphology of apoptosis*. Cell and Tissue Research, 2000. **301**(1): p. 5-17.

245. Krysko, D.V., *et al.*, *Apoptosis and necrosis: Detection, discrimination and phagocytosis*. *Methods*, 2008. **44**(3): p. 205-221.
246. Fink, S.L. and B.T. Cookson, *Caspase-1-dependent pore formation during pyroptosis leads to osmotic lysis of infected host macrophages*. *Cellular Microbiology*, 2006. **8**(11): p. 1812-1825.
247. Slee, E.A., *et al.*, *Ordering the Cytochrome c-initiated Caspase Cascade: Hierarchical Activation of Caspases-2, -3, -6, -7, -8, and -10 in a Caspase-9-dependent Manner*. *The Journal of Cell Biology*, 1999. **144**(2): p. 281-292.
248. Bergsbaken, T., S.L. Fink, and B.T. Cookson, *Pyroptosis: host cell death and inflammation*. *Nat Rev Micro*, 2009. **7**(2): p. 99-109.
249. Kufer, T.A. and P.J. Sansonetti, *Sensing of bacteria: NOD a lonely job*. *Current Opinion in Microbiology*, 2007. **10**(1): p. 62-69.
250. Bergsbaken, T., S.L. Fink, and B.T. Cookson, *Pyroptosis: Host cell death and inflammation*. *Nature Reviews Microbiology*, 2009. **7**(2): p. 99-109.
251. Bryant, C. and K.A. Fitzgerald, *Molecular mechanisms involved in inflammasome activation*. *Trends in Cell Biology*, 2009. **19**(9): p. 455-464.
252. Dowds, T.A., *et al.*, *Regulation of cryopyrin/Pypaf1 signaling by pyrin, the familial Mediterranean fever gene product*. *Biochemical and Biophysical Research Communications*, 2003. **302**(3): p. 575-580.
253. Netea, M.G., *et al.*, *Neutralization of IL-18 Reduces Neutrophil Tissue Accumulation and Protects Mice Against Lethal Escherichia coli and Salmonella typhimurium Endotoxemia*. *The Journal of Immunology*, 2000. **164**(5): p. 2644-2649.
254. Frantz, S., *et al.*, *Targeted deletion of caspase-1 reduces early mortality and left ventricular dilatation following myocardial infarction*. *Journal of Molecular and Cellular Cardiology*, 2003. **35**(6): p. 685-694.
255. Melnikov, V.Y., *et al.*, *Impaired IL-18 processing protects caspase-1-deficient mice from ischemic acute renal failure*. *The Journal of Clinical Investigation*, 2001. **107**(9): p. 1145-1152.
256. Uwamahoro, N., *et al.*, *The Pathogen Candida albicans Hijacks Pyroptosis for Escape from Macrophages*. *mBio*, 2014. **5**(2).
257. Westwater, C., E. Balish, and D.A. Schofield, *Candida albicans-Conditioned Medium Protects Yeast Cells from Oxidative Stress: a Possible Link between Quorum Sensing and Oxidative Stress Resistance*. *Eukaryotic Cell*, 2005. **4**(10): p. 1654-1661.
258. Wheeler, R.T., *et al.*, *Dynamic, Morphotype-Specific Candida albicans β -Glucan Exposure during Infection and Drug Treatment*. *PLoS Pathog*, 2008. **4**(12): p. e1000227.
259. Bahn, Y.-S., *et al.*, 2007. *Nat Rev Micro*, Sensing the environment: lessons from fungi. **5**(1).

260. Griffiths, G., *On vesicles and membrane compartments*. Protoplasma, 1996. **195**(1-4): p. 37-58.
261. Uwamahoro¹, N., *et al.*, *The pathogen Candida albicans hijacks pyroptosis for escape from macrophages*. mBIO, 2014. **Accepted**.
262. Brown, G.D. and S. Gordon, *Immune recognition: A new receptor for [beta]-glucans*. Nature, 2001. **412**(6851): p. 36-37.
263. Groß, O., *Measuring the Inflammasome*, in *Leucocytes*, R.B. Ashman, Editor. 2012, Humana Press. p. 199-222.
264. Miao, E.A., J.V. Rajan, and A. Aderem, *Caspase-1-induced pyroptotic cell death*. Immunological Reviews, 2011. **243**(1): p. 206-214.
265. Wellington, M., *et al.*, *Candida albicans Triggers NLRP3-Mediated Pyroptosis in Macrophages*. Eukaryotic Cell, 2014. **13**(2): p. 329-340.
266. Cheng, S.-C., *et al.*, *The dectin-1/inflammasome pathway is responsible for the induction of protective T-helper 17 responses that discriminate between yeasts and hyphae of Candida albicans*. Journal of Leukocyte Biology, 2011. **90**(2): p. 357-366.
267. Fernández-Arenas, E., *et al.*, *Candida albicans actively modulates intracellular membrane trafficking in mouse macrophage phagosomes*. Cellular Microbiology, 2009. **11**(4): p. 560-589.
268. Marr, K.A., *et al.*, *Early Events in Macrophage Killing of Aspergillus fumigatus Conidia: New Flow Cytometric Viability Assay*. Clinical and Diagnostic Laboratory Immunology, 2001. **8**(6): p. 1240-1247.
269. Mora-Montes, H., *et al.*, *Interactions Between Macrophages and Cell Wall Oligosaccharides of Candida albicans*, in *Host-Fungus Interactions*, A.C. Brand and D.M. MacCallum, Editors. 2012, Humana Press. p. 247-260.
270. Brothers, K.M., Z.R. Newman, and R.T. Wheeler, *Live Imaging of Disseminated Candidiasis in Zebrafish Reveals Role of Phagocyte Oxidase in Limiting Filamentous Growth*. Eukaryotic Cell, 2011. **10**(7): p. 932-944.
271. Lo, H.-J., *et al.*, *Nonfilamentous C. albicans Mutants Are Avirulent*. Cell. **90**(5): p. 939-949.
272. Miao, E.A., *et al.*, *Caspase-1-induced pyroptosis is an innate immune effector mechanism against intracellular bacteria*. Nat Immunol, 2010. **11**(12).
273. Kayagaki, N., *et al.*, *Non-canonical inflammasome activation targets caspase-11*. Nature, 2011. **479**(7371): p. 117-121.
274. Kayagaki, N., *et al.*, *Noncanonical Inflammasome Activation by Intracellular LPS Independent of TLR4*. Science, 2013. **341**(6151): p. 1246-1249.
275. Hagar, J.A., *et al.*, *Cytoplasmic LPS Activates Caspase-11: Implications in TLR4-Independent Endotoxic Shock*. Science, 2013. **341**(6151): p. 1250-1253.

276. Chinen, *et al.*, *Candida albicans* suppresses nitric oxide (NO) production by interferon-gamma (IFN- γ) and lipopolysaccharide (LPS)-stimulated murine peritoneal macrophages. *Clinical & Experimental Immunology*, 1999. **115**(3): p. 491-497.
277. Lionakis, M.S. and M.G. Netea, *Candida* and Host Determinants of Susceptibility to Invasive Candidiasis. *PLoS Pathog*, 2013. **9**(1): p. e1003079.
278. Marcil, A., *et al.*, *Candida albicans* Killing by RAW 264.7 Mouse Macrophage Cells: Effects of *Candida* Genotype, Infection Ratios, and Gamma Interferon Treatment. *Infection and Immunity*, 2002. **70**(11): p. 6319-6329.
279. Moriwaki, K. and F.K.-M. Chan, *RIP3: a molecular switch for necrosis and inflammation*. *Genes & Development*, 2013. **27**(15): p. 1640-1649.
280. Marakalala, M.J., *et al.*, *Differential Adaptation of Candida albicans In Vivo Modulates Immune Recognition by Dectin-1*. *PLoS Pathog*, 2013. **9**(4): p. e1003315.
281. Ferwerda, B., *et al.*, *Human Dectin-1 Deficiency and Mucocutaneous Fungal Infections*. *New England Journal of Medicine*, 2009. **361**(18): p. 1760-1767.
282. Rosenthal, D.C., *et al.*, *Genetic Variation in the Dectin-1/CARD9 Recognition Pathway and Susceptibility to Candidemia*. *Journal of Infectious Diseases*, 2011. **204**(7): p. 1138-1145.
283. Hise, A.G., *et al.*, *An Essential Role for the NLRP3 Inflammasome in Host Defense against the Human Fungal Pathogen Candida albicans*. *Cell Host & Microbe*. **5**(5): p. 487-497.
284. van de Veerdonk, F.L., *et al.*, *The inflammasome drives protective Th1 and Th17 cellular responses in disseminated candidiasis*. *European Journal of Immunology*, 2011. **41**(8): p. 2260-2268.
285. Risley, M.D., *et al.*, *The Mediator complex protein Med31 is required for embryonic growth and cell proliferation during mammalian development*. *Developmental Biology*, 2010. **342**(2): p. 146-156.
286. Lionakis, M.S., *et al.*, *CX3CR1-dependent renal macrophage survival promotes Candida control and host survival*. *The Journal of Clinical Investigation*, 2013. **123**(12): p. 5035-5051.
287. Joshi, V.D., *et al.*, *Role of Caspase 1 in Murine Antibacterial Host Defenses and Lethal Endotoxemia*. *Infection and Immunity*, 2002. **70**(12): p. 6896-6903.

***Appendix 1 Appendix figures and tables for
Chapter 3***

Appendix Table 1. Go Term process for down- regulated genes in the *med31Δ/Δ* mutant hits

GOID	GO term	Cluster frequency (%)	Background frequency (%)	Corrected <i>p</i>-value	False discovery rate (%)
9987	cellular process	63.7	46.3	0.000000455	0.00
44699	single-organism process	61.4	37.0	0.000000000	0.00
44763	single-organism cellular process	46.4	29.2	0.000000093	0.00
50896	response to stimulus	29.4	16.5	0.000007520	0.00
65007	biological regulation	27.1	16.6	0.002020000	0.00
51716	cellular response to stimulus	24.5	14.5	0.001770000	0.00
50789	regulation of biological process	23.2	15.0	0.072040000	0.00
50794	regulation of cellular process	21.9	13.6	0.038290000	0.00
30447	filamentous growth	20.9	8.8	0.000000030	0.00
40007	growth	20.9	9.0	0.000000075	0.00
42221	response to chemical	19.3	8.7	0.000004250	0.00
6950	response to stress	18.0	9.2	0.000790000	0.00
44182	filamentous growth of a population of unicellular organisms	16.3	6.9	0.000007850	0.00
33554	cellular response to stress	16.0	8.6	0.014260000	0.00
60255	regulation of macromolecule metabolic process	15.7	8.8	0.048060000	0.00
70887	cellular response to chemical stimulus	15.4	7.4	0.001410000	0.00
10468	regulation of gene expression	15.4	7.6	0.002700000	0.00
19219	regulation of nucleobase-containing compound metabolic process	14.7	7.7	0.017360000	0.00
31326	regulation of cellular biosynthetic process	14.7	7.8	0.022780000	0.00
9889	regulation of biosynthetic process	14.7	7.8	0.023340000	0.00
51171	regulation of nitrogen compound metabolic process	14.7	7.8	0.024510000	0.00

2001141	regulation of RNA biosynthetic process	14.4	6.7	0.001110000	0.00
6355	regulation of transcription, DNA-templated	14.4	6.7	0.001110000	0.00
51252	regulation of RNA metabolic process	14.4	6.8	0.001710000	0.00
2000112	regulation of cellular macromolecule biosynthetic process	14.4	7.5	0.020270000	0.00
10556	regulation of macromolecule biosynthetic process	14.4	7.5	0.021320000	0.00
9605	response to external stimulus	13.7	5.2	0.000007690	0.00
7154	cell communication	12.7	6.4	0.030850000	0.00
31667	response to nutrient levels	12.4	4.6	0.000023600	0.00
9991	response to extracellular stimulus	12.4	4.6	0.000027000	0.00
31669	cellular response to nutrient levels	12.1	4.4	0.000025400	0.00
31668	cellular response to extracellular stimulus	12.1	4.5	0.000030400	0.00
71496	cellular response to external stimulus	12.1	4.5	0.000047400	0.00
48518	positive regulation of biological process	12.1	5.7	0.009550000	0.00
9607	response to biotic stimulus	11.8	4.5	0.000130000	0.00
48522	positive regulation of cellular process	10.8	4.6	0.004480000	0.00
42493	response to drug	10.8	5.3	0.085490000	0.00
42594	response to starvation	10.5	4.3	0.002930000	0.00
36180	filamentous growth of a population of unicellular organisms in response to biotic stimulus	10.1	4.0	0.001420000	0.00
9267	cellular response to starvation	10.1	4.1	0.003550000	0.00
48519	negative regulation of biological process	10.1	4.8	0.079680000	0.00
6357	regulation of transcription from RNA polymerase II promoter	9.5	3.7	0.003590000	0.00
40008	regulation of growth	8.8	2.9	0.000200000	0.00
71216	cellular response to biotic stimulus	8.8	3.8	0.033700000	0.00

36170	filamentous growth of a population of unicellular organisms in response to starvation	8.2	3.4	0.035630000	0.00
10628	positive regulation of gene expression	7.8	2.3	0.000160000	0.00
1900428	regulation of filamentous growth of a population of unicellular organisms	7.8	2.5	0.000520000	0.00
10570	regulation of filamentous growth	7.8	2.5	0.000820000	0.00
10604	positive regulation of macromolecule metabolic process	7.8	3.1	0.030140000	0.00
9893	positive regulation of metabolic process	7.8	3.4	0.096490000	0.00
45893	positive regulation of transcription, DNA-templated	7.5	2.3	0.000550000	0.00
1902680	positive regulation of RNA biosynthetic process	7.5	2.5	0.002740000	0.00
51254	positive regulation of RNA metabolic process	7.5	2.6	0.003910000	0.00
45935	positive regulation of nucleobase-containing compound metabolic process	7.5	2.7	0.007040000	0.00
10557	positive regulation of macromolecule biosynthetic process	7.5	2.7	0.009770000	0.00
51173	positive regulation of nitrogen compound metabolic process	7.5	2.7	0.009770000	0.00
31328	positive regulation of cellular biosynthetic process	7.5	2.8	0.020820000	0.00
9891	positive regulation of biosynthetic process	7.5	2.8	0.020820000	0.00
71554	cell wall organization or biogenesis	7.2	2.8	0.058860000	0.00
45944	positive regulation of transcription from RNA polymerase II promoter	6.5	1.9	0.001110000	0.00
42710	biofilm formation	6.5	2.1	0.008310000	0.00
44010	single-species biofilm formation	5.9	2.0	0.038810000	0.00
43900	regulation of multi-organism process	4.9	1.3	0.013940000	0.00

1901605	alpha-amino acid metabolic process	4.9	1.4	0.032830000	0.00
70783	growth of unicellular organism as a thread of attached cells	4.6	0.9	0.001000000	0.00
70784	regulation of growth of unicellular organism as a thread of attached cells	3.9	0.9	0.011080000	0.00
1900429	negative regulation of filamentous growth of a population of unicellular organisms	3.9	0.9	0.013310000	0.00
60258	negative regulation of filamentous growth	3.9	0.9	0.014570000	0.00
1901700	response to oxygen-containing compound	3.9	0.9	0.015930000	0.00
45926	negative regulation of growth	3.9	0.9	0.017400000	0.00
122	negative regulation of transcription from RNA polymerase II promoter	3.9	1.0	0.054360000	0.00
16049	cell growth	2.9	0.5	0.024430000	0.00
1901606	alpha-amino acid catabolic process	2.6	0.4	0.009880000	0.00
7124	pseudohyphal growth	2.6	0.4	0.021770000	0.00
9063	cellular amino acid catabolic process	2.6	0.5	0.082080000	0.00
45990	carbon catabolite regulation of transcription	2.3	0.3	0.016610000	0.00
9112	nucleobase metabolic process	2.3	0.3	0.055690000	0.00
43708	cell adhesion involved in biofilm formation	2.3	0.3	0.064900000	0.00
31670	cellular response to nutrient	2.3	0.3	0.075320000	0.00
70785	negative regulation of growth of unicellular organism as a thread of attached cells	2.0	0.2	0.037640000	0.00
7109	cytokinesis, completion of separation	1.6	0.1	0.004610000	0.00
6551	leucine metabolic process	1.3	0.1	0.032870000	0.00
6012	galactose metabolic process	1.3	0.1	0.082920000	0.00
33499	galactose catabolic process via UDP-galactose	1.0	0.0	0.012260000	0.00

Appendix Table 2. Go Term process for up- regulated genes in the *med31*Δ/Δ mutant hits

GOID	GO term	Cluster frequency (%)	Background frequency (%)	Corrected P-value	False discovery rate (%)
9987	cellular process	62.1	46.3	0.005280	0.50
8152	metabolic process	51.1	35.9	0.008740	0.44
44699	single-organism process	50.5	37.0	0.057770	0.71
71840	cellular component organization or biogenesis	31.1	16.4	0.000210	0.00
44710	single-organism metabolic process	30.5	18.7	0.034140	0.91
16043	cellular component organization	28.4	14.1	0.000130	0.00
6996	organelle organization	22.1	9.7	0.000150	0.00
7005	mitochondrion organization	10.0	2.3	0.000048	0.00
33108	mitochondrial respiratory chain complex assembly	3.7	0.3	0.001480	0.00
10821	regulation of mitochondrion organization	2.6	0.1	0.000300	0.00
45727	positive regulation of translation	2.6	0.2	0.014200	0.40
17004	cytochrome complex assembly	2.6	0.2	0.044340	0.77
70129	regulation of mitochondrial translation	2.1	0.1	0.001950	0.00
70131	positive regulation of mitochondrial translation	1.6	0.0	0.039210	0.83
10822	positive regulation of mitochondrion organization	1.6	0.1	0.067870	0.67

Appendix 1, Table 3. Go SLIM classification by process of all significantly altered genes in the *C. albicans med31ΔΔ* mutant

GO-Slim term	Cluster frequency	Genes annotated to the term
biological unknown	process 125 out of 510 genes, 24.5%	<i>ABP2, BUL1, ECM18, ECM331, GTT11, HOC1, HRQ2, HRT2, HYR3, IFD3, LDG3, MPRL36, MRPL33, MRPL37, PGA38, PRN3,PRN4, PSP1, SNG4, TLO10, TLO7, orf19.1002, orf19.1083, orf19.1121, orf19.1140, orf19.1152, orf19.1189, orf19.1240, orf19.1277,orf19.1485, orf19.1486, orf19.1562, orf19.1653, orf19.1709, orf19.1717, orf19.1800, orf19.1857, orf19.1913, orf19.1964, orf19.2048,orf19.2049, orf19.206, orf19.2125, orf19.2165, orf19.2204, orf19.2398, orf19.2515, orf19.2521, orf19.2529.1, orf19.2575, orf19.2730,orf19.2846, orf19.2887, orf19.3087.1, orf19.3248, orf19.3302, orf19.3323, orf19.3335, orf19.334, orf19.3360, orf19.3448, orf19.3461,orf19.3475, orf19.3480, orf19.3615, orf19.3678, orf19.4046, orf19.4204, orf19.4358, orf19.4450.1, orf19.4600.1, orf19.4735,orf19.4751, orf19.4763, orf19.4814, orf19.4819, orf19.4921.1, orf19.4951, orf19.4952, orf19.5014, orf19.5019, orf19.5070,orf19.5132, orf19.5235, orf19.5282, orf19.5288.1, orf19.5365, orf19.5412, orf19.5431, orf19.551, orf19.5522, orf19.5626, orf19.5686,orf19.5775, orf19.5785, orf19.5813, orf19.5840, orf19.5920, orf19.6017, orf19.6156, orf19.6184, orf19.6244, orf19.639.1, orf19.642,orf19.6484, orf19.6660, orf19.670.2, orf19.6709, orf19.6730, orf19.6770, orf19.6818, orf19.6896, orf19.699, orf19.7051, orf19.7085,orf19.7091, orf19.716, orf19.7173, orf19.7210, orf19.7250, orf19.727, orf19.7300, orf19.7507, orf19.94, orf19.951</i>
regulation of process	of biological 99 out of 510 genes, 19.4%	<i>ADAEC, AGP2, AHR1, ALS1, ARC18, ARF1, CAS5, CDC68, CEK1, CHS7, CLN3, CPH2, CTA26, CTA4, CUP9, DAD3, DCK1,DCK2, DED1, DEF1, DOT5, DOT6, DPB4, EFG1,</i>

		<i>ESC4, FCRI, FKH2, GAL1, GAL10, GAL4, GPR1, HAL9, HAP2, HAP31,HGT1, HYM1, MAC1, MAF1, MHP1, MIG1, NDE1, NRG1, PDE2, PGA1, PGA13, PGA26, PHB2, PHO4, PST2, PTP3, RAD54,RHO2, RIM101, RME1, ROB1, RPB4, RPM2, RRP6, SFU1, SHA3, SNO1, , SRR1, STP3, STP4, SUC1, SUT1, TEC1,TRR1, TRY6, TYE7, URA2, ZCF1, ZCF13, ZCF16, orf19.1604, orf19.1619, orf19.173, orf19.1794, orf19.2064, orf19.215, orf19.2175,orf19.2201, orf19.2308, orf19.2516, orf19.3007, orf19.3854, orf19.439, orf19.4657, orf19.5026, orf19.512, orf19.5459, orf19.5515,orf19.5618, orf19.5620, orf19.5953, orf19.6563.1, orf19.7196, orf19.7538</i>
response to chemical	80 out of 510 genes, 15.7%	<i>ADE1, ADE2, AHR1, ARC18, CAS5, CDR1, CEK1, CIS2, CLN3, CPH2, CTA4, DAC1, DDR48, DIP5, DOT5, EFG1, FCRI,FCY21, FKH2, GAD1, GAL1, GAL10, GAL4, GPR1, GSL1, HAP2, HAP31, HGT1, HOL4, HSP104, HSP21, HYM1, IFF6, LEU4,MET14, MET3, MIG1, NRG1, OPT1, PDE2, PGA23, PGA26, PGA31, PHO4, PTP3, RBT4, RIM101, RRP6, SEN2, SFU1, SHA3,SNQ2, SOD4, SOD5, STP3, TAF19, TEC1, TIP1, TRR1, TYE7, UTP22, VPS28, YTH1, ZCF16, orf19.1308, orf19.1723, orf19.173,orf19.2175, orf19.276, orf19.304, orf19.3228, orf19.341, orf19.3854, orf19.4116, orf19.439, orf19.5401, orf19.5620, orf19.6586,orf19.7029, orf19.7522</i>
response to stress	78 out of 510 genes, 15.3%	<i>ADAEC, ADE1, ADE2, AHR1, CAS5, CDR1, CEK1, CPH2, CTF18, DAC1, DCK1, DCK2, DDR48, DED1, DOT5, DPB4, ECM29,EFG1, ESC4, EXO1, FCRI, FGR14, FGR6, FGR6-3, FGR6-4, GAD1, GAL10, GIR2, GPR1, GPX2, HGT1, HSM3, HSP104,HSP21, HYM1, MAL2, MET14, MET3, MHP1, NRG1, PDE2, PGA26, PHHB, PHO4, PRI2, PTC8, PYC2, RAD7, REV3, RIM101,RPB4, SFU1, SHA3, SNQ2, SOD4, SOD5, , SRR1, SSU1, TEC1, TRR1, TYE7, VAM3, YTM1, ZCF13, orf19.1210,orf19.2175, orf19.2208, orf19.2926, orf19.3481,</i>

filamentous growth	77 out of 510 genes, 15.1%	<p>orf19.3854, orf19.439, orf19.512, orf19.5620, orf19.6720, orf19.7196, orf19.7213, orf19.7538 <i>ADE5,7, AHRI, ALS1, CAS5, CEK1, CHS7, CHT1, CLN3, CPH2, CTA4, CUP9, DAC1, DCK1, DCK2, DDR48, DEF1, DOT6, DPB4, ECM29, EFG1, ENA2, ESC4, FCR1, FGR14, FGR6, FGR6-1, FGR6-3, FGR6-4, FKH2, GAL10, GIR2, GPR1, HAL9, HGT1, HSP21, HYM1, MAC1, MAL2, MHP1, MIG1, MNT1, NRG1, PDE2, PGA1, PGA13, PGA26, PHHB, PHO4, PTC8, RHO2, RIM101, ROB1, RPB4, SHA3, SNQ2, , SRR1, SSU1, STP3, STP4, SUC1, TEC1, TYE7, VAM3, VPS28, YTM1, ZCF13, ZCF16, orf19.1085, orf19.1300, orf19.2397.3, orf19.2761, orf19.3228, orf19.6720, orf19.6868, orf19.6874, orf19.7111</i></p>
transport	70 out of 510 genes, 13.7%	<p><i>AGP2, ARC18, ARF1, BET4, CDR1, CFL1, CFL4, CHS7, CLC1, COX19, DIP5, ECM21, ENA2, FCY21, GAL1, GIT2, GNPI, HGT1, HGT3, HOL4, HSP31, HXT5, IFC3, MAC1, MAS2, OPT1, OPT4, PIR1, RHO2, RPB4, SDS24, SEC5, SHA3, SMF12, SNQ2, SSU1, TIM13, TIP1, USO1, UTP22, VAM3, VCX1, VMA11, VMA5, VPS28, YHB4, orf19.1195, orf19.1210, orf19.1308, orf19.1564, orf19.1795.1, orf19.1855, orf19.2078, orf19.2302, orf19.304, orf19.3222, orf19.3228, orf19.3406, orf19.341, orf19.4292, orf19.4731, orf19.4981, orf19.5022, orf19.5095, orf19.516, orf19.5618, orf19.6264.3, orf19.6522, orf19.7193, orf19.954</i></p>
organelle organization	67 out of 510 genes, 13.1%	<p><i>ABP140, ACS1, ARC18, BBC1, CDC68, CLN3, COX19, CTF18, DAD3, DCP2, DPB4, ESC4, EXO1, FKH2, GCF1, IFC3, INN1, MAS2, MRP20, PEX11, PHB2, PHO4, PRI2, RAD54, RAD7, RHO2, RIM1, RIM101, RME1, ROB1, RPM2, RRP6, SEC5, , TIM13, TIP1, USO1, VAM3, YTM1, orf19.1085, orf19.1195, orf19.1483, orf19.185, orf19.215, orf19.2201, orf19.3007, orf19.3223.1, orf19.3581, orf19.409, orf19.4292, orf19.439, orf19.4657, orf19.5459, orf19.5515, orf19.5618, orf19.6100, orf19.6246, orf19.6458.1, orf19.6563.1,</i></p>

			orf19.6607, orf19.6639, orf19.6861, orf19.7111, orf19.7196, orf19.7450, orf19.7538, orf19.954
response to drug		45 out of 510 genes, 8.8%	<i>AHR1, ARC18, CAS5, CDR1, CEK1, CLN3, CPH2, DIP5, EFG1, FCRI, FCY21, GSLL1, HAP31, HGT1, HOL4, HYM1, LEU4, MIG1, NRG1, OPT1, PDE2, PGA23, PGA31, RBT4, RIM101, RRP6, SEN2, SNQ2, STP3, TAF19, TIP1, UTP22, VPS28, YTH1</i> , orf19.1308, orf19.173, orf19.304, orf19.3228, orf19.341, orf19.3854, orf19.4116, orf19.5401, orf19.6586, orf19.7029, orf19.7522
RNA metabolic process		40 out of 510 genes, 7.8%	<i>ABP140, CDC68, CTA4, DBP2, DBP7, DCP2, DTD2, FKH2, PRI2, PRP22, PWP2, RNY11, ROBI, RPB4, RPM2, RRP6, SEN2, , SUC1, TAF19, TSR1, TYE7, UTP22, YTH1, ZCF13</i> , orf19.1356, orf19.1387, orf19.1578, orf19.1619, orf19.1687, orf19.1794, orf19.3481, orf19.5239, orf19.5334, orf19.5459, orf19.5767, orf19.6458.1, orf19.6847, orf19.7196, orf19.7265
carbohydrate process	metabolic	31 out of 510 genes, 6.1%	<i>ARA1, CHS7, CHT1, CHT3, EXG2, GAL1, GAL10, GAL7, GLK4, GSLL1, HSP104, HSP21, INO1, LEU2, MAL2, MDH1-3, MNN12, MNN22, MNT1, NDE1, PCK1, PYC2, RHD1, SCW11, SUC1</i> , orf19.1092, orf19.2308, orf19.338, orf19.3840, orf19.7214, orf19.7426
pathogenesis		28 out of 510 genes, 5.5%	<i>ADE2, ADE5,7, AHR1, ALS1, CAS5, CEK1, CHS7, CSH1, DAC1, EFG1, HSP104, HSP21, LEU2, MNT1, NRG1, PDE2, PGA26, RBT4, RHD3, RIM101, SAP7, SOD5, , SRR1, TEC1, TYE7, VAM3, VPS28</i>
DNA metabolic process		27 out of 510 genes, 5.3%	<i>ADAEC, CDC68, CTF18, DDR48, DPB4, ESC4, EXO1, FGR14, FKH2, HSM3, POL93, PRI2, RAD54, RAD7, REV3, RNR3, ROBI</i> , orf19.2669, orf19.2926, orf19.3581, orf19.3840, orf19.439, orf19.6469, orf19.6861, orf19.7213, orf19.7538
cellular	protein	26 out of 510 genes, 5.1%	<i>ACS1, BET4, CEK1, GAL10, GAL7, MNN12, MNN22, MNT1, PTC8, PTP3, RAD7, SHA3</i> ,

modification process		<i>UBP1</i> , orf19.1085, orf19.1092,orf19.1619, orf19.1959, orf19.229, orf19.2761, orf19.3237, orf19.35, orf19.3840, orf19.3854, orf19.6246, orf19.6861, orf19.7426
cell cycle	22 out of 510 genes, 4.3%	<i>CEK1</i> , <i>CHT3</i> , <i>CLN3</i> , <i>CTF18</i> , <i>DAD3</i> , <i>DIT2</i> , <i>ENG1</i> , <i>EXO1</i> , <i>FKH2</i> , <i>HYM1</i> , <i>INN1</i> , <i>PHHB</i> , <i>PWP2</i> , <i>RAD54</i> , <i>RIM101</i> , <i>RME1</i> , <i>SCW11</i> , <i>SDS24</i> , orf19.1619, orf19.3854, orf19.7450
biofilm formation	22 out of 510 genes, 4.3%	<i>AHR1</i> , <i>ALS1</i> , <i>ALS5</i> , <i>ALS6</i> , <i>CAS5</i> , <i>CAT2</i> , <i>CSH1</i> , <i>DEF1</i> , <i>EAP1</i> , <i>EFG1</i> , <i>HSP104</i> , <i>NRG1</i> , <i>PDE2</i> , <i>PGA1</i> , <i>PGA26</i> , <i>ROB1</i> , <i>SUC1</i> , <i>TEC1</i> , <i>TRY6</i> , <i>TYE7</i> , <i>VAM3</i>
interspecies interaction between organisms	20 out of 510 genes, 3.9%	<i>ALS1</i> , <i>ALS5</i> , <i>ALS6</i> , <i>CAS5</i> , <i>CPH2</i> , <i>CTA4</i> , <i>CYB2</i> , <i>DEF1</i> , <i>EAP1</i> , <i>EFG1</i> , <i>MNT1</i> , <i>NRG1</i> , <i>PDE2</i> , <i>PGA1</i> , <i>RIM101</i> , <i>SOD4</i> , <i>SOD5</i> , <i>TEC1</i> , <i>ZCF1</i> , <i>ZCF13</i>
cellular homeostasis	20 out of 510 genes, 3.9%	<i>ADE5,7</i> , <i>DOT5</i> , <i>GPR1</i> , <i>MAC1</i> , <i>SFU1</i> , <i>SMF12</i> , <i>TRR1</i> , <i>VAM3</i> , <i>VCX1</i> , <i>VMA5</i> , orf19.1195, orf19.2302, orf19.2516, orf19.3228,orf19.3854, orf19.4843, orf19.5022, orf19.5334, orf19.5618, orf19.6100
cell wall organization	19 out of 510 genes, 3.7%	<i>CAS5</i> , <i>CEK1</i> , <i>DCK1</i> , <i>DIT2</i> , <i>HYM1</i> , <i>MHP1</i> , <i>MNT1</i> , <i>PDE2</i> , <i>PGA1</i> , <i>PGA13</i> , <i>PGA26</i> , <i>PGA31</i> , <i>PHHB</i> , <i>PIR1</i> , <i>RHD3</i> , <i>RHO2</i> , <i>VPS28</i> , orf19.215, orf19.6741
vesicle-mediated transport	17 out of 510 genes, 3.3%	<i>ARC18</i> , <i>BET4</i> , <i>CHS7</i> , <i>CLC1</i> , <i>ECM21</i> , <i>SDS24</i> , <i>SEC5</i> , <i>TIP1</i> , <i>USO1</i> , <i>VAM3</i> , orf19.2078, orf19.4292, orf19.4731, orf19.5095,orf19.5618, orf19.6264.3, orf19.7193
lipid metabolic process	16 out of 510 genes, 3.1%	<i>ARE2</i> , <i>AYR1</i> , <i>CAT2</i> , <i>ERG251</i> , <i>FAA21</i> , <i>INO1</i> , <i>OPI3</i> , <i>PEX11</i> , orf19.100, orf19.1092, orf19.1890, orf19.276, orf19.2761, orf19.3283,orf19.4066, orf19.6100
growth of unicellular organism as a thread of attached cells	13 out of 510 genes, 2.5%	<i>AHR1</i> , <i>CEK1</i> , <i>CPH2</i> , <i>CTA4</i> , <i>EFG1</i> , <i>GAL10</i> , <i>GPR1</i> , <i>HAL9</i> , <i>NRG1</i> , <i>TEC1</i> , <i>ZCF13</i> , orf19.3228
hyphal growth	12 out of 510 genes, 2.4%	<i>ALS1</i> , <i>CEK1</i> , <i>CLN3</i> , <i>EFG1</i> , <i>ENA2</i> , <i>HYM1</i> , <i>MIG1</i> , <i>RHO2</i> , <i>SUC1</i> , <i>VAM3</i> , orf19.1085, orf19.7111

cell adhesion	12 out of 510 genes, 2.4%	<i>AHR1, ALS1, ALS5, ALS6, CSH1, DEF1, EAP1, EFG1, MNT1, PDE2, PGAI, TEC1</i>
ribosome biogenesis	12 out of 510 genes, 2.4%	<i>DBP2, DBP7, PWP2, RRP6, TSRI, UTP22, YTM1, orf19.1578, orf19.1687, orf19.3797, orf19.512, orf19.7107</i>
cytokinesis	11 out of 510 genes, 2.2%	<i>CHT3, ENG1, HYM1, INN1, PWP2, RIM101, SCW11, SDS24, orf19.1619, orf19.7450</i>
signal transduction	10 out of 510 genes, 2%	<i>ARF1, CEK1, DCK1, DCK2, GPR1, PDE2, RHO2, RIM101, SRR1, orf19.5620</i>
cytoskeleton organization	9 out of 510 genes, 1.8%	<i>ABP140, ARC18, BBC1, CTF18, DAD3, RHO2, orf19.215, orf19.6246, orf19.7450</i>
protein catabolic process	9 out of 510 genes, 1.8%	<i>RAD7, UBP1, VPS28, orf19.1085, orf19.229, orf19.6861, orf19.7193, orf19.7196, orf19.7265</i>
generation of precursor metabolites and energy	8 out of 510 genes, 1.6%	<i>ACS1, AOX1, AOX2, CAT2, COX15, NDE1, UCF1, orf19.3283</i>
translation	8 out of 510 genes, 1.6%	<i>DED1, GIR2, MRP20, RPM2, orf19.185, orf19.5239, orf19.5812, orf19.7012</i>
protein folding	6 out of 510 genes, 1.2%	<i>CHS7, ERO1, HSP104, PHB2, orf19.7183, orf19.954</i>
pseudohyphal growth	6 out of 510 genes, 1.2%	<i>CPH2, EFG1, GPR1, NRG1, TEC1, orf19.3228</i>
cell development	6 out of 510 genes, 1.2%	<i>CEK1, DIT2, EFG1, NRG1, PHHB, RIM101</i>
vitamin metabolic process	5 out of 510 genes, 1%	<i>SNO1, SNZ1, SPE3, orf19.4589, orf19.7306</i>
cellular respiration	4 out of 510 genes, 0.8%	<i>AOX1, AOX2, CAT2, orf19.3283</i>
conjugation	4 out of 510 genes, 0.8%	<i>CEK1, IFF6, OPT1, orf19.7196</i>
nucleus organization	2 out of 510 genes, 0.4%	<i>RAD54, orf19.4657</i>
cell budding	2 out of 510 genes, 0.4%	<i>CLN3, HYM1</i>
can not be mapped to a GO slim term	44 out of 510 genes, 8.6%	<i>AAT1, ARG3, ARO10, AYR2, CDC21, CDG1, DAO1, DLD1, FCA1, FDH1, FRP2, GCV2, GDH2, GDH3, GLX3, IFR2, MAE1, MET13, MET15, MNN4-4, POT1-2, RCE1, SAP98, SER2, SHM2, STF2, TRP1, XYL2, orf19.1117, orf19.1180, orf19.1272, orf19.1306,</i>

not yet annotated	22 out of 510 genes, 4.3%	orf19.1589.1, orf19.1774, orf19.1888, orf19.2269, orf19.2284, orf19.2671, orf19.279, orf19.3810, orf19.449, orf19.4633, orf19.4907, orf19.5730 <i>FET35</i> , orf19.1071, orf19.1125, orf19.13, orf19.1437, orf19.2222.1, orf19.2353, orf19.2659, orf19.3145.4, orf19.3386, orf19.3479, orf19.3641, orf19.4155.12, orf19.4421, orf19.4485, orf19.4552, orf19.5192, orf19.6301, orf19.6865, orf19.6964, orf19.7005, orf19.7028
-------------------	---------------------------	---

Appendix 1, Table 4. Go Slim functions *down-regulated* in the *med31*Δ/Δ mutant

GO-Slim term	Cluster frequency	Genes annotated to the term
molecular unknown	function 112 out of 315 genes, 35.6%	<i>ABP2, AGP2, ALS6, DEF1, ECM18, FGR6-1, FGR6-3, FGR6-4, HSM3, HSP21, HYM1, HYR3, IFD3, IFF6, INN1, MNN22, PGA13,PGA26, PGA38, PRN3, PSP1, RHD1, RHD3, SNG4, STF2, UCF1, UTP22, YTM1, orf19.1002, orf19.1083, orf19.1189, orf19.1240,orf19.1272, orf19.1277, orf19.1486, orf19.1562, orf19.1653, orf19.1717, orf19.1800, orf19.1890, orf19.1913, orf19.1964, orf19.2049,orf19.206, orf19.2078, orf19.215, orf19.2208, orf19.2397.3, orf19.2398, orf19.2521, orf19.2529.1, orf19.2575, orf19.3007, orf19.3087.1,orf19.3228, orf19.3302, orf19.3323, orf19.3335, orf19.334, orf19.3360, orf19.3448, orf19.3475, orf19.3615, orf19.3678, orf19.4046,orf19.409, orf19.4450.1, orf19.4814, orf19.4907, orf19.4921.1, orf19.4951, orf19.4952, orf19.5019, orf19.512, orf19.5282, orf19.5288.1,orf19.5365, orf19.5412, orf19.5431, orf19.551, orf19.5626, orf19.5775, orf19.5785, orf19.6017, orf19.6184, orf19.6244, orf19.642,orf19.6586, orf19.6639, orf19.6660, orf19.670.2, orf19.6720, orf19.6730, orf19.6741, orf19.6770, orf19.6896, orf19.699, orf19.7051,orf19.7085, orf19.7091, orf19.7107, orf19.7111, orf19.7173, orf19.7183, orf19.7193, orf19.7210, orf19.7250, orf19.727, orf19.7300,orf19.7450, orf19.7507, orf19.951</i>
hydrolase activity	41 out of 315 genes, 13.0%	<i>ARF1, CDR1, CHT1, CHT3, CTF18, DAC1, DBP2, DBP7, DCP2, DED1, DTD2, ENA2, ENG1, FCA1, HSP104, MAL2, PDE2, PRP22,PTC8, PTP3, RCE1, RPM2, RRP6, SAP98, SER2, SNO1, SNQ2, SNZ1, UBPI, URA2, orf19.100, orf19.1121, orf19.1687,</i>

		orf19.1959,orf19.279, orf19.3481, orf19.449, orf19.4657, orf19.6818, orf19.7029, orf19.7213
oxidoreductase activity	31 out of 315 genes, 9.8%	<i>AOX1, AOX2, AYR2, CDG1, CFL1, DIT2, ERG251, ERO1, FDH1, FET35, FRP2, GCV2, GDH2, GPX2, LEU2, MAE1, NDE1, RNR3, SOD5, YHB4</i> , orf19.1117, orf19.1306, orf19.1774, orf19.2175, orf19.2284, orf19.2671, orf19.3283, orf19.3810, orf19.4589, orf19.4843,orf19.5730
DNA binding	27 out of 315 genes, 8.6%	<i>ADAEC, AHR1, CAS5, CPH2, CTA4, CUP9, DOT6, EFG1, FKH2, GAL4, MIG1, NRG1, PHO4, RIM101, RME1, ROB1, SFU1, STP4,SUC1, TEC1, TYE7, ZCF13, ZCF16</i> , orf19.173, orf19.5026, orf19.6874, orf19.7213
transferase activity	26 out of 315 genes, 8.3%	<i>AAT1, ABP140, ADAEC, ARG3, FGR14, GAL1, GAL7, GSL1, LEU4, MNN12, MNT1, POT1-2, SHA3, SHM2, SPE3, URA2</i> , orf19.1619, orf19.2308, orf19.3283, orf19.35, orf19.3840, orf19.3854, orf19.4116, orf19.6246, orf19.6469, orf19.6847
transporter activity	23 out of 315 genes, 7.3%	<i>CDR1, DIP5, ENA2, FCY21, GIT2, GNP1, HGT1, HOL4, HSP31, IFC3, OPT1, OPT4, SMF12, SNQ2, SSU1</i> , orf19.1308, orf19.1855,orf19.304, orf19.3222, orf19.3406, orf19.341, orf19.5022, orf19.6522
protein binding	22 out of 315 genes, 7%	<i>ABP140, AHR1, ALS1, ALS5, BBC1, CAS5, CPH2, DAD3, EAP1, ECM21, ECM29, GAL4, HSP104, MAF1, PHO4, SUT1, TRY6,TYE7, VAM3, VPS28</i> , orf19.4292, orf19.5618
RNA binding	10 out of 315 genes, 3.2%	<i>DCP2, DED1, FGR14, PRP22, PWP2, YTH1</i> , orf19.1578, orf19.5334, orf19.5767, orf19.6469
helicase activity	8 out of 315 genes, 2.5%	<i>DBP2, DBP7, DED1, PRP22</i> , orf19.1687, orf19.3481, orf19.6818, orf19.7213
lyase activity	6 out of 315 genes, 1.9%	<i>ADE2, ARO10, GAD1, PCK1, PHHB</i> , orf19.5730

protein kinase activity	5 out of 315 genes, 1.6%	<i>SHA3</i> , orf19.1619, orf19.35, orf19.3840, orf19.3854
ligase activity	4 out of 315 genes, 1.3%	<i>ADE1</i> , <i>ADE5,7</i> , <i>URA2</i> , orf19.3237
peptidase activity	4 out of 315 genes, 1.3%	<i>RCE1</i> , <i>SAP98</i> , <i>UBP1</i> , orf19.1959
phosphatase activity	4 out of 315 genes, 1.3%	<i>PTC8</i> , <i>PTP3</i> , <i>SER2</i> , orf19.4657
protein binding	4 out of 315 genes, 1.3%	<i>CAS5</i> , <i>GAL4</i> , , <i>TEC1</i>
transcription factor activity		
nucleotidyltransferase activity	3 out of 315 genes, 1%	<i>FGR14</i> , <i>GAL7</i> , orf19.6469
structural molecule activity	3 out of 315 genes, 1%	<i>ECM29</i> , <i>MHP1</i> , <i>PIR1</i>
isomerase activity	3 out of 315 genes, 1%	<i>ADE2</i> , <i>ERO1</i> , <i>GAL10</i>
signal transducer activity	2 out of 315 genes, 0.6%	<i>GPRI</i> , <i>SRR1</i>
can not be mapped to a GO slim term	16 out of 315 genes, 5.1%	<i>DCK1</i> , <i>DCK2</i> , <i>FCR1</i> , <i>HAL9</i> , <i>SCW11</i> , <i>SDS24</i> , <i>STP3</i> , <i>TSR1</i> , orf19.1387, orf19.1604, orf19.2064, orf19.2669, orf19.2730, orf19.5813,orf19.5953, orf19.6868
not yet annotated	13 out of 315 genes, 4.1%	FGR6, orf19.1071, orf19.1437, orf19.2659, orf19.3641, orf19.4155.12, orf19.4485, orf19.4552, orf19.5401, orf19.6301, orf19.6964,orf19.7005, orf19.7028

Appendix 1, Table 5. Go Slim processes *down-regulated* in the *med31*Δ/Δ mutant

GO-Slim term	Cluster frequency	Genes annotated to the term
biological unknown	process 76 out of 315 genes, 24.1%	<i>ABP2, ECM18, HYR3, IFD3, PGA38, PRN3, PSP1, SNG4</i> , orf19.1002, orf19.1083, orf19.1121, orf19.1189, orf19.1240, orf19.1277,orf19.1486, orf19.1562, orf19.1653, orf19.1717, orf19.1800, orf19.1913, orf19.1964, orf19.2049, orf19.206, orf19.2398, orf19.2521,orf19.2529.1, orf19.2575, orf19.2730, orf19.3087.1, orf19.3302, orf19.3323, orf19.3335, orf19.334, orf19.3360, orf19.3448,orf19.3475, orf19.3615, orf19.3678, orf19.4046, orf19.4450.1, orf19.4814, orf19.4921.1, orf19.4951, orf19.4952, orf19.5019,orf19.5282, orf19.5288.1, orf19.5365, orf19.5412, orf19.5431, orf19.551, orf19.5626, orf19.5775, orf19.5785, orf19.5813, orf19.6017,orf19.6184, orf19.6244, orf19.642, orf19.6660, orf19.670.2, orf19.6730, orf19.6770, orf19.6818, orf19.6896, orf19.699, orf19.7051,orf19.7085, orf19.7091, orf19.7173, orf19.7210, orf19.7250, orf19.727, orf19.7300, orf19.7507, orf19.951
regulation of biological process	69 out of 315 genes, 21.9%	<i>ADAEC, AGP2, AHRI, ALS1, ARF1, CAS5, CPH2, CTA4, CUP9, DAD3, DCK1, DCK2, DED1, DEF1, DOT6, EFG1, FCRI,FKH2, GAL1, GAL10, GAL4, GPRI, HAL9, HGT1, HYM1, MAF1, MHP1, MIG1, NDE1, NRG1, PDE2, PGA13, PGA26, PHO4,PTP3, RIM101, RME1, ROB1, RPM2, RRP6, SFUI, SHA3, SNO1, , SRR1, STP3, STP4, SUC1, SUT1, TEC1, TRY6,TYE7, URA2, ZCF13, ZCF16</i> , orf19.1604, orf19.1619, orf19.173, orf19.2064, orf19.215, orf19.2175, orf19.2308, orf19.3007,orf19.3854, orf19.4657, orf19.5026, orf19.512, orf19.5618, orf19.5953

filamentous growth	63 out of 315 genes, 20%	<i>ADE5,7, AHR1, ALS1, CAS5, CHT1, CPH2, CTA4, CUP9, DAC1, DCK1, DCK2, DEF1, DOT6, ECM29, EFG1, ENA2, FCRI, FGR14, FGR6, FGR6-1, FGR6-3, FGR6-4, FKH2, GAL10, GPR1, HAL9, HGT1, HSP21, HYM1, MAL2, MHP1, MIG1, MNT1, NRG1, PDE2, PGA13, PGA26, PHHB, PHO4, PTC8, RIM101, ROB1, SHA3, SNQ2, , SRR1, SSU1, STP3, STP4, SUC1, TEC1, TYE7, VAM3, VPS28, YTM1, ZCF13, ZCF16, orf19.2397.3, orf19.3228, orf19.6720, orf19.6868, orf19.6874, orf19.7111</i>
response to chemical	57 out of 315 genes, 18.1%	<i>ADE1, ADE2, AHR1, CAS5, CDR1, CPH2, CTA4, DAC1, DIP5, EFG1, FCRI, FCY21, FKH2, GAD1, GAL1, GAL10, GAL4, GPR1, GSL1, HGT1, HOL4, HSP104, HSP21, HYM1, IFF6, LEU4, MIG1, NRG1, OPT1, PDE2, PGA26, PHO4, PTP3, RIM101, RRP6, SFU1, SHA3, SNQ2, SOD5, STP3, TEC1, TYE7, UTP22, VPS28, YTH1, ZCF16, orf19.1308, orf19.173, orf19.2175, orf19.304, orf19.3228, orf19.341, orf19.3854, orf19.4116, orf19.5401, orf19.6586, orf19.7029</i>
response to stress	56 out of 315 genes, 17.8%	<i>ADAEC, ADE1, ADE2, AHR1, CAS5, CDR1, CPH2, CTF18, DAC1, DCK1, DCK2, DED1, ECM29, EFG1, FCRI, FGR14, FGR6, FGR6-3, FGR6-4, GAD1, GAL10, GPR1, GPX2, HGT1, HSM3, HSP104, HSP21, HYM1, MAL2, MHP1, NRG1, PDE2, PGA26, PHHB, PHO4, PTC8, RIM101, SFU1, SHA3, SNQ2, SOD5, , SRR1, SSU1, TEC1, TYE7, VAM3, YTM1, ZCF13, orf19.2175, orf19.2208, orf19.3481, orf19.3854, orf19.512, orf19.6720, orf19.7213</i>
transport	40 out of 315 genes, 12.7%	<i>AGP2, ARF1, CDR1, CFL1, DIP5, ECM21, ENA2, FCY21, GAL1, GIT2, GNP1, HGT1, HOL4, HSP31, IFC3, OPT1, OPT4, PIR1, SDS24, SHA3, SMF12, SNQ2, SSU1, UTP22, VAM3, VPS28, YHB4, orf19.1308, orf19.1855, orf19.2078, orf19.304, orf19.3222, orf19.3228, orf19.3406, orf19.341, orf19.4292, orf19.5022, orf19.5618, orf19.6522, orf19.7193</i>
response to drug	34 out of 315 genes, 10.8%	<i>AHR1, CAS5, CDR1, CPH2, DIP5, EFG1, FCRI, FCY21, GSL1, HGT1, HOL4, HYM1,</i>

		<i>LEU4, MIG1, NRG1, OPT1, PDE2,RIM101, RRP6, SNQ2, STP3, UTP22, VPS28, YTH1, orf19.1308, orf19.173, orf19.304, orf19.3228, orf19.341, orf19.3854,orf19.4116, orf19.5401, orf19.6586, orf19.7029</i>
organelle organization	27 out of 315 genes, 8.6%	<i>ABP140, BBC1, CTF18, DAD3, DCP2, FKH2, IFC3, INN1, PHO4, RIM101, RME1, ROB1, RPM2, RRP6, , VAM3, YTM1, orf19.215, orf19.3007, orf19.409, orf19.4292, orf19.4657, orf19.5618, orf19.6246, orf19.6639, orf19.7111, orf19.7450</i>
RNA metabolic process	27 out of 315 genes, 8.6%	<i>ABP140, CTA4, DBP2, DBP7, DCP2, DTD2, FKH2, PRP22, PWP2, ROB1, RPM2, RRP6, , SUC1, TSR1, TYE7, UTP22,YTH1, ZCF13, orf19.1387, orf19.1578, orf19.1619, orf19.1687, orf19.3481, orf19.5334, orf19.5767, orf19.6847</i>
pathogenesis	23 out of 315 genes, 7.3%	<i>ADE2, ADE5,7, AHR1, ALS1, CAS5, DAC1, EFG1, HSP104, HSP21, LEU2, MNT1, NRG1, PDE2, PGA26, RHD3, RIM101,SOD5, , SRR1, TEC1, TYE7, VAM3, VPS28</i>
carbohydrate metabolic process	20 out of 315 genes, 6.3%	<i>CHT1, CHT3, GAL1, GAL10, GAL7, GSL1, HSP104, HSP21, LEU2, MAL2, MNN12, MNN22, MNT1, NDE1, PCK1, RHD1,SCW11, SUC1, orf19.2308, orf19.3840</i>
biofilm formation	19 out of 315 genes, 6.0%	<i>AHR1, ALS1, ALS5, ALS6, CAS5, DEF1, EAP1, EFG1, HSP104, NRG1, PDE2, PGA26, ROB1, , SUC1, TEC1, TRY6,TYE7, VAM3</i>
cell cycle	18 out of 315 genes, 5.7%	<i>CHT3, CTF18, DAD3, DIT2, ENGI, FKH2, HYM1, INN1, PHHB, PWP2, RIM101, RME1, SCW11, SDS24, , orf19.1619,orf19.3854, orf19.7450</i>
cellular protein modification process	16 out of 315 genes, 5.1%	<i>GAL10, GAL7, MNN12, MNN22, MNT1, PTC8, PTP3, SHA3, UBPI, orf19.1619, orf19.1959, orf19.3237, orf19.35, orf19.3840,orf19.3854, orf19.6246</i>
interspecies interaction between organisms	16 out of 315 genes, 5.1%	<i>ALS1, ALS5, ALS6, CAS5, CPH2, CTA4, DEF1, EAP1, EFG1, MNT1, NRG1, PDE2, RIM101, SOD5, TEC1, ZCF13</i>
cell wall organization	15 out of 315 genes, 4.8%	<i>CAS5, DCK1, DIT2, HYM1, MHP1, MNT1, PDE2, PGA13, PGA26, PHHB, PIR1, RHD3,</i>

		<i>VPS28, orf19.215, orf19.6741</i>
growth of unicellular organism as a thread of attached cells	12 out of 315 genes, 3.8%	<i>AHR1, CPH2, CTA4, EFG1, GAL10, GPR1, HAL9, NRG1, , TEC1, ZCF13, orf19.3228</i>
DNA metabolic process	12 out of 315 genes, 3.8%	<i>ADAEC, CTF18, FGR14, FKH2, HSM3, RNR3, ROB1, orf19.2669, orf19.3840, orf19.6469, orf19.7213</i>
cytokinesis	11 out of 315 genes, 3.5%	<i>CHT3, ENG1, HYM1, INN1, PWP2, RIM101, SCW11, SDS24, , orf19.1619, orf19.7450</i>
ribosome biogenesis	11 out of 315 genes, 3.5%	<i>DBP2, DBP7, PWP2, RRP6, TSR1, UTP22, YTM1, orf19.1578, orf19.1687, orf19.512, orf19.7107</i>
cellular homeostasis	11 out of 315 genes, 3.5%	<i>ADE5,7, GPR1, SFUI, SMF12, VAM3, orf19.3228, orf19.3854, orf19.4843, orf19.5022, orf19.5334, orf19.5618</i>
cell adhesion	10 out of 315 genes, 3.2%	<i>AHR1, ALS1, ALS5, ALS6, DEF1, EAP1, EFG1, MNT1, PDE2, TEC1</i>
hyphal growth	8 out of 315 genes, 2.5%	<i>ALS1, EFG1, ENA2, HYM1, MIG1, SUC1, VAM3, orf19.7111</i>
cytoskeleton organization	7 out of 315 genes, 2.2%	<i>ABP140, BBC1, CTF18, DAD3, orf19.215, orf19.6246, orf19.7450</i>
signal transduction	7 out of 315 genes, 2.2%	<i>ARF1, DCK1, DCK2, GPR1, PDE2, RIM101, SRR1</i>
vesicle-mediated transport	7 out of 315 genes, 2.2%	<i>ECM21, SDS24, VAM3, orf19.2078, orf19.4292, orf19.5618, orf19.7193</i>
pseudohyphal growth	6 out of 315 genes, 1.9%	<i>CPH2, EFG1, GPR1, NRG1, TEC1, orf19.3228</i>
generation of precursor metabolites and energy	5 out of 315 genes, 1.6%	<i>AOX1, AOX2, NDE1, UCF1, orf19.3283</i>
cell development	5 out of 315 genes, 1.6%	<i>DIT2, EFG1, NRG1, PHHB, RIM101</i>

lipid metabolic process	4 out of 315 genes, 1.3%	<i>ERG251</i> , orf19.100, orf19.1890, orf19.3283
vitamin metabolic process	4 out of 315 genes, 1.3%	<i>SNO1</i> , <i>SNZ1</i> , <i>SPE3</i> , orf19.4589
cellular respiration	3 out of 315 genes, 1%	<i>AOX1</i> , <i>AOX2</i> , orf19.3283
protein folding	3 out of 315 genes, 1%	<i>ERO1</i> , <i>HSP104</i> , orf19.7183
protein catabolic process	3 out of 315 genes, 1%	<i>UBP1</i> , <i>VPS28</i> , orf19.7193
conjugation	2 out of 315 genes, 0.6%	<i>IFF6</i> , <i>OPT1</i>
translation	2 out of 315 genes, 0.6%	<i>DED1</i> , <i>RPM2</i>
nucleus organization	1 out of 315 genes, 0.3%	orf19.4657
cell budding	1 out of 315 genes, 0.3%	<i>HYM1</i>
can not be mapped to a GO slim term	28 out of 315 genes, 8.9%	<i>AAT1</i> , <i>ARG3</i> , <i>ARO10</i> , <i>AYR2</i> , <i>CDG1</i> , <i>FCA1</i> , <i>FDH1</i> , <i>FRP2</i> , <i>GCV2</i> , <i>GDH2</i> , <i>MAE1</i> , <i>POT1-2</i> , <i>RCE1</i> , <i>SAP98</i> , <i>SER2</i> , <i>SHM2</i> , <i>STF2</i> , orf19.1117, orf19.1272, orf19.1306, orf19.1774, orf19.2284, orf19.2671, orf19.279, orf19.3810, orf19.449, orf19.4907, orf19.5730
not yet annotated	12 out of 315 genes, 3.8%	FET35, orf19.1071, orf19.1437, orf19.2659, orf19.3641, orf19.4155.12, orf19.4485, orf19.4552, orf19.6301, orf19.6964, orf19.7005, orf19.7028

Appendix 1, Table 6. Go SLIM classification by component of all significantly altered genes in the *C. albicans med31*Δ/Δ mutant

GO-Slim term	Cluster frequency	Genes annotated to the term
cytoplasm	256 out of 510 genes, 50.2%	<i>AAT1, ABP140, ACS1, ADE1, ADE2, ADE5,7, AGP2, AOX1, AOX2, ARA1, ARC18, ARE2, ARG3, ARO10, AYR1, BBC1, BET4,CAS5, CAT2, CDR1, CEK1, CHS7, CHT3, CIS2, CLC1, COX15, COX19, CSH1, CTF18, CYB2, DBP2, DCK1, DCP2, DDR48,DED1, DIP5, DOT5, DOT6, DTD2, ECM18, ECM21, ECM29, EFG1, ENA2, ERO1, EXO1, FAA21, FCA1, FCY21, FDH1, FKH2,GAD1, GAL1, GAL10, GAL7, GCF1, GCV2, GDH2, GDH3, GIR2, GLX3, GTT11, HOC1, HRT2, HSM3, HSP104, HYM1, INN1,INO1, LEU2, LEU4, MAE1, MAF1, MAL2, MAS2, MDH1-3, MET13, MET14, MET15, MET3, MIG1, MNT1, MPRL36, MRP20,MRPL33, MRPL37, NDE1, OPI3, OPT1, PCK1, PDE2, PEX11, PHB2, PHHB, PHO4, POT1-2, PRI2, PSP1, PTP3, PWP2,PYC2, RAD54, RCE1, REV3, RHO2, RIM1, RME1, RNR3, RNY11, RPB4, RPM2, SDS24, SEC5, SEN2, SER2, SHA3, SHM2,SMF12, SNO1, SNQ2, SNZ1, , SPE3, SRR1, SSU1, STF2, STP3, SUT1, TIM13, TIP1, TRP1, TRR1, TSR1, UBP1, UCF1,URA2, USO1, VAM3, VCX1, VMA11, VMA5, VPS28, XYL2, YTH1, orf19.1083, orf19.1085, orf19.1092, orf19.1180, orf19.1195,orf19.1210, orf19.1272, orf19.1300, orf19.1306, orf19.1308, orf19.1356, orf19.1387, orf19.1483, orf19.1485, orf19.1564, orf19.1687,orf19.1723, orf19.173, orf19.1794, orf19.1795.1, orf19.185, orf19.1857, orf19.1888, orf19.1959, orf19.2064, orf19.2078, orf19.215,orf19.2175, orf19.2201,</i>

		orf19.2208, orf19.2269, orf19.2302, orf19.2575, orf19.2671, orf19.276, orf19.2761, orf19.279, orf19.2887,orf19.3007, orf19.3222, orf19.3228, orf19.3237, orf19.3283, orf19.338, orf19.3406, orf19.341, orf19.3480, orf19.3481, orf19.3581,orf19.3615, orf19.3797, orf19.3810, orf19.3840, orf19.3854, orf19.409, orf19.4204, orf19.4292, orf19.4358, orf19.439, orf19.449,orf19.4589, orf19.4633, orf19.4657, orf19.4731, orf19.4735, orf19.4751, orf19.4763, orf19.4843, orf19.4907, orf19.4981, orf19.5014,orf19.5022, orf19.5095, orf19.516, orf19.5235, orf19.5239, orf19.5334, orf19.5365, orf19.5459, orf19.5515, orf19.5618, orf19.5620,orf19.5730, orf19.5840, orf19.5953, orf19.6100, orf19.6246, orf19.6264.3, orf19.639.1, orf19.6458.1, orf19.6563.1, orf19.6607,orf19.6639, orf19.6660, orf19.6720, orf19.6741, orf19.6818, orf19.6847, orf19.7012, orf19.7029, orf19.7051, orf19.7107, orf19.7111,orf19.7183, orf19.7193, orf19.7196, orf19.7210, orf19.7214, orf19.7306, orf19.7426, orf19.7450, orf19.954
nucleus	137 out of 510 genes, 26.9%	<i>ADE1, AHR1, ARC18, BET4, CAS5, CDC21, CDC68, CEK1, CHT3, CLN3, COX19, CTA26, CTA4, CTF18, CUP9, DAD3, DBP2,DBP7, DCP2, DOT5, DOT6, DPB4, DTD2, ECM29, EFG1, ESC4, EXO1, FCA1, FCRI, FKH2, GAL10, GAL4, GAL7, GDH3,GIR2, GLX3, HAL9, HAP2, HAP31, HRT2, HSM3, HSP104, MAC1, MAF1, MAL2, MET13, MET14, MET15, MIG1, NRG1, PDE2,PHHB, PHO4, PRI2, PRP22, PTP3, PWP2, RAD54, RAD7, REV3, RHO2, RIM101, RME1, ROB1, RPB4, RPM2, RRP6, SEN2,SER2, SFU1, SHA3, , SPE3, SRR1, STF2, STP3, STP4, SUC1, SUT1, TAF19, TEC1, TIM13, TRR1, TSR1, TYE7, UCF1,UTP22, YTH1, YTM1, ZCF1, ZCF13, ZCF16, orf19.1085, orf19.1180, orf19.1272, orf19.1306, orf19.1578,</i>

		<p>orf19.1604, orf19.1619,orf19.1687, orf19.1723, orf19.173, orf19.1857, orf19.1888, orf19.2175, orf19.2269, orf19.229, orf19.2926, orf19.3237, orf19.3581,orf19.3615, orf19.3810, orf19.4116, orf19.439, orf19.4633, orf19.5026, orf19.512, orf19.5334, orf19.5459, orf19.5620, orf19.5812,orf19.5813, orf19.5953, orf19.6246, orf19.6458.1, orf19.6730, orf19.6847, orf19.6861, orf19.7051, orf19.7107, orf19.7210,orf19.7213, orf19.7214, orf19.7265, orf19.7306, orf19.7538, orf19.954</p>
cellular component unknown	129 out of 510 genes, 25.3%	<p><i>ABP2, ADAEC, AYR2, BUL1, CDG1, CPH2, DAC1, DAO1, DCK2, DEF1, DIT2, DLD1, FGR14, FGR6-1, FGR6-3, FGR6-4,FRP2, GLK4, GPX2, HRQ2, IFD3, IFR2, LDG3, MNN12, MNN22, MNN4-4, POL93, PRN3, PRN4, PTC8, SAP98, SNG4, TLO10,TLO7, TRY6, YHB4,</i> orf19.100, orf19.1002, orf19.1117, orf19.1121, orf19.1140, orf19.1152, orf19.1189, orf19.1240, orf19.1277,orf19.1486, orf19.1562, orf19.1589.1, orf19.1709, orf19.1717, orf19.1774, orf19.1800, orf19.1890, orf19.1913, orf19.1964,orf19.2048, orf19.2125, orf19.2165, orf19.2284, orf19.2308, orf19.2398, orf19.2515, orf19.2516, orf19.2521, orf19.2529.1,orf19.2669, orf19.2730, orf19.2846, orf19.3087.1, orf19.3223.1, orf19.3248, orf19.3302, orf19.3323, orf19.334, orf19.3360,orf19.3448, orf19.3461, orf19.3475, orf19.35, orf19.3678, orf19.4046, orf19.4450.1, orf19.4600.1, orf19.4814, orf19.4819,orf19.4921.1, orf19.4951, orf19.4952, orf19.5019, orf19.5070, orf19.5132, orf19.5282, orf19.5288.1, orf19.5412, orf19.5431,orf19.551, orf19.5522, orf19.5626, orf19.5686, orf19.5767, orf19.5775, orf19.5785, orf19.5920, orf19.6017, orf19.6156, orf19.6184,orf19.6244, orf19.642, orf19.6469, orf19.6484, orf19.6586, orf19.670.2, orf19.6709, orf19.6770, orf19.6868, orf19.6874, orf19.6896,orf19.699, orf19.7085, orf19.7091, orf19.716, orf19.7173,</p>

membrane	100 out of 510 genes, 19.6%	<p>orf19.7250, orf19.727, orf19.7300, orf19.7507, orf19.7522, orf19.94,orf19.951</p> <p><i>AGP2, AOX1, AOX2, ARE2, AYRI, CDR1, CFL1, CFL4, CHS7, CLC1, COX15, DCK1, DIP5, EAP1, ECM331, ENA2, ERG251,ERO1, EXG2, FCY21, GIT2, GNP1, GPR1, GSL1, HGT1, HGT3, HOC1, HOL4, HSP31, HXT5, IFC3, IFF6, MET15, MNT1, NDE1,OPT1, OPT4, PEX11, PHB2, RCE1, RHD1, RHD3, RHO2, SEN2, SHM2, SMF12, SNQ2, SSU1, TIP1, URA2, USO1, VAM3,VCX1, VMA11, VMA5, VPS28, orf19.1092, orf19.1210, orf19.1308, orf19.1483, orf19.1564, orf19.1653, orf19.1794, orf19.1795.1,orf19.1855, orf19.2049, orf19.2078, orf19.2204, orf19.2302, orf19.276, orf19.2761, orf19.304, orf19.3222, orf19.3228, orf19.3335,orf19.3406, orf19.341, orf19.4066, orf19.409, orf19.4116, orf19.4292, orf19.4657, orf19.4763, orf19.4843, orf19.4981, orf19.5022,orf19.5095, orf19.516, orf19.5515, orf19.5618, orf19.5730, orf19.6100, orf19.6522, orf19.6563.1, orf19.6607, orf19.6741, orf19.7111,orf19.7183, orf19.7426, orf19.954</i></p>
mitochondrion	87 out of 510 genes, 17.1%	<p><i>AAT1, ACS1, AOX1, AOX2, ARC18, ARG3, AYRI, CAT2, CDR1, CEK1, COX15, COX19, CTF18, CYB2, DBP2, ECM18, ENA2,FAA21, GCF1, GCV2, GDH2, GDH3, LEU4, MAE1, MAL2, MAS2, MET13, MET3, MNT1, MPRL36, MRP20, MRPL33, MRPL37,NDE1, OPI3, PEX11, PHB2, PHHB, POT1-2, PSP1, REV3, RIM1, RPM2, SEN2, SNQ2, SRR1, TIM13, TRR1, URA2, orf19.1195,orf19.1300, orf19.1356, orf19.1483, orf19.1485, orf19.1687, orf19.1794, orf19.185, orf19.2175, orf19.2201, orf19.3237, orf19.3283,orf19.3480, orf19.3481, orf19.3797, orf19.409, orf19.4204, orf19.4358, orf19.439, orf19.449, orf19.4657, orf19.4751, orf19.4763,orf19.5014, orf19.5022, orf19.5235, orf19.5459, orf19.5515, orf19.6100, orf19.639.1,</i></p>

		orf19.6563.1, orf19.6607, orf19.6639,orf19.6818, orf19.7012, orf19.7111, orf19.7214, orf19.954
endomembrane system	54 out of 510 genes, 10.6%	<i>AGP2, ARE2, AYR1, CEK1, CHS7, CHT3, CLC1, DIP5, ERO1, GTT11, HOC1, HSP104, MIG1, MNT1, OPI3, OPT1, PEX11,PRI2, RCE1, SMF12, SSU1, TIP1, UBPI, USO1, VCX1, VMA11, VPS28, orf19.1092, orf19.1564, orf19.1795.1, orf19.2064,orf19.2078, orf19.2302, orf19.276, orf19.2761, orf19.3222, orf19.3228, orf19.341, orf19.4116, orf19.4292, orf19.4657, orf19.4731,orf19.4907, orf19.4981, orf19.5095, orf19.516, orf19.5618, orf19.6264.3, orf19.6720, orf19.6741, orf19.7183, orf19.7196, orf19.7426,orf19.954</i>
plasma membrane	43 out of 510 genes, 8.4%	<i>AGP2, AOX2, CDR1, CFL1, CFL4, CLC1, COX15, DIP5, EAP1, ECM331, ENA2, ERG251, EXG2, FCY21, GPR1, GSL1, HGT1,HGT3, IFC3, IFF6, MET15, MNT1, NDE1, OPT1, OPT4, PHB2, RHD3, RHO2, SHM2, SMF12, SNQ2, SSU1, VMA5, orf19.1564,orf19.2049, orf19.276, orf19.3335, orf19.341, orf19.409, orf19.4116, orf19.5095, orf19.5730, orf19.6741</i>
endoplasmic reticulum	36 out of 510 genes, 7.1%	<i>AGP2, ARE2, AYR1, CHS7, CHT3, DIP5, ERO1, GTT11, MNT1, OPI3, OPT1, PEX11, RCE1, SMF12, SSU1, TIP1, UBPI, VCX1,VMA11, orf19.1092, orf19.1564, orf19.1795.1, orf19.2064, orf19.2302, orf19.276, orf19.2761, orf19.3222, orf19.341, orf19.4907,orf19.4981, orf19.5095, orf19.516, orf19.6264.3, orf19.7183, orf19.7426, orf19.954</i>
cell wall	26 out of 510 genes, 5.1%	<i>ALS1, ALS5, ALS6, CHT1, CHT3, CSH1, DDR48, EAP1, ECM331, ENG1, EXG2, GLX3, HYR3, IFF6, INO1, MET15, PGA13,PGA31, PHHB, PIR1, PST2, RHD3, SCW11, SOD4, SOD5, XYL2</i>

ribosome	21 out of 510 genes, 4.1%	<i>MAL2, MPRL36, MRP20, MRPL33, MRPL37, STF2, orf19.1485, orf19.185, orf19.1959, orf19.2201, orf19.2887, orf19.3480,orf19.3797, orf19.4204, orf19.4633, orf19.4751, orf19.5235, orf19.5515, orf19.639.1, orf19.7012, orf19.7107</i>
mitochondrial envelope	21 out of 510 genes, 4.1%	<i>AOX1, AYRI, COX15, COX19, CYB2, NDE1, PHB2, SEN2, TIM13, TRR1, orf19.1300, orf19.1483, orf19.1794, orf19.409,orf19.4763, orf19.5515, orf19.6563.1, orf19.6607, orf19.7111, orf19.7214, orf19.954</i>
Golgi apparatus	18 out of 510 genes, 3.5%	<i>AYRI, CLC1, DIP5, HOC1, MNT1, OPT1, TIP1, USO1, orf19.2078, orf19.3222, orf19.3228, orf19.4292, orf19.4731, orf19.5618,orf19.6264.3, orf19.6720, orf19.6741, orf19.7196</i>
vacuole	16 out of 510 genes, 3.1%	<i>AGP2, AYRI, CIS2, DIP5, FCY21, MNT1, RNY11, VAM3, VCX1, VMA11, orf19.1210, orf19.1308, orf19.3222, orf19.3406,orf19.4843, orf19.7193</i>
extracellular region	16 out of 510 genes, 3.1%	<i>CHT1, CHT3, ENG1, FDH1, GDH3, MAL2, MNT1, PIR1, RBT4, RHD3, RNY11, SAP7, SCW11, SOD4, SOD5, SPE3</i>
chromosome	16 out of 510 genes, 3.1%	<i>CDC68, CTA26, CTF18, CUP9, DAD3, DOT6, DPB4, EFG1, PRI2, REV3, ROBI, TEC1, TYE7, orf19.229, orf19.7213, orf19.7538</i>
site of polarized growth	13 out of 510 genes, 2.5%	<i>ABP140, CEK1, CHS7, CHT3, HYMI, INNI, RHO2, SEC5, SHM2, orf19.2887, orf19.5095, orf19.5840, orf19.7450</i>
nucleolus	13 out of 510 genes, 2.5%	<i>DBP2, DBP7, MAF1, PWP2, RRP6, TSRI, UTP22, YTM1, orf19.1578, orf19.1619, orf19.512, orf19.6458.1, orf19.6730</i>
cytoskeleton	12 out of 510 genes, 2.4%	<i>ABP140, ARC18, BBC1, BET4, CDC68, CEK1, DAD3, INNI, MHP1, RAD7, orf19.229, orf19.7450</i>
cellular bud	9 out of 510 genes, 1.8%	<i>CHS7, CHT3, HYMI, INNI, SEC5, orf19.2887, orf19.5095, orf19.6741, orf19.7450</i>

cell cortex	8 out of 510 genes, 1.6%	<i>ABP140, ARC18, BBC1, INN1, SEC5</i> , orf19.5095, orf19.6741, orf19.7450
peroxisome	7 out of 510 genes, 1.4%	<i>CAT2, CYB2, FAA21, MDH1-3, PEX11, SRR1</i> , orf19.7111
cytoplasmic membrane-bounded vesicle	7 out of 510 genes, 1.4%	<i>CLC1, TIP1, USO1</i> , orf19.2078, orf19.3228, orf19.5022, orf19.6264.3
microtubule organizing center	5 out of 510 genes, 1%	<i>BET4, CDC68, CEK1, RAD7</i> , orf19.229
hyphal tip	1 out of 510 genes, 0.2%	<i>CEK1</i>
can not be mapped to a GO slim term	8 out of 510 genes, 1.6%	<i>ARF1, HSP21, PGAI, PGA23, PGA26, PGA38</i> , orf19.206, orf19.2397.3
not yet annotated	24 out of 510 genes, 4.7%	<i>FET35, FGR6</i> , orf19.1071, orf19.1125, orf19.13, orf19.1437, orf19.2222.1, orf19.2353, orf19.2659, orf19.3145.4, orf19.3386,orf19.3479, orf19.3641, orf19.4155.12, orf19.4421, orf19.4485, orf19.4552, orf19.5192, orf19.5401, orf19.6301, orf19.6865,orf19.6964, orf19.7005, orf19.7028

Appendix 1, Table 7. Significantly altered genes of the complete transcriptome analysis data for the *med31Δ/Δ* mutant.

The significantly differentially expressed Genes from the Volcano Plot built by comparing "Experiment med31 " with itself, using the Genes in the "all genes" Gene list.

Multiple Testing Correction: None. Which Genes were differentially expressed was defined by Normalized Value: 1.5 and a P-value Cutoff: 0.05

More information of full transcriptome analysis at <http://www.ncbi.nlm.nih.gov/pmc/articles/PMC3320594/#pgen.1002613.s001>

Systematic	P-value	Normalized	Common	Description
orf19.5557	0.00112	8.877082	<i>MNN4-4</i>	Putative mannosyltransferase; transcription is upregulated in a mutant lacking the Ssk1p response regulator protein or in a <i>nik1</i> homozygous null mutant, but not in <i>chk1</i> or <i>sln1</i> null mutants; pheromone induced
orf19.6078	0.000579	5.409864	<i>POL93</i>	Predicted ORF in retrotransposon Tca8 with similarity to the Pol region of retrotransposons encoding reverse transcriptase, protease and integrase; downregulated in response to ciclopirox olamine; induced upon biofilm formation
orf19.7585	3.66E-05	4.600788	<i>INO1</i>	Inositol-1-phosphate synthase; enzyme of inositol biosynthesis; antigenic in human; repressed by farnesol (in biofilm) or caspofungin; regulated during planktonic growth; upstream inositol/choline regulatory element; glycosylation predicted
orf19.4477	0.00103	4.039404	<i>CSH1</i>	Member of aldo-keto reductase family, similar to aryl alcohol dehydrogenases; role in adhesion to fibronectin, cell surface hydrophobicity; regulated by temperature, growth phase, benomyl, macrophage interaction; azole resistance associated
orf19.13	0.0117	3.817329		Putative glucokinase; regulated upon yeast-hyphal switch; regulated by Efg1p; fluconazole-induced; induced in core stress response; shows colony morphology-related gene regulation by Ssn6p; merged with orf19.734 in Assembly 20
orf19.5025	0.0166	3.705716	<i>MET3</i>	Putative ATP sulfurlyase of sulfate assimilation; repressed by Met or Cys, Sfu1p, or in fluconazole-resistant isolate; strongly induced on biofilm formation, even in presence of Met and Cys; Hog1p-, caspofungin-, possibly adherence-induced
orf19.6116	0.0336	3.69303	<i>GLK4</i>	Protein described as a glucokinase; decreased expression in hyphae compared to yeast-form cells
orf19.3461	0.00166	3.601725		Predicted ORF in Assemblies 19, 20 and 21; oxidative stress-induced via Cap1p; transcription is induced in response to alpha pheromone in SpiderM medium
orf19.6202	0.000156	3.233906	<i>RBT4</i>	Similar to plant pathogenesis-related proteins; required for virulence in mouse systemic, rabbit corneal infections; not required for filamentation; secretion signal; TUP1/RFG1/SSN6/HOG1 repressed; serum, hyphal, pheromone, alkaline-induced
orf19.5620	0.033	3.195529		Predicted ORF in Assemblies 19, 20 and 21; regulated by Gcn4p; induced in response to amino

				acid starvation (3-aminotriazole treatment); increased transcription is observed upon benomyl treatment or in an azole-resistant strain that overexpresses MDR1
orf19.251	0.0143	3.04965		ThiJ/PfpI protein family; antigenic (Cand a 3 allergen); binds human immunoglobulin E; 2 N-glycosylation motifs; alkaline, fluconazole, Hog1p-downregulated; induced in core stress response or by oxidative stress (via Cap1p)
orf19.2048	0.0498	2.767925		Transcription is positively regulated by Sfu1p
orf19.4255	0.00375	2.638032	<i>ECM331</i>	GPI-anchored protein; mainly at plasma membrane, also at cell wall; caspofungin induced; Plc1p-regulated; repressed by Rim101p, Hog1p; colony morphology-related gene regulation by Ssn6p; induced in <i>cyr1</i> homozygous null mutant yeast-form cel
orf19.3145.4	0.00751	2.558054		ORF Predicted by Annotation Working Group; removed from Assembly 20
orf19.3740	0.0248	2.453572	<i>PGA23</i>	Putative GPI-anchored protein of unknown function; transcription is negatively regulated by Rim101p; regulated by Cyr1p; shows colony morphology-related gene regulation by Ssn6p
orf19.5686	0.000151	2.412262		Predicted ORF in Assemblies 19, 20 and 21
orf19.6484	0.0118	2.373322		Predicted ORF in Assemblies 19, 20 and 21
orf19.7522	4.12E-06	2.345423		Predicted ORF in Assemblies 19, 20 and 21; mutation confers hypersensitivity to amphotericin B
orf19.272	0.000815	2.33923	<i>FAA21</i>	Predicted acyl CoA synthetase; upregulated upon phagocytosis; transcription is regulated by Nrg1p and Mig1p
orf19.1180	0.0109	2.260603		Predicted ORF in Assemblies 19, 20 and 21
orf19.5645	0.00658	2.237586	<i>MET15</i>	O-acetylhomoserine O-acetylserine sulfhydrylase; involved in sulfur amino acid biosynthesis; immunogenic; Hog1p, biofilm, possibly adherence-induced; brown colony color of homozygous mutant in Pb(2+) medium is visual selection marker
orf19.5094	0.0489	2.208094	<i>BUL1</i>	Protein not essential for viability; macrophage/pseudohyphal-induced; similar to <i>S. cerevisiae</i> Bullp, which may be involved in selection of substrates for ubiquitination
orf19.4082	0.0331	2.1819	<i>DDR48</i>	Immunogenic stress-associated protein; regulated by filamentous growth pathways; induced by benomyl, caspofungin, or in azole-resistant strain; Hog1p, farnesol, alkaline downregulated; similar to <i>S. cerevisiae</i> Ddr48p
orf19.4624	0.00331	2.168487	<i>HRT2</i>	Protein described as having a role in Ty3 transposition; decreased expression in hyphae compared to yeast-form cells; protein detected by mass spec in stationary phase cultures
orf19.2516	0.00158	2.145445		Predicted ORF in Assemblies 19, 20 and 21
orf19.4981	0.0169	2.13885		Predicted ORF in Assemblies 19, 20 and 21
orf19.716	0.0195	2.13818		Predicted ORF in Assemblies 19, 20 and 21; regulated by Nrg1p, Tup1p; transcription is

				repressed in response to alpha pheromone in SpiderM medium
orf19.4716	0.011	2.113491	<i>GDH3</i>	Protein described as similar to NADP-glutamate dehydrogenase; hyphal downregulated expression; transcription is regulated by Nrg1p, Plc1p; downregulated by Efg1p; upregulated by Rim101p at pH 8; ciclopirox olamine induced
orf19.338	0.0167	2.063332		Predicted ORF in Assemblies 19, 20 and 21; Hog1p-downregulated; shows colony morphology-related gene regulation by Ssn6p; protein detected by mass spec in stationary phase cultures
orf19.1300	0.00293	2.060488		Predicted ORF in Assemblies 19, 20 and 21
orf19.1589.1	0.011	2.038194		ORF added to Assembly 21 based on comparative genome analysis
orf19.1857	0.000629	2.022316		Protein not essential for viability
orf19.2885	0.00374	2.013147	<i>PRI2</i>	Gene adjacent to CDC68; divergently transcribed with CDC68
orf19.6709	0.00457	2.007273		Predicted ORF in Assemblies 19, 20 and 21
orf19.5037	0.00669	2.004664		Protein not essential for viability
orf19.1092	0.00112	1.970606		Predicted ORF in Assemblies 19, 20 and 21
orf19.6607	0.00204	1.970538		Predicted ORF in Assemblies 19, 20 and 21
orf19.4358	0.0166	1.970043		Predicted ORF in Assemblies 19, 20 and 21
orf19.5840	0.000275	1.964379		Predicted ORF in Assemblies 19, 20 and 21
orf19.2062	0.0334	1.955213	<i>SOD4</i>	Copper- and zinc-containing superoxide dismutase; role in response to host innate immune ROS; regulated on white-opaque switching; ciclopirox olamine induced; caspofungin repressed; member of family that includes SOD1, SOD4, SOD5, and SOD6
orf19.3612	0.0271	1.95196	<i>PST2</i>	Putative NADH:quinone oxidoreductase; similar to 1,4-benzoquinone reductase; immunogenic in mice; benomyl treatment induces transcription; oxidative stress-induced via Cap1p; fungal-specific (no human/murine homolog), farnesol-downregulated
orf19.3797	0.000537	1.939901		Predicted ORF in Assemblies 19, 20 and 21
orf19.7214	0.000876	1.933288		Similar to glucan 1,3-beta-glucosidase; regulated by Nrg1p, Tup1p; possibly regulated by Tac1p; induced upon biofilm formation; induced by nitric oxide; induced during cell wall regeneration; detected by mass spec in stationary phase
orf19.7068	0.0133	1.882253	<i>MAC1</i>	Transcriptional regulator of CTR1, which encodes a copper transporter; activates CTR1 transcription under low-copper conditions; ectopic expression causes copper-sensitive stimulation of filamentation in <i>S. cerevisiae</i>
orf19.5192	0.00137	1.882085		Predicted ORF from Assembly 19; removed from Assembly 20

orf19.2754	0.0458	1.873925		Predicted ORF in Assemblies 19, 20 and 21
orf19.7625	0.0115	1.871306	<i>PGA1</i>	Putative GPI-anchored protein of unknown function; induced during cell wall regeneration
orf19.94	0.0094	1.8681		Predicted ORF in Assemblies 19, 20 and 21
orf19.6486	0.00139	1.865975	<i>LDG3</i>	Predicted ORF in Assemblies 19, 20 and 21; induced upon biofilm formation
orf19.405	0.0412	1.858371	<i>VCX1</i>	Putative H ⁺ /Ca ²⁺ antiporter; fungal-specific (no human or murine homolog)
orf19.5000	7.37E-07	1.853678	<i>CYB2</i>	Protein described as precursor protein of cytochrome b2; transcriptionally regulated by iron; expression greater in high iron; alkaline downregulated; shows colony morphology-related gene regulation by Ssn6p
orf19.2165	0.00974	1.852237		Predicted ORF in Assemblies 19, 20 and 21; induced by nitric oxide
orf19.1723	0.00844	1.834498		Predicted ORF in Assemblies 19, 20 and 21
orf19.6947	0.00907	1.813512	<i>GTT11</i>	Predicted ORF in Assemblies 19, 20 and 21; induced by nitric oxide
orf19.4356	0.00307	1.799181	<i>HGT3</i>	Putative glucose transporter of the major facilitator superfamily; the <i>C. albicans</i> glucose transporter family comprises 20 members; 12 probable membrane-spanning segments, extended C terminus; expressed in rich medium with 2% glucose
orf19.756	0.0017	1.793211	<i>SAP7</i>	Member of the secreted aspartyl proteinase family; expression detected during human oral infection; regulated by Ssn6p; role in murine intravenous infection; induced during, but not required for, murine vaginal infection
orf19.2886	0.000263	1.787408	<i>CEK1</i>	ERK-family protein kinase, required for wild-type yeast-hyphal switching, mating efficiency, and virulence in a mouse model; Cst20p-Hst7p-Cek1p-Cph1p MAPK pathway regulates mating, and invasive hyphal growth under some conditions
orf19.2396	0.000353	1.785828	<i>IFR2</i>	Increased transcription is observed upon benomyl treatment; transcription is upregulated in response to treatment with ciclopirox olamine, alpha pheromone; regulated by oxidative stress (via Cap1p) and osmotic stress (via Hog1p)
orf19.1039	0.0054	1.782475		Predicted ORF in Assemblies 19, 20 and 21
orf19.6167	0.00179	1.780897	<i>AYR1</i>	Protein described as putative oxidoreductase; transcriptionally induced by interaction with macrophage
orf19.946	0.0284	1.774209	<i>MET14</i>	Predicted ORF in Assemblies 19, 20 and 21; predicted role in sulfur metabolism; induced upon biofilm formation; possibly adherence-induced
orf19.1483	0.0234	1.773485		Predicted ORF in Assemblies 19, 20 and 21
orf19.2735	0.0109	1.760793	<i>SEN2</i>	Predicted ORF in Assemblies 19, 20 and 21; mutation confers hypersensitivity to toxic ergosterol analog, and to amphotericin B; has intron in 5'-UTR

orf19.2884	0.0192	1.75648	<i>CDC68</i>	Functional homolog of <i>S. cerevisiae</i> Cdc68p, which is a transcription elongation factor; essential; possible drug target
orf19.4633	0.000141	1.75562		Predicted ORF in Assemblies 19, 20 and 21
orf19.400	0.00132	1.752598	<i>GCF1</i>	HMG box-containing mitochondrial (mt) protein; binds to mt DNA and to the HWP1 promoter; mutant phenotype and functional complementation of an <i>S. cerevisiae</i> abf2 mutation suggest a role in mt genome replication and maintenance
orf19.5515	0.000127	1.748567		Predicted ORF in Assemblies 19, 20 and 21
orf19.2269	0.000173	1.748259		Putative 3-phosphoserine phosphatase; fungal-specific (no human or murine homolog); increased transcription is observed upon benomyl treatment or in an azole-resistant strain that overexpresses MDR1
orf19.2302	0.00393	1.744693		Predicted ORF in Assemblies 19, 20 and 21
orf19.2222.1	0.0172	1.741771		ORF Predicted by Annotation Working Group; merged with orf19.2660 in Assembly 20
orf19.7538	0.00286	1.739729		Predicted ORF in Assemblies 19, 20 and 21
orf19.7265	0.0258	1.736566		Predicted ORF in Assemblies 19, 20 and 21
orf19.6096	0.0196	1.731309	<i>TRP1</i>	Phosphoribosylanthranilate isomerase; enzyme of tryptophan biosynthesis; expected to be unifunctional, unlike trifunctional enzyme of some other fungi; complements <i>E. coli</i> trpC or <i>S. cerevisiae</i> trp1 mutant; CCT1 and TRP1 genes overlap
orf19.5132	0.0321	1.727941		Predicted ORF in Assemblies 19, 20 and 21
orf19.4290	0.00708	1.724194	<i>TRR1</i>	Putative thioredoxin reductase; upregulated in presence of human neutrophils; regulated by Tsa1p, Tsa1Bp; induced by nitric oxide; peroxide-induced; oxidative stress-induced via Cap1p; fungal-specific (no human/murine homolog)
orf19.5417	0.00259	1.723615	<i>DOT5</i>	Alkaline downregulated
orf19.1485	0.00679	1.720811		Predicted ORF in Assemblies 19, 20 and 21
orf19.1932	0.0341	1.71908	<i>CFLA</i>	Similar to ferric reductase, C-terminal region; expression greater in low iron; transcription is negatively regulated by Sfu1p; ciclopirox olamine induced; shows colony morphology-related gene regulation by Ssn6p
orf19.288	0.00702	1.709314		Predicted ORF in Assemblies 19, 20 and 21
orf19.639.1	0.0188	1.706143		ORF Predicted by Annotation Working Group
orf19.2204	0.00101	1.702359		Predicted ORF in Assemblies 19, 20 and 21
orf19.4731	0.000879	1.701039		Predicted ORF in Assemblies 19, 20 and 21

orf19.4600.1	0.0433	1.700511		ORF Predicted by Annotation Working Group
orf19.1356	2.27E-06	1.696588		Predicted ORF in Assemblies 19, 20 and 21
orf19.1888	0.0275	1.695417		Predicted ORF in Assemblies 19, 20 and 21
orf19.276	0.0294	1.689134		Predicted ORF in Assemblies 19, 20 and 21; increased transcription is observed in an azole-resistant strain that overexpresses MDR1
orf19.2511.1	0.0164	1.682074	<i>MRPL33</i>	ORF predicted by Annotation Working Group; increased expression observed in an <i>ssr1</i> homozygous null mutant; transcription is upregulated in both intermediate and mature biofilms
orf19.954	0.00213	1.681929		Predicted ORF in Assemblies 19, 20 and 21
orf19.5004	0.0419	1.680228	<i>RAD54</i>	Protein similar to <i>S. cerevisiae</i> Rad54p, which is a DNA-dependent ATPase involved in DNA repair; induced under hydroxyurea treatment
orf19.789	0.00809	1.677074	<i>PYC2</i>	Putative pyruvate carboxylase, binds to biotin cofactor; up-regulated in mutant lacking the Ssk1p response regulator protein, upon benomyl treatment, or in an azole-resistant strain overexpressing MDR1
orf19.516	0.0149	1.674573		Predicted ORF in Assemblies 19, 20 and 21
orf19.4751	0.000111	1.674256		Predicted ORF in Assemblies 19, 20 and 21
orf19.5235	0.00016	1.672747		Protein not essential for viability; protein level decreased in stationary phase cultures
orf19.2846	0.00438	1.664617		Predicted ORF in Assemblies 19, 20 and 21; induced in core caspofungin response; transcription regulated upon yeast-hyphal switch
orf19.3223.1	0.0114	1.661614		Predicted ORF; described as 12kDa subunit of mitochondrial NADH-ubiquinone oxidoreductase; gene has intron
orf19.2952	0.000582	1.660474	<i>EXG2</i>	Protein similar to <i>S. cerevisiae</i> Exg2p, which is an exo-1,3-beta-glucosidase; predicted Kex2p substrate; induced during cell wall regeneration
orf19.2353	0.0119	1.657397		Predicted ORF from Assembly 19; merged with orf19.1840 in Assembly 20
orf19.7196	0.00192	1.654088		Protein described as a vacuolar protease; upregulated in the presence of human neutrophils
orf19.517	0.0257	1.65305	<i>HAP31</i>	Protein described as a transcription factor that regulates CYC1; transcriptionally regulated by iron; expression greater in high iron
orf19.2461	0.000437	1.651223	<i>PRN4</i>	Protein with similarity to pirins; increased transcription is observed upon benomyl treatment
orf19.1125	0.0394	1.649334		Predicted ORF from Assembly 19; merged with orf19.2165 in Assembly 20
orf19.3656	0.00127	1.648344	<i>COX15</i>	Transcription is regulated by Nrg1p and Tup1p; alkaline downregulated
orf19.3445	0.000871	1.647885	<i>HOC1</i>	Protein with similarity to mannosyltransferases; similar to <i>S. cerevisiae</i> Hoc1p and <i>C. albicans</i>

				Och1p
orf19.2172	0.00116	1.647637	<i>ARA1</i>	D-Arabinose dehydrogenase; in dehydro-D-arabinono-1,4-lactone biosynthesis; NADP+ cofactor; active toward D-arabinose, L-fucose, L-xylose, L-galactose; inhibited by metal ions, thiol group-specific reagents; induced on polystyrene adherence
orf19.1795.1	0.0398	1.644288		ORF added to Assembly 21 based on comparative genome analysis
orf19.2483	0.00514	1.64014	<i>RIM1</i>	Predicted ORF in Assemblies 19, 20 and 21; protein level decreased in stationary phase cultures
orf19.6295	0.000419	1.637186	<i>MAS2</i>	Predicted ORF in Assemblies 19, 20 and 21; protein level decreased in stationary phase cultures
orf19.2166	0.000742	1.636999		Predicted ORF in Assemblies 19, 20 and 21
orf19.2887	0.00054	1.635622	<i>MET13</i>	Predicted ORF in Assemblies 19, 20 and 21; ketoconazole-induced; amphotericin B repressed
orf19.5459	0.0139	1.631619		Putative protein of unknown function, transcription is upregulated in an RHE model of oral candidiasis and in clinical isolates from HIV+ patients with oral candidiasis; predicted ORF in Assemblies 19, 20 and 21
orf19.6458.1	0.0234	1.628647		ORF Predicted by Annotation Working Group
orf19.5239	2.66E-05	1.626316		Predicted ORF in Assemblies 19, 20 and 21; oxidative stress-induced via Cap1p
orf19.2248	0.0295	1.625625	<i>ARE2</i>	Acyl CoA:sterol acyltransferase (ASAT); uses cholesterol and oleoyl-CoA substrates; protoberberine derivative drug inhibits enzyme activity; 7 putative transmembrane regions; ketoconazole-induced
orf19.145	0.00043	1.621885	<i>RPB4</i>	Protein similar to <i>S. cerevisiae</i> Rpb4p, which is a component of RNA polymerase II; transposon mutation affects filamentous growth
orf19.6563.1	0.00162	1.6216		ORF Predicted by Annotation Working Group
orf19.7306	0.027	1.619479		Protein of aldo-keto reductase family; increased transcription associated with MDR1 overexpression, benomyl or long-term fluconazole treatment; overexpression does not affect drug or oxidative stress sensitivity
orf19.2125	0.000126	1.618466		Predicted ORF in Assemblies 19, 20 and 21
orf19.1743	0.000324	1.618018	<i>ACSI</i>	Putative acetyl-CoA synthetase, similar to <i>S. cerevisiae</i> Acs1p; upregulated in the presence of human neutrophils; fluconazole-downregulated; regulated by Nrg1p and Mig1p; shows colony morphology-related gene regulation by Ssn6p
orf19.5014	0.0199	1.617514		Predicted ORF in Assemblies 19, 20 and 21
orf19.6865	0.0215	1.615571		Predicted ORF from Assembly 19; merged with orf19.2631 in Assembly 20
orf19.5812	0.0319	1.613057		Predicted ORF in Assemblies 19, 20 and 21

orf19.1152	0.0463	1.612679		Predicted ORF in Assemblies 19, 20 and 21; regulated by Gcn2p and Gcn4p; induced in core stress response
orf19.74	0.0105	1.608947	<i>SEC5</i>	Predicted exocyst component; ortholog of <i>S. cerevisiae</i> Sec5p; merged with orf19.75 in Assembly 21
orf19.2088	0.0272	1.606075		Predicted ORF in Assemblies 19, 20 and 21
orf19.1794	0.0159	1.604762		Predicted ORF in Assemblies 19, 20 and 21
orf19.3065	2.79E-05	1.602601	<i>DAO1</i>	Putative D-amino acid oxidase; transcription is regulated upon yeast-hyphal switch
orf19.6100	3.21E-05	1.602063		Protein not essential for viability; similar to <i>S. cerevisiae</i> Crd1p, which is cardiolipin synthase; transcription is upregulated in clinical isolates from HIV+ patients with oral candidiasis
orf19.7676	0.0274	1.601831	<i>XYL2</i>	Protein described as similar to D-xylulose reductase; immunogenic in mouse; soluble protein in hyphae; Hog1p-induced; induced during cell wall regeneration; caspofungin or fluconazole-induced; Mnl1p-induced in weak acid stress
orf19.1089	0.0148	1.601562	<i>PEX11</i>	Putative protein involved in fatty acid oxidation; expression is Tac1p-dependent
orf19.7389	0.00289	1.598004	<i>REV3</i>	Protein not essential for viability; similar to <i>S. cerevisiae</i> Rev3p, which is a subunit of DNA polymerase zeta
orf19.3581	0.00845	1.597515		Predicted ORF in Assemblies 19, 20 and 21
orf19.1228	0.017	1.59736	<i>HAP2</i>	CCAAT-binding factor regulates low-iron (chelation) induction of FRP1 transcription, and under these conditions CBF comprises Hap43p and probably Hap2p and Hap3p
orf19.6861	0.00664	1.595342		Predicted ORF in Assemblies 19, 20 and 21
orf19.4763	0.00645	1.594072		Protein not essential for viability
orf19.3480	0.00163	1.590259		Predicted ORF in Assemblies 19, 20 and 21
orf19.1140	0.00101	1.590074		Predicted ORF in Assemblies 19, 20 and 21; possibly spurious ORF (Annotation Working Group prediction)
orf19.7012	0.036	1.585916		Predicted ORF in Assemblies 19, 20 and 21
orf19.4204	0.0296	1.585916		Predicted ORF in Assemblies 19, 20 and 21
orf19.3350	0.00626	1.585345	<i>MRP20</i>	Protein described as component of mitochondrial ribosome; decreased expression in hyphae compared to yeast-form cells
orf19.6156	0.0132	1.582963		Predicted ORF in Assemblies 19, 20 and 21
orf19.4735	0.00775	1.582627		Predicted ORF in Assemblies 19, 20 and 21
orf19.5805	0.0149	1.579052	<i>DLD1</i>	Putative D-lactate dehydrogenase; transcription is specific to white cell type; shows colony

				morphology-related gene regulation by Ssn6p; transcription is upregulated in both intermediate and mature biofilms
orf19.1564	0.00926	1.578584		Predicted ORF in Assemblies 19, 20 and 21
orf19.6587	5.75E-05	1.578268		Protein similar to <i>S. cerevisiae</i> Ydr152wp; transposon mutation affects filamentous growth
orf19.4591	0.000849	1.577796	<i>CAT2</i>	Major carnitine acetyl transferase localized in peroxisomes and mitochondria; involved in intracellular acetyl-CoA transport; transcriptionally induced in macrophage; farnesol-upregulated in biofilm; Hog1p-downregulated
orf19.2629	0.00102	1.577517		Predicted ORF in Assemblies 19, 20 and 21
orf19.7680	0.00189	1.576935	<i>CTA26</i>	Putative transcriptional activator; downregulated by Efg1p; transcription is upregulated in an RHE model of oral candidiasis; member of a family of telomere-proximal genes
orf19.7446	0.000784	1.573003	<i>OPI3</i>	Putative phosphatidylethanolamine N-methyltransferase of phosphatidylcholine biosynthesis; downregulation correlates with clinical development of fluconazole resistance; amphotericin B repressed; caspofungin repressed
orf19.755	0.0258	1.572058	<i>MRPL37</i>	Predicted ORF in Assemblies 19, 20 and 21; shows colony morphology-related gene regulation by Ssn6p
orf19.3205	0.00282	1.566239		Predicted ORF in Assemblies 19, 20 and 21
orf19.5302	0.0258	1.565018	<i>PGA31</i>	Cell wall protein; putative GPI anchor; expression is regulated upon white-opaque switching; induced during cell wall regeneration; possibly spurious ORF (Annotation Working Group prediction)
orf19.1210	0.0015	1.563869		Predicted ORF in Assemblies 19, 20 and 21
orf19.4967	0.00163	1.562726	<i>COX19</i>	Predicted ORF in Assemblies 19, 20 and 21; Plc1p-regulated
orf19.1085	0.0346	1.561583		Predicted ORF in Assemblies 19, 20 and 21
orf19.5467	0.00493	1.556072	<i>TLO7</i>	Member of a family of telomere-proximal genes of unknown function; may be spliced <i>in vivo</i>
orf19.6053	0.000594	1.552345	<i>CIS2</i>	Putative role in regulation of biogenesis of the cell wall; upregulated in biofilm; Gcn4p-regulated
orf19.4421	0.000504	1.551854		Processing alpha glucosidase I, involved in N-linked protein glycosylation and assembly of cell wall beta 1,6 glucan; merged with orf19.4719 in Assembly 20
orf19.5973	0.0392	1.549712		Predicted ORF in Assemblies 19, 20 and 21
orf19.1195	0.00117	1.548998		Predicted ORF in Assemblies 19, 20 and 21
orf19.4384	0.0433	1.548743	<i>HXT5</i>	Protein described as a sugar transporter; transcription is upregulated in response to treatment with ciclopirox olamine; Snf3p-induced; alkaline downregulated; shows colony morphology-related

				gene regulation by Ssn6p
orf19.2444	0.0225	1.548489	<i>CHS7</i>	Protein required for wild-type chitin synthase III activity; similar to (but not functional homolog of) <i>S. cerevisiae</i> Chs7p, which effects ER export of Chs3p; induced in homozygous <i>cyr1</i> null mutant hyphae and <i>ras1</i> yeast-form cells
orf19.3074	0.00164	1.544797	<i>TLO10</i>	Member of a family of telomere-proximal genes of unknown function
orf19.4819	0.0233	1.544793		Predicted ORF in Assemblies 19, 20 and 21
orf19.1493	0.00738	1.543473	<i>RAD7</i>	Protein similar to <i>S. cerevisiae</i> Rad7p, which is a subunit of the Nucleotide Excision Repair Factor 4; induced under hydroxyurea treatment
orf19.2201	0.00384	1.541372		Predicted ORF in Assemblies 19, 20 and 21
orf19.185	0.00128	1.539813		Predicted ORF in Assemblies 19, 20 and 21
orf19.5174	0.000709	1.536971	<i>TAF19</i>	Predicted ORF in Assemblies 19, 20 and 21; mutation confers hypersensitivity to amphotericin B
orf19.2761	7.78E-05	1.535966		Predicted ORF in Assemblies 19, 20 and 21; induced by nitric oxide in <i>yhb1</i> mutant; possibly spurious ORF (Annotation Working Group prediction)
orf19.439	0.00113	1.535489		Predicted ORF in Assemblies 19, 20 and 21
orf19.5522	1.13E-05	1.534996		Predicted ORF in Assemblies 19, 20 and 21; possibly spurious ORF (Annotation Working Group prediction)
orf19.3479	0.041	1.534096		Predicted ORF in Assemblies 19, 20 and 21
orf19.6538	0.00676	1.53342	<i>VMA11</i>	Predicted ortholog of <i>S. cerevisiae</i> Tfp3p, which is the c' subunit of the V0 subcomplex of the vacuolar ATPase; required for hemoglobin-iron utilization
orf19.3926	0.0264	1.532394		Predicted ORF in Assemblies 19, 20 and 21
orf19.229	0.024	1.531777		Predicted ORF in Assemblies 19, 20 and 21
orf19.1960	0.0364	1.531248	<i>CLN3</i>	G1 cyclin; depletion causes abolished budding and hyphal growth defects; likely to be essential; farnesol regulated, upregulated in biofilm; functional in <i>S. cerevisiae</i> ; similar to <i>S. cerevisiae</i> Cln3p, which is a G1-specific cyclin
orf19.5070	0.0316	1.53041		Predicted ORF in Assemblies 19, 20 and 21; transcriptionally regulated by iron; expression greater in low iron; similar to cell-wall mannoproteins; ; regulated by osmotic and oxidative stress via Hog1p
orf19.4594	0.0308	1.530271		Predicted ORF in Assemblies 19, 20 and 21
orf19.3549	0.00148	1.528976	<i>CDC21</i>	Predicted ORF in Assemblies 19, 20 and 21; flucytosine induced; transcription is downregulated in both intermediate and mature biofilms

orf19.3386	0.011	1.525249		ORF Predicted by Annotation Working Group; removed from Assembly 20
orf19.5323	0.0308	1.524832	<i>MDH1-3</i>	Predicted malate dehydrogenase; farnesol regulated
orf19.3951	0.000983	1.524696	<i>TIP1</i>	Predicted ORF in Assemblies 19, 20 and 21; mutation confers hypersensitivity to toxic ergosterol analog
orf19.4066	0.000389	1.523195		Predicted ORF in Assemblies 19, 20 and 21; Hog1p-downregulated
orf19.5920	9.75E-06	1.520128		Predicted ORF in Assemblies 19, 20 and 21; possibly spurious ORF (Annotation Working Group prediction)
orf19.6264.3	0.00746	1.518869		ORF Predicted by Annotation Working Group
orf19.1445	0.0483	1.518734	<i>ESC4</i>	Protein similar to <i>S. cerevisiae</i> Esc4p, which represses transposition; transposon mutation affects filamentous growth
orf19.2515	0.00056	1.517957		Predicted ORF in Assemblies 19, 20 and 21
orf19.5095	0.00108	1.517627		Predicted ORF in Assemblies 19, 20 and 21; caspofungin induced
orf19.7426	0.00672	1.516994		Predicted ORF in Assemblies 19, 20 and 21
orf19.121	0.00516	1.516633	<i>ARC18</i>	Predicted ORF in Assemblies 19, 20 and 21; mutation confers hypersensitivity to cytochalasin D
orf19.926	3.68E-07	1.515161	<i>EXO1</i>	Predicted ORF in Assemblies 19, 20 and 21; cell-cycle regulated periodic mRNA expression
orf19.255	0.0274	1.514486		Predicted zinc-cluster protein of unknown function; possibly transcriptionally regulated upon hyphal formation; intron in 5'-UTR
orf19.3248	0.000444	1.511345		Predicted ORF in Assemblies 19, 20 and 21
orf19.1709	0.0337	1.506605		Predicted ORF in Assemblies 19, 20 and 21; alkaline downregulated; shows colony morphology-related gene regulation by Ssn6p
orf19.2926	0.000216	1.505279		Predicted ORF in Assemblies 19, 20 and 21
orf19.2204.2	0.00553	1.503046		ORF Predicted by Annotation Working Group (see Locus History Note for Assembly 19 correction)
orf19.7173	0.00637	0.665784		Predicted ORF in Assemblies 19, 20 and 21
orf19.7414	3.34E-05	0.665405	<i>ALS6</i>	ALS family protein; expression in <i>S. cerevisiae</i> confers adhesion to gelatin; macrophage-induced gene; N-terminal adhesion domain; ALS family includes cell-surface glycoproteins, some with adhesin function
orf19.2972	0.0371	0.665167	<i>PDE2</i>	Cyclic nucleotide phosphodiesterase, high affinity; role in moderating signaling via cAMP; required for wild-type virulence, hyphal growth, switching, and cell wall, but not for pseudohyphal growth; expressed shortly after hyphal induction

orf19.2545	0.0124	0.664842	<i>DOT6</i>	Predicted ORF in Assemblies 19, 20 and 21; repressed upon high-level peroxide stress
orf19.6730	0.0298	0.664561		Predicted ORF in Assemblies 19, 20 and 21
orf19.7111	5.09E-05	0.664272		Predicted ORF in Assemblies 19, 20 and 21
orf19.6387	0.000283	0.664002	<i>HSP104</i>	Functional homolog of <i>S. cerevisiae</i> Hsp104p; has chaperone and prion propagation activity in <i>S. cerevisiae</i> ; guanidine-insensitive; heat shock/stress induced; downregulated in biofilm upon treatment with farnesol; no human or murine homolog
orf19.3087.1	0.00627	0.663781		ORF added to Assembly 21 based on comparative genome analysis
orf19.5775	0.0188	0.663514		Predicted ORF in Assemblies 19, 20 and 21; member of a family encoded by FGR6-related genes in the RB2 repeat sequence
orf19.6902	0.00107	0.661202	<i>DBP7</i>	Predicted ORF in Assemblies 19, 20 and 21; transcription is upregulated in both intermediate and mature biofilms
orf19.3228	0.00195	0.661055		Predicted ORF in Assemblies 19, 20 and 21; mutation confers hypersensitivity to amphotericin B
orf19.3007	0.0104	0.660659		Predicted ORF in Assemblies 19, 20 and 21
orf19.3239	0.00545	0.660557	<i>CTF18</i>	Predicted ORF in Assemblies 19, 20 and 21; cell-cycle regulated periodic mRNA expression
orf19.5610	0.0189	0.660459	<i>ARG3</i>	Alkaline downregulated; Gcn4p-regulated
orf19.5736	0.000642	0.659841	<i>ALS5</i>	Adhesin; ALS family protein; highly variable; expression in <i>S. cerevisiae</i> causes adhesion to human epithelium, endothelium or ECM, endothelial invasiveness by endocytosis, and, at high abundance, ECM-induced aggregation; has amyloid domain
orf19.6621	0.0118	0.659493	<i>MHP1</i>	Protein similar to <i>S. cerevisiae</i> Mhp1p, which is involved in microtubule stabilization; transposon mutation affects filamentous growth; possibly transcriptionally regulated upon hyphal formation
orf19.2208	0.00138	0.659315		Predicted ORF in Assemblies 19, 20 and 21
orf19.5813	1.34E-05	0.658904		Predicted ORF in Assemblies 19, 20 and 21
orf19.4814	0.0157	0.658298		Predicted ORF in Assemblies 19, 20 and 21
orf19.2462	0.0358	0.6577	<i>PRN3</i>	Predicted ORF in Assemblies 19, 20 and 21; similar to pirin; transcriptionally activated by Mnl1p under weak acid stress
orf19.1717	0.00132	0.657545		Predicted ORF in Assemblies 19, 20 and 21
orf19.1959	9.91E-05	0.657077		Predicted ORF in Assemblies 19, 20 and 21
orf19.512	0.00368	0.655235		Predicted ORF in Assemblies 19, 20 and 21; essential; <i>S. cerevisiae</i> ortholog is essential
orf19.5953	7.36E-06	0.655134		Predicted ORF in Assemblies 19, 20 and 21

orf19.554	0.0113	0.654596	<i>DIT2</i>	Monoxygenase of the cytochrome P450 family involved in chlamyospore formation; produces N,N'-bisformyl dityrosine from N-formyltyrosine; transcription is regulated by Nrg1p, Mig1p, and Tup1p
orf19.5767	0.0151	0.654211		Predicted ORF in Assemblies 19, 20 and 21
orf19.6373	6.32E-06	0.653308		Predicted ORF in Assemblies 19, 20 and 21
orf19.559	0.000729	0.652604	<i>FGRI4</i>	Protein encoded in retrotransposon Zorro3 with similarity to retroviral endonuclease-reverse transcriptase proteins; lacks an ortholog in <i>S. cerevisiae</i> ; transposon mutation affects filamentous growth
orf19.4869	0.00523	0.651844	<i>SFU1</i>	Transcriptional regulator of iron-responsive genes; represses some iron utilization genes when iron is present; not required for wild-type hyphal growth; has two GATA1-like zinc fingers separated by Cys-rich iron-sensing region
orf19.6818	0.000881	0.651046		Predicted ORF in Assemblies 19, 20 and 21
orf19.6244	0.00926	0.650884		Predicted ORF in Assemblies 19, 20 and 21
orf19.1401	0.00442	0.646922	<i>EAP1</i>	Cell wall adhesin required for cell-cell adhesion and biofilm formation; GPI anchored; Efg1p-regulated; suppresses polystyrene or cell adhesion, filamentation, invasive growth defects of <i>S. cerevisiae</i> flo8 or flo11 mutant
orf19.2730	0.0304	0.646709		Predicted ORF in Assemblies 19, 20 and 21
orf19.176	0.0018	0.646459	<i>OPT4</i>	Oligopeptide transporter; detected at germ tube plasma membrane by mass spectrometry; transcriptionally induced upon phagocytosis by macrophage; fungal-specific (no human or murine homolog); merged with orf19.2292 in Assembly 20
orf19.2078	0.039	0.646384		Predicted ORF in Assemblies 19, 20 and 21
orf19.1890	0.00162	0.645151		Predicted ORF in Assemblies 19, 20 and 21
orf19.1308	0.00678	0.644933		Predicted membrane transporter, member of the drug:proton antiporter (14 spanner) (DHA2) family, major facilitator superfamily (MFS)
orf19.1578	2.24E-05	0.64468		Predicted ORF in Assemblies 19, 20 and 21
orf19.2360	0.00422	0.644605	<i>URA2</i>	Predicted ORF in Assemblies 19, 20 and 21; flucytosine induced; macrophage/pseudohyphal-induced; intron in 5'-UTR
orf19.4815	0.016	0.643448	<i>YTM1</i>	Protein similar to <i>S. cerevisiae</i> Ytm1p, which is involved in biogenesis of the large ribosomal subunit; transposon mutation affects filamentous growth; protein level decreased in stationary phase cultures
orf19.2049	0.0383	0.643269		Predicted ORF in Assemblies 19, 20 and 21; heterozygous null mutant displays sensitivity to

				virgineone
orf19.3311	0.00671	0.6425	<i>IFD3</i>	Transcription is regulated by Mig1p
orf19.7484	0.00316	0.642422	<i>ADE1</i>	Phosphoribosylaminoimidazole succinocarboxamide synthetase, enzyme of adenine biosynthesis; not induced during GCN response, in contrast to the <i>S. cerevisiae</i> ortholog; fungal-specific (no human or murine homolog)
orf19.4679	1.57E-06	0.642323	<i>AGP2</i>	Protein described as an amino acid permease; hyphal downregulated; regulated upon white-opaque switching; induced in core caspofungin response, during cell wall regeneration, or by flucytosine; fungal-specific (no human or murine homolog)
orf19.1665	0.015	0.642054	<i>MNT1</i>	Alpha-1,2-mannosyl transferase; adds second mannose during cell-wall mannoprotein biosynthesis; required for wild-type virulence and adherence to epithelial cells; predicted type II membrane protein of Golgi; fungal-specific
orf19.7107	0.00127	0.641868		Predicted ORF in Assemblies 19, 20 and 21
orf19.4589	0.0144	0.641761		Predicted ORF in Assemblies 19, 20 and 21
orf19.1569	0.0312	0.641516	<i>UTP22</i>	Predicted ORF in Assemblies 19, 20 and 21; decreased expression observed in an <i>ssr1</i> homozygous null mutant; decreased expression in response to prostaglandins; heterozygous null mutant exhibits resistance to parnafungin
orf19.173	0.0155	0.641144		Putative transcription factor with zinc finger DNA-binding motif; transcriptionally activated by Mnl1p under weak acid stress
orf19.3323	0.00597	0.640532		Predicted ORF in Assemblies 19, 20 and 21; possibly spurious ORF (Annotation Working Group prediction)
orf19.7250	0.0204	0.640298		Predicted ORF in Assemblies 19, 20 and 21
orf19.6824	1.63E-06	0.640172		Predicted ORF in Assemblies 19, 20 and 21; appears to be <i>C. albicans</i> -specific; induced upon biofilm formation; transcription is repressed in response to alpha pheromone in SpiderM medium
orf19.7561	0.02	0.639803	<i>DEF1</i>	Protein required for filamentous growth and for escape from epithelial cells and dissemination in an RHE model; transcription induced in oral candidiasis clinical isolates; induced by fluconazole, high cell density; hyphally regulated
orf19.796	0.03	0.639704	<i>HYMI</i>	Mo25 family domain protein of RAM cell wall integrity signaling network; role in cell separation, azole sensitivity; required for hyphal growth
orf19.7507	0.000635	0.639577		Predicted ORF in Assemblies 19, 20 and 21
orf19.3529	0.00973	0.638372	<i>ABP2</i>	Protein of unknown function; induced in response to alpha pheromone in SpiderM medium
orf19.4871	0.0259	0.637732	<i>ERO1</i>	Protein described as similar to <i>S. cerevisiae</i> Ero1p, which has a role in formation of disulfide

				bonds in the endoplasmic reticulum; fluconazole-induced; transcriptionally activated by Mnl1p under weak acid stress
orf19.2495	0.013	0.637656	<i>GSL1</i>	Subunit of beta-1,3-glucan synthase; 10 predicted membrane-spanning regions; caspofungin induced; mRNA abundance declines after yeast-to-hyphal transition; similar to <i>S. cerevisiae</i> Fks3p; fungal-specific (no human or murine homolog)
orf19.4195.1	0.0119	0.63743	<i>FCA1</i>	Cytosine deaminase; enzyme of pyrimidine salvage; functional homolog of <i>S. cerevisiae</i> Fcy1p; mutation is associated with resistance to flucytosine (5-FC) in a clinical isolate; hyphal downregulated; gene has intron
orf19.5618	0.000871	0.636909		Predicted ORF in Assemblies 19, 20 and 21
orf19.7183	0.000333	0.635756		Predicted ORF in Assemblies 19, 20 and 21
orf19.5917	0.0241	0.635135	<i>STP3</i>	Transcription factor; regulates SAP2, OPT1 expression and thereby protein catabolism for nitrogen source; activated via amino-acid-induced proteolytic processing; macrophage/pseudohyphal-repressed
orf19.3840	0.000128	0.635043		Predicted ORF in Assemblies 19, 20 and 21
orf19.6417	0.00239	0.634853	<i>TSR1</i>	Predicted ORF in Assemblies 19, 20 and 21; decreased expression in response to prostaglandins
orf19.2250	0.00167	0.634494	<i>SPE3</i>	Predicted ORF in Assemblies 19, 20 and 21
orf19.4670	3.49E-05	0.633506	<i>CAS5</i>	Putative zinc finger transcription factor; cell wall damage response; required for wild-type transcriptional response to caspofungin; mutant caspofungin hypersensitive; downregulated in core stress response; avirulent, reduced CFU in mice
orf19.5843	0.0269	0.633226		Predicted ORF in Assemblies 19, 20 and 21; Plc1p-regulated; greater mRNA abundance observed in a <i>cyr1</i> homozygous null mutant than in wild type; possibly spurious ORF (Annotation Working Group prediction)
orf19.1277	0.0304	0.632682		Predicted ORF in Assemblies 19, 20 and 21; repressed by Rgt1p
orf19.1083	0.00332	0.631912		Predicted ORF in Assemblies 19, 20 and 21; macrophage-induced gene; possibly spurious ORF (Annotation Working Group prediction)
orf19.5389	0.00054	0.631	<i>FKH2</i>	Forkhead transcription factor; morphogenesis regulator; required for wild-type hyphal transcription, cell separation, and for virulence in cell culture; mutant lacks true hyphae, is constitutively pseudohyphal; upregulated in RHE model
orf19.3615	0.00219	0.629519		Predicted ORF in Assemblies 19, 20 and 21; induced in core caspofungin response; increased expression observed in an <i>ssr1</i> homozygous null mutant; induced by nitric oxide in <i>yhb1</i> mutant
orf19.1240	0.00628	0.629088		Predicted ORF in Assemblies 19, 20 and 21; fungal-specific (no human or murine homolog)

orf19.5061	0.00851	0.629019	<i>ADE5,7</i>	Enzyme of adenine biosynthesis; interacts with Vps34p; required for hyphal growth and virulence; flucytosine induced; not induced during GCN response, in contrast to the <i>S. cerevisiae</i> ortholog
orf19.5412	0.00634	0.62823		Predicted ORF in Assemblies 19, 20 and 21
orf19.3222	0.0349	0.628179		Predicted ORF in Assemblies 19, 20 and 21; fungal-specific (no human or murine homolog)
orf19.5191	0.0203	0.627872	<i>FGR6-1</i>	Protein lacking an ortholog in <i>S. cerevisiae</i> ; member of a family encoded by FGR6-related genes in the RB2 repeat sequence; transposon mutation affects filamentous growth
orf19.3237	7.26E-07	0.627716		Predicted ORF in Assemblies 19, 20 and 21
orf19.575	7.35E-05	0.627311	<i>HYR3</i>	Putative GPI-anchored protein of unknown function; similar to Hyr1p; transcriptionally regulated by iron; expression greater in high iron; clade-specific repeat variation
orf19.304	0.00337	0.625892		Putative transporter similar to MDR proteins; fungal-specific (no human or murine homolog)
orf19.3554	0.0119	0.625776	<i>AAT1</i>	Protein described as aspartate aminotransferase; soluble protein in hyphae; macrophage-induced protein; alkaline upregulated; amphotericin B repressed; gene used for strain identification by multilocus sequence typing, farnesol-induced
orf19.58	8.23E-05	0.625378	<i>RRP6</i>	Predicted ORF in Assemblies 19, 20 and 21; mutation confers hypersensitivity to 5-fluorocytosine (5-FC), 5-fluorouracil (5-FU), and tubercidin (7-deazaadenosine)
orf19.2758	0.0241	0.623478	<i>PGA38</i>	Putative GPI-anchored protein of unknown function; repressed during cell wall regeneration
orf19.297	0.000415	0.622752	<i>DTD2</i>	Predicted ORF in Assemblies 19, 20 and 21
orf19.4546	2.06E-05	0.621921	<i>HOL4</i>	Protein described as an ion transporter; alkaline upregulated by Rim101p; Plc1p-regulated; caspofungin repressed
orf19.699	0.0391	0.621173		Predicted ORF in Assemblies 19, 20 and 21
orf19.6017	0.0106	0.619215		Predicted ORF in Assemblies 19, 20 and 21
orf19.2832	0.0275	0.619133	<i>INN1</i>	Protein with similarity to <i>S. cerevisiae</i> Inn1p, which is an essential protein of the contractile actomyosin ring required for ingression of the plasma membrane into the bud neck during cytokinesis; contains a C2 membrane targeting domain
orf19.5365	0.000522	0.617877		Predicted ORF in Assemblies 19, 20 and 21; decreased transcription is observed upon fluphenazine treatment or in an azole-resistant strain that overexpresses CDR1 and CDR2
orf19.4072	0.0181	0.617779	<i>IFF6</i>	Putative GPI-anchored protein of unknown function; opaque-specific transcription; macrophage-induced gene
orf19.3871	0.0238	0.617615		Predicted ORF in Assemblies 19, 20 and 21

orf19.2808	1.53E-06	0.617501		Predicted zinc-finger protein of unknown function, not essential for viability
orf19.2791	7.40E-05	0.617266		Predicted ORF in Assemblies 19, 20 and 21
orf19.551	3.21E-05	0.617185		Predicted ORF in Assemblies 19, 20 and 21
orf19.3490	0.0109	0.616017	<i>FGR6-4</i>	Protein lacking an ortholog in <i>S. cerevisiae</i> ; member of a family encoded by FGR6-related genes in the RB2 repeat sequence; transposon mutation affects filamentous growth
orf19.1387	0.00441	0.615909		Predicted ORF in Assemblies 19, 20 and 21
orf19.3825	0.00706	0.615306	<i>RCE1</i>	Protein induced during the mating process
orf19.279	0.00416	0.614308		Predicted ORF in Assemblies 19, 20 and 21
orf19.4485	0.000199	0.614076		Predicted ORF from Assembly 19; removed from Assembly 20
orf19.1687	0.00209	0.613796		Predicted ORF in Assemblies 19, 20 and 21
orf19.6847	0.000178	0.613713		Predicted ORF in Assemblies 19, 20 and 21; virulence-group-correlated expression
orf19.4951	0.0165	0.61296		Predicted ORF in Assemblies 19, 20 and 21; possibly spurious ORF (Annotation Working Group prediction)
orf19.3276	1.19E-05	0.612095	<i>PWP2</i>	Predicted ORF in Assemblies 19, 20 and 21; downregulated during core stress response; decreased expression in response to prostaglandins; physically interacts with TAP-tagged Nop1p
orf19.6246	0.00151	0.611507		Predicted ORF in Assemblies 19, 20 and 21
orf19.1619	0.000594	0.611289		Predicted ORF in Assemblies 19, 20 and 21
orf19.7028	0.0447	0.611142		Predicted ORF in Assemblies 19, 20 and 21; merged with orf19.7027 in Assembly 21
orf19.5906	0.00537	0.610887	<i>ADE2</i>	Phosphoribosylaminoimidazole carboxylase; enzyme of adenine biosynthesis; required for wild-type growth and virulence in immunosuppressed mouse systemic infection; not induced during GCN response, in contrast to <i>S. cerevisiae</i> ortholog
orf19.5615	0.012	0.609904	<i>AYR2</i>	Predicted ORF in Assemblies 19, 20 and 21; shows colony morphology-related gene regulation by Ssn6p
orf19.1332	0.000325	0.609813	<i>SNG4</i>	Predicted ORF in Assemblies 19, 20 and 21; transcriptionally activated by Mnl1p under weak acid stress; shows Mob2p-dependent hyphal regulation
orf19.7193	0.000353	0.609743		Predicted ORF in Assemblies 19, 20 and 21
orf19.2575	0.0115	0.609525		Predicted ORF in Assemblies 19, 20 and 21
orf19.6420	0.00373	0.608855	<i>PGA13</i>	Putative GPI-anchored protein; described as similar to mucins; induced during cell wall regeneration, and during core caspofungin response; regulated by Tsa1p, Tsa1Bp in minimal media at 37 deg and by Cyr1p, Nrg1p, Tup1p, Rlm1p

orf19.727	0.0323	0.608147		Predicted ORF in Assemblies 19, 20 and 21; member of a family encoded by FGR6-related genes in the RB2 repeat sequence; possibly spurious ORF (Annotation Working Group prediction)
orf19.1071	0.0253	0.607603		Predicted ORF from Assembly 19; possibly spurious ORF (Annotation Working Group prediction); merged with orf19.5203 in Assembly 20
orf19.816	0.017	0.607036	<i>DCK2</i>	Predicted ORF in Assemblies 19, 20 and 21; similar to <i>S. cerevisiae</i> Ylr422wp; transposon mutation affects filamentous growth; transcriptionally activated by Mnl1p under weak acid stress
orf19.4907	0.00106	0.605239		Predicted ORF in Assemblies 19, 20 and 21; increased transcription is observed upon fluphenazine treatment; possibly transcriptionally regulated by Tac1p; induced by nitric oxide; fungal-specific (no human or murine homolog)
orf19.6881	0.0193	0.60456	<i>YTH1</i>	Protein described as an mRNA cleavage and polyadenylation specificity factor; transcription is regulated upon yeast-hyphal switch; decreased expression in hyphae compared to yeast-form cells; fluconazole or flucytosine induced
orf19.212	0.00275	0.603991	<i>VPS28</i>	Protein involved in proteolytic activation of Rim101p, which regulates pH response; role in echinocandin, azole sensitivity; similar to <i>S. cerevisiae</i> Vps28p, which is a subunit of the ESCRT I protein sorting complex
orf19.206	0.00892	0.603342		Predicted ORF in Assemblies 19, 20 and 21
orf19.5750	0.0211	0.602508	<i>SHM2</i>	Cytoplasmic serine hydroxymethyltransferase; complements the glycine auxotrophy of an <i>S. cerevisiae</i> shm1 null shm2 null gly1-1 triple mutant; antigenic in human; soluble protein in hyphae; farnesol-upregulated in biofilm
orf19.3664	0.016	0.601984	<i>HSP31</i>	Protein repressed during the mating process
orf19.7610	0.00753	0.601912	<i>PTP3</i>	Protein not essential for viability; similar to <i>S. cerevisiae</i> Ptp3p, which is a protein tyrosine phosphatase; hyphal induced; alkaline upregulated; regulated by Efg1p, Ras1p, cAMP pathways
orf19.5759	0.0022	0.601752	<i>SNQ2</i>	Protein similar to <i>S. cerevisiae</i> Ssq2p transporter; member of PDR subfamily of ABC family; transposon mutation affects filamentation; benomyl-induced transcription; detected at yeast-form cell plasma membrane by mass spec
orf19.7668	0.0185	0.60128	<i>MAL2</i>	Alpha-glucosidase that hydrolyzes sucrose; required for sucrose utilization; transcriptionally regulated by Suc1p; expression induced by maltose, repressed by glucose; transposon mutation affects filamentous growth; upregulated in RHE model
orf19.3190	0.00307	0.601164	<i>HAL9</i>	Protein with Zn(2)-Cys(6) binuclear cluster; gene in zinc cluster region of Chr. 5; transcriptionally activated by Mnl1p in weak acid; similar to <i>S. cerevisiae</i> Hal9p, which is a putative transcription factor involved in salt tolerance
orf19.3676	7.56E-07	0.601035	<i>ABP140</i>	Protein similar to <i>S. cerevisiae</i> actin-binding protein Abp140p; induced upon biofilm formation

orf19.7517	0.0224	0.600501	<i>CHT1</i>	Chitinase; putative N-terminal catalytic domain; has secretory signal sequence; lacks S/T region and N-glycosylation motifs of Chs2p and Chs3p; alkaline downregulated; expression not detected in yeast-form or hyphal cells
orf19.852	0.00529	0.599612	<i>SAP98</i>	Predicted ORF in Assemblies 19, 20 and 21; regulated by Gcn2p and Gcn4p; expressed in opaque MTLa/MTLa cells
orf19.7392	0.00233	0.599554		Predicted ORF in Assemblies 19, 20 and 21
orf19.6773	0.00158	0.598725	<i>ECM29</i>	Protein similar to <i>S. cerevisiae</i> Ecm29p; transposon mutation affects filamentous growth
orf19.4900	0.00176	0.598531		Predicted ORF in Assemblies 19, 20 and 21
orf19.2646	0.0011	0.597482		Predicted zinc-finger protein of unknown function, not essential for viability
orf19.671	0.0115	0.595755	<i>PSP1</i>	Protein repressed during the mating process
orf19.4046	0.000369	0.591307		Putative transcription factor containing a Zn(2)-Cys(6) binuclear cluster; predicted ORF in Assemblies 19, 20 and 21
orf19.7080	0.00372	0.590661	<i>LEU2</i>	Isopropyl malate dehydrogenase; enzyme of leucine biosynthesis; upregulated in the presence of human whole blood or polymorphonuclear (PMN) cells; protein level decreased in stationary phase cultures
orf19.5730	0.00106	0.590374		Predicted ORF in Assemblies 19, 20 and 21; clade-associated gene expression
orf19.3481	0.0105	0.589772		Putative protein of unknown function, transcription is activated in the presence of elevated CO ₂ ; predicted ORF in Assemblies 19, 20 and 21
orf19.2173	0.0446	0.589499	<i>MAF1</i>	Protein described as affecting nucleocytoplasmic transport and synthesis of RNA Polymerase III; decreased expression in hyphae compared to yeast-form cells; caspofungin repressed
orf19.7450	5.36E-05	0.588207		Predicted ORF in Assemblies 19, 20 and 21
orf19.7367	0.000702	0.588066	<i>UBP1</i>	Protein described as ubiquitin carboxyl-1-terminal hydrolase
orf19.3335	0.000126	0.586216		Predicted ORF in Assemblies 19, 20 and 21; shows colony morphology-related gene regulation by Ssn6p; repressed by nitric oxide
orf19.6868	0.00117	0.585553		Predicted ORF in Assemblies 19, 20 and 21
orf19.2397.3	0.00174	0.58522		ORF Predicted by Annotation Working Group
orf19.7112	0.000871	0.585201	<i>FRP2</i>	Protein described as ferric reductase; alkaline upregulated by Rim101p; fluconazole-downregulated; upregulated in the presence of human neutrophils; possibly adherence-induced
orf19.5838	0.000225	0.585142		Predicted ORF in Assemblies 19, 20 and 21
orf19.339	0.0287	0.583908	<i>NDE1</i>	Putative NADH dehydrogenase that could act alternatively to complex I in respiration;

				caspofungin repressed; fungal-specific (no human or murine homolog); transcription is upregulated in both intermediate and mature biofilms
orf19.2175	0.0308	0.58262		Predicted ORF in Assemblies 19, 20 and 21; induced by nitric oxide
orf19.2046	0.0211	0.582112	<i>POT1-2</i>	Putative peroxisomal 3-ketoacyl CoA thiolase
orf19.642	0.00458	0.580809		Predicted ORF in Assemblies 19, 20 and 21
orf19.1978	0.0358	0.580707	<i>GIT2</i>	Putative glycerophosphoinositol permease; fungal-specific (no human or murine homolog); transcription is repressed in response to alpha pheromone in SpiderM medium
orf19.3475	0.00363	0.580383		Described as a Gag-related protein; hyphal induced; downregulation correlates with clinical development of fluconazole resistance; repressed by nitric oxide, 17-beta-estradiol, ethynyl estradiol
orf19.4292	0.0143	0.579382		Predicted ORF in Assemblies 19, 20 and 21
orf19.7247	0.0404	0.579246	<i>RIM101</i>	Transcription factor involved in alkaline pH response; required for alkaline-induced hyphal growth; role in virulence in mouse systemic infection; activated by C-terminal proteolytic cleavage; mediates both positive and negative regulation
orf19.1121	0.000117	0.576399		Predicted ORF in Assemblies 19, 20 and 21
orf19.1357	7.16E-05	0.576374	<i>FCY21</i>	High affinity, high capacity, hypoxanthine-adenine-guanine-cytosine/ H ⁺ symporter; purine-cytosine permease of pyrimidine salvage; similar to <i>S. cerevisiae</i> Fcy2p; mutation confers resistance to 5-fluorocytosine (5-FC)
orf19.5315	0.0154	0.575819	<i>FGR6</i>	Protein lacking an ortholog in <i>S. cerevisiae</i> ; transposon mutation affects filamentous growth; removed from Assembly 20
orf19.5845	0.0362	0.575603	<i>RNR3</i>	Protein described as large subunit of ribonucleotide reductase; transcriptionally regulated by iron; expression greater in low iron
orf19.7381	0.0449	0.575548	<i>ZCF37</i>	Predicted zinc-finger protein of unknown function; not essential for viability
orf19.3066	0.0159	0.57285	<i>ENG1</i>	Endo-1,3-beta-glucanase required for cell separation after division, orthologous to <i>S. cerevisiae</i> Dse4p; caspofungin repressed; fungal-specific (no human or murine homolog); repressed in response to alpha pheromone in SpiderM medium
orf19.6184	7.79E-05	0.568816		Predicted ORF in Assemblies 19, 20 and 21; possibly spurious ORF (Annotation Working Group prediction)
orf19.6958	0.00232	0.568543	<i>ECM18</i>	Predicted ORF in Assemblies 19, 20 and 21
orf19.4712	0.00252	0.567439	<i>FGR6-3</i>	Protein lacking an ortholog in <i>S. cerevisiae</i> ; member of a family encoded by FGR6-related genes in the RB2 repeat sequence; transposon mutation affects filamentous growth

orf19.1193	0.0193	0.566949	<i>GNPI</i>	Protein described as similar to asparagine and glutamine permease; fluconazole or caspofungin induced; transcription is regulated by Nrg1p, Mig1p, Tup1p, Gcn2p, Gcn4p, and alkaline regulated by Rim101p; fungal-specific
orf19.449	0.0156	0.566381		Predicted ORF in Assemblies 19, 20 and 21; possible phosphatidyl synthase; transcription reduced upon yeast-hyphal switch; protein detected by mass spec in stationary phase cultures
orf19.868	0.000797	0.565457	<i>ADAEC</i>	Transcription is specific to white cell type
orf19.6469	0.00083	0.563102		Predicted ORF in retrotransposon Tca11 with similarity to the Gag-Pol region of retrotransposons, which encodes nucleocapsid-like protein, reverse transcriptase, protease, and integrase
orf19.2521	0.000232	0.561259		Predicted ORF in Assemblies 19, 20 and 21
orf19.4318	0.00777	0.56018	<i>MIG1</i>	Transcriptional repressor; regulates genes for utilization of carbon sources; Tup1p-dependent and -independent functions; upregulated in biofilm; hyphal downregulated; caspofungin repressed; functional homolog of <i>S. cerevisiae</i> Mig1p
orf19.4155.12	0.000443	0.559591		ORF Predicted by Annotation Working Group; removed from Assembly 20
orf19.35	0.014	0.559415		Predicted ORF in Assemblies 19, 20 and 21
orf19.7300	0.0208	0.557491		Predicted ORF in Assemblies 19, 20 and 21
orf19.5019	0.0108	0.556879		Predicted ORF in Assemblies 19, 20 and 21
orf19.7213	0.00369	0.556479		Putative ATP-dependent RNA helicase; fungal-specific (no human or murine homolog)
orf19.7005	0.00493	0.555637		Predicted ORF from Assembly 19; removed from Assembly 20
orf19.1604	0.0321	0.555094		Predicted ORF in Assemblies 19, 20 and 21; Gal4p-like DNA-binding domain
orf19.1847	0.000767	0.554081	<i>ARO10</i>	Aromatic decarboxylase of the Ehrlich fusel oil pathway of aromatic alcohol biosynthesis; pH-regulated (alkaline downregulated); protein abundance is affected by <i>URA3</i> expression in the CAI-4 strain background
orf19.2398	0.000462	0.554076		Predicted ORF in Assemblies 19, 20 and 21; possible increased transcription in an azole-resistant strain that overexpresses CDR1 and CDR2; possibly transcriptionally regulated by Tac1p; induced by Mnl1p under weak acid stress
orf19.5026	7.57E-06	0.55232		Putative transcription factor with zinc finger DNA-binding motif
orf19.1800	0.0486	0.550772		Predicted ORF in Assemblies 19, 20 and 21
orf19.6896	0.00215	0.550141		Predicted ORF in Assemblies 19, 20 and 21; member of a family encoded by FGR6-related genes in the RB2 repeat sequence

orf19.7210	8.64E-06	0.548582		Predicted ORF in Assemblies 19, 20 and 21
orf19.171	0.00442	0.547023	<i>DBP2</i>	Predicted ORF in Assemblies 19, 20 and 21; flucytosine induced; downregulated in core stress response
orf19.215	0.00963	0.546938		Predicted ORF in Assemblies 19, 20 and 21
orf19.2270	0.000818	0.545943	<i>SMF12</i>	Protein not essential for viability; similar to <i>S. cerevisiae</i> Smf1p, which is a manganese transporter; Gcn4p-regulated; alkaline upregulated; caspofungin repressed
orf19.1206	0.00898	0.542704	<i>FET35</i>	Protein with similarity to multicopper ferroxidase; transcriptionally activated in low iron conditions; transcription is repressed by Sfu1p and activated under weak acid stress by Mnl1p; merged with orf19.4215 in Assembly 20
orf19.5022	0.00187	0.542692		Predicted ORF in Assemblies 19, 20 and 21
orf19.4952	1.71E-05	0.538147		Predicted ORF in Assemblies 19, 20 and 21
orf19.4921.1	0.0351	0.537837		ORF added to Assembly 21 based on comparative genome analysis
orf19.2308	0.0388	0.534149		Predicted ORF in Assemblies 19, 20 and 21
orf19.1913	0.00169	0.530611		Predicted ORF in Assemblies 19, 20 and 21
orf19.6741	0.0366	0.529154		Predicted ORF in Assemblies 19, 20 and 21; regulated by Nrg1p, Tup1p
orf19.7313	0.0242	0.528818	<i>SSUI</i>	Protein similar to <i>S. cerevisiae</i> Ssu1p sulfite transport protein; transposon mutation affects filamentous growth; regulated by Gcn2p and Gcn4p; induced by nitric oxide
orf19.610	0.000612	0.525688	<i>EFG1</i>	Transcriptional repressor; required for white-phase cell type; hyphal growth, metabolism, cell-wall gene regulator; roles in adhesion, virulence; Cph1p and Efg1p have role in host cytokine response; bHLH; binds E-box; T206 phosphorylated
orf19.7029	0.0201	0.52308		Predicted ORF in Assemblies 19, 20 and 21; mutation confers hypersensitivity to toxic ergosterol analog
orf19.1153	0.0158	0.516484	<i>GADI</i>	Protein described as glutamate decarboxylase; macrophage-downregulated gene; alkaline downregulated; amphotericin B induced; transcriptionally activated by Mnl1p under weak acid stress
orf19.4657	0.0013	0.515581		Predicted ORF in Assemblies 19, 20 and 21
orf19.6070	0.00614	0.51463	<i>ENA2</i>	Protein described as sodium transporter; transcription is upregulated in response to ciclopirox olamine; alkaline upregulated by Rim101p; repressed upon high-level peroxide stress; upregulated in oral candidiasis clinical isolates
orf19.4116	0.0156	0.512017		Protein not essential for viability

orf19.1964	0.0133	0.511279		Putative protein of unknown function; downregulated upon fluphenazine treatment; upregulated upon benomyl treatment and in an RHE model; regulated by Nrg1p, Tup1p
orf19.5875	0.000936	0.510624	<i>VAM3</i>	Predicted ORF in Assemblies 19, 20 and 21
orf19.2948	0.0144	0.509147	<i>SNO1</i>	Protein of unknown function expressed during stationary phase; transcription is regulated by Tup1p, Efg1p
orf19.5401	0.004	0.507141		Predicted ORF in Assemblies 19, 20 and 21; mutation confers hypersensitivity to toxic ergosterol analog; decreased transcription is observed upon fluphenazine treatment
orf19.1486	0.00487	0.506785		Predicted ORF in Assemblies 19, 20 and 21; possibly spurious ORF (Annotation Working Group prediction)
orf19.3641	0.00491	0.50539		Expression is regulated upon white-opaque switching; merged with orf19.84 in Assembly 20
orf19.2942	0.00134	0.504627	<i>DIP5</i>	Putative permease for dicarboxylic amino acids; mutation confers hypersensitivity to toxic ergosterol analog; transcriptionally induced upon phagocytosis by macrophage; Gcn4p-regulated; upregulated by Rim101p at pH 8
orf19.2064	0.032	0.504182		Putative transcription factor with zinc finger DNA-binding motif
orf19.6447	0.00846	0.498876	<i>ARF1</i>	ADP-ribosylation factor, probable GTPase involved in intracellular transport; one of several <i>C. albicans</i> ADP-ribosylation factors; N-myristoylprotein; substrate of Nmt1p
orf19.7374	0.00956	0.497344	<i>CTA4</i>	Predicted transcription factor involved in response to nitric oxide; downregulated upon adherence to polystyrene; induced by nitric oxide; transcriptionally activated by Mnl1p under weak acid stress
orf19.3283	0.00321	0.495502		Predicted ORF in Assemblies 19, 20 and 21
orf19.7051	0.000235	0.493678		Predicted ORF in Assemblies 19, 20 and 21
orf19.3749	0.039	0.491973	<i>IFC3</i>	Oligopeptide transporter; transcriptionally induced upon phagocytosis by macrophage; induced by BSA or peptides; fluconazole-induced; upregulated by Rim101p at pH 8; virulence-group-correlated expression; no human or murine homolog
orf19.5785	0.0312	0.488996		Predicted ORF in Assemblies 19, 20 and 21; greater mRNA abundance observed in a <i>cyr1</i> or <i>ras1</i> homozygous null mutant than in wild type; induced by nitric oxide; possibly spurious ORF (Annotation Working Group prediction)
orf19.3360	0.0176	0.487556		Predicted ORF in Assemblies 19, 20 and 21; possibly spurious ORF (Annotation Working Group prediction)
orf19.6522	0.0168	0.486342		Putative allantoin permease; fungal-specific (no human or murine homolog); Gcn4p-regulated
orf19.1855	0.00194	0.484793		Predicted membrane transporter, member of the anion:cation symporter (ACS) family, major

				facilitator superfamily (MFS); Gcn4p-regulated; flucytosine induced; ketoconazole-repressed; oxidative stress-induced via Cap1p
orf19.6639	0.00782	0.484169		Predicted ORF in Assemblies 19, 20 and 21
orf19.2107.1	0.0258	0.483707	<i>STF2</i>	Protein involved in ATP biosynthesis; decreased expression in hyphae compared to yeast-form cells; downregulated by Efg1p; transcription is upregulated in clinical isolates from HIV+ patients with oral candidiasis
orf19.3810	0.00446	0.483379		Predicted ORF in Assemblies 19, 20 and 21
orf19.2060	0.0211	0.480563	<i>SOD5</i>	Copper- and zinc-containing superoxide dismutase; protective role against oxidative stress; induced by neutrophil contact, hyphal growth, caspofungin, osmotic or oxidative stress; member of a gene family including SOD1, SOD4, SOD5, and SOD6
orf19.951	0.0137	0.479724		Predicted ORF in Assemblies 19, 20 and 21; transcription downregulated upon yeast-hyphal switch; fluconazole-induced; possibly spurious ORF (Annotation Working Group prediction)
orf19.1263	0.0154	0.478152	<i>CFL1</i>	Protein similar to ferric reductase Fre10p; possible functional homolog of <i>S. cerevisiae</i> Fre1p (reports differ); transcription is negatively regulated by Sfu1p, copper, amphotericin B, caspofungin; induced by ciclopirox olamine
orf19.5338	0.00143	0.477903	<i>GAL4</i>	Putative transcription factor with zinc cluster DNA-binding motif; ortholog of <i>S. cerevisiae</i> Gal4p, but is not involved in the regulation of galactose utilization genes; caspofungin repressed
orf19.2157	0.0154	0.476609	<i>DAC1</i>	N-acetylglucosamine-6-phosphate (GlcNAcP) deacetylase; enzyme of N-acetylglucosamine utilization; required for wild-type hyphal growth and virulence in mouse systemic infection; gene is GlcNAc-induced
orf19.1562	0.011	0.471445		Predicted ORF in Assemblies 19, 20 and 21; transcription is repressed in response to alpha pheromone in SpiderM medium
orf19.48	0.0465	0.470746		Predicted ORF in Assemblies 19, 20 and 21; likely to be essential for growth, based on an insertional mutagenesis strategy; virulence-group-correlated expression
orf19.5118	0.00124	0.469446	<i>SDS24</i>	Protein described as similar to <i>S. cerevisiae</i> Ybr214wp; transcription regulated by Mig1p and Tup1p; fluconazole-induced
orf19.54	0.0214	0.468246	<i>RHD1</i>	Putative beta-mannosyltransferase, required for the addition of beta-mannose to the acid-labile fraction of cell wall phosphopeptidomannan; member of a 9-gene family; transcriptionally regulated on yeast-hyphal and white-opaque switches
orf19.1253	0.0144	0.463877		Predicted ORF in Assemblies 19, 20 and 21; transcriptionally activated by Mnl1p under weak acid stress
orf19.6000	3.16E-06	0.463774	<i>CDR1</i>	Multidrug transporter of ATP-binding cassette (ABC) superfamily; transports phospholipids in an

				in-to-out direction; transcription induced by beta-estradiol, progesterone, corticosteroid, or cholesterol
orf19.1272	1.36E-05	0.463725		Predicted ORF in Assemblies 19, 20 and 21
orf19.220	0.000891	0.462377	<i>PIR1</i>	Structural protein of cell wall; 1,3-beta-glucan-linked; O-glycosylated by Pmt1p; N-mannosylated; tandem repeats; heterozygous mutant has cell wall defects; hyphal repressed; Hog1p, fluconazole, hypoxia induced; iron, Efg1p, Plc1p regulated
orf19.3675	0.031	0.46018	<i>GAL7</i>	Predicted ORF in Assemblies 19, 20 and 21; macrophage/pseudohyphal-repressed
orf19.815	0.000332	0.456965	<i>DCK1</i>	Putative guanine nucleotide exchange factor required for embedded filamentous growth; activates Rac1p; contains a DOCKER domain; similar to adjacent DCK2 and to <i>S. cerevisiae</i> Ylr422wp; regulated by Nrg1p
orf19.6874	0.00354	0.45673		Predicted ORF in Assemblies 19, 20 and 21
orf19.2284	0.0105	0.455543		Predicted ORF in Assemblies 19, 20 and 21
orf19.1331	0.00029	0.452789	<i>HSM3</i>	Protein not essential for viability; similar to <i>S. cerevisiae</i> Hsm3p, which may be involved in DNA mismatch repair
orf19.334	0.0186	0.452403		Predicted ORF in Assemblies 19, 20 and 21
orf19.100	0.0234	0.452318		Predicted ORF in Assemblies 19, 20 and 21
orf19.4843	0.000146	0.450159		Predicted ORF in Assemblies 19, 20 and 21
orf19.1002	0.0337	0.449649		Predicted ORF in Assemblies 19, 20 and 21; possibly spurious ORF (Annotation Working Group prediction)
orf19.6770	0.0221	0.448797		Predicted ORF in Assemblies 19, 20 and 21
orf19.341	0.0213	0.44521		Putative spermidine export pump; fungal-specific (no human or murine homolog)
orf19.5431	0.0165	0.4439		Predicted ORF in Assemblies 19, 20 and 21
orf19.2947	0.0188	0.441762	<i>SNZ1</i>	Detected in stationary phase cultures; soluble in hyphae; induced on yeast to hyphal switch, in response to 3-aminotriazole, or in azole-resistant strain overexpressing MDR1; regulated by Gcn4p, macrophage; no human/murine homolog
orf19.7637	0.0355	0.428356	<i>YHB4</i>	Protein related to flavohemoglobins; not required for wild-type nitric oxide resistance; has predicted globin, FAD-binding, and NAD(P)-binding domains but lacks some conserved residues of flavohemoglobins; no mRNA detected
orf19.6514	0.0211	0.425696	<i>CUP9</i>	Protein of unknown function, upregulated in clinical isolates from HIV+ patients with oral candidiasis; transcription reduced upon yeast-hyphal switch; ketoconazole-induced; Plc1p-regulated; shows colony morphology-related Ssn6p regulation

orf19.7150	0.00685	0.42168	<i>NRG1</i>	Transcriptional repressor; regulates hyphal genes, virulence genes, chlamyospore development, and genes involved in rescue and stress responses; effects both Tup1p-dependent (major) and -independent (minor) regulation
orf19.7319	0.00515	0.418703	<i>SUC1</i>	Putative transcriptional regulator with N-terminal zinc finger; regulates alpha-glucosidase in <i>C. albicans</i> and <i>S. cerevisiae</i> ; in <i>S. cerevisiae</i> , complements <i>suc2</i> mutant sucrose utilization defect and <i>mal13</i> mutant maltase defect
orf19.1944	0.0015	0.417498	<i>GPR1</i>	Putative G-protein-coupled receptor of plasma membrane; required for wild-type hyphal growth; acts in cAMP-PKA pathway; reports differ on role in cAMP-mediated glucose signaling; Gpr1p C terminus binds Gpa2p; regulates HWPI and ECE1
orf19.3406	1.84E-05	0.41687		Predicted ORF in Assemblies 19, 20 and 21; member of conserved Mcm1p regulon
orf19.7586	0.00407	0.414925	<i>CHT3</i>	Chitinase, major; functional homolog of <i>S. cerevisiae</i> Cts1p; 4 N-glycosylation motifs; possible O-mannosylated region; putative signal peptide; hyphal-repressed; farnesol upregulated in biofilm; regulated by Efg1p, Cyr1p, Ras1p
orf19.385	0.024	0.4137	<i>GCV2</i>	Putative protein of glycine catabolism; downregulated by Efg1p; Hog1p-induced; upregulated by Rim101p at acid pH; transcription is activated in the presence of elevated CO ₂ ; protein detected by mass spec in stationary phase cultures
orf19.4998	0.00311	0.410706		Predicted ORF in Assemblies 19, 20 and 21; caspofungin repressed
orf19.3854	0.000169	0.410661		Protein similar to <i>S. cerevisiae</i> Sat4p; amphotericin B induced; clade-associated gene expression
orf19.4631	0.00762	0.40561	<i>ERG251</i>	Predicted ORF in Assemblies 19, 20 and 21; ketoconazole-induced; amphotericin B, caspofungin repressed
orf19.2671	0.000491	0.402614		Predicted ORF in Assemblies 19, 20 and 21; Plc1p-regulated
orf19.3448	0.000718	0.399897		Predicted ORF in Assemblies 19, 20 and 21; ketoconazole-repressed; possibly spurious ORF (Annotation Working Group prediction)
orf19.3678	0.00144	0.39974		Protein not essential for viability
orf19.1306	0.00325	0.397487		Predicted ORF in Assemblies 19, 20 and 21
orf19.1653	0.000925	0.397107		Predicted ORF in Assemblies 19, 20 and 21; possibly spurious ORF (Annotation Working Group prediction)
orf19.409	0.0368	0.395374		Predicted membrane protein; similar to <i>S. cerevisiae</i> Ynr018Wp
orf19.1437	0.000195	0.392816		Transcription is negatively regulated by Sfu1p; removed from Assembly 20
orf19.5305	1.65E-05	0.389951	<i>RHD3</i>	Putative GPI-anchored protein that localizes to the cell wall; transcription is decreased upon yeast-hyphal switch; transcriptionally regulated by iron; expression greater in high iron; clade-

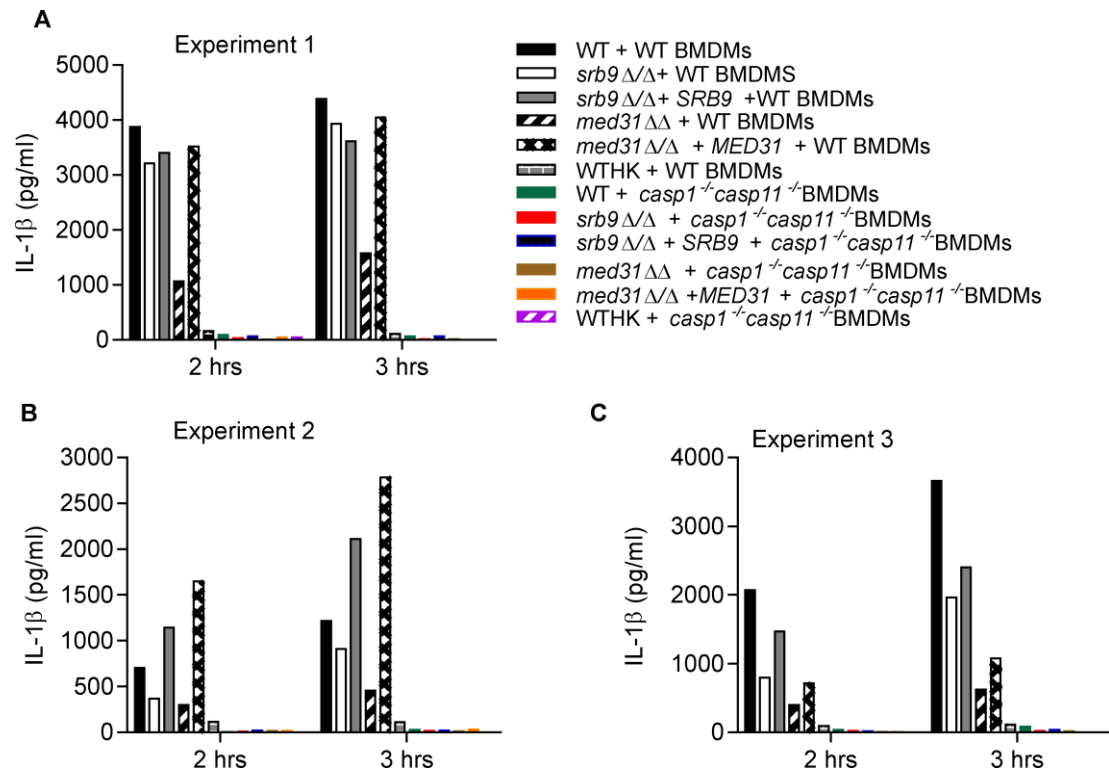
				associated gene expression
orf19.6086	0.00211	0.389919	<i>LEU4</i>	Putative 2-isopropylmalalate synthase; regulated by Nrg1p, Mig1p, Tup1p, Gcn4p; upregulated in the presence of human whole blood or polymorphonuclear (PMN) cells; macrophage/pseudohyphal-repressed after 16h; fungal-specific
orf19.7091	0.000747	0.389613		Predicted ORF in Assemblies 19, 20 and 21; induced by nitric oxide
orf19.6720	0.0141	0.376265		Predicted ORF in Assemblies 19, 20 and 21; similar to <i>S. cerevisiae</i> Ydr090cp; transposon mutation affects filamentous growth
orf19.2602	0.00493	0.369784	<i>OPT1</i>	Oligopeptide transporter; transports 3-to-5-residue peptides; alleles are distinct, one has intron; not ABC or PTR type transporter; suppresses <i>S. cerevisiae</i> ptr2-2 mutant defects; induced by BSA or peptides; Stp3p, Hog1p regulated
orf19.4033	3.94E-05	0.369632	<i>PRP22</i>	Protein described as an RNA-dependent ATPase; induced upon adherence to polystyrene; transcriptionally activated by Mnl1p under weak acid stress
orf19.4438	0.0442	0.36677	<i>RME1</i>	Protein similar to <i>S. cerevisiae</i> meiotic regulator Rme1p; white-specific transcription; upregulation correlates with clinical development of fluconazole resistance; transcription is not regulated during rat oral infection
orf19.7085	0.0143	0.366157		Predicted ORF in Assemblies 19, 20 and 21; induced in core stress response; induced by heavy metal (cadmium) stress via Hog1p; oxidative stress-induced via Cap1p; induced by Mnl1p under weak acid stress; macrophage-downregulated
orf19.2475	0.0149	0.361199	<i>PGA26</i>	Putative GPI-anchored protein of unknown function; transcriptionally regulated by iron; expression greater in high iron; induced during cell wall regeneration; possibly spurious ORF (Annotation Working Group prediction)
orf19.3302	0.0405	0.360498		Predicted ORF in Assemblies 19, 20 and 21; transcription downregulated upon yeast-hyphal switch; transcriptionally activated by Mnl1p under weak acid stress
orf19.1774	0.0156	0.352149		Predicted ORF in Assemblies 19, 20 and 21; transcription is upregulated in an RHE model of oral candidiasis; virulence-group-correlated expression
orf19.2079	0.00604	0.347598	<i>PHHB</i>	Transposon mutation affects filamentous growth
orf19.638	0.0499	0.341712	<i>FDH1</i>	Putative formate dehydrogenase, oxidizes formate to produce CO ₂ ; induced during macrophage infection; fluconazole-downregulated; Mig1p regulated; downregulated by Efg1p under yeast, not hyphal, growth conditions; predicted to be cytosolic
orf19.4887	0.0222	0.338658	<i>ECM21</i>	Protein not essential for viability; similar to <i>S. cerevisiae</i> Ecm21p (may have cell wall role); alkaline upregulated by Rim101p; fluconazole induced; caspofungin repressed; downregulated inazole-resistant strain overexpressing MDR1

orf19.2192	0.00599	0.336967	<i>GDH2</i>	Putative NAD-specific glutamate dehydrogenase; fungal-specific (no human or murine homolog); transcription is regulated by Nrg1p, Mig1p, Tup1p, and Gcn4p
orf19.5288.1	6.13E-05	0.335136		ORF added to Assembly 21 based on comparative genome analysis
orf19.1429	0.0336	0.324095	<i>SOH1</i>	Predicted ORF in Assemblies 19, 20 and 21; cell-cycle regulated periodic mRNA expression
orf19.3803	0.0111	0.311183	<i>MNN22</i>	Protein described as similar to Golgi alpha-1,2-mannosyltransferase; regulated by Tsa1p, Tsa1Bp in minimal media at 37 deg; Hog1p-induced; induced by nitric oxide; downregulated in core stress response
orf19.6586	0.0126	0.310892		Predicted ORF in Assemblies 19, 20 and 21; increased transcription is observed upon benomyl treatment or in an azole-resistant strain that overexpresses MDR1; shows colony morphology-related gene regulation by Ssn6p; macrophage-downregulated gene
orf19.4774	0.0173	0.31022	<i>AOX1</i>	Alternative oxidase; low abundance; constitutively expressed; one of two isoforms (Aox1p and Aox2p); involved in a cyanide-resistant respiratory pathway present in plants, protists, and some fungi, although absent from <i>S. cerevisiae</i>
orf19.7314	0.00822	0.303503	<i>CDG1</i>	Protein described as similar to cysteine dioxygenases; expression is regulated upon white-opaque switching; transcription is upregulated in both intermediate and mature biofilms
orf19.5334	0.0182	0.302231		Predicted ORF in Assemblies 19, 20 and 21; transcription regulated upon yeast-hyphal switch
orf19.4527	0.014	0.299649	<i>HGT1</i>	High-affinity glucose transporter, member of major facilitator superfamily; transcription induced by progesterone and by drugs including chloramphenicol and benomyl; likely essential for growth, based on an insertional mutagenesis strategy
orf19.6964	0.0162	0.299391		Predicted ORF from Assembly 19; removed from Assembly 20
orf19.6817	0.00681	0.297804	<i>FCR1</i>	Putative zinc cluster transcription factor; negative regulator of fluconazole, ketoconazole, brefeldin A resistance; transposon mutation affects filamentous growth; partially suppresses <i>S. cerevisiae</i> pdr1 pdr3 mutant fluconazole sensitivity
orf19.3419	0.00388	0.295747	<i>MAE1</i>	Malic enzyme, mitochondrial; transcription regulated by Mig1p and Tup1p; shows colony morphology-related gene regulation by Ssn6p
orf19.1187	0.00119	0.291984	<i>CPH2</i>	Transcriptional activator of hyphal growth; Myc bHLH family: directly regulates Tec1p, which regulates hypha-specific genes; probably homodimeric, phosphorylated; enhances <i>S. cerevisiae</i> nitrogen starvation-induced pseudohyphal growth
orf19.3893	2.34E-05	0.282536	<i>SCW11</i>	Cell wall protein; transcription is decreased in mutant lacking ACE2; downregulated in core caspofungin response; transcriptionally regulated by iron; expression greater in high iron
orf19.4773	0.0247	0.279674	<i>AOX2</i>	Alternative oxidase; induced by antimycin A, some oxidants; growth- and carbon-source-regulated; one of two isoforms (Aox1p and Aox2p); involved in cyanide-resistant respiratory

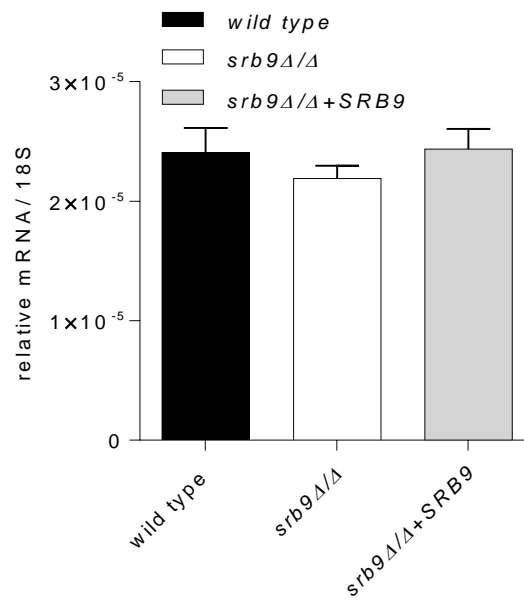
				pathway that is absent from <i>S. cerevisiae</i>
orf19.3669	0.00189	0.260733	<i>SHA3</i>	Protein similar to <i>S. cerevisiae</i> Sha3p, which is a serine/threonine kinase involved in glucose transport; transposon mutation affects filamentous growth; fluconazole-induced; ketoconazole-repressed; induced in response to alpha pheromone
orf19.6660	0.0183	0.252933		Predicted ORF in Assemblies 19, 20 and 21
orf19.4698	0.000439	0.250611	<i>PTC8</i>	Predicted type 2C protein phosphatase, serine/threonine-specific; required for hyphal growth; induced under stress
orf19.2669	5.82E-05	0.246219		Predicted ORF in retrotransposon Tca4 with similarity to the Pol region of retrotransposons encoding reverse transcriptase, protease and integrase; downstream from RHD2 with similarity to the Gag region encoding nucleocapsid-like protein
orf19.822	0.0352	0.24605		Protein detected in some, not all, biofilm extracts; fluconazole-downregulated; greater mRNA abundance observed in <i>cyr1</i> or <i>ras1</i> homozygous null mutant than in wild type; protein detected by mass spec in stationary phase cultures
orf19.909	0.000449	0.241573	<i>STP4</i>	Putative transcription factor with zinc finger DNA-binding motif; induced in core caspofungin response; shows colony morphology-related gene regulation by <i>Ssn6p</i> ; induced by 17-beta-estradiol, ethynyl estradiol
orf19.6301	0.0026	0.240573		Predicted ORF from Assembly 19; clade-associated gene expression; removed from Assembly 20
orf19.2529.1	0.0145	0.240372		ORF added to Assembly 21 based on comparative genome analysis
orf19.4342	0.00411	0.232675		Predicted ORF in Assemblies 19, 20 and 21
orf19.4552	6.59E-06	0.23171		Predicted ORF from Assembly 19; removed from Assembly 20
orf19.5282	0.0141	0.221252		Predicted ORF in Assemblies 19, 20 and 21; decreased expression in hyphae compared to yeast-form cells; regulated by <i>Efg1p</i> and <i>Efh1p</i> ; intron in 5'-UTR; transcriptionally activated by <i>Mnl1p</i> under weak acid stress
orf19.5908	0.00129	0.212989	<i>TEC1</i>	TEA/ATTS transcription factor involved in regulation of hypha-specific genes; required for wild-type biofilm formation; regulates <i>BCR1</i> ; directly transcriptionally regulated by <i>Cph2p</i> under some growth conditions; alkaline upregulated
orf19.85	1.06E-05	0.212084	<i>GPX2</i>	Similar to glutathione peroxidase; expression greater in high iron; alkaline upregulated by <i>Rim101p</i> ; transcriptionally induced by alpha factor or interaction with macrophage; regulated by <i>Efg1p</i> ; caspofungin repressed
orf19.1117	0.00907	0.206126		Predicted ORF in Assemblies 19, 20 and 21; similar to <i>Candida boidinii</i> formate dehydrogenase; virulence-group-correlated expression

orf19.5741	0.00126	0.191546	<i>ALSI</i>	Adhesin; ALS family of cell-surface glycoproteins; adhesion, virulence roles; immunoprotective; in band at hyphal base; amyloid domain; biofilm-induced; Rfg1p, Ssk1p, growth-regulated; strain background affects expression
orf19.1189	0.00155	0.17644		Predicted ORF in Assemblies 19, 20 and 21; transcription regulated upon yeast-hyphal switch; transcriptionally activated by Mnl1p under weak acid stress
orf19.4941	0.0217	0.171761	<i>TYE7</i>	Putative bHLH (basic region, helix-loop-helix) transcription factor; hyphally regulated via Cph1p, Cyr1p; flucytosine, Hog1p induced; amphotericin B, caspofungin repressed; downregulated in azole-resistant strain overexpressing MDR1
orf19.4450.1	0.00363	0.168425		ORF Predicted by Annotation Working Group
orf19.3670	0.00726	0.157816	<i>GALI</i>	Galactokinase; transcription regulated by galactose; transcription regulated by Mig1p and Tup1p; not required for systemic mouse virulence; farnesol-downregulated in biofilm; fluconazole-induced
orf19.7514	0.00152	0.155544	<i>PCK1</i>	Phosphoenolpyruvate carboxykinase; role in gluconeogenesis; regulated by hyphal switch, carbon source; repressed on glucose; induced by fluconazole, phagocytosis, H ₂ O ₂ ; predicted ATP-dependent, dimeric; predicted PKC phosphorylation sites
orf19.3672	0.0292	0.154387	<i>GAL10</i>	UDP-glucose 4-epimerase, required for galactose utilization; mutant shows cell wall defects and increased filamentation; fluconazole-induced; protein detected by mass spec in stationary phase cultures
orf19.2659	0.0171	0.151961		Predicted ORF from Assembly 19; downregulation correlates with clinical development of fluconazole resistance; decreased expression in hyphae compared to yeast-form cells; Ras1p-regulated; merged with orf19.1354 in Assembly 20
orf19.1354	0.0348	0.147131	<i>UCFI</i>	Transcriptionally regulated by iron or by yeast-hyphal switch; expression greater in high iron, decreased upon yeast-hyphal switch; downregulation correlates with clinical development of fluconazole resistance; Ras1p-regulated
orf19.5626	0.00564	0.132816		Predicted ORF in Assemblies 19, 20 and 21; Plc1p-regulated; transcriptionally activated by Mnl1p under weak acid stress
orf19.670.2	0.000753	0.077765		ORF Predicted by Annotation Working Group

Appendix 2 Appendix figures for Chapter 4



Appendix 2, Figure 1. Actual experimental results of IL-1 β levels depicted in Figure 4.14. Results of the individual experiments used in Figure 4.13, with absolute values of secreted IL-1 β (pg/ml). For the *srb9* Δ/Δ mutant, data from the experiment described for panel C and the experiments described for panel D were combined for the graph in Figure 4.13



Appendix 2, Figure 2. *URA3* expression levels of the *srb9Δ/Δ* mutant within macrophages. *C. albicans* strains were co-incubated with macrophages for 4 hours and RNA was extracted as as conducted in Figure 4.8A. The expression of *URA3* was determined using quantitative PCR. Shown are the levels of wild type, *srb9Δ/Δ* and *srb9Δ/Δ+SRB9* cells relative to 18s rRNA. The average of three experiments and the SEM are shown.